CURRENT CHALLENGES IN FUNDAMENTAL PHYSICS

by

DANIEL EGANA-UGRINOVIC

A dissertation submitted to the

Graduate School - New Brunswick

Rutgers, The State University of New Jersey

In partial fulfillment of the requirements

For the degree of

Doctor of Philosophy

Graduate Program in Physics and Astronomy

Written under the direction of

Scott Thomas

And approved by

_____

_____

_____

_____

_____

New Brunswick, New Jersey

October, 2016

ABSTRACT OF THE DISSERTATION

Current challenges in fundamental physics

By Daniel Egana-Ugrinovic

Dissertation Director:
Professor Scott Thomas

The discovery of the Higgs boson at the Large Hadron Collider completed the Standard Model of particle physics. The Standard Model is a remarkably successful theory of fundamental physics, but it suffers from severe problems. It does not provide an explanation for the origin or stability of the electroweak scale nor for the origin and structure of flavor and CP violation. It predicts vanishing neutrino masses, in disagreement with experimental observations. It also fails to explain the matter-antimatter asymmetry of the universe, and it does not provide a particle candidate for dark matter. In this thesis we provide experimentally testable solutions for most of these problems and we study their phenomenology.

Acknowledgements

In the grand scheme of the human situation, I believe that my journey through graduate school was tremendously easy. What other conclusion might one possibly reach?. I had most of the things that many people in this unfair world do not have; a profoundly loving family, excellent friends and guidance from professionals which exceptional clarity of mind.

Gratefulness is not really what I feel for my family. Instead, I feel that in the complex process of the expansion of the universe, things confabulated in the most unlikely way for me to end up by the sea. It all smells great, I hear everything, it is all good. This is all my mother's and father's work and love, my sister's smiles and my brother's games. This is all yours, all was given to me, I just sat down and grew up. I found nothing but happiness in the equilibrated way of life you showed me. The professional condition cannot be separated from the human one.

The other part of the work was done by those in academia who taught me. Somehow my high school teacher managed to let me see that Newton's laws were nothing trivial, while I was playing soccer with my friends inside the classroom. In college, Viktor Slusarenko, Ivan Schmidt, Claudio Dib in physics and Jaime Glaria, Ricardo Rojas, Marcelo Salgado and others in engineering allowed me to see the beauty in mathematics and physics, and rescued me from a millionaire future as an engineer, to show me a poorer but happier future as a physicist.

At the NHETC, I found all the source of knowledge I needed and all the support from an outstanding group of scientists. My advisor, Scott Thomas, tried to teach me as hard as he could. Most of what he taught me I did it in another way, somehow I am too stubborn, thanks for the patience. All around, besides the valuable technical knowledge and the constant lessons on academic rigor, I learned from him things that will persist as years pass by

Always try to outsmart the calculation

What is that? Write down an equation for that!

Do not be too afraid of being wrong, people are wrong all the time

Finally, Scott had the most valuable quality of an advisor, which is to believe on his student's abilities, supporting him when needed. That did most of the trick.

I also must dedicate some words to David Shih. He invested lots of his time to teach me many of techniques I learned early in my PhD, and supported me during my whole career at the NHETC. From him I also learned my initial lessons on academic precision. I am also very grateful to Nathaniel Craig. He trusted in my abilities, and supported me during the postdoc application season any time I asked him for help. Thanks Nathaniel.

I am very grateful for the constant support that the NHETC provided and in particular to Daniel Friedan. Daniel made sure to provide all the resources within his capabilities for me to have a successful stay at the NHETC, and was the protecting figure any time something extra academic would go wrong. Also I want to thank the Physics Department at Rutgers for providing all the support for summer schools and trips, they were crucial for my academic training.

I also want to thank the postdocs at the NHETC. I learned most of my cosmology knowledge from Chang-Sub Shin and Angelo Monteux. I also enjoyed many discussions with Matthew Baumgart and Marco Farina.

And finally, I want to thank my friends, who were like my family during these great 5 years. Majo, Dani, Pietro, Ana, Miriam, Valia, Vilmi, Eleni, Sebastian, Isidora, Cristina and many others. Without you, I would have still gone through grad school, but it would have been very boring.

In the end, I did not really do much. Somehow I still get to write my name on the title page, and here below.

Daniel Egana-Ugrinovic

New High Energy Theory Center

June 2016

Table of Contents

Abstract ii

Acknowledgements iii

Table of Contents v

List of Figures viii

1 Introduction and Summary 1

2 A complete model for all known and required CP violation 6

2.1 The puzzle of CP violation 6

2.2 Nelson-Barr model and leptonic CP phases 9

2.2.1 The effective theory below the scale $M_A^{D,L}$ 12

2.2.2 The effective theory below the RH neutrino mass scale 15

2.2.3 Supersymmetry breaking and renormalization of $\overline{\theta}$ 16

2.3 Predictions for IR physics 17

2.3.1 Parameter counting using invariants 18

2.3.2 Solving for the unknown model parameters using leptonic data 21

2.3.3 Results and predictions for electroweak scale physics 24

2.4 Predictions for UV physics and thermal leptogenesis 30

2.4.1 Parameter counting using invariants 31

2.4.2 Thermal leptogenesis 34

3 125 GeV Higgs from Tree-level A-terms 41

3.1 Introduction 41

3.2 A non-MFV model 45

3.3 An MFV model . . . 49
3.4 A composite model from Seiberg duality . . . 52
3.4.1 Electric theory . . . 52
3.4.2 Magnetic theory . . . 53
3.4.3 Complete model with spectators . . . 54
3.5 Conclusions of this chapter . . . 57

4 Effective Theory of Higgs Sector Vacuum States 58

4.1 Introduction . . . 58
4.2 A Higgs and a heavy real scalar singlet . . . 61
4.2.1 The model . . . 61
4.2.2 Mass eigenstates and couplings in the mixing language . . . 63
4.2.2.1 Scattering amplitudes . . . 67
4.2.3 The low energy effective theory . . . 69
4.2.3.1 Scattering amplitudes . . . 75
4.3 The two Higgs doublet model . . . 77
4.3.1 Mass eigenstates . . . 83
4.3.1.1 The T conserving case . . . 84
4.3.1.2 The general T violating case . . . 85
4.3.2 Couplings of the Higgs boson . . . 88
4.3.3 Scattering amplitudes . . . 92
4.4 The low energy effective theory of the 2HDM . . . 94
4.4.1 Diagrams and derivation of the EFT . . . 95
4.4.2 The low energy theory of the Higgs doublet . . . 100
4.4.3 The Low energy theory of the Higgs boson . . . 103
4.4.4 Scattering amplitudes . . . 110
4.5 The EFT of the 2HDM with Glashow-Weinberg conditions . . . 111
4.5.1 Type I . . . 112
4.5.2 Type II: $\lambda_1^u = \lambda_2^d = \lambda_2^\ell = 0$ . . . 115
4.5.3 Type III . . . 118
4.5.4 Type IV . . . 120
4.6 T violation in types I-IV 2HDM . . . 122
4.7 The electron EDM . . . 126

4.8 Conclusions of this chapter 128

5 Conclusions and Outlook **134**

Appendices

A Flavor invariants **137**

A.1 Flavor Invariants in the Standard Model 137

A.2 Flavor Invariants in a type I seesaw model 144

B The little A/m^2 problem for arbitrary couplings **147**

C EDM functions **149**

D Solution to the EWSB condition for the condensate phase ξ in the $\mathbb{Z}_2$ symmetric limit **151**

Bibliography **153**

List of Figures

2.1 The puzzle of CP violation 9

2.2 Tree level contribution to wave function renormalization 12

2.3 Mixing angles as a function of the lightest neutrino mass 25

2.4 CP violating phases and mixing angles 28

2.5 CP violating phases and mixing angles with improved measurements 29

2.6 CP violating phases and mixing angles leading to correct sign of baryon asymmetry . . 30

2.7 Correlations in predictions for the leptonic sector 31

2.8 Correlations in predictions for the leptonic sector with improved measurements 32

2.9 Correlations in predictions for the leptonic sector with correct sign of baryon asymmetry 33

2.10 Right handed neutrino mass and baryon asymmetry 39

2.11 Correlation between the baryon asymmetry and predictions for the PMNS phases 39

2.12 Correlation between the right handed neutrino mass needed for baryogenesis and predictions for the PMNS phases 40

3.1 Contours of the Higgs mass in the $(A_t, m_{\tilde{t}_1})$ plane in an NMFV model 47

3.2 Typical spectrum in an NMFV model 48

3.3 Contours of the Higgs mass in the $(A_t, m_{\tilde{t}_1})$ plane in an MFV model 51

3.4 Typical spectrum in an MFV model 52

4.1 At dimension four and six generates the operators $(H^\dagger H)^2$ and $\partial_\mu(H^\dagger H)\partial^\mu(H^\dagger H)$. . . . 71

4.2 At dimension six generates the operator $(H^\dagger H)^3$. 71

4.3 At dimension six generates the operator $(H^\dagger H)^3$. 71

4.4 At dimension eight generates the operator $(H^\dagger H)^4$. This diagrams represents the leading order correction in λ_S, and is considered only for illustrative purposes. 71

4.5 Diagrams with two m_{12}^2 insertions and gauge boson legs 96

4.6 Diagrams with two λ_6 insertions and gauge boson legs 97
4.7 Diagrams with one λ_6 and one $(\tilde{m}^2_{12})^*$ insertion 98
4.8 Diagrams with a $\tilde{\lambda}_3$ vertex 99
4.9 Diagrams with one Yukawa 100
4.10 Diagrams with two Yukawas 101
4.11 Limits on effective dimension six CP violating phase 128
4.12 Limits on the Higgs potential CP violating combination 129
4.13 Limits on the CP violating effective top Yukawa 130
4.14 Limits on the CP violating effective tau Yukawa 131

Chapter 1

Introduction and Summary

The completion of the Standard Model of particle physics (SM) with the discovery of the Higgs boson [1, 2] and the success of the standard model of Big Bang cosmology (ΛCDM) opened a new era for fundamental physics. Both the SM and ΛCDM are tremendously successful models, but they fail to explain the origin of the electroweak (EW) scale, the flavor and CP violating structure of the SM, the origin of the matter-antimatter asymmetry and the particle nature of dark matter. It is remarkable that in the next few years, the experimental program of particle physics and cosmology might intersect with the phenomenology of the proposed theoretical solutions of all these problems. In this work we study possible solutions to these problems which are within reach of current or proposed experiments.

The Standard Model is is a Quantum Field Theory (QFT). QFT is the most successful theoretical framework to describe fundamental physics to date. As an example, the SM correctly describes the measured decay rates of all known elementary and composite particles with an unmatched precision which in some cases, as in the rare decay of B_s mesons to muons, are as small as a part in a billion [3]. Another remarkable example is the SM prediction for the magnetic moment of the electron, which has been calculated to tenth order in an expansion in the electric coupling [4], and is consistent with the experimental measurement to one part in one billion [5]. The SM is also consistent with the cosmology of the early universe. As an example, together with the standard model of Big Bang cosmology, it provides consistent predictions for the primordial abundance of light elements D,[3] He,[4] He and ^{7}Li, which span nine orders of magnitude from ^{4}He/H ~ 0.08 to ^{7}Li/H $\sim 10^{-10}$ and were synthesized only a few minutes after the Big Bang [6].

The SM, however, has severe consistency problems. In the modern understanding the Standard Model is an effective theory in the Wilsonian sense [7]. There are two intrinsic energy scales in the

Standard Model, which are the QCD confinement scale $\Lambda_{\rm QCD} \sim 220\,\text{MeV}$ and the electroweak scale which here will be parametrized by the Higgs mass $m_H = 125\,\text{GeV}$. The next fundamental scale is the Planck scale, $M_P = 1.22 \times 10^{19}\,\text{GeV}$, which is wildly separated from the electroweak scale. In effective field theory, a theory with validity up to the Planck scale should provide a microscopic description for the origin and stability under quantum corrections of the smaller energy scales in the theory. As an example, the QCD confinement scale is elegantly explained in our current theory by a mechanism called dimensional transmutation, which provides a dynamical connection between the dimensionless strong coupling constant and the QCD scale, and explains its smallness with respect to the electroweak scale. In the SM there is no such dynamical mechanism nor a symmetry to explain the smallness of the Higgs mass with respect to the Planck mass. Without extremely precise cancellations between parameters in the theory, the dynamics of the microscopic theory would naturally drive the electroweak scale, together with the Higgs mass, to values close to the Planck scale, in strong disagreement with experimental data. If the cancellations are not enforced by a reason, as an underlying symmetry, the parameters of the theory must be "unnaturally" tuned to provide these cancellations. This is the problem of the origin and stability of the electroweak scale, which is usually called the "Hierarchy Problem" [8].

A possible solution for the Hierarchy Problem is supersymmetry [9, 10]. In supersymmetry, fermions and bosons are related by the action of the supersymmetry group generators. In supersymmetry, the smallness of the Higgs mass with respect to the Planck is related to the smallness of the mass of its fermionic partners, which may be explained on symmetry grounds. If supersymmetry is only broken softly (*i.e.*, it is preserved at high energies), the stability of the electroweak scale under renormalization to higher scales is due to the non-renormalization theorem of supersymmetric theories [11, 12], which protects certain quantities from perturbative radiative corrections. The precise origin of the electroweak scale can be explained with a microscopic mechanism of supersymmetry breaking, which then could dynamically induce EWSB at a small scale. Supersymmetry also provides new particles that can be dark matter candidates.

Nature is, however, not supersymmetric. As a consequence, a phenomenologically viable mechanism for supersymmetry breaking is needed. This is a particularly delicate issue for flavor physics. Supersymmetry breaking parameters generically induce flavor changing processes which are strongly constrained by experiments. For this reason, a particularly attractive model for supersymmetry breaking is gauge mediated supersymmetry breaking (GMSB). A review of GMSB can be found in [13]. Gauge interactions are flavor blind so they cannot lead to flavor violating processes. Unfortunately, the simplest untuned models of gauge mediation are inconsistent with the value of the

Higgs mass [14]. It is pressing to build models which retain the main features of GMSB, while being consistent with the Higgs mass and avoiding the reintroduction of the Hierarchy Problem. In this work we address this issue and present the possibly simplest extension of GMSB which satisfies these criterions [15, 16].

The problem of the flavor structure and of the microscopic origin of CP violation in the Standard Model are also two of the most important issues in fundamental physics. The masses of the quark and lepton sector seem hierarchical, but we have no explanation for this fact, and neither do we have an explanation for the origin of neutrino masses. In addition, the structure of flavor and CP violation are related in the Standard Model; in our current understanding, both flavor CP violation are contained in the CKM [17, 18] and PMNS [19, 20] matrices. We have no explanation for the origin of these matrices. And intriguingly, CP violation in the strong interactions (the "strong CP phase") is allowed by all symmetries, but is experimentally constrained to be less than one part in a billion from measurements of the neutron electric dipole moment [21]. This is the so called strong CP problem. Finally, CP violation is a crucial component for explaining the excess of matter over antimatter in the universe. The Standard Model, however, does not contain enough CP violation to account for this excess, which is yet another indication that our theory is incomplete.

All these problems might be related to each other, in what we call in this work "the puzzle of CP violation". Supersymmetry might play an important role in this puzzle. If a microscopic model is built that is consistent with the flavor and CP structure of the Standard Model, supersymmetry preserves this structure down to accessible energy scales thanks to the non-renormalization theorem. In this thesis we present a complete, calculable, predictive and experimentally testable supersymmetric model for all known and required CP violation in nature, which represents a full solution to the puzzle of CP violation. The model explains all flavor mixing and CP violation spontaneously, through condensates of so called Barr-Nelson fields, while it explains the origin of neutrino masses through mixing with right handed neutrinos. Making use of the model background symmetries, it is possible to impose all known data on the parameter space, and derive precise predictions for the lightest neutrino mass and all the CP violating phases of the PMNS matrix, which have not been measured. As a consequence, the model might be experimentally confirmed or falsified.

The models which will be presented in this work, as well as many other extensions of the Standard Model, possess characteristic phenomenological features that may be experimentally probed. In particular, most extensions of the Standard Model, including supersymmetry, have extended Higgs sectors. Extended Higgs sectors contain additional Higgs particles, *i.e.*, new scalar particles with no quantum numbers near the electroweak scale. These new vacuum states can mix with the Higgs

boson, modify the Standard Model predictions for its interactions, and lead to new signatures at colliders or other types of experiments. In particular, the Higgs sector of all supersymmetric models contain at least one additional SU(2) Higgs doublet [22]. These kind of extensions of the Higgs sector are called "Two Higgs Doublet Models" (2HDM). Two Higgs Doublet Models are not only interesting for supersymmetry, but also are interesting for electroweak baryogenesis [23] and axion models [24, 25], to name a few additional motivations. Moreover, they fall into a very constrained class of theories of extended Higgs sectors that are consistent with electroweak precision tests by construction, since they do not modify the Standard Model prediction for the ρ parameter at tree level [26], which is defined as

$$\rho = \frac{m_W^2}{m_Z^2 \cos\theta_W} \tag{1.0.1}$$

where θ_W is the Weinberg angle. In the Standard Model at tree level $\rho = 1$, consistent with the measured experimental value $\rho = 1.0008^{+0.0017}_{-0.007}$.

The Higgs sector has already been partially probed at colliders [27–29] and no new physics has been found. This suggests that if additional Higgs particles exists, they are likely to be heavier than the Higgs boson, such that by decoupling its effects in the Standard Model Higgs sector are suppressed. The most powerful available tool to analyze new physics near the decoupling limit is wilsonian effective field theory. In this thesis we present a complete analysis of the tree level low energy effective theory of the 2HDM. We identify all the effects in the low energy theory that might be seen at colliders or low energy experiments, classifying the modifications to the Higgs interactions by a concept of effective operator dimension, and organizing all flavor and CP violating effects in the same way.

One of the main outputs of the effective field theory analysis, is that we find that the main types of 2HDM studied in the literature including the ones corresponding to supersymmetric theories, *i.e.* 2HDM with Glashow Weinberg conditions, [30], contain only one CP violating phase at leading order in an operator expansion. This CP violating phase can be constrained by current measurements of the electron electric dipole moment, so we finally present in this work a complete study of the limits in all the types of 2HDM with Glashow Weinberg conditions.

The topics in this thesis are presented from microscopic physics to larger scales. In chapter 2 we start with a supersymmetric effective theory which is a full solution to the puzzle of CP violation. The model is valid up to energies near the unification scale 10^{15} GeV. The model explains the baryon asymmetry of the universe and provides a mechanism for neutrino masses. Supersymmetry provides a solution to the hierarchy problem, and a detailed model of gauge mediated supersymmetry breaking

at energy scales of 100 TeV consistent with the Higgs mass, is presented in section 3. Supersymmetry also provides a motivation to study extensions of the Higgs sector around the TeV scale, and the complete organization of extended Higgs sectors within effective field theory at tree level is presented in chapter 4. The operator analysis of extended Higgs sectors identifies novel CP violating effects at low energies, and a detailed study of CP violation at energy scales of the electron is presented in the same chapter. Further technical details are left for appendices. The phenomena covered in this thesis span twenty-four orders of magnitude in energy, from the unification scale down to scale of the neutrino masses.

Chapter 2

A complete model for all known and required CP violation

2.1 The puzzle of CP violation

There is a CP puzzle in the Standard model and many of its extensions. In the quark sector of the Standard Model there is a large CP violating phase in the CKM matrix, and its effects on experimental observables depend on the flavor structure of the quark sector [17] [18] [31]. In particular, its effects are heavily suppressed by quark mixing angles. Neither the origin of the CP violating phase nor the origin of the flavor structure of the quark sector may be understood within the framework of the Standard Model. Moreover, once the Standard Model is extended to allow for neutrino masses, there are additional CP violating phases in the PMNS matrix of the lepton sector [19] [20], which lead to effects that depend on the flavor structure of the lepton sector. Neither the origin of neutrino masses nor of the flavor structure of the lepton sector is understood within the Standard Model. Moreover, even if there is experimentally confirmed CP violation in the CKM matrix, CP violation is experimentally absent from all experiments testing CP violation in $SU(3)_C$ interactions. $SU(3)_C$ interactions allow for a CP violating parameter $\overline{\theta}$ in the QCD Lagrangian term $\frac{i\overline{\theta}}{32\pi^2}G_{\mu\nu}\tilde{G}^{\mu\nu}$. Current limits on electric dipole moments of the neutron [21] set a strong constraint on CP violation in the strong interactions, $\overline{\theta} < 10^{-10}$. No symmetry or dynamical reason in the Standard Model can explain the smallness of this parameter. This is commonly referred to as the *strong CP problem*. Finally, CP violation is one of the three Sakharov conditions needed for baryogenesis [32], so it is crucial for the cosmological evolution of our universe. The Standard Model, however, does not contain enough CP violation to explain the asymmetry in our universe.

The origin of CP violation in the quark and lepton sector, its relation to the flavor structure of the quark and lepton sectors, the absence in CP violation in the strong interactions and the needed CP violation to explain the baryon asymmetry in the universe, might all be related in a puzzle of CP violation, and might all have a common microscopic explanation. A schematic depiction of the puzzle of CP violation and the relations between its different components is provided in figure 2.1.

Different classes of solutions aim to explain the strong CP problem, which is one of the parts of the puzzle of CP violation. The Peccei-Quinn mechanism [24, 25] introduces an anomalous $U(1)_{PQ}$ symmetry, a low-energy remnant of which is the QCD axion, which has not been observed in experiments. A different class of solutions, first introduced by Nelson [33] and Barr [34], aims to solve the strong CP problem and to provide an explanation for the origin of CP violation in the quark sector. Here, at a high scale the theory is CP-conserving, that is, $\overline{\theta} = 0$ and all parameters in the Lagrangian are real, *i.e.*, there is no explicit CP violation. CP violation is only spontaneously broken at lower scales, and is communicated to the quark sector without inducing a strong CP phase. A minimal model useful to understand the Nelson-Barr (NB) mechanism was introduced in Ref. [35]. In this model, in addition to the SM fields, a set of neutral scalar field S_a and vector-like down-type quarks $D + \overline{D}$ are introduced with the following interactions:

$$M D\overline{D} + \kappa_{aj} S_a D\overline{d}_j + \lambda^d_{ij} Q_i H \overline{d}_j + \dots \tag{2.1.1}$$

where the dots represent CP conserving SM like interactions, as well as the potential for the fields S_a. For what concerns the latter, it just needs to produce complex vev's $\langle S_a \rangle$, and a generic polynomial potential is satisfactory. Below the scale of spontaneous CP violation, which we call the Nelson-Barr scale, the physical QCD vacuum angle is given by

$$i\overline{\theta} = i\mathrm{Arg}\left(\det M_d\right) = i\mathrm{Arg}\begin{vmatrix} \lambda^d_{ij} v_d & \kappa_{ai}\langle S_a\rangle \\ 0 & M \end{vmatrix} \tag{2.1.2}$$

where we have already set to zero the "bare" angle θ and $\mathrm{Arg}\det m_u$, which vanishes because the high-energy theory is CP-conserving. Because M_d is a triangular matrix with real elements on the diagonal, its determinant is real and $\overline{\theta}$ vanishes. Moreover, there is mixing between the light and heavy down-type quarks, meaning that at low energies the 3×3 down-type Yukawa matrix will have complex components.

In non-supersymmetric versions of the Nelson-Barr mechanism, there are contributions to $\overline{\theta}$ both at tree-level, coming from non-renormalizable operators (such as $S^\dagger_a S^b \overline{D} D$), as well as radiatively, via four-scalar interactions (such as $S_a S_b H^\dagger H$ or $S^\dagger_a S^\dagger_b S_c S_d$) which cannot be forbidden by any

symmetry compatible with the Lagrangian (2.1.1). This implies a relatively low scale for the CP-breaking scale, $M < 10^8$ GeV, too low to account for the CP-violating phases needed for thermal leptogenesis. For this reason, we require the model to be supersymmetric at high energies: with supersymmetry, such non-holomorphic operators are forbidden. There are potentially large loop corrections to $\overline{\theta}$ that involve soft squark masses [36–38], but those can be avoided in the case of degeneracy and proportionality of the soft masses, such as in low-scale gauge mediation, which we will require.

The simple supersymmetric Nelson-Barr solution to the strong CP problem is the starting point for finding a complete solution to the whole puzzle of CP violation. In Nelson-Barr models CP violation in the quark sector, which is part of the puzzle, is originated spontaneously. Since the flavor structure of the quark and lepton sectors, and the origin of CP violation in the lepton sector are the remaining parts of the puzzle, we extend the simple supersymmetric Nelson-Barr model so that all *known and required CP violation and flavor mixing* are originated spontaneously. In our model, baryogenesis is achieved via thermal leptogenesis due to out of equilibrium decays of right handed neutrinos. In order to introduce CP-violation in the leptonic sector, we extend the model of Eq. (2.1.1) to the leptonic sector by introducing a vector-like $\mathbf{5} + \overline{\mathbf{5}}$ multiplet and considering GUT-unified couplings of the Standard Model $\mathbf{5}_i = (\overline{d}_i, L_i)$ multiplet to the NB sector. Thus, the CP violating phases and part of the flavor structure and mass hierarchies of the leptonic sector are related to the ones in the quark sector by an unification Ansatz.

Common numerical techniques to analyze the parameter space of our model are not adequate, due to the complexity of the flavor structure in the Standard Model. For this reason, we proceed analytically by presenting a full list of polynomial flavor invariants for the quark and lepton sector. Polynomial flavor invariants are useful tools to describe flavor physics and CP violation. Using flavor invariants, we are able to show that all the relevant parameters for low energy physics in our model can be fixed from known data, so that the model is able to not only realize all observed low energy phenomena, but also to give strong predictions on the parameters of the lepton sector that have not yet been measured. In particular, we show that the model reproduces quark and lepton masses and mixing angles, predicts the leptonic CP phases in the PMNS matrix, predicts the mass of the lightest neutrino to be in a very narrow range between 10^{-2}meV and 10^{-3}meV, solves the strong CP problem, for given right handed neutrino masses predicts the CP violating phases required for leptogenesis entirely from low energy data and reproduces the observed baryon asymmetry through thermal leptogenesis. The precision of the predictions depend entirely on the precision of current measurements of quark and lepton masses and mixing angles.

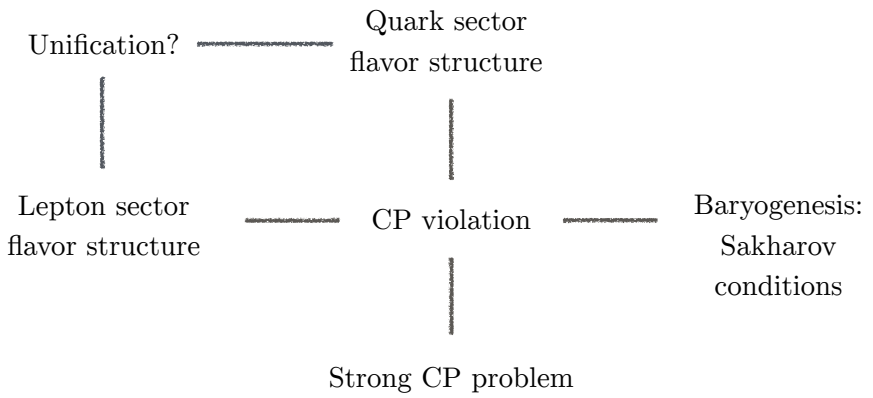

Figure 2.1: The puzzle of CP violation. In the quark sector, CP violation is contained in the CKM phase and its effects depend on its flavor structure. In the lepton sector, CP violation is contained in the PMNS matrix, and its effects depend on its flavor structure, so CP violation may also be related with the problem of the origin of neutrino masses. CP violation in the lepton and quark sector may be related through unification. CP violation is also fundamental for baryogenesis, and finally, it represents a problem for explaining the experimentally absent strong CP phase.

The outline of this chapter is as follows. In Section 2.2, we introduce our model, a supersymmetric version of Eq. (2.1.1) with GUT-unified couplings between the NB sector and the MSSM fields. Then, we systematically investigate the physics form the UV to the IR, describing the effective field theories at each scale and finding non-trivial conditions for the couplings in the EFT arising from the unification Ansatz. In Section 2.3, we solve for the model parameters in terms of observed IR data, such as fermion masses and mixing angles. In addition, we are able to solve for unobserved parameters such as the lightest neutrino mass and the CP phases in the PMNS matrix, which are predictions of our model. In Section 2.4 we turn our attention to physics at the RH neutrino mass scale: we discuss the Boltzmann equations that describe leptogenesis and find the final asymmetry as a function of known IR observables and the RH neutrino masses. Appendix A contains a technical discussion of flavor invariants.

2.2 Nelson-Barr model and leptonic CP phases

We begin by describing the supersymmetric model. In this section we do not consider any supersymmetry breaking effects. A short discussion of supersymmetry breaking is postponed to section (2.2.3), and a full discussion of a gauge mediated supersymmetry breaking mechanism is postponed

to section 3. We consider the field content of a supersymmetric type I seesaw model, with three RH neutrinos N_1, N_2, N_3 which are SM singlets. We also add singlet fields S_{jA}, $A = 1, 2$, $j = 1, 2, 3$ which are called Nelson-Barr fields and two vector-like matter $SU(5)$ GUT multiplets $5_A + \overline{5}_A$, $A = 1, 2$. The setup requires two families GUT multiplets for reasons that will be discussed later. The components of the vector like pair are defined as

$$5_A = (D_A, \overline{L}_A), \qquad \overline{5}_A = (\overline{D}_A, L_A). \tag{2.2.1}$$

The Nelson-Barr fields have complex expectation values $\langle S_{jA} \rangle$ which spontaneously break CP at a scale which we call the Nelson-Barr scale M_{CP}. This is the only source of CP breaking in the whole theory. We take the Nelson-Barr scale to be much larger than the electroweak scale, but below the unification scale. The masses of the vector like fields are also at the Nelson-Barr scale.

We now describe the interactions. At the unification scale we consider a canonical Kähler potential for simplicity. Dropping one loop corrections, the Kähler potential at the Nelson-Barr scale is also canonical[1].

The superpotential at the Nelson-Barr scale is given by

$$\begin{aligned} &\tilde{\lambda}^d_{ij}\ Q_i H_d \overline{d}_j - \tilde{\lambda}^u_{ij}\ Q_i H_u \overline{u}_j - \tilde{\lambda}^\ell_{ij}\ L_i H_d \overline{\ell}_j + \mu H_u H_d, \\ &- \tilde{\lambda}^N_{ij}\ L_i H_u N_j + \frac{1}{2} M_{ij} N_i N_j \\ &+\ M^{D,L}_{AB} \Big[D_A \overline{D}_B + L_A \overline{L}_B \Big] + \lambda\, S_{jA} \Big[D_A \overline{d}_j + \overline{L}_A L_j \Big] \end{aligned} \tag{2.2.2}$$

Note that in the last line of (2.2.2), we have imposed a unification *Ansatz* for the interactions of the heavy vector-like matter fields. Note also that the superpotential (2.2.2) contains basically the interactions of a supersymmetric type I seesaw model, plus a mass for the vector like matter fields, and Yukawas for the Nelson-Barr fields.

We dedicate the rest of this section to describe the superpotential, its parameters and the Nelson-Barr mechanism. The lagrangian has a $U(3)_Q \times U(3)_{\overline{u}} \times U(3)_{\overline{d}} \times U(3)_L \times U(3)_{\overline{\ell}} \times U(3)_N$ flavor background symmetry, which corresponds to the background symmetry of a type I seesaw model.

The Nelson-Barr mechanism to solve the strong CP problem is implemented as follows. We impose CP to be a symmetry of the Lagrangian. As a consequence, all couplings in (2.2.2) can be taken to be real in some flavor basis. We also impose that the Higgs condensate does not break CP spontaneously,

$$\langle H_u^\dagger H_u \rangle = v_u^2, \qquad \langle H_d^\dagger H_d \rangle = v_d^2, \qquad \mathrm{Arg}\langle H_u H_d \rangle = 0, \pi. \tag{2.2.3}$$

[1] Adding one loop corrections does not significantly affect the discussion, because the corrections are mainly coming from gauge loops and are flavor blind, so the flavor structure of the model to be presented is left unmodified. A more detailed discussion is left for future work.

We allow for CP to be broken only spontaneously by the Nelson-Barr fields. We remain agnostic about the origin of the Nelson-Barr condensate, examples on how to spontaneously break CP through singlet condensates are available in the literature [38] . We treat the S_{jA} fields as flavor and CP breaking spurions and define

$$\zeta_{jA} \equiv \lambda \langle S_{jA} \rangle \tag{2.2.4}$$

The above structure of CP breaking leads to a vanishing $SU(3)_C$ vacuum angle, as we now show. At tree level, the physical $SU(3)_C$ vacuum angle of the supersymmetric theory is given by

$$i\overline{\theta} = i\mathrm{Arg}\big(e^{i\theta} \det m_u \det M_d \big)$$

where θ is the unphysical, basis dependent theta angle in the Lagrangian and

$$m_u = \tilde{\lambda}^u v_u \qquad M_d = \begin{pmatrix} \tilde{\lambda}^d v_d & \zeta \\ 0 & M^{D,L}_{AB} \end{pmatrix} \tag{2.2.5}$$

Since CP is a symmetry of the Lagrangian, the bare theta angle is zero, $\theta = 0$ and $\tilde{\lambda}^u, v_d, M^{D,L}$ are real, so at tree level the physical theta angle is zero $\overline{\theta} = 0$. All CP violation is contained in ζ, which does not affect $\overline{\theta}$. This is the Nelson-Barr solution of the strong CP problem [33, 34, 39]. Note that due to supersymmetric non-renormalization, $\overline{\theta}$ remains zero at all orders of perturbation theory.

The MSSM Yukawas are not explicitly unified, but the vector like pair $5_A + \overline{5}_A$ has an $SU(5)$ unified mass term. It also has an $SU(5)$ unified marginal interaction with the MSSM $SU(5)$ multiplet $\overline{5}_j = (\overline{d}_j, L_j)$ and Nelson-Barr fields. This unification Ansatz is an important part of our model.

In addition to the unification Ansatz, we also consider that *all flavor mixing is is induced by interaction with the Nelson-Barr sector*, such that for $\langle S_{jA} \rangle = 0$ there is no flavor mixing. This Ansatz can be naturally obtained in UV completions with horizontal symmetries, and it is super-technically natural so it is protected. From the perspective of the flavor symmetries, it means that we can work in a flavor basis in which all the couplings not involving Nelson-Barr fields can be simultaneously diagonalized

$$\tilde{\lambda}^f_{ij} = \delta_{ij}\, \tilde{\lambda}^f_i \qquad M_{ij} = \delta_{ij}\, M_i \tag{2.2.6}$$

where $f = d, u, \ell, N$ and all entries along the diagonals are real, since CP is only spontaneously broken. Also, without loss of generality we can work in a basis where the vector like mass matrix $M^{D,L}_{AB}$ is diagonal

$$M^{D,L}_{AC} = \delta_{AC} M^{D,L}_C \tag{2.2.7}$$

where no sum over C is intended.

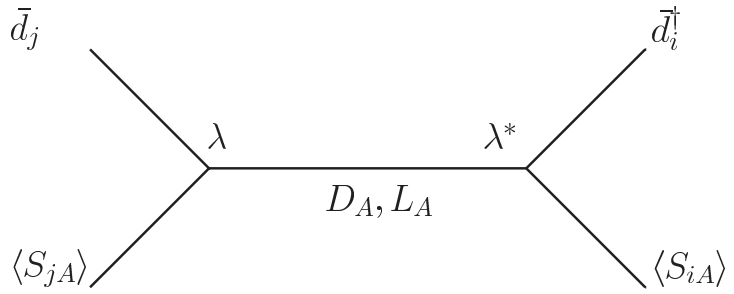

Figure 2.2: Integrating out the vector like fields D_A, L_A lead to wave function renormalization for the superfields $\overline{d}_i$ and L_i. The unification condition ensures that the wave function renormalization matrices for $\overline{d}_i$ and L_i are the same.

Note that from the perspective of the flavor symmetries, the unification Ansatz and the conditions (2.2.6) for the origin of flavor mixing, mean that in our model, there exists a basis in which the couplings of the Nelson-Barr fields to $\overline{d}_j$ and L_j are the same *and* all the couplings in (2.2.6) are diagonal and real. This basis is unique: any transformation acting on L_j would make either the RH neutrino Yukawa or the RH neutrino mass complex. Any transformation acting on $\overline{d}_j$ without acting on L_j at the same time would break the unification Ansatz. Finally, any transformation acting on $\overline{u}_j$ would make the up type quark Yukawa complex.

Finally, the mass scales are taken as follows. We consider the masses of the vector like pairs $M_1^{D,L}, M_2^{D,L}$ to be at the Nelson-Barr scale,

$$M_{CP} \sim M_1^{D,L} \sim M_2^{D,L} \sim \zeta_{j1} \sim \zeta_{j2} \tag{2.2.8}$$

This is a coincidence of scales that may be realized dynamically, and it will not be discussed here for brevity. In order to consider leptogenesis via out-of-equilibrium decay to the RH neutrinos, the masses of the vector like fields $M_A^{D,L}$ are assumed to be larger than M_1, M_2, M_3. We also consider hierarchical RH neutrinos $M_2, M_3 > M_1$, as in the simplest thermal leptogenesis setup [40].

2.2.1 The effective theory below the scale $M_A^{D,L}$

We now derive the effective theory at energies below the scale $M^{D,L}$ by integrating out the heavy vector like multiplet at tree level. In the large $M^{D,L}$ limit, the equations of motion for the vector like fields give

$$\overline{5}_A = -\left[\frac{\zeta_{jA}}{M_A^{D,L}}\right]\overline{5}_j \qquad\qquad M_A^{D,L} 5_A = 0 \tag{2.2.9}$$

where we sum over j, but no sum over A is intended and ζ is given by (2.2.4).

Using the field equations (2.2.9) in the superpotential (2.2.2), we get the effective superpotential

$$\begin{aligned}&\tilde{\lambda}^d_{ij}\ Q_i H_d \overline{d}_j - \tilde{\lambda}^u_{ij}\ Q_i H_u \overline{u}_j - \tilde{\lambda}^\ell_{ij}\ L_i H_d \overline{\ell}_j + \mu H_u H_d \\ &- \tilde{\lambda}^N_{ij}\ L_i H_u N_j + \frac{1}{2} M_{ij} N_i N_j \end{aligned} \tag{2.2.10}$$

with all real couplings. The low energy Kähler potential can be obtained by using the equations of motion (2.2.9) in the canonical UV potential. The result is

$$\begin{aligned}&\mathcal{Z}^d_{ij}\ \overline{d}^\dagger_i \overline{d}_j + \mathcal{Z}^L_{ij}\ L^\dagger_i L_j + Q^\dagger_i Q_i + \overline{u}^\dagger_i \overline{u}_i + \overline{\ell}^\dagger_i \overline{\ell}_i \\ &\qquad + N^\dagger_i N_i + H^\dagger_u H_u + H^\dagger_d H_d \end{aligned} \tag{2.2.11}$$

where the hermitian wave function renormalization matrices are

$$\mathcal{Z}^d_{ij} = \mathcal{Z}^L_{ij} = \mathcal{Z}^{\text{tree}}_{ij} \tag{2.2.12}$$

$\mathcal{Z}^{\text{tree}}$ includes the identity piece of the wave function renormalization matrix and the tree level contribution to wave function renormalization from integrating out the heavy GUT multiplets, as represented in figure 2.2. $\mathcal{Z}^{\text{tree}}$ is given by

$$\mathcal{Z}^{\text{tree}}_{ij} = \delta_{ij} + \frac{\zeta_{iA}\zeta^*_{jA}}{\left(M^{D,L}_A\right)^2} \tag{2.2.13}$$

$\mathcal{Z}^{\text{tree}}$ is the only source of CP violation in the low energy theory. Note from the definition of the spurion ζ (2.2.4), that in the limit $\left|\langle S_{jA}\rangle\right| \ll M^{D,L}_A$ and holding λ, we get $|\zeta_{jA}| \ll M^{D,L}_A$. In this limit $\mathcal{Z}^{\text{tree}}$ vanishes, and there is no observable CP violation in the effective theory. In this limit, the model fails to accommodate the CP violating phase in the CKM matrix and the observed baryon asymmetry. In order to get large CP violation in the effective theory we take $\left|\langle S_{jA}\rangle\right| \sim M^{D,L}_A$. Moreover, by direct calculation of the Jarlskog invariant in the IR theory, it may be shown that the CKM phase of the low energy theory is non vanishing only if the volume

$$\text{Im}\left[\mathcal{Z}^{\text{tree}}_{12}\,\mathcal{Z}^{\text{tree}*}_{13}\,\mathcal{Z}^{\text{tree}}_{23}\right] \tag{2.2.14}$$

is non vanishing. If one considers only one family of GUT multiplets $5_A, \overline{5}_A$ the off diagonal terms of the wave function renormalization matrix $\mathcal{Z}^{\text{tree}}$ form a bivector, and the volume form (2.2.14) vanishes. A minimum of two families of GUT multiplets are needed for non-vanishing volume (2.2.14), and for a non-vanishing CKM phase.

Note that there is a unique flavor basis in which the Ansatz that the Yukawas of the UV completion and the RH neutrino mass matrix are real and diagonal, and the wave function renormalization matrix for $\overline{d}$ and L is the same from unification. The proof is by contradiction. Assume there is a

$U(3)_N \times U(3)_L \times U(3)_\ell \times U(3)_{\overline{d}} \times U(3)_Q \times U(3)_{\overline{u}}$ flavor transformation different from the identity that takes us to a new basis in which the aforementioned Ansatz hold. The $U(3)_N$ part of the transformation would make the RH neutrino mass matrix off diagonal and/or complex, so it must be set to the identity. As a consequence, we must also set the $U(3)_L$ part of the transformation to the identity, since any $U(3)_L$ transformation would make the RH neutrino Yukawas off diagonal and/or complex. Now, the $U(3)_\ell$ part of the transformation would make the lepton Yukawas off diagonal and/or complex, so it must also must be set to one. The unification Ansatz forces us to set the $U(3)_{\overline{d}}$ transformation equal to the $U(3)_L$ transformation, so it is also set to the identity. As a consequence, the $U(3)_Q$ transformation must be set to one, to keep the down type quark Yukawa real and diagonal. Finally, this also enforces the $U(3)_{\overline{u}}$ part of the transformation to be the identity, to keep the up type Yukawa real and diagonal, completing the proof. This means that we cannot perform any flavor transformation to get rid of Lagrangian parameters in our model, so the nine elements of the wave function renormalization matrix, the nine elements of the real diagonal Yukawas, and the three RH neutrino masses are the complete set of twenty-one independent physical parameters in the quark and lepton sector of our theory. Below the energy scale of the three RH neutrino masses, there are only eighteen independent physical parameters in the quark and lepton sector.

We now make the Kähler potential canonical by the field redefinitions

$$\Phi \;=\; \sqrt{\mathcal{Z}^\Phi}\,\Phi' \qquad\qquad \Phi = \overline{d}, L \tag{2.2.15}$$

The field redefinitions affect the superpotential. Using (4.4.26) in (2.2.10) and dropping the primes we get the low energy effective superpotential

$$\begin{aligned} &\lambda^d_{ij}\; Q_i H_d \overline{d}_j - \lambda^u_{ij}\; Q_i H_u \overline{u}_j - \lambda^\ell_{ij}\; L_i H_d \overline{\ell}_j + \mu H_u H_d \\ &- \lambda^N_{ij}\; L_i H_u N_j + \frac{1}{2} M_{ij} N_i N_j \end{aligned} \tag{2.2.16}$$

with Yukawa couplings

$$\begin{aligned} \lambda^d_{ij} &= \left[\left(\mathcal{Z}^d\right)^{-1/2}\right]_{kj} \tilde{\lambda}^d_{ik} = \left[\left(\mathcal{Z}^{\text{tree}}\right)^{-1/2}\right]_{kj} \tilde{\lambda}^d_{ik} \\ \lambda^\ell_{ij} &= \left[\left(\mathcal{Z}^L\right)^{-1/2}\right]_{ki} \tilde{\lambda}^\ell_{kj} = \left[\left(\mathcal{Z}^{\text{tree}}\right)^{-1/2}\right]_{ki} \tilde{\lambda}^\ell_{ik} \\ \lambda^N_{ij} &= \left[\left(\mathcal{Z}^L\right)^{-1/2}\right]_{ki} \tilde{\lambda}^N_{kj} = \left[\left(\mathcal{Z}^{\text{tree}}\right)^{-1/2}\right]_{ki} \tilde{\lambda}^N_{ik} \\ \lambda^u_{ij} &= \tilde{\lambda}^u_{ij}. \end{aligned} \tag{2.2.17}$$

where in the second equality in each line we made use of the (2.2.12).

The matrices $\tilde{\lambda}^d, \tilde{\lambda}^\ell, \tilde{\lambda}^N$, $\tilde{\lambda}^u$ and M_{ij} are diagonal, real matrices as specified in (2.2.6). The expression for the Yukawas (2.2.17) may be translated into non-trivial conditions for the low energy

theory. The first condition is that the $SU(3)_C$ vacuum angle vanishes,

$$\overline{\theta} = \mathrm{Arg}\,\mathrm{det}(\lambda_u \lambda_d) = -\frac{1}{2}\mathrm{Arg}\,\mathrm{det}(\mathcal{Z}^d) + \mathrm{Arg}\,\mathrm{det}(\tilde{\lambda}_u \tilde{\lambda}_d) = 0 \tag{2.2.18}$$

where we used the reality of $\tilde{\lambda}_u, \tilde{\lambda}_d$ and the hermiticity of the wave function renormalization matrices. This is the low energy description of the Nelson-Barr mechanism. Supersymmetry ensures that (2.2.18) is an exact result to all orders of perturbation theory. The second condition is that the leptonic Yukawas are related to the down type Yukawas by

$$\lambda^\ell = (\lambda^d)^T \Gamma^\ell, \qquad \lambda^N = \lambda^{dT} \Gamma^N. \tag{2.2.19}$$

where Γ^ℓ and Γ^N are diagonal, real matrices. In terms of couplings of the UV completion they are given by

$$\Gamma^\ell_{ij} = \left[\left(\tilde{\lambda^d}\right)^{-1} \tilde{\lambda}^\ell\right]_{ij} \tag{2.2.20}$$

$$\Gamma^N_{ij} = \left[\left(\tilde{\lambda^d}\right)^{-1} \tilde{\lambda}^N\right]_{ij}. \tag{2.2.21}$$

The conditions (2.2.18) and (2.2.19) are a consequence of the UV completion. They are non-trivial, in the sense that in a general case (in the most general MSSM with a type I seesaw model) there exists no flavor basis in which (2.2.18) and/or (2.2.19) hold. From (4.6.2) we do not obtain non-trivial conditions on λ^u and λ^d, since in general, in the MSSM quark sector there is always a flavor basis in which λ^u is diagonal and λ^d is specified by a real diagonal matrix times a hermitian matrix.

The theory with canonical Kähler potential, superpotential (2.2.16) and Yukawas given by (2.2.17), or equivalently, with the non trivial conditions (2.2.18) and (2.2.19), is the final form of our effective theory in this section. The effective theory corresponds to a type I seesaw model where the origin of all flavor mixing and CP violation is in an hermitian wave function renormalization matrix (2.2.13), so that the $SU(3)_C$ vacuum angle is zero. Supersymmetry ensures that the vacuum angle stays zero at all orders of perturbation theory .

2.2.2 The effective theory below the RH neutrino mass scale

In this section we present the effective theory at a scale just below the lightest right handed neutrino mass M_1 by integrating out the RH neutrinos at tree level. We neglect the effects of RG running between the mass scale of the vector like GUT multiplets $M_A^{D,L}$ and the RH neutrino mass scale. We consider both scales to be separated by only a couple of orders of magnitude. The superpotential

of our seesaw model (2.2.22) below the right handed neutrino mass scale has the form

$$\begin{aligned}&\lambda^d_{ij}\ Q_i H_d \overline{d}_j - \lambda^u_{ij}\ Q_i H_u \overline{u}_j - \lambda^\ell_{ij}\ L_i H_d \overline{\ell}_j + \mu H_u H_d \\ &+ \lambda^\nu_{ij}(L_i H_u)(L_j H_u)\end{aligned} \tag{2.2.22}$$

where λ^ν_{ij} is given by

$$\lambda^\nu = \lambda^N M^{-1} (\lambda^N)^T . \tag{2.2.23}$$

The non trivial condition for the strong CP angle (2.2.18) together with supersymmetry impose a vanishing $SU(3)_C$ vacuum angle at all orders in perturbation theory. Also, from the non trivial conditions for the Yukawas (2.2.19), λ^ℓ and λ^ν are related to the down type Yukawas

$$\lambda^\ell = \left(\lambda^d\right)^T \Gamma^\ell \qquad \lambda^\nu = \left(\lambda^d\right)^T \left[\Gamma^N M^{-1} \Gamma^N\right] \lambda^d \tag{2.2.24}$$

where Γ^ℓ and Γ^N are real, diagonal matrices defined in (2.2.21). The right handed neutrino mass matrix M is also real and diagonal in the basis we work on.

The effective theory corresponds to the MSSM with massive neutrinos and non trivial conditions (2.2.18) and (2.2.24), ensuring vanishing $\overline{\theta}$ and relations between the quark and lepton flavor parameters, respectively.

Finally, for completeness we define the mass matrices of the quarks, charged leptons and neutrinos as

$$m^u = v_u \lambda^u \qquad m^d = v_d \lambda^d \qquad m^\ell = v_d \lambda^\ell \qquad m^\nu = v_u^2 \lambda^\nu . \tag{2.2.25}$$

Defining the real, diagonal matrix Γ^m

$$\Gamma^m = \frac{v_u^2}{v_d^2} \left[\Gamma^N M^{-1} \Gamma^N\right] \tag{2.2.26}$$

and using 2.2.25, we may rewrite the non-trivial conditions (2.2.24) in terms of the mass matrices

$$m^\ell = \left(m^d\right)^T \Gamma^\ell \qquad m^\nu = \left(m^d\right)^T \Gamma^m m^d \tag{2.2.27}$$

where Γ^ℓ and Γ^m are some real, diagonal matrices.

2.2.3 Supersymmetry breaking and renormalization of $\overline{\theta}$

In the beginning of this section, it was shown that the supersymmetric model leads to $\overline{\theta} = 0$ at all orders in perturbation theory due to the non-renormalization of the superpotential. We now briefly comment on the effects of supersymmetry breaking on the renormalization of $\overline{\theta}$. Renormalization of $\overline{\theta}$ can arise from the renormalization of any of the terms in

$$\overline{\theta} = 8\pi^2 \,\mathrm{Im}\,\tau - 3\mathrm{Arg}\, m_{\tilde{g}} - 3\mathrm{Arg}\, v_u v_d - \mathrm{Arg}\ \det(\lambda_u \lambda_d), \tag{2.2.28}$$

once supersymmetry is broken. From (2.2.28) we immediately see that in order for the mechanism not to be spoiled by SUSY breaking, the SUSY breaking sector has to be CP conserving, to avoid a phase for the gluino mass or b_μ term. This is consistent with our assumptions, since we consider all CP breaking to come from the Nelson-Barr sector.

To illustrate the general features of the corrections to $\overline{\theta}$, consider the renormalization of the Yukawas once supersymmetry breaking is taken into account, which can be multiplicative $(\delta_{ik} + \varepsilon^{u,d}_{ik})\lambda^{u,d}_{kj}$ with $\varepsilon^{u,d}_{ik}$ hermitian, or additive, $\lambda^{u,d}_{ij} + \varepsilon^{u,d}_{ij}$, with $\varepsilon^{u,d}_{ij}$ arbitrary.

The multiplicative corrections come from wave function renormalization matrices $\mathcal{Z}^\Phi$, with Φ being the SM fields in the fundamental representaiton of $SU(3)_C$, and lead to a contribution to $\overline{\theta}$ given by $\prod_\Phi \text{Arg det}(\mathcal{Z}^\Phi)$. This contribution always vanishes (with or without SUSY breaking) due to the hermiticity of the wave function renormalization matrices.

The additive contributions are potentially dangerous. There are two types of additive corrections. The first ones are the flavor aligned corrections, and are just proportional to the Yukawas themselves, $\lambda^{u,d}_{ij} + \varepsilon^{u,d}\lambda^{u,d}_{ij}$, where $\varepsilon^{u,d}$ can be potentially complex. These kind of corrections may be generated when SUSY breaking is mediated by gauge interactions. The aligned additive contributions do not lead to large renormalization of $\overline{\theta}$, since as noted in [37] their effect in renormalizing $\overline{\theta}$ must be proportional to the Jarlskob invariant. This motivates us to choose gauge mediation as our SUSY mediation mechanism. The second type of additive corrections are flavor misaligned. In our model, they may be generated by gauge mediation diagrams that also contain loops of the heavy vector like quarks $D, \overline{D}$, or loops of Nelson-Barr fields. These diagrams come first at three loops, and are parametrically suppressed by M^2_{SUSY}/M^2_{CP}. In section 2.4 we will argue that in our model, in order to consider successful leptogenesis, we must take $M_{CP} \gtrsim 10^{10}\,\text{GeV}$, and to avoid gravitino overproduction we need $M_{SUSY} \sim 100\,\text{TeV}$. This leads to $M^2_{SUSY}/M^2_{CP} \lesssim 10^{-10}$. Together with the three loop suppression, this gives contributions to $\overline{\theta}$ of order 10^{-16}, much below the current experimental limits.

2.3 Predictions for IR physics

The objective of this section is to impose the constraints from the quark and lepton sector data on the effective theory described in section 2.2.2, and to obtain predictions once all the model parameters have been fixed.

In this section we make use of a technical description of the flavor symmetries and flavor invariants of the MSSM with massive neutrinos, which is left for appendix A.1. Flavor invariants

are combinations of Lagrangian parameters that are independent of the flavor basis in which they are evaluated. For this reason, all flavor invariants are physical, they can be related to measurable quantities. Examples of flavor invariants are masses, mixing angles and CP violating phases. In terms of Lagrangian parameters, these invariants are in general complicated non-polynomial expressions. For instance, quark masses are proportional to the roots of the characteristic equations of the Yukawa matrices. In appendix A.1 we describe complete sets invariants which are simpler, polynomial combinations of Lagrangian parameters. The polynomial invariants will be used in this section.

2.3.1 Parameter counting using invariants

The fermionic sector of the SM with massive neutrinos and vanishing strong CP phase contains twenty-two measurable parameters, of which ten correspond to the quark sector and twelve to the leptonic sector. The ten measurable parameters of the quark sector are six masses, three mixing angles and the CKM phase. All the measurable parameters in the quark sector are known with good accuracy [2]. The twelve measurable parameters of the leptonic sector are six masses, three mixing angles and three CP violating phases. Of these twelve parameters, only eight have been measured, namely the three charged lepton masses, two neutrino mass splittings (up to a discrete ordering) and the three mixing angles [41]. A summary table of the measured running parameters in the quark and lepton sector at the scales m_Z and at 10^{12} GeV is presented in table 2.1.

In this section we show that in our model, due to the non-trivial conditions (2.2.27), only eighteen out of the twenty-two measurable parameters of the fermionic sector can be chosen to be independent.

The proof is by direct counting. We choose the first ten independent measurable parameters to be the quark masses and CKM matrix elements. The twelve measurable parameters of the lepton sector cannot be chosen to be independent, because the lepton and quark sector Lagrangian parameters are related by the non-trivial conditions (2.2.27). In order to identify the independent measurable parameters in the lepton sector, we start by listing a complete set of polynomial leptonic invariants. Any complete set of leptonic invariants specify all the measurable parameters of the lepton sector, so the list must contain twelve invariants, and an invertible map between the invariants and the lepton masses and elements of the PMNS matrix must exist. In appendix A we build a complete list of polynomial invariants and show that the invertible map exists. Here we closely follow that list, but we choose to build the invariants in terms of the leptonic mass matrices (2.2.25) instead of

[2] The largest uncertainty being in the mass of the up quark, with a non-zero value strongly suggested by lattice QCD simulations.

yukawa matrices. The list of twelve invariants is

$$
\begin{aligned}
&\mathrm{Tr}[(m^{\ell}m^{\ell\dagger})^n]\\
&\mathrm{Tr}[(m^{\nu}m^{\nu\dagger})^n]\\
&\mathrm{Tr}\,\Big(\big[\,m^{\ell}m^{\ell\dagger},m^{\nu}m^{\nu\dagger}\,\big]^2\Big)\\
&\mathrm{Tr}\,\Big(\big[\,m^{\ell}m^{\ell\dagger},m^{\nu}m^{\nu\dagger}\,\big]^2\,(m^{\ell}m^{\ell\dagger})\Big)\\
&\mathrm{Tr}\,\Big(\big[\,m^{\ell}m^{\ell\dagger},m^{\nu}m^{\nu\dagger}\,\big]^2\,(m^{\nu}m^{\nu\dagger})\Big)\\
&\mathrm{Tr}\,\Big(\big[\,m^{\ell}m^{\ell\dagger},m^{\nu}m^{\nu\dagger}\,\big]^3\Big)\\
&\mathrm{Tr}\,\Big(\big[\,m^{\ell}m^{\ell\dagger},m^{\nu}(m^{\ell}m^{\ell\dagger})^{*}m^{\nu\dagger}\,\big]^3\Big)\\
&\mathrm{Tr}\,\Big(\big[\,m^{\ell}m^{\ell\dagger},m^{\nu}m^{\nu\dagger}\,\big]\,\Big(m^{\nu}(m^{\ell}m^{\ell\dagger})^{*}m^{\nu\dagger}\Big)\Big)
\end{aligned}
\tag{2.3.1}
$$

where $n=1,2,3$. Using the non-trivial conditions (2.2.27) in (2.3.1) and the cyclic property of the trace, the list may be rewritten as

$$
\begin{aligned}
\mathrm{Tr}\;(m^{\ell}m^{\ell\dagger})^n &= \mathrm{Tr}\,\Big(\,(\Gamma^{\ell})^2\,(m^{d}m^{d\dagger})^{*}\,\Big)^n\\
\mathrm{Tr}\;(m^{\nu}m^{\nu\dagger})^n &= \mathrm{Tr}\,\Big(\Gamma^{m}\,m^{d}m^{d\dagger}\Gamma^{m}\,(m^{d}m^{d\dagger})^{*}\Big)^n
\end{aligned}
$$

$$
\begin{aligned}
\mathrm{Tr}\,\big[\,m^{\ell}m^{\ell\dagger},m^{\nu}m^{\nu\dagger}\,\big]^2 &= \mathrm{Tr}\,\Big[\,(\Gamma^{\ell})^2\,(m^{d}m^{d\dagger})^{*}\,,\,\Gamma^{m}\,m^{d}m^{d\dagger}\Gamma^{m}\,(m^{d}m^{d\dagger})^{*}\,\Big]^2\\
\mathrm{Tr}\,\Big(\big[\,m^{\ell}m^{\ell\dagger},m^{\nu}m^{\nu\dagger}\,\big]^2\,(m^{\ell}m^{\ell\dagger})\Big) &= \mathrm{Tr}\,\Big(\Big[(\Gamma^{\ell})^2\,(m^{d}m^{d\dagger})^{*},\Gamma^{m}\,m^{d}m^{d\dagger}\Gamma^{m}\,(m^{d}m^{d\dagger})^{*}\Big]^2\\
&\qquad \Gamma^{\ell}\,(m^{d}m^{d\dagger})^{*}\Big)\\
\mathrm{Tr}\,\Big(\big[m^{\ell}m^{\ell\dagger},m^{\nu}m^{\nu\dagger}\,\big]^2\,(m^{\nu}m^{\nu\dagger})\Big) &= \mathrm{Tr}\,\Big(\Big[\,(\Gamma^{\ell})^2\,(m^{d}m^{d\dagger})^{*},\Gamma^{m}\,m^{d}m^{d\dagger}\Gamma^{m}\,(m^{d}m^{d\dagger})^{*}\,\Big]^2\\
&\qquad \Gamma^{m}\,m^{d}m^{d\dagger}\Gamma^{m}\,(m^{d}m^{d\dagger})^{*}\,\Big)
\end{aligned}
$$

$$
\begin{aligned}
\mathrm{Tr}\,\big[\,m^{\ell}m^{\ell\dagger},m^{\nu}m^{\nu\dagger}\,\big]^3 &= \mathrm{Tr}\,\Big[\,(\Gamma^{\ell})^2\,(m^{d}m^{d\dagger})^{*}\;,\;\Gamma^{m}\,m^{d}m^{d\dagger}\Gamma^{m}\,(m^{d}m^{d\dagger})^{*}\,\Big]^3\\
\mathrm{Tr}\,\big[\,m^{\ell}m^{\ell\dagger},m^{\nu}(m^{\ell}m^{\ell\dagger})^{*}m^{\nu\dagger}\,\big]^3 &= \mathrm{Tr}\,\Big[\,(\Gamma^{\ell})^2\,(m^{d}m^{d\dagger})^{*}\;,\\
&\qquad \Gamma^{m}m^{d}m^{d\dagger}(\Gamma^{\ell})^2m^{d}m^{d\dagger}\Gamma^{m}(m^{d}m^{d\dagger})^{*}\Big]^3\\
\mathrm{Tr}\,\Big(\big[m^{\ell}m^{\ell\dagger},m^{\nu}m^{\nu\dagger}\big]m^{\nu}(m^{\ell}m^{\ell\dagger})^{*}m^{\nu\dagger}\Big) &= \mathrm{Tr}\,\Big(\Big[\,(\Gamma^{\ell})^2\,(m^{d}m^{d\dagger})^{*}\;,\;\Gamma^{m}\,m^{d}m^{d\dagger}\Gamma^{m}\,(m^{d}m^{d\dagger})^{*}\,\Big]\\
&\qquad \Gamma^{m}m^{d}m^{d\dagger}(\Gamma^{\ell})^2m^{d}m^{d\dagger}\Gamma^{m}(m^{d}m^{d\dagger})^{*}\Big)
\end{aligned}
\tag{2.3.2}
$$

where $n = 1, 2, 3$ and Γ^ℓ and Γ^m are real, diagonal matrices, which must be interpreted as model parameters coming from the UV completion. The twelve polynomial leptonic invariants 2.3.2 are completely specified by Γ^ℓ and Γ^m, and $m^d m^{d\dagger}$.

In a general basis, the matrices $m^u m^{u\dagger}$ and $m^d m^{d\dagger}$ are given by

$$m_u m_u^\dagger = U_{Q_u}\,\mathrm{diag}(m_u^2, m_c^2, m_t^2)\,U_{Q_u}^\dagger \tag{2.3.3}$$

$$m_d m_d^\dagger = U_{Q_d}\,\mathrm{diag}(m_d^2, m_s^2, m_b^2)\,U_{Q_d}^\dagger \tag{2.3.4}$$

while the CKM matrix is given by

$$V_{\mathrm{CKM}} = U_{Q_u}^T U_{Q_d}^* \tag{2.3.5}$$

In the basis we work on, in which m^u is diagonal, the most general matrix U_{Q_u} is

$$U_{Q_u} = e^{-i\gamma}\mathrm{diag}(1, e^{-i\gamma_1}, e^{-i\gamma_2}) \tag{2.3.6}$$

where $\gamma, \gamma_1, \gamma_2$ are unspecified phases. Then, in this basis

$$U_{Q_d} = \left[U_{Q_u}^\dagger\right]^{-1} V_{\mathrm{CKM}}^* = e^{i\gamma}\mathrm{diag}(1, e^{i\gamma_1}, e^{i\gamma_2}) V_{\mathrm{CKM}}^* \tag{2.3.7}$$

Using (2.3.7) in (2.3.4), we can express the matrix $m^d m^{d\dagger}$ in terms of the ten quark sector measurable parameters and two unknown phases γ_1, γ_2

$$m^d m^{d\dagger} = \mathrm{diag}(1, e^{i\gamma_1}, e^{i\gamma_2})\, V_{\mathrm{CKM}}^*\, \mathrm{diag}(m_d^2, m_s^2, m_b^2)\, V_{\mathrm{CKM}}^T\, \mathrm{diag}(1, e^{-i\gamma_1}, e^{-i\gamma_2}). \tag{2.3.8}$$

In the quark sector, the phases γ_1, γ_2 are not observable since they can be rotated away by a $U(3)_Q$ transformation. But thanks to the non-trivial conditions (2.2.27), they show up in the leptonic invariants 2.3.2, so they become physical. Another way to understand that these phases are observable, is to recall that in our model there is only one single primordial phase in all the theory, related to the vacuum expectation values of the Nelson-Barr fields. The phases γ_1, γ_2 are related to this primordial phase through (2.2.13) and (4.6.2), so they are physical. We interpret these phases as model parameters coming from the UV completion.

Using (2.3.8) in the list (2.3.1), we obtain that the twelve polynomial invariants can be expressed in terms of the ten quark sector measured parameters and eight model parameters: γ_1, γ_2, Γ_{ii}^ℓ, Γ_{ii}^m, $i = 1, 2, 3$. These eight model parameters are fixed by the eight measured parameters of the leptonic sector (the charged lepton masses, neutrino mass splittings, and mixing angles). We describe in the next section how to numerically fix the model parameters with lepton sector data. This count is the final result of this section: in our model, the twenty-two measurable parameters of the fermionic sector can be specified from the ten measured parameters of the quark sector and the eight measured

parameters of the lepton sector. The lightest neutrino mass and the three CP violating phases of the PMNS matrix are *predictions of the model*. Note that the results are independent on $\tan\beta$. This is to be expected, the only physical meaning of $\tan\beta$ is in the couplings of Higgs fields to fermions and in the MSSM Higgs potential. Our analysis relies on invariants constructed out of down type mass matrices, and as such it could be carried out after all Higgs fields have been integrated out and no $\tan\beta$ dependence is left in the theory.

Note that when using the non-trivial conditions (2.2.27), quark sector data enters into the leptonic invariants. This is important, since it means that some of the hierarchical structure of the quark sector is inherited to the leptonic sector. This is a consequence of the unification Ansatz.

2.3.2 Solving for the unknown model parameters using leptonic data

In this section we describe the algorithm to solve for the eight model parameters γ_1, γ_2, Γ^{ℓ}_{ii}, Γ^{m}_{ii}, $i = 1, 2, 3$ using the eight measured parameters of the lepton sector. This section is technical, the reader interested in the results can skip to the next section.

The eight model parameters γ_1, γ_2, Γ^{ℓ}_{ii}, Γ^{m}_{ii}, $i = 1, 2, 3$ are parameters of an effective theory just below the scale M_1 (the mass of the lightest RH neutrino), which for practical purposes in this section is taken to be $\sim 10^{10}$ GeV. In order to impose the constraints from IR data on the model parameters, the measured parameters of the quark and lepton sector need to be evolved to the scale M_1 using the MSSM renormalizaton group equations. We show the corresponding renormalized values in Table 2.1, which are taken from Refs [42, 43], where we have taken the results for $\tan\beta = 10$. As the MSSM RGE equations depend on $\tan\beta$, this introduces a slight dependence of our result on $\tan\beta$.

All masses, mixing angles and the CKM phase in this section correspond to the values at the scale $M_1 \sim 10^{10}$ GeV. In this section, when we refer to observed parameters it should be understood that we have in mind the renormalized values at this high scale.

We start by defining the PMNS matrix. In a general basis, the lepton mass matrices are given by

$$\begin{aligned} m^{\ell} &= U_{L_d}\ \mathrm{diag}(m_e, m_\mu, m_\tau)\ U_{\ell}^{\dagger} \\ m^{\nu} &= U_{L_u}\ \mathrm{diag}(m_{\nu e}, m_{\nu\mu}, m_{\nu\tau})\ U_{L_u}^{T} \end{aligned} \tag{2.3.9}$$

the PMNS matrix is then the basis independent unitary matrix

$$U_{\mathrm{PMNS}} = U_{L_d}^{T} U_{L_u}^{*} \tag{2.3.10}$$

Quarks	$m_u\,(\mathrm{MeV})$	$m_d\,(\mathrm{MeV})$	$m_c\,(\mathrm{MeV})$	$m_s\,(\mathrm{GeV})$	$m_t\,(\mathrm{GeV})$	$m_b\,(\mathrm{GeV})$
$\mu = M_Z$	$1.28^{+0.50}_{-0.42}$	$2.91^{+1.24}_{-1.20}$	55^{+16}_{-15}	0.624 ± 0.083	172.5 ± 3.0	2.89 ± 0.09
$\mu = 10^{12}\,\mathrm{GeV}$	$0.65^{+0.27}_{-0.22}$	$1.12^{+0.49}_{-0.47}$	21 ± 6	0.319 ± 0.047	$119.4^{+4.9}_{-4.4}$	1.24 ± 0.05

Leptons	$m_e\,(\mathrm{MeV})$	$m_\mu\,(\mathrm{MeV})$	$m_\tau\,(\mathrm{MeV})$	$\Delta m^2_{21}\,(\mathrm{eV}^2)$	$\Delta m^2_{32}\,(\mathrm{eV}^2)$
$\mu = M_Z$	0.4865	102.718	1746.2	$(7.53 \pm 0.18) \times 10^{-5}$	$(2.51 \pm 0.10) \times 10^{-3}$
$\mu = 10^{12}\,\mathrm{GeV}$	0.4124	87.088	1645.31	$(9.41 \pm 0.22) \times 10^{-5}$	$(3.21 \pm 0.13) \times 10^{-3}$

$\sin\theta_{12}^{\mathrm{CKM}}$	$\sin\theta_{23}^{\mathrm{CKM}}$	$\sin^2\theta_{13}^{\mathrm{CKM}}$	δ^{CKM}
$0.22537^{+0.0006}_{-0.0006}$	$0.0413^{+0.0014}_{-0.0014}$	$0.00347^{+0.00031}_{-0.00029}$	$1.251^{+0.064}_{-0.066}$

$\sin^2\theta_{12}^{\mathrm{PMNS}}$	$\sin^2\theta_{23}^{\mathrm{PMNS}}$	$\sin^2\theta_{13}^{\mathrm{PMNS}}$
$0.3036^{+0.0014}_{-0.0012}$	$0.514^{+0.055}_{-0.056}$	$0.0230^{+0.0021}_{-0.0024}$

Table 2.1: Observed IR parameters. Top: Running quark and lepton masses in the MSSM with $\tan\beta = 10$ from $\mu = M_Z$ to $\mu = 10^{12}\,\mathrm{GeV}$. The running values are taken from Ref. [42]; for the neutrino mass splittings, updated experimental values have been used [44, 45]. Bottom: The experimental values for the mixing angles and CP phases, taken from the PDG [41]. Those do not run appreciably.

Note that the matrix U_{L_d} is defined in (2.3.9) only up to right multiplication by a diagonal unitary matrix, which can always be absorbed in the definition of $U_\ell^\dagger$. Different choices for the diagonal matrix lead to different parametrizations of the PMNS matrix. In the standard parametrization described in appendix A, the PMNS matrix is given in terms of the experimentally measured mixing angles $\theta_{12}, \theta_{13}, \theta_{23}$ and the unknown CP violating phases δ_{13}, λ_2 and λ_3 by

$$U_{\mathrm{PMNS}} = \begin{pmatrix} c_{12}c_{13} & s_{12}c_{13} & s_{13}e^{-i\delta_{13}} \\ -s_{12}c_{23} - c_{12}s_{23}s_{13}e^{i\delta_{13}} & c_{12}c_{23} - s_{12}s_{23}s_{13}e^{i\delta_{13}} & s_{23}c_{13} \\ s_{12}s_{23} - c_{12}c_{23}s_{13}e^{i\delta_{13}} & -c_{12}s_{23} - s_{12}c_{23}s_{13}e^{i\delta_{13}} & c_{23}c_{13} \end{pmatrix} \begin{pmatrix} 1 & 0 & 0 \\ 0 & e^{i\lambda_2} & 0 \\ 0 & 0 & e^{i\lambda_3} \end{pmatrix} \tag{2.3.11}$$

where $s_{ij} = \sin\theta_{ij}$ and $c_{ij} = \cos\theta_{ij}$.

We now describe how to solve for the model parameters. We first solve for Γ^ℓ_{ii}, $i = 1, 2, 3$. Using (2.3.9) we can express the first three invariants of the list (2.3.2) as functions of charged lepton masses

$$\mathrm{Tr}\ (m^\ell m^{\ell\dagger})^n = m_e^{2n} + m_\mu^{2n} + m_\tau^{2n} = \mathrm{Tr}\Big[\Big(\left(\Gamma^\ell\right)^2 V_{\mathrm{CKM}}\, \mathrm{diag}(m_d^2, m_s^2, m_b^2)\, V_{\mathrm{CKM}}^\dagger \Big)^n \Big] \tag{2.3.12}$$

where $n = 1, 2, 3$. These three equations allow us to solve for Γ^ℓ_{ii}, $i = 1, 2, 3$ using the known renormalized values of the CKM matrix and charged fermion masses. Note that the solutions for Γ^ℓ_{ii}, $i = 1, 2, 3$ are independent of γ_1, γ_2, Γ^m_{ii}, $i = 1, 2, 3$ and the unknown CP violating phases of the PMNS matrix. This is an important simplification for the numerical computations, which is seen

transparently in (2.3.12) thanks to the use of polynomial invariants. We leave the presentation of explicit numerical solutions for the next section.

The next step is to solve for Γ^m_{ii}, $i = 1, 2, 3$. Using (2.3.9) in the second line of invariants in (2.3.1) we get

$$\begin{aligned} \mathrm{Tr}\ (m^\nu m^{\nu\dagger})^n &= m_{\nu_1}^{2n} + m_{\nu_2}^{2n} + m_{\nu_3}^{2n} \\ &= \mathrm{Tr}\Big[\Big(\Gamma^m\, V^*_{\rm CKM}\, \mathrm{diag}(m_d^2, m_s^2, m_b^2)\, V^T_{\rm CKM}\, \mathrm{diag}(1, e^{-2i\gamma_1}, e^{-2i\gamma_2}) \\ &\qquad \Gamma^m\, V_{\rm CKM}\, \mathrm{diag}(m_d^2, m_s^2, m_b^2)\, V^\dagger_{\rm CKM}\, \mathrm{diag}(1, e^{2i\gamma_1}, e^{2i\gamma_2}) \Big)^n \Big] \end{aligned} \tag{2.3.13}$$

In these equations the quark masses, elements of the CKM matrix and neutrino mass splittings are known, and they allow us to solve for Γ^m_{ii}, $i = 1, 2, 3$ as a function of γ_1, γ_2 and the unknown lightest neutrino mass $m_{\nu 1}$. There is no simple analytic solution to these equations, so we solve them numerically in the ranges $0 \leq \gamma_1 < \pi$, $0 \leq \gamma_2 < \pi$ and $0 \leq m_{\nu 1} < 1\mathrm{eV}$, where the last upper bound is of the order of the experimental upper bound on the lightest neutrino mass [].

The final step is to solve for γ_1, γ_2 and $m_{\nu 1}$ by using the known leptonic mixing angles. The easiest way to find the solutions is to directly find the PMNS matrix as a function of γ_1, γ_2 and $m_{\nu 1}$, and solve for the values of γ_1, γ_2 and $m_{\nu 1}$ that lead to the experimentally measured mixing angles. This is done as follows. We repeat here the non-trivial conditions (2.2.27)

$$m^\ell = \big(m^d\big)^T \Gamma^\ell \qquad\qquad m^\nu = \big(m^d\big)^T \Gamma^m(\gamma_1, \gamma_2, m_{\nu 1})\, m^d \tag{2.3.14}$$

where now Γ^ℓ is known and Γ^m is a known function of γ_1, γ_2 and $m_{\nu 1}$, so we are only missing the matrix m^d. From (2.3.8) we know the combination $m^d m^{d\dagger}$ as a function of γ_1, γ_2 and known data from the quark sector. Any matrix m^d satisfying (2.3.8) leads to the same physical results, because all the polynomial quark and lepton invariants are written only in terms of the combination $m^d m^{d\dagger}$. This means that we can choose

$$m^d = \mathrm{diag}(1, e^{i\gamma_1}, e^{i\gamma_2})\, V^*_{\rm CKM}\, \mathrm{diag}(m_d, m_s, m_b) \tag{2.3.15}$$

Using (2.3.15) in (2.3.14) we obtain the leptonic mass matrices as a function of γ_1, γ_2 and $m_{\nu 1}$,

$$\begin{aligned} m^\ell(\gamma_1, \gamma_2, m_{\nu 1}) &= \mathrm{diag}(m_d, m_s, m_b)\, V^\dagger_{\rm CKM}\, \mathrm{diag}(1, e^{i\gamma_1}, e^{i\gamma_2}) \Gamma^\ell \\ m^\nu(\gamma_1, \gamma_2, m_{\nu 1}) &= \mathrm{diag}(m_d, m_s, m_b)\, V^\dagger_{\rm CKM}\, \mathrm{diag}(1, e^{i\gamma_1}, e^{i\gamma_2}) \Gamma^m(\gamma_1, \gamma_2, m_{\nu 1}) \\ &\qquad \mathrm{diag}(1, e^{i\gamma_1}, e^{i\gamma_2})\, V^*_{\rm CKM}\, \mathrm{diag}(m_d, m_s, m_b) \end{aligned} \tag{2.3.16}$$

where Γ^ℓ is known and Γ^m is a known function of γ_1, γ_2 and $m_{\nu 1}$. We now diagonalize the matrices $m^\ell(\gamma_1, \gamma_2, m_{\nu 1}), m^\nu(\gamma_1, \gamma_2, m_{\nu 1})$ and using (2.3.10) we find the PMNS matrix as a function of γ_1, γ_2

and $m_{\nu 1}$ (in the interval $0 \leq \gamma_1 < \pi$, $0 \leq \gamma_2 < \pi$ and $0 \leq m_{\nu 1} < 1\text{eV}$). It is important to make sure to express the PMNS matrix in the standard form (2.3.11). Finally, we use

$$\begin{aligned} |U_{\text{PMNS}}(\gamma_1, \gamma_2, m_{\nu 1})|_{13} &= |s_{13}| \\ |U_{\text{PMNS}}(\gamma_1, \gamma_2, m_{\nu 1})|_{12} &= |s_{12} c_{13}| \\ |U_{\text{PMNS}}(\gamma_1, \gamma_2, m_{\nu 1})|_{23} &= |s_{23} c_{13}| \end{aligned} \tag{2.3.17}$$

The three equations (2.3.17) allow us to solve for γ_1, γ_2 and $m_{\nu 1}$ in terms of the known mixing angles. This immediately gives as an output the first prediction: the mass of the lightest neutrino $m_{\nu 1}$. Using the now known values of γ_1, γ_2 and $m_{\nu 1}$, we can now numerically compute the whole PMNS matrix, and we can extract from it the Dirac and Majorana phases $\delta_{13}, \lambda_2, \lambda_3$, which are the remaining three predicted physical parameters.

Two final technical comments are in order. First, the equations (2.3.12) have twelve solutions and the equations (2.3.13) have forty-eight solutions. Only a small subset of the solutions are real (recall that Γ^ℓ and Γ^m must be real matrices), but in general there is more than one set of real solutions for the model parameters. Correspondingly, it is to be expected that the model will give as an output a discrete set of predictions for the yet unmeasured parameters of the lepton sector. Second, all the experimentally measured parameters of the quark and lepton sector that we use in our calculations, are only known up to the experimental uncertainties. The quark masses, elements of the CKM matrix, lepton masses and neutrino mass splittings are known with good precision, so it is a good approximation to use their experimentally measured central value in the calculations. The mixing angles in the lepton sector are known less precisely. At this point, their 3σ experimental error bands allow for deviations as large as $\sim 50\%$ from the measured central values [41]. This means that instead of getting a discrete set of solutions for γ_1, γ_2 and Γ^m_{ii}, $i = 1, 2, 3$, we are only able to obtain a discrete set of ranges, that are consistent with the mixing angles at some level of the experimental uncertainties. Correspondingly, the predictions of our model will also lie in some ranges. A better measurement of the leptonic mixing angles would make the predictions of the model more precise.

2.3.3 Results and predictions for electroweak scale physics

In this section we present the results and predictions for electroweak scale physics in our model. Here we make use of the algorithm described in section 2.3.2 to numerically fix the eight model parameters γ_1, γ_2, Γ^ℓ_{ii}, Γ^m_{ii}, $i = 1, 2, 3$ with lepton sector data. Once the model parameters are fixed by data, the allowed values for the lightest neutrino mass and CP violating phases of the PMNS matrix are obtained as an output.

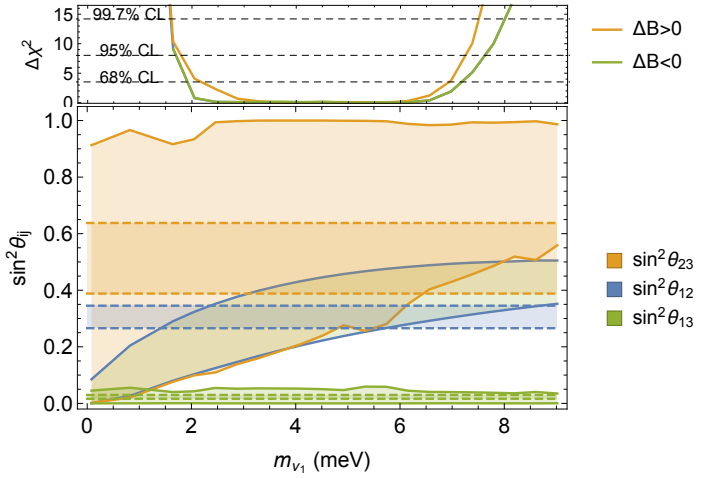

Figure 2.3: Bands of mixing angles as a function of m_{ν_1} for the model of section 2.2.2 (solid) and 3σ bands of experimentally measured mixing angles (dashed). The model mixing angle bands as functions of m_{ν_1} are obtained by imposing quark sector data (masses, mixing angles and CKM phase), charged lepton masses and neutrino mass splittings as constraints, and scanning over the unconstrained model parameter space. In the top adjoining panel, we show the minimum $\Delta\chi^2$ for each value of m_{ν_1} separating the solutions leading to different signs of the baryon asymmetry, as discussed in Sec. 2.4.

To understand some general features of the model, we start by constraining the model parameters only by using the known charged lepton masses and neutrino mass splittings. This is done by solving equations (2.3.12)–(2.3.13). At this stage we do not make use of the known lepton mixing angles, so there are still three unknown model parameters. We can trade one of the model parameters for the unknown mass of the lightest neutrino m_{ν_1}. The remaining two free parameters are taken to be the phases γ_1 and γ_2, which are defined in 2.3.8.

The first result is that we find no solutions to equations (2.3.12)–(2.3.13) that correspond to an inverted hierarchy scenario, so the hierarchy is predicted to be normal. The reason is that our model inherits the mass hierarchies from the quark sector through the unification Ansatz. This disfavors an inverted hierarchy, which differently from the quark sector hierarchy, always contains nearly degenerate mass eigenstates regardless of the value of the lightest neutrino mass.

In figure 2.3 we present the bands of leptonic mixing angles obtained in our model after solving equations (2.3.12)–(2.3.13) and scanning over all values of γ_1, γ_2. The bands are delimited by solid lines, and plotted as a function of the lightest neutrino mass m_{ν_1}. In the same figure, the bands delimited by dashed lines are the experimentally allowed regions for the same angles (at 3σ). We immediately see that the model tends to give mixing angles that fall roughly in the correct experimental range and order ($s^2_{23} \gtrsim s^2_{13} > s^2_{13}$). In particular, s^2_{13} tends to correctly be the smallest mixing angle. This is a nice consequence of the unification Ansatz: in the quark sector s^2_{13} is the

smallest mixing angle, and this feature is conveniently carried out to the leptonic sector. Note also that the three angles fall within their experimentally allowed values only for a small window of lightest neutrino mass. This range must be understood as a prediction, once the mixing angles are constrained by data, the lightest neutrino mass is an output of the model.

To make this last statement more precise, in the top panel of figure 2.3 we also show the value of a combined chi-squared test for the three measured mixing angles,[3] $\Delta\chi^2 \equiv \sum_{ij} \Delta\chi^2(\sin^2\theta_{ij})$, as a function of m_{ν_1}, marginalized over all values of γ_1 and γ_2. The dashed horizontal lines correspond to $\Delta\chi^2 = 3.52, 8.03$ and 14.16 respectively, or equivalently, to CL intervals of $68\%, 95\%$ and 99.7% for a χ^2 distribution with three degrees of freedom. At 3σ, the *predicted range* for the lightest neutrino mass which is consistent with all the experimentally measured data from the quark and lepton sector is

$$2 \times 10^{-3}\,\text{eV} < m_{\nu_1} < 9.5 \times 10^{-3}\,\text{eV} \tag{2.3.18}$$

We now move on to the predictions on the CP violating phases of the PMNS matrix. In figure 2.4 we plot the CP violating phases versus the known mixing angles. The figures are obtained by fixing the lightest neutrino mass at $m_{\nu 1} = 5 \times 10^{-3}$eV and selecting the points γ_1, γ_2 that fulfill the chi-squared test mentioned above $\Delta\chi^2 \equiv \sum_{ij} \Delta\chi^2(\sin^2\theta_{ij})$ at $1\sigma, 2\sigma$ or 3σ. The points colored with orange, purple and black fulfill the chi-squared test at $68\%, 95\%$ and 99.7% confidence level, respectively. These points must be considered to be consistent with all the experimentally measured data from the quark and lepton sector. These plots are *not* scatter plots, they are the plots obtained by imposing all known data from the quark and lepton sector in the model parameters. The red diamond corresponds to the minimum value of the chi-squared test (the best fit point). The model parameters corresponding to the best fit point are presented for reference in table 2.2.[4].

In the leftmost panels, as a check that we solved for the model parameters correctly, we show how the mixing angles fall within the allowed experimental ranges, while in the three right panels we show the corresponding predicted CP violating phases. The phases are generically not vanishing in the sense that they do not show any preference for a null value. On the other hand, at the 3σ level, we cannot provide a sharp prediction for the CP phases. This is not a limitation of the model, but of the current experimental uncertainties of the measured mixing angles. Better measurement of the mixing angles will provide sharper predictions: for example, if future experimental uncertainties

[3] The individual likelihood distributions are taken from the original experimental results of the KamLand, T2K and Daya Bay collaborations [44–46]

[4] Additionally, we only show the the region of the parameter space yielding the correct sign of the baryon asymmetry. We will explain this in more details in Sec. 2.4

are reduced by a factor of 3 for each mixing angle (with the central value staying the same), only the black points will be allowed (at the 99.7% CL), corresponding to $\delta \approx \frac{\pi}{4}, \frac{5\pi}{4}, \lambda_2 \simeq 0, \pi, \lambda_3 \simeq \frac{\pi}{2}$.

In table 2.2 we give the full set of UV parameters $\gamma_1, \gamma_2, \Gamma^\ell_{ii}$ and Γ^m_{ii}, $i = 1, 2, 3$ corresponding to the red diamond in Figure 2.4, as well as the predicted leptonic CP phases and lightest neutrino mass. We see that there are large hierarchies between the different elements of the diagonal matrices Γ^ℓ and Γ^m. The reason is that due to the unification Ansatz, the same hierarchy of the quark masses would be inherited to the leptonic sector, if all the elements of Γ^ℓ and Γ^m were of the same order. The hierarchical structure of Γ^ℓ and Γ^m allows us to accommodate the correct hierarchies measured in the leptonic sector. Note that the large value of Γ^ℓ_{11} does not represent a problem for perturbativity: from (2.2.21) and (2.2.26) we see that all the elements of Γ^ℓ and Γ^m can be achieved with perturbative values of $\tilde{\lambda}^d, \tilde{\lambda}^\ell$ and $\tilde{\lambda}^N$.

γ_1	γ_2	Γ^ℓ_{11}	Γ^ℓ_2	Γ^ℓ_{33}	$\Gamma^m_{11}(\mathrm{GeV}^{-1})$	$\Gamma^m_{22}(\mathrm{GeV}^{-1})$	$\Gamma^m_{33}(\mathrm{GeV}^{-1})$
0.74	0.64	52.4	0.196	0.022	826.9×10^{-10}	-28.5×10^{-10}	0.036×10^{-10}

$\sin^2\theta_{12}$	$\sin^2\theta_{23}$	$\sin^2\theta_{13}$	$\Delta\chi^2$	$m_{\nu_1}(\mathrm{eV})$	δ	λ_2	λ_3
0.3038	0.5264	0.0228	0.024	5×10^{-3}	5.272	0.118	1.547

Table 2.2: Top: Numerical values of the model parameters for the benchmark point shown as a red diamond in Figure 2.4. The eight parameters are fixed by the three charged lepton masses, two neutrino mass splittings and three leptonic mixing angles. Bottom: The mixing angles, well matched by their experimentally measured central values (as shown by the small $\Delta\chi^2$) and the predicted output of the mdoel: the lightest neutrino mass m_{ν_1} (with a normal hierarchy) and the three CP violating phases of the PMNS matrix.

It should be noted that the above predictions about the leptonic CP phases are rather sensitive to the particular choice of $m_{\nu_1} = 5 \times 10^{-3}$eV for the lightest neutrino mass. We illustrate this effect in Figure 2.7, where we show predictions for the CP phases δ, λ_2 and λ_3 as a function of the lightest neutrino mass m_{ν_1}. The color scheme is the same as in Fig. 2.4, with points within the experimental 1, 2 and 3σ ranges for the mixing angles respectively marked in black, purple and orange. Within the current experimental uncertainties, the CP phases are completely generic, but improvements in the experimental precision can sharpen the predictions and give non-trivial correlations between $\delta, \lambda_2, \lambda_3$ and m_{ν_1} as well as between individual CP phases.

Finally, we conclude this section by discussing the experimental outlook to confirm or disprove our model. First, the predicted range (2.3.18) for m_{ν_1} is too low for current and projected direct neutrino mass experiments looking for an endpoint in the beta decay spectrum. On the other hand, in our model the sum of neutrino masses is restricted to the narrow range $0.060\,\mathrm{eV} < \sum_\nu m_\nu < 0.073\,\mathrm{eV}$, below the current PLANCK 95%CL upper bound, $\sum_\nu m_\nu < 0.23\,\mathrm{eV}$ [47] and just within

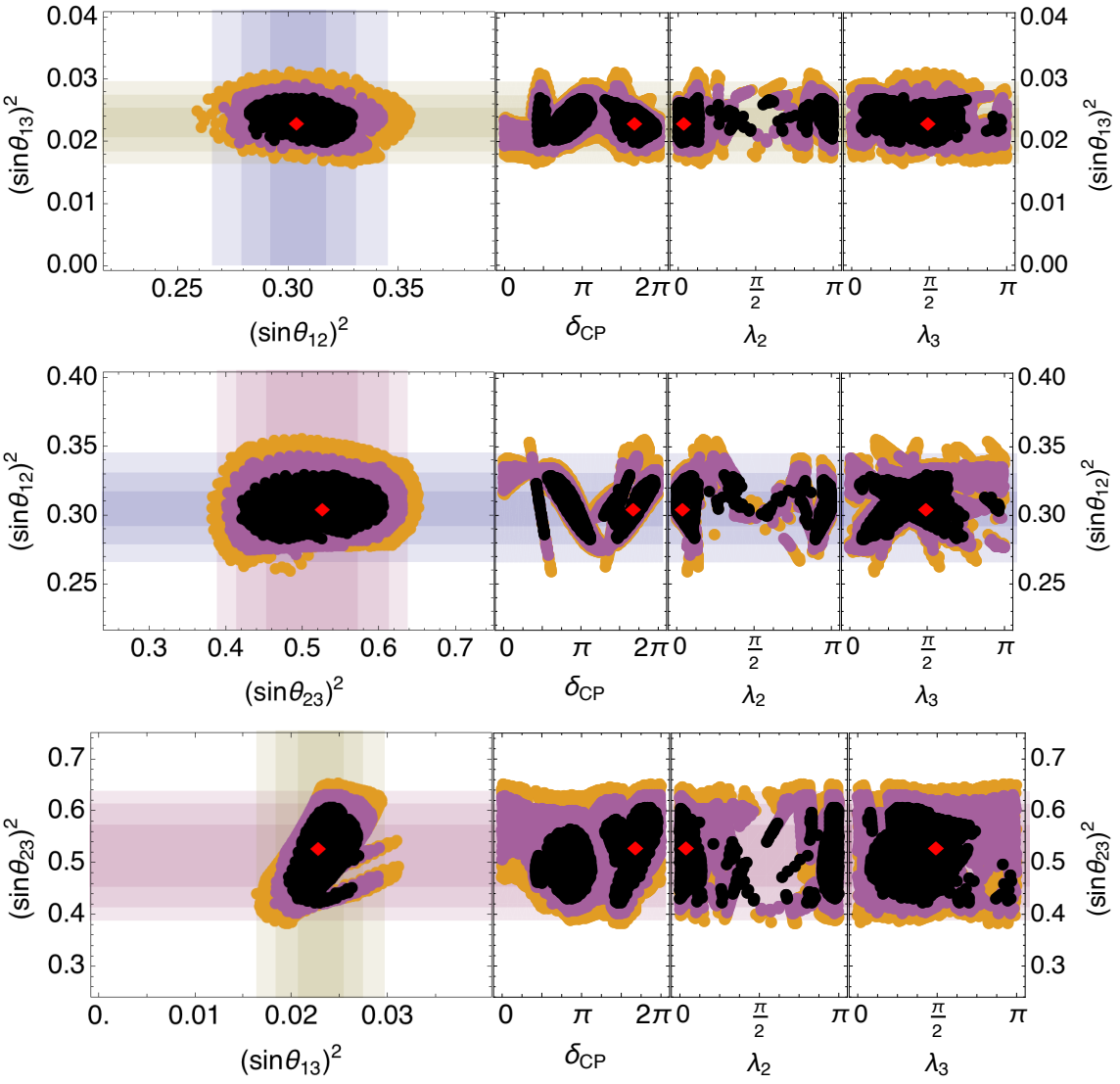

Figure 2.4: Plots of $\sin^2\theta_{ij}$, $ij = 12, 23, 13$ and the CP violating phases of the PMNS matrix $\delta, \lambda_2, \lambda_3$ versus $\sin^2\theta_{kl}$, $kl = 13, 12, 23$ for the model of section 2.2.2 constrained by IR data as explained in section 2.3.1. These plots are *not* scatter plots. The lightest neutrino mass is fixed at $m_{\nu_1} = 5 \times 10^{-3}$ eV. The colored bands show the 1σ to 3σ experimental limits for each mixing angle. Regions are colored according to a chi-squared test for the three measured mixing angles, considered as independent variables. Orange, purple and black circles are solutions that fall within 3σ, 2σ and 1σ of the chi-squared test. The red diamond is the best fit point described in Table 2.2.

the reach of future galaxy surveys probing Large Scale Structures. Second, the CKM-like phase δ will be measured at the DUNE experiment with a resolution that could approach $O(10°)$ [48]. A measurement of δ would *overconstrain* our model, and when paired with significantly improved uncertainties in the lepton mixing angles it holds the potential of definitely confirming or excluding it. On the other hand, when considering the existing uncertainties, a measurement of δ would sharpen the predicted range for m_{ν_1}, which in turn would also improve the predictions for the Majorana

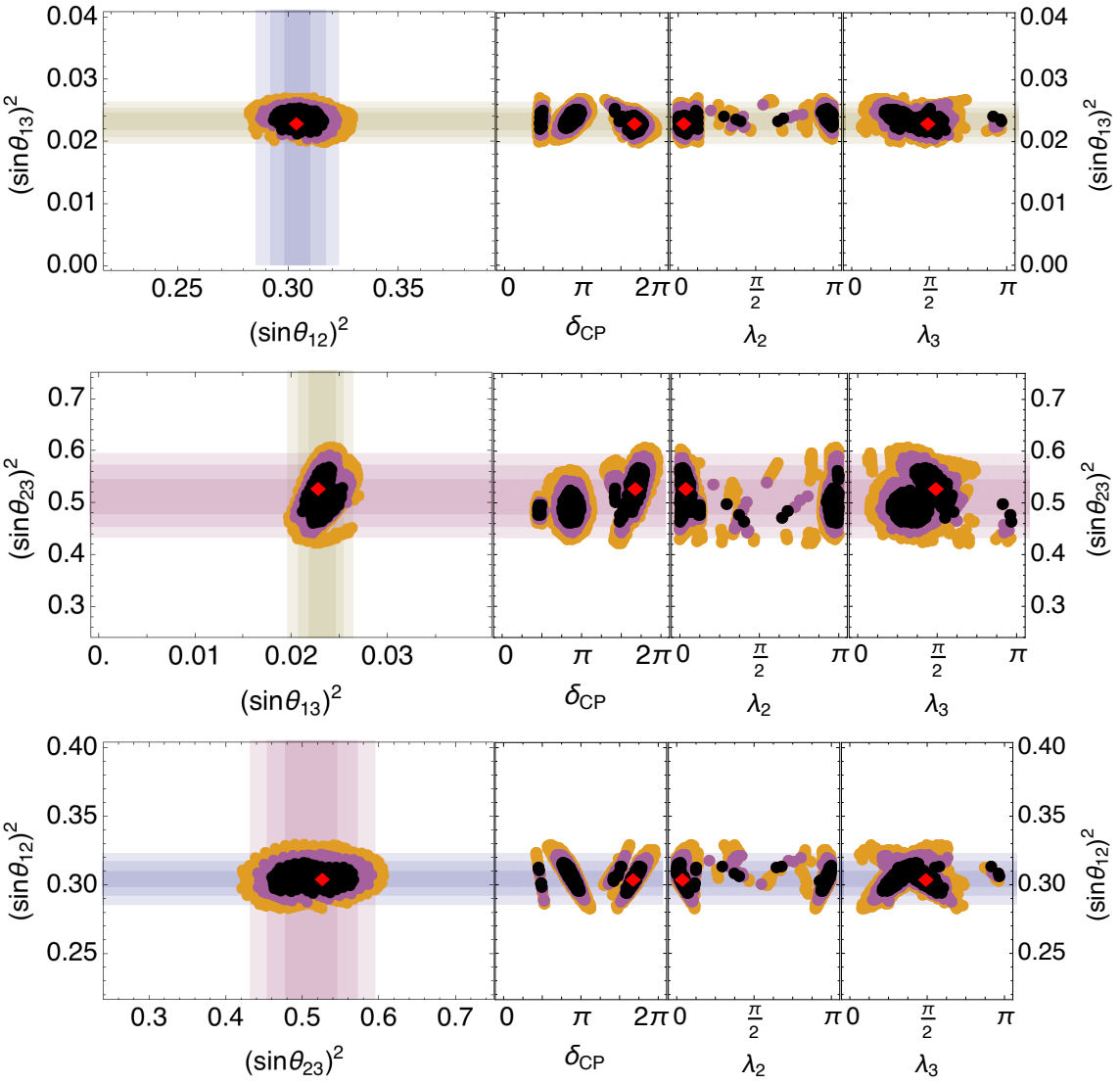

Figure 2.5: Same as Fig. 2.4, but with a projected 3× improvement in the experimental errors for the mixing angles (assuming the central values stay the same). Now the predictions for the CP phases are more precise.

phases λ_2, λ_3 (see Fig. 2.7).

Another process depending on CP-violating phases is neutrinoless double-beta decay; in this case, λ_2 and λ_3 enter the expression for the neutrinoless decay mass parameter $m_{0\nu\beta\beta} = \left|\sum_i m_{\nu_i} (U_{\rm PMNS})_{ei})^2\right|$, where the PMNS matrix is fully calculable in our model. For example, the best fit point in Table 2.2 yields $m_{0\nu\beta\beta} = 6 \times 10^{-3}\,\text{eV}$. Given that a lightest neutrino mass in the range $10^{-3}\,\text{eV} < m_{\nu_1} < 10^{-2}\,\text{eV}$ and a normal hierarchy are predicted, we fall in the parameter space region where a "throat" appears in the $m_{\nu_1} - m_{0\nu\beta\beta}$ plane, signaling cancellations between different factors in $m_{0\nu\beta\beta}$. With the currently large uncertainties for the mixing angles leading to a

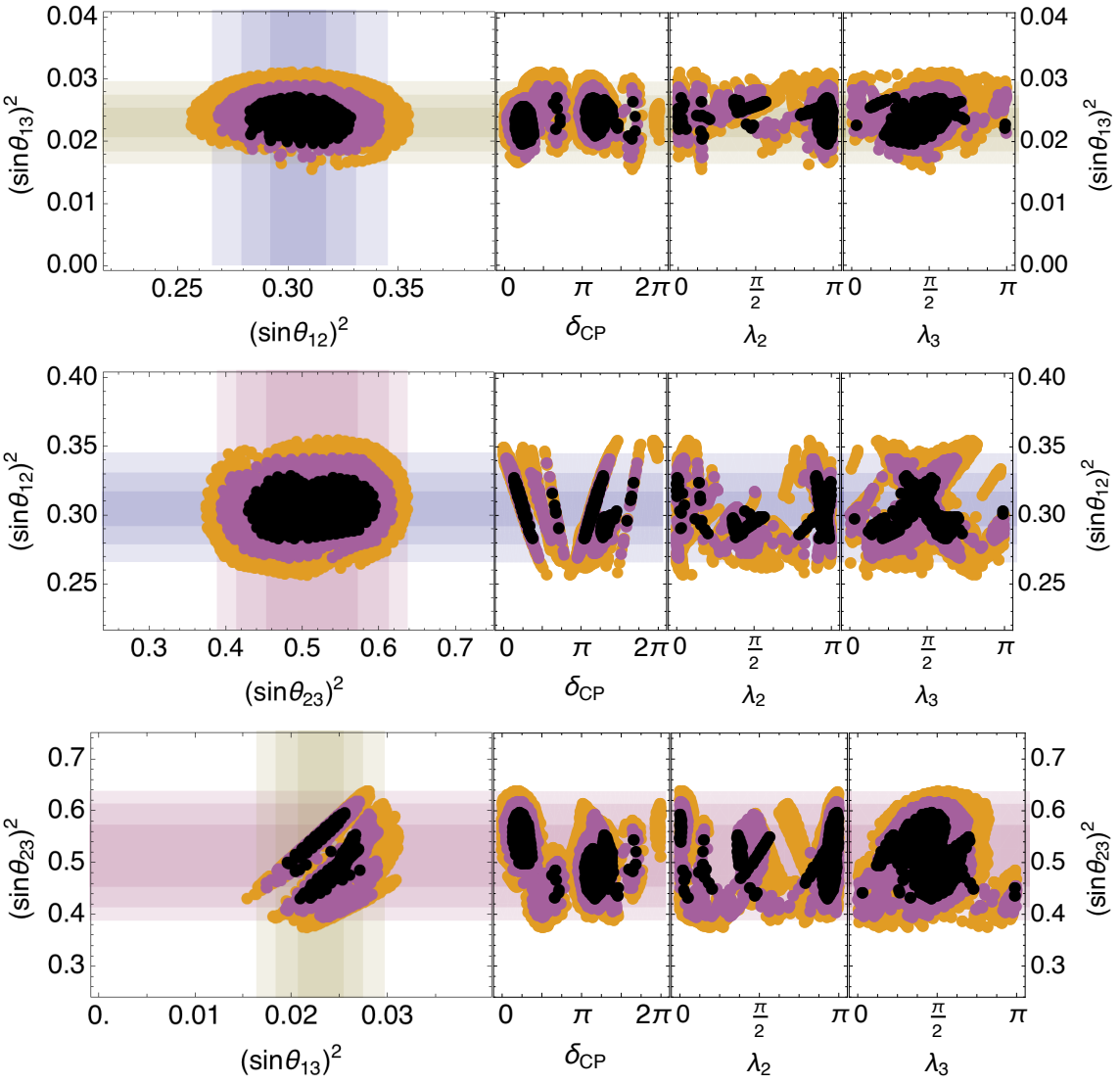

Figure 2.6: Same as Fig. 2.4, but including only points leading to the wrong sign of the baryon asymmetry. This illustrates how requiring the correct sign of the asymmetry leads to different predictions for IR physics.

wide range of predictions for λ_2 and λ_3, we are not able to exclude such cancellations: instead, we find points lying within 1σ from the mixing angles that yield a very small neutrinoless double-beta decay parameter, of order 10^{-4}eV, well below the future experimental reach.

2.4 Predictions for UV physics and thermal leptogenesis

We have seen that the effective theory presented in section 2.2.2, which is valid below the scale of the RH neutrino masses, is completely specified by known IR data. In this section, we move up in energies and we study the constraints from the quark and lepton sector data on the effective theory

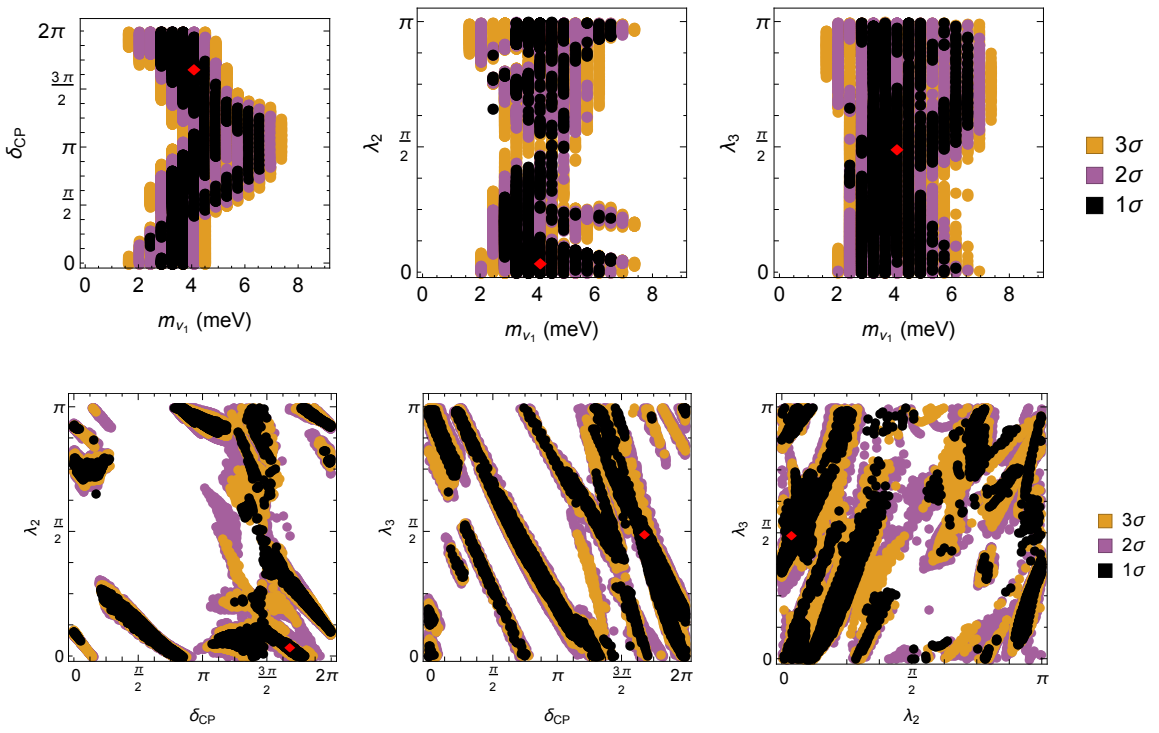

Figure 2.7: Correlations between the predictions of our model. Top: correlation between the leptonic CP phases $\delta, \lambda_2, \lambda_3$ and the lightest neutrino mass m_{ν_1}. Bottom: correlation between the different leptonic CP phases. Points within the 68%, 95% and 99.7% CL intervals for the leptonic mixing angles are respectively marked in orange, purple and black, and the best fit point of Table 2.2 is shown as ared diamond. Only points leading to the correct baryon asymmetry are shown.

described in section 2.2.1, which is valid between the scale of the RH neutrino masses and the scale of spontaneous CP breaking. A complete analysis of this effective theory is crucial for our purposes, since it is the theory that contains all the relevant information for leptogenesis.

As we did in section 2.3, in this section we use a formal description of flavor symmetries and polynomial invariants, now for a type I seesaw model. The description of the polynomial invariants of a type I seesaw model is left for appendix A.2.

2.4.1 Parameter counting using invariants

The leptonic sector of a general type I seesaw model with three right handed neutrinos contains twenty-one independent observables (six CP violating phases and fifteen real observables), as described in the appendix A.2. Twelve of these parameters correspond to the twelve leptonic observables at the electroweak scale, namely the six charged lepton masses and the six elements of the PMNS matrix. The remaining independent nine physical parameters, which we call UV observables, are not measurable at the electroweak scale, and they correspond to the three RH neutrino masses

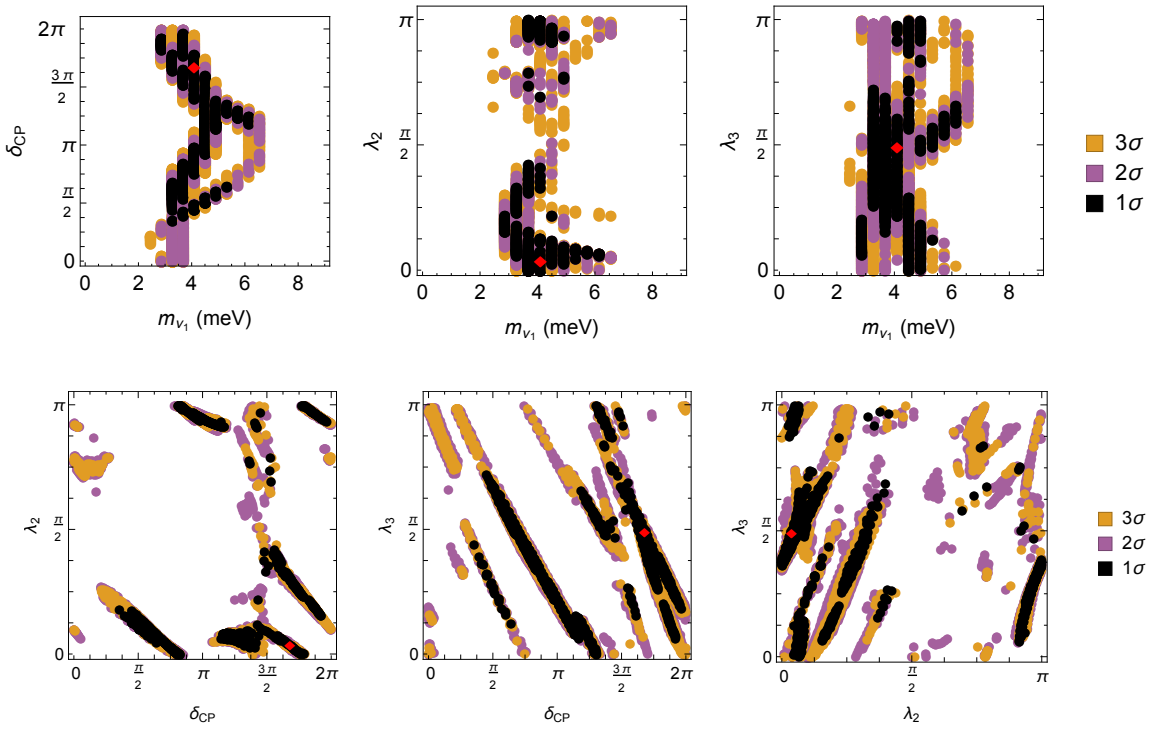

Figure 2.8: Same as Fig. 2.7, but with a projected 2× improvement in the experimental errors for the lepton mixing angle (assuming the central values stay the same).

and six elements of a complex orthogonal matrix defined in (A.2.4). Of these last six elements, three are real and three are complex, so we will loosely call them "UV mixing angles" and "UV CP violating phases".

Due to the conditions (2.2.19), the effective theory presented in section 2.2.1 is not the most general type I seesaw model, and not all of the twenty-one observables are independent. Moreover, constraints on the nine UV observables can be made from data at the electroweak scale. We now show that the twenty-one observables are all fixed by known data at the electroweak scale, the RH neutrino masses and $\tan\beta$.

First, note that as described in section 2.3.1, the twelve observable parameters at the electroweak scale are completely specified in our model by known data at the electroweak scale from the quark and lepton sector. As explained in section 2.3.1 this is non-trivial, since not all the elements of the PMNS nor the mass of the lightest neutrino matrix have been measured to date. These yet unmeasured parameters are predicted by our model. No knowledge of $\tan\beta$ or the RH neutrino masses is required to specify the value of these twelve IR observables.

On the other hand, the nine UV observables cannot be chosen to be independent, due to the non-trivial conditions (2.2.19). To identify the independent UV observables, we first list a complete

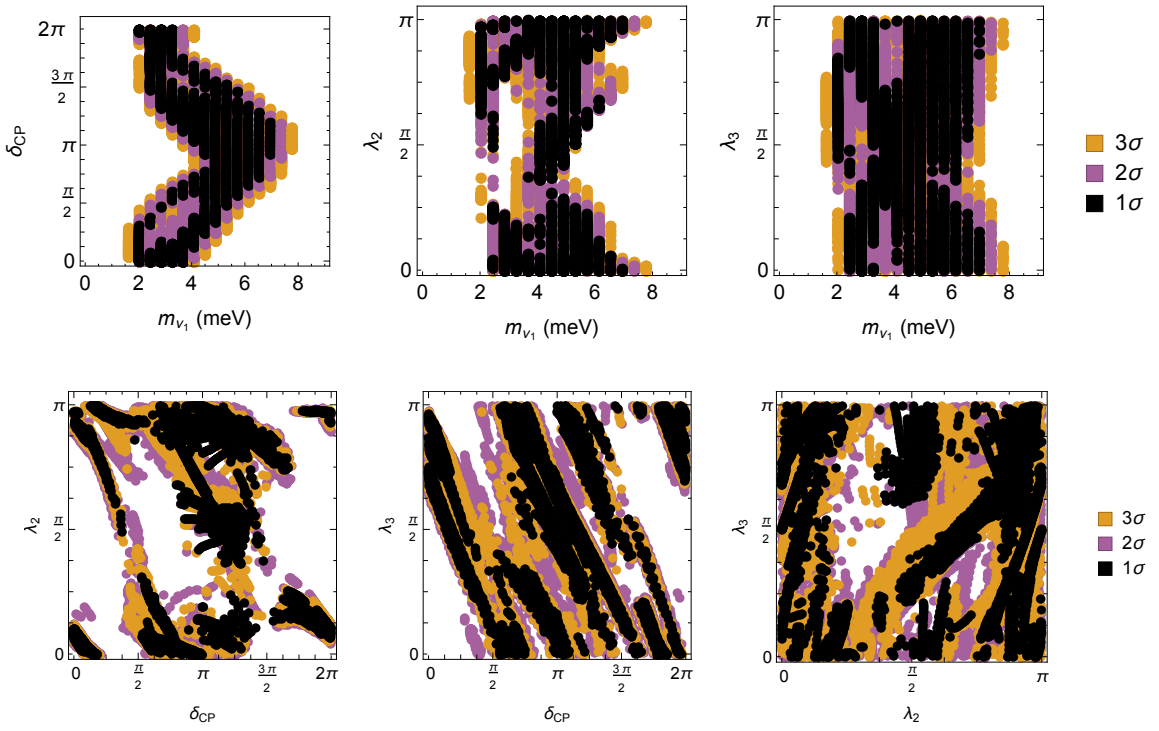

Figure 2.9: Same as Fig. 2.7, but for points leading to the wrong sign of the baryon asymmetry.

set of nine UV polynomial invariants (A.2.7)-(A.2.13)

$$\begin{aligned}
&\text{Tr}\ \left(M^* M\right)^n \\
&\text{Tr}\ \left[\lambda_N^\dagger \lambda_N, M^* M\right]^2 \\
&\text{Tr}\ \left[\lambda_N^\dagger \lambda_N, M^* \lambda_N^\dagger \lambda_N M\right]^2 \\
&\text{Tr}\ \left(\left[\lambda_N^\dagger \lambda_N, M^* M\right]^2 \left(M^* \lambda_N^\dagger \lambda_N M\right)\right) \\
&\text{Tr}\ \left[\lambda_N^\dagger \lambda_N, M^* M\right]^3 \\
&\text{Tr}\ \left[\lambda_N^\dagger \lambda_N, M^* \lambda_N^\dagger \lambda_N M\right]^3 \\
&\text{Tr}\ \left(\left[\lambda_N^\dagger \lambda_N, M^* M\right] \left(M^* \lambda_N^\dagger \lambda_N M\right)\right)
\end{aligned} \tag{2.4.1}$$

where $n = 1, 2, 3$. The UV polynomial invariants can be completely specified by taking traces involving the matrices M and $\lambda^{N\dagger}\lambda^N$ in any basis. In the basis we work on the right-handed neutrino mass matrix M is diagonal and real, as specified in equation (2.2.6)

$$M_{ij} = \delta_{ij} M_i \tag{2.4.2}$$

The eigenvalues M_i cannot be predicted in our model. Note that the hierarchy of the RH neutrino mass matrix is physically meaningful. For instance, swapping the values of M_1 and M_2 leads to

different physical results, since it leads to different values for the polynomial invariants (2.4.1).

On the other hand, using the non-trivial conditions (2.2.19) the matrix $\lambda^{N\dagger}\lambda^N$ can be written as

$$\lambda^{N\dagger}\lambda^N = \Gamma^N(\lambda^d\lambda^{d\dagger})^*\Gamma^N \tag{2.4.3}$$

where Γ^N is a real, diagonal matrix defined in (2.2.21). It is related to the real, diagonal matrix Γ^m (which is known from measured IR data, see section 2.3.1), through (2.2.26),

$$\frac{v_d^2}{v_u^2}\Gamma^m = \Gamma^N M^{-1}\Gamma^N \tag{2.4.4}$$

Since Γ^N and M are real diagonal matrices, from (2.4.4) we obtain

$$\Gamma^N = \frac{v_d}{v_u}\sqrt{M}\sqrt{\Gamma^m} \tag{2.4.5}$$

Using (2.4.5) in (2.4.3) and $m^d = v_d\lambda^d$ we get

$$\lambda^{N\dagger}\lambda^N = \frac{1}{v_u^2}\sqrt{M}^{\,\dagger}\sqrt{\Gamma^m}^{\,\dagger}(m^d m^{d\dagger})^*\sqrt{M}\sqrt{\Gamma^m} \tag{2.4.6}$$

Note that $\sqrt{M}$ and $\sqrt{\Gamma^m}$ can contain imaginary elements, since the real diagonal matrices M and Γ^m need not be positive. Finally, using the known expression for $m^d m^{d\dagger}$ (2.3.8) in (2.4.6) we get

$$\begin{aligned}\lambda^{N\dagger}\lambda^N \;=\; & \frac{1}{v^2\sin^2\beta}\sqrt{M}^{\,\dagger}\sqrt{\Gamma^m}^{\,\dagger}\Big[\mathrm{diag}(1,e^{i\gamma_1},e^{i\gamma_2})\,V_{\mathrm{CKM}}^*\,\mathrm{diag}(m_d^2,m_s^2,m_b^2)\\ & V_{\mathrm{CKM}}^T\,\mathrm{diag}(1,e^{-i\gamma_1},e^{-i\gamma_2})\Big]^*\;\sqrt{M}\sqrt{\Gamma^m}\end{aligned} \tag{2.4.7}$$

As discussed in section 2.3.1, the parameters γ_1, γ_2 and the three elements of the real diagonal matrix Γ^m can be obtained from known data at the electroweak scale. The only unknowns in (2.4.7) are $\tan\beta$ and the three RH neutrino masses that set the diagonal matrix M.

We are now ready to do the parameter counting. Using (2.4.2) and (2.4.7) in (2.4.1), we see that the nine UV invariants can be fixed by known IR data and four unknown model parameters: the three RH neutrino masses M_i, $i = 1, 2, 3$ and $\tan\beta$. Given these four unknown model parameters, the three "UV mixing angles" and three "UV CP violating phases" can be predicted. This is the final result of this section.

2.4.2 Thermal leptogenesis

Thermal leptogenesis is a very simple mechanism to generate the observed baryon asymmetry. We now briefly summarize the mechanism and then apply the predictions of our model to generate the asymmetry.

For simplicity, we consider hierarchical RH neutrinos, $M_a \ll M_b, M_c$, where a, b, c take different values from 1 to 3. Which one of the RH neutrinos N_1, N_2, N_3 is the lightest is relevant, as discussed in section 2.4.1. In thermal leptogenesis, a large population of N_a is produced thermally from scattering of the Higgs with leptons when $T > M_a$. N_a might or might not reach its equilibrium number density $n_{N_a}^{\rm eq} \approx n_\gamma$, depending on the strength of its Yukawa coupling with the Higgs. If the Yukawas of the RH neutrinos to the Higgs doublet and lepton doublets contain a CP violating phase, any change of the N_a abundance through these interactions generates a lepton asymmetry. Any time an asymmetry is generated, it tends to be washed out by the inverse process, since it represents a chemical disequilibrium. In the end, the interplay of the production of RH neutrinos, their decay and the washout process leads to a residual asymmetry, but only if the process gets out of equilibrium at some point of the evolution. If it does not, any remaining asymmetry will be washed out.

The interplay of production, decay and washout is contained in the Boltzmann equations for the RH neutrino abundance and the lepton (and slepton) asymmetry. We consider the simplified Boltzmann equations [49]

$$\frac{d}{dx}\left(Y_{N_a}(x)\right) = -\left(Kx\frac{K_1(x)}{K_2(x)}\right)\left(Y_{N_a}(x) - Y_{N_a}^{\rm eq}(x)\right) \tag{2.4.8}$$

$$\frac{d}{dx}\left(\Delta Y_{L_\alpha+\tilde{L}_\alpha}(x)\right) = \left(Kx\frac{K_1(x)}{K_2(x)}\right)\left[2\epsilon_\alpha\left(Y_{N_a}(x) - Y_{N_a}^{\rm eq}(x)\right) - \frac{1}{2}\left(\frac{K_{\alpha\alpha}}{K}\frac{Y_{N_a}^{\rm eq}(x)}{Y_L^{\rm eq}(x)}\right)\Delta Y_{L_\alpha}(x)\right] \tag{2.4.9}$$

where $K_{1,2}(x)$ are the modified Bessel function of the second kind and

$$\begin{aligned} x &= \frac{M_a}{T} \\ Y_{N_a, L_\alpha+\tilde{L}_\alpha} &= \frac{n_{N_a, L_\alpha+\tilde{L}_\alpha}}{s} \\ K_{\alpha\alpha} &= \frac{\Gamma_{N_a\to L_\alpha}}{H|_{T=M_a}} \\ K &= \sum_\alpha K_{\alpha\alpha} \end{aligned} \tag{2.4.10}$$

and the CP asymmetry parameter is defined as

$$\epsilon_\alpha = \frac{\Gamma_{N_a\to L_\alpha H_u} - \Gamma_{N_a\to \overline{L}_\alpha H_u^*}}{\Gamma_{N_a\to L H_u} + \Gamma_{N_a\to \overline{L} H_u^*}} \tag{2.4.11}$$

In the equation for the evolution of the lepton asymmetry (2.4.9), the first term on the right hand side corresponds to the contribution to the asymmetry due to production and decay of the RH neutrinos when there exists CP violation. The second term is the washout term which tends to erase any asymmetry. Note that the solution for the asymmetry in the simplified Boltzmann equations are linear in ϵ_α. In particular, $\Delta Y_{L_\alpha+\tilde{L}_\alpha}(\lambda\epsilon_\alpha) = \lambda \Delta Y_{L_\alpha+\tilde{L}_\alpha}(\epsilon_\alpha)$.

The corresponding baryon asymmetry over the entropy density is [49]

$$\frac{n_B}{s} \simeq -\frac{10}{31}\sum_\alpha \Delta Y_{L_\alpha+\tilde{L}_\alpha}. \tag{2.4.12}$$

The numerical prefactor takes into account that the lepton asymmetry is not entirely converted into a baryon asymmetry by sphaleron processes. The input from microscopic physics enters in (2.4.9) through $K_{\alpha\alpha}$ and ϵ_α. In terms of the Yukawas of the seesaw model and the light neutrino mass matrix they are given by [49]

$$\begin{aligned} K_{\alpha\alpha} &= \frac{M_a}{H|_{T=M_a}}\left[\frac{\lambda^{N*}_{\alpha a}\lambda^N_{\alpha a}}{8\pi}\right] \\ \epsilon_\alpha &= -\frac{3M_a}{8\pi v_u^2\,\lambda^{N*}_{\beta a}\lambda^N_{\beta a}}\mathrm{Im}\left[\lambda^N_{\alpha a}(m^{\nu*}_{\alpha\beta}\lambda^N_{\beta a})\right] \end{aligned} \tag{2.4.13}$$

where only sum over the index β is intended, $H|_{T=M_a} = 1.66\, g_*^{1/2} M_a^2/M_{Pl}$ and in the MSSM, $g_* = 228.75$.

CP violation enters in the calculation through the asymmetry parameter ϵ_α. In a general type I seesaw model, the CP violation needed for leptogenesis is uncorrelated with the CP violating phases of the PMNS matrix [50]. The asymmetry parameter ϵ_α is only sensitive to the UV CP violating phases, that cannot be measured in experiments below the scale of the RH neutrino masses. Our model, however, is not a general type I seesaw model, since it contains non-trivial conditions (2.2.19) relating different Yukawa matrices. This provides relations between different observables. In section 2.4.1 we showed that in our model, all the UV observables, including the UV CP violating phases, are fixed by known data from the IR, the three RH neutrino masses and $\tan\beta$. Moreover, since thermal leptogenesis relies only on the decay of the lightest RH neutrino, one might expect that in our model, only the knowledge of the lightest RH neutrino mass and $\tan\beta$ are needed to calculate the resulting baryon asymmetry from leptogenesis. We now show that this statement is correct and calculate the baryon asymmmetry by explicitly obtaining $\lambda^N_{\alpha a}$ and m^ν, which determine $K_{\alpha\alpha}$ and ϵ_α.

First, note from (2.4.7) that the matrix $\lambda^{N\dagger}\lambda^N$ is a known function of IR data and the RH neutrino masses. Also note that any matrix λ^N satisfying (2.4.7) leads to the same physical results, because all the polynomial invariants (2.4.1) depend only on the combination $\lambda^{N\dagger}\lambda^N$. Then, we are free to choose

$$\lambda^N = \frac{1}{v_u}\Big[\mathrm{diag}(m_d, m_s, m_b)\, V^T_{\mathrm{CKM}}\, \mathrm{diag}(1, e^{-i\gamma_1}, e^{-i\gamma_2})\Big]^*\, \sqrt{M}\sqrt{\Gamma^m} \tag{2.4.14}$$

where in section 2.3.1 we obtained the real diagonal matrix Γ_m and the phases γ_1, γ_2 from known IR data. In the basis we work on, M is diagonal, so we commute it with Γ_m and we obtain the

element α, a of the matrix λ^N

$$\lambda^N_{\alpha a} = \frac{1}{v_u}\Big[\mathrm{diag}(m_d, m_s, m_b)\, V^T_{\rm CKM}\, \mathrm{diag}(1, e^{-i\gamma_1}, e^{-i\gamma_2})\sqrt{\Gamma^m}^{\,*}\Big]^*_{\alpha a}\, \sqrt{M_a} \tag{2.4.15}$$

On the other hand, the neutrino mass matrix is known from (2.3.16), we repeat the expression here for convenience

$$\begin{aligned} m^\nu &= \mathrm{diag}(m_d, m_s, m_b)\, V^\dagger_{\rm CKM}\, \mathrm{diag}(1, e^{i\gamma_1}, e^{i\gamma_2})\Gamma^m \\ &\quad\ \mathrm{diag}(1, e^{i\gamma_1}, e^{i\gamma_2})\, V^*_{\rm CKM}\, \mathrm{diag}(m_d, m_s, m_b) \end{aligned} \tag{2.4.16}$$

where γ_1, γ_2 and the real diagonal matrix Γ^m are known from IR data.

Using (2.4.15) and (2.4.16) in (2.4.13) we immediately see that $K_{\alpha\alpha}$ and the CP asymmetry ϵ_α are completely specified by IR physics and the mass of the lightest RH neutrino, M_a. No knowledge of the masses of the heavier RH neutrinos is needed, in the range of validity of the calculations.

We now give a numerical example, using the benchmark point of Table 2.2. We consider the lightest neutrino mass to be M_1. Using the model parameters of Table 2.2 in (2.4.15) and (2.4.16), we obtain the flavored CP asymmetry parameters

$$\epsilon_1 \simeq \frac{1.07\cdot 10^{-9}}{\sin^2\beta}\left[\frac{|M_1|}{10^{10}\,\mathrm{GeV}}\right] \qquad \epsilon_2 \simeq -\frac{4.21\cdot 10^{-7}}{\sin^2\beta}\left[\frac{|M_1|}{10^{10}\,\mathrm{GeV}}\right] \qquad \epsilon_3 \simeq \frac{1.17\cdot 10^{-8}}{\sin^2\beta}\left[\frac{|M_1|}{10^{10}\,\mathrm{GeV}}\right] \tag{2.4.17}$$

where $\tan\beta = 10$. The CP asymmetries are linear in $|M_1|$. As a consequence, the baryon asymmetry is also linear in $|M_1|$. Using (2.4.17) in (2.4.12) and numerically solving the Boltzmann equations we obtain

$$\frac{n_B}{s} \simeq \frac{8.29\cdot 10^{-10}}{\sin^2\beta}\left[\frac{|M_1|}{10^{10}\,\mathrm{GeV}}\right] \tag{2.4.18}$$

For our benchmark point, the correct baryon asymmetry can be obtained for $M_1 \simeq 10^9\,\mathrm{GeV}$. Equation (2.4.18) is a prediction of our model: the baryon asymmetry is linear in $|M_1|/\sin^2\beta$, and the proportionality constant is predicted by making use of known IR data.

The benchmark point of table 2.2 is the best fit value for the model parameters as determined by the low energy data. More generally, scanning over the set of model parameters that are consistent with all the IR data up to the experimental uncertainties, we find that for $\tan\beta = 10$, the correct baryon asymmetry can be obtained in a range

$$10^{-9}\,\mathrm{GeV} \lesssim |M_1| \tag{2.4.19}$$

One special feature of our model is that the sign of baryon asymmetry is part of the prediction: in our unified framework, the definition of "matter" in the quark sector (as given by the sign

of the CKM phase determining CP violation in say, kaon mixing) defines "matter" in the lepton sector. Thus, only the *negative* sign of the lepton asymmetry is phenomenologically acceptable. As described above, known IR data ultimately determines (up to experimental uncertainties) the sign of the asymmetry parameters ϵ_α and of the final baryon asymmetry. In reality, within the experimental uncertainties in the lepton sector both signs of the asymmetry are still allowed. Different signs are correlated with different predictions for the CP phases in the PMNS matrix.

We illustrate this effect in Fig. 2.10, where we set the lightest (left-handed) neutrino mass to the best fit value $m_{\nu_1} = 5 \times 10^{-3}$ and display the allowed parameter space for the UV parameters γ_1, γ_2 (for presentation purposes, we choose the linear combinations $(\gamma_1 - \gamma_2, \gamma_1 + \gamma_2)$ for the axes). In the white region, there are no solutions to Eq. (2.3.13) to reproduce the observed light neutrino masses, while in the colored region solutions exist: there, the correct (positive) sign is given in the yellow/red tones and the incorrect sign in blue tones. Because the Boltzmann equations are homogeneous in $|M_1|$, we can also display the value of the lightest right-handed neutrino mass needed to achieve the correct absolute value of the baryon asymmetry n_B/s, with different hues of red and blue corresponding to different values in the range $|M_1| = 10^9 - 10^{11}$ GeV. Finally, we also show contours delimiting regions consistent with the lepton mixing angles at 1,2, and 3σ, according to the χ^2 test described in Sec. 2.3.3. In a world with perfect experimental resolution for the mixing angles, some of these regions will disappear and one will shrink to the black diamond, corresponding to the benchmark point described in Table 2.2. In section 2.3.3 and Figs. 2.4, 2.7, we only displayed the points leading to the correct sign of the baryon asymmetry. This lead to sharper predictions for the IR data $m_{\nu_1}, \delta, \lambda_2$ and λ_3.

In Fig. 2.11, we show the correlation between the baryon asymmetry and the predictions for yet-to-be-measured IR observables, where for concreteness the RH neutrino mass is set as $M_1 = 10^{11}$ GeV. This should be compared to the experimental value, $n_B/s = (0.8 \pm 0.2) \times 10^{-11}$ [47]. The benchmark point in Table 2.2 gives the correct baryon asymmetry when $M_1 = 10^{11}$ GeV. As in the previous section, we use a color scheme where points consistent with the measured leptonic mixing angles at the $68\%, 95\%$ and 99.7% CL are purple, orange and black, respectively. Only points with $n_B/s > 0$ are consistent with the baryon asymmetry being generated after sphaleron processing of the epton asymmetry from thermal leptogenesis.[5] Because the asymmetry parameters $\epsilon_{1,2,3}$ are linear in $|M_1|$, even points in Fig. 2.11 that do not yield the correct magnitude of the baryon

[5]However, it is possible to decouple baryogenesis from the IR predictions of our model if it is assumed that a different mechanism was responsible for the generation of the baryon asymmetry: in this case, our unified model still describes all the IR observables and predicts the correlations described in Section 2.3. In particular, the correlations show in Fig. 2.9 will now also be phenomenologically acceptable.

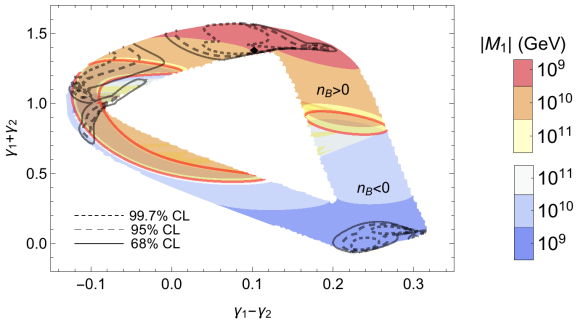

Figure 2.10: Values of the lightest RH neutrino mass M_1 required to achieve the observed magnitude for the baryon asymmetry, for $m_{\nu_1} = 5 \times 10^{-3}$ eV and as a function of the UV parameters γ_1, γ_2 (here reparametrized in the $(\gamma_1 - \gamma_2, \gamma_1 + \gamma_2)$ plane for clarity). Colored regions give solutions to Eqs. (2.3.12)–(2.3.13), before enforcing agreement with the lepton mixing angles. Regions shaded in red (blue) give the correct (wrong) sign for the baryon asymmetry, and are separated by the red lines. Note that at each point in the γ_1, γ_2 plane there are up to 6×24 distinct solutions for Eqs. (2.3.12)–(2.3.13), some of which will yield different mixing angles and baryon asymmetries; for example, in the region enclosed by red lines solutions exist for both signs of n_B, meaning that this region can give the correct (positive) baryon asymmetry. Black contours with continuous, dashed and dotted lines demarcate respectively the parameter space regions laying within the $68\%, 95\%$ and 99.7% CL intervals for the leptonic mixing angles. Taking into account the lepton mixing angles, phenomenologically acceptable regions are the red regions enclosed by the continuous black contours. The benchmark point of table 2.2 is shown as a black diamond.

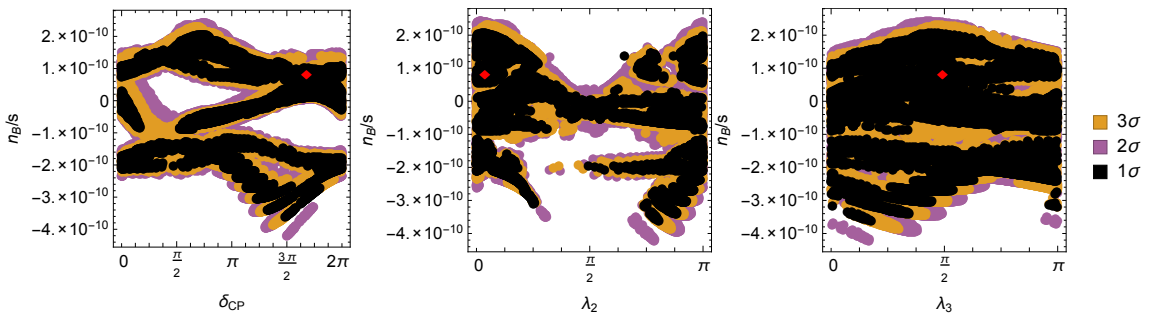

Figure 2.11: Correlation between the baryon asymmetry and the IR parameters of our model, for $|M_1| = 10^{11}$ GeV. Points within the $68\%, 95\%$ and 99.7% CL intervals for the leptonic mixing angles are respectively marked in orange, purple and black, and the benchmark point of Table 2.2 is shown as ared diamond.

asymmetry will be able to, for different values of $|M_1|$. We illustrate this in Fig. 2.12, where we show the correlation between the value of $|M_1|$ needed to reproduce the observed baryon asymmetry and the IR CP-violating phases δ_{CP}, λ_2 and λ_3. The correlation between δ_{CP} and $|M_1|$ is particularly strong, and a future measurement of the Dirac neutrino phase has the power of predicting the RH neutrino mass scale. As in the previous sections, it is worth noting that a better experimental resolution for the lepton angles will sharpen these predictions.

We conclude with some comments on the cosmology of our model. First, note that for the lepto-

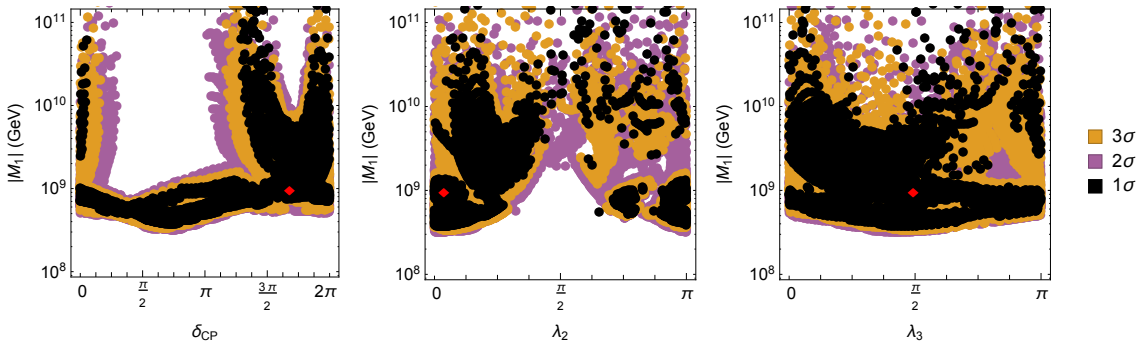

Figure 2.12: Correlation between the RH neutrino mass scale $|M_1|$ and the IR observables of our model, obtained by requiring that the correct matter-antimatter asymmetry is generated during leptogenesis. Points within the 68%, 95% and 99.7% CL intervals for the leptonic mixing angles are respectively marked in orange, purple and black, and the benchmark point of Table 2.2 is shown as ared diamond.

genesis mechanism to work, the reheating temperature after inflation T_R should be higher than the lightest RH neutrino mass, *i.e.* it should be larger than $10^9 - 10^{11}$ GeV. The reheating temperature is also bounded from above by M_{CP}. The reason is that when CP is spontaneously broken, there can be discrete number of vacua and long-lived domain wall will be generically produced. A lower reheating temperature assures that domain walls have been inflated away. Thus, a set of necessary conditions for successful leptogenesis in our model are (2.4.19) and

$$M_a \lesssim T_R \lesssim M_{CP} \tag{2.4.20}$$

The high reheating temperature leads to cosmological constraints on the gravitino mass. For thermalized gravitinos in the early universe, the gravitino energy density is

$$\Omega_{\psi_{3/2}} h^2 = \frac{200}{g_*(T_{fr})} \left[\frac{m_{3/2}}{\text{keV}}\right] \tag{2.4.21}$$

where T_{fr} is the freeze-out temperature for gravitino production. To avoid overclosure of the universe, the gravitino has to be light. Moreover, astrophysical constraint on structure formation set the strong bound $m_{3/2} < 16\,\text{eV}$ [51]. Correspondingly, the supersymmetry breaking messenger scale is constrained to be $M_m \lesssim 100\,\text{TeV}$. In this way, a cosmological history that include leptogenesis at high temperatures automatically prevents a sizable contribution to $\overline{\theta}$.

Chapter 3

125 GeV Higgs from Tree-level A-terms

3.1 Introduction

In the previous chapter, we built a supersymmetric model to solve the puzzle of CP violation in the Standard Model. Experimental evidence indicates that if supersymmetry is a symmetry of nature, it must be broken at low energy scales. A particularly well motivated supersymmetry breaking mechanism is gauge mediated SUSY breaking (GMSB, for a review and original references, see [13]). Since gauge interactions are flavor blind, gauge mediated supersymmetry breaking does not induce flavor breaking effects that would be heavily constrained by flavor experiments. In this chapter, we build a detailed model of gauge mediated supersymmetry breaking, which is consistent with all the low energy phenomenology.

In particular, the discovery of the Higgs boson with a mass near 125 GeV [1, 2] has important consequences for physics beyond the Standard Model, especially supersymmetry. In the MSSM, it implies that the stops must either be very heavy or have a large trilinear coupling ("A-term") with the Higgs [14, 52–59]. The large A-term scenario is more interesting from several points of view. It is less fine-tuned and it allows for lighter ($\sim$ 1 TeV) stops that are still within reach of the LHC. It also presents an interesting model-building challenge – prior to the discovery of the Higgs, mechanisms for generating the A-terms from an underlying model of SUSY-breaking mediation were not well-explored.

In the framework of gauge mediated SUSY-breaking, the problem of how to obtain large A-terms becomes especially acute. In GMSB, the A-terms are always negligibly small at the messenger scale. If the messenger scale is sufficiently high and the gluino sufficiently heavy, a sizable weak scale A-term with relatively light stops may be generated through RG-running [14]. However,

this setup is in strong tension with electroweak symmetry breaking (EWSB) [60]. This strongly motivates extending gauge mediation with additional MSSM-messenger couplings that generate A-terms through threshold corrections at the messenger scale.

In all models for A-terms considered since the observation of a Higgs boson at 125 GeV [61–74], the focus has been on generating A-terms at one-loop level through weakly coupled messengers. Integrating out the messengers produces one or more of the following Kähler operators

$$\frac{1}{16\pi^2}\frac{1}{M}X^\dagger H_u^\dagger H_u \ , \qquad \frac{1}{16\pi^2}\frac{1}{M}X^\dagger Q_3^\dagger Q_3 \ , \qquad \frac{1}{16\pi^2}\frac{1}{M}X^\dagger \overline{u}_3^\dagger \overline{u}_3 \tag{3.1.1}$$

Here X is a field that spontaneously breaks SUSY, and M is the messenger scale. After substituting $\langle X\rangle = \theta^2 F_X$ and integrating out the auxiliary components of the MSSM fields, one obtains the desired A-term

$$\mathcal{L} \supset y_t A_t H_u Q_3 \overline{u}_3 \quad , \quad A_t \sim \frac{1}{16\pi^2}\frac{F_X}{M} \tag{3.1.2}$$

This setup has the advantage that the A-terms come out parametrically the same size as the other soft masses in GMSB (one-loop gaugino masses, two-loop scalar mass-squareds). However, one-loop A-terms from (3.1.1) introduce a host of complications as well. First and foremost is the "A/m^2 problem" [62]: in addition to the A-terms, one also generates a scalar mass-squared at one-loop, completely analogous with the more well-known μ/B_μ problem. A one-loop scalar mass-squared would overwhelm the GMSB contributions and lead to serious problems with fine-tuning and/or EWSB. Previous solutions to the A/m^2 problem include taking the messengers to be those of minimal gauge mediation [62], or having the hidden sector be a strongly-coupled SCFT [64, 65].

In this chapter, we will explore a new solution to the A/m^2 problem: models where the A-terms are generated *at tree-level in the MSSM-messenger couplings*. The advantage with this approach is that there is simply no A/m^2 problem to begin with, since at worst any accompanying sfermion mass-squareds would be tree-level as well. An added benefit of this approach is that it will lead us to a consider an interesting new operator for the A-terms: one which arises in the effective *superpotential*, rather than in the Kähler potential. As we will see, this superpotential operator will have qualitatively different effects on the MSSM soft terms as compared to Kähler potential operators.

The basic setup is quite simple. To generate a tree-level A-term, either the Higgs or stops must mix with the messengers in the mass-matrix. For example, consider the superpotential

$$W = X' H_u \tilde{\phi} + \lambda_u^{ij} \phi Q_i \overline{u}_j + M \tilde{\phi}\phi \tag{3.1.3}$$

Here X' is another spurion for SUSY-breaking, and ϕ, $\tilde{\phi}$ are heavy messenger fields. Upon integrating out the messengers at the scale M, one generates the effective superpotential operator

$$W_{eff} \supset -\frac{\lambda_u^{ij}}{M} X' H_u Q_i \overline{u}_j \tag{3.1.4}$$

Note that because of the SUSY non-renormalization theorem, W_{eff} can *only* arise at tree-level, so it is perfectly suited for our purposes. In order to produce an A-term of the correct size, one must have[1]

$$\frac{F_{X'}}{M} \sim \mathcal{O}(\text{TeV}) \tag{3.1.5}$$

The tree-level A-term originating from (3.1.4) is minimally flavor violating (MFV), provided that the operator in (3.1.4) generates the full up-type Yukawa coupling of the MSSM. For this to work, X' should acquire a lowest component vev of size $\sim M$.

The interesting complication in these models comes from the fact that when integrating out the messengers, in addition to the superpotential operator (3.1.4), a Kähler potential operator is also generated at tree-level. For example, in the model (3.1.3), one generates the term:

$$K_{eff} \supset \frac{1}{M^2} X'^{\dagger} X' H_u^{\dagger} H_u \tag{3.1.6}$$

(For a more general treatment of the Kähler operators, see appendix A.) This leads to a soft mass for H_u of roughly the same order as the A-term:

$$\delta m_{H_u}^2 = -\frac{y_t^2}{|\lambda_u^{33}|^2} |A_t|^2 \tag{3.1.7}$$

For $\lambda_u^{33} \lesssim 1$, this represents a large, irreducible contribution to $m_{H_u}^2$, and correspondingly to the fine-tuning of the electroweak scale. This is another manifestation of the "little A/m^2 problem" encountered in [62], whereby a large A-term was accompanied by an equally large sfermion mass-squared. In [62], the situation was even worse, because the contribution was irreducible with a fixed coefficient:

$$\delta m_{H_u}^2 = |A_t|^2 \tag{3.1.8}$$

There both the A-terms and the irreducible contribution to $m_{H_u}^2$ (3.1.8) originated from integrating out the auxiliary components of the MSSM fields in the first Kähler operator in (3.1.1). Since we are starting instead with the effective superpotential operator (3.1.4), the coefficient in (3.1.7) is free to vary in our present models. Importantly, however, we will see that the sign in (3.1.7) is always

[1] Note that this is a loop factor smaller than the usual GMSB relation. A smaller F-term satisfying this hierarchy can easily be dynamically generated using weakly-coupled messengers, see e.g. [75]. In this chapter we will simply assume that $F_{X'}$ of the right size can be obtained somehow and not explore it any further.

negative, such that (3.1.7) does not jeopardize electroweak symmetry breaking, in contrast to the relation in (3.1.8).

In this chapter, we will consider various ways to alleviate the fine-tuning problem introduced by the little A/m^2 problem (3.1.7). Clearly, if λ_{33} is taken to be large (e.g. $\lambda_{33} \sim 3$), then the little A/m^2 problem is ameliorated. This requires a UV completion at a relatively low scale. We will provide such a UV completion in this chapter, using a novel application of Seiberg duality [76, 77].

Alternatively, one can consider non-MFV models obtained from (3.1.3) by exchanging the role played by H_u with $\overline{u}_3$:[2]

$$W = X'\overline{u}_3\tilde{\phi}_u + \kappa H_u Q_3 \phi_u + M\tilde{\phi}_u\phi_u \tag{3.1.9}$$

For this model the expression analogous to (3.1.7) contains $m^2_{\overline{u}_3}$ instead of $m^2_{H_u}$. As in [63], the fine-tuning is greatly reduced with respect to the perturbative MFV case because the stop contribution to $m^2_{H_u}$ is diluted by a loop factor. Moreover, the situation is even better than in [63], because in that case there were still sizeable two-loop contributions to $m^2_{H_u}$, whereas here the contribution is solely to the squarks.

An important thing to note about the framework for generating tree-level A-terms presented in this chapter is that it can in principle be tacked on to any mediation mechanism for the rest of the MSSM soft terms; the framework itself does not lead to a particularly compelling choice. This is in contrast to the one-loop models considered previously, whereby the A-term messengers also contributed to the MSSM soft spectrum through minimal gauge mediation, and thus GMSB was the most economical choice. Moreover, the tree-level A-term module does not affect the overall phenomenology much; the one essential difference occurs in the non-MFV models, where the stops can be split by several TeV due to the non-MFV analogue of (3.1.8).

For simplicity and concreteness, in this chapter we will couple our models to minimal gauge mediation (MGM) [79–81]. We will see that after imposing the Higgs mass constraint, the models are typically out of reach of Run I LHC; however they will be accessible (especially the lightest stop) at 14 TeV LHC. Finally, we will estimate the fine tuning in these models and show that they achieve essentially the best tuning possible in the MSSM (percent level).

The remainder of this chapter is organized as follows: Since no strongly coupled UV completion is needed for the non-MFV models, we discuss those first in section 2, as well as their phenomenology when coupled to minimal gauge mediation. In section 3 we analyze the MFV example in a similar

[2]Because these models are not MFV, one should worry about the potential constraints from precision flavor and CP observables. This is beyond the scope of this work (see however [78]). We will assume for simplicity (as in [63]) that the coupling κ is real and fully aligned with the third generation. We will also focus on the $\overline{u}_3$ model because then the flavor violation is limited to the up-squark sector and the constraints are much weaker.

way. In section 4, we UV complete the MFV model using Seiberg duality. Finally, in the conclusions we list some potential future directions suggested by our work. A general discussion of the little A/m^2 problem and Landau poles in models for tree-level A-terms is left for appendix B.

3.2 A non-MFV model

As discussed in the introduction, the non-MFV model (3.1.9) has a less severe version of the little A/m^2 problem, and thus does not need an immediate UV completion, unlike the MFV model (3.1.3). Since the story is simpler here, let us start by analyzing the non-MFV model in detail. Apart from the issues of flavor alignment discussed in the introduction, the form of the renormalizable superpotential (3.1.9) is the most general that couples the spurion, messengers and MSSM fields up to terms that are irrelevant for our purposes (powers of the spurion X' and a small soft mass for the messenger pair from $X'\phi_u\tilde{\phi}_u$).

After diagonalizing the mass matrix and integrating out $\phi_u, \tilde{\phi}_u$ at the messenger scale M, we obtain the IR effective theory

$$\begin{aligned} W_{eff} &\supset -\kappa \frac{X'}{M} H_u Q_3 \overline{u}_3 \\ K_{eff} &\supset \frac{X'^\dagger X'}{M^2} \overline{u}_3^\dagger \overline{u}_3 + \frac{\kappa^2}{M^2} H_u^\dagger H_u Q_3^\dagger Q_3 \end{aligned} \tag{3.2.1}$$

The irrelevant operator induced in the low energy superpotential leads to an A-term for the corresponding MSSM fields after substituting $\langle X' \rangle = \theta^2 F_{X'}$. However, an additional contribution to $m^2_{\overline{u}_3}$ from the first term in the Kähler potential is also induced, such that

$$\delta m^2_{\overline{u}_3} = -\frac{y_t^2}{\kappa^2} A_t^2 \tag{3.2.2}$$

Note that the contribution to $m^2_{\overline{u}_3}$ is negative, so to avoid a tachyonic right handed stop, it must be cancelled off by additional contributions at the messenger scale (e.g. from GMSB) or from MSSM renormalization group running from the messenger scale down to the weak scale. If $\kappa \sim 1$, the fine tuning from (3.2.2) is comparable to the fine tuning from the A-term itself, since both enter the running of $m^2_{H_u}$ in exactly the same fashion. Taking $\kappa > 1$ therefore does not substantially improve the overall fine tuning of the model. One major improvement relative to the non-MFV models considered in [63] is that there are no sizeable contributions generated to $m^2_{H_u}$ from integrating out the messengers.

To study the phenomenology of a model with tree-level A-terms and a 125 GeV Higgs, we must add our tree-level A-term module (3.1.9) to an underlying model for the rest of the MSSM soft masses. While in principle any model could be used, GMSB is a particularly well-motivated choice

given the SUSY flavor problem. So for simplicity and concreteness, let us now specialize to the case of minimal gauge mediation (MGM) with $\mathbf{5} \oplus \overline{\mathbf{5}}$ messengers [79–81].

The parameter space of our model is as follows. The MGM sector of the model is characterized by four parameters: messenger index N_m, $\tan\beta$, messenger scale M and SUSY-breaking mass scale $\frac{F_X}{M}$, where F_X is the highest component vev of the SUSY breaking spurion. We take the masses of the additional messengers in (3.1.9) to be the same scale M for simplicity. We consider μ and B_μ to be determined by the EWSB conditions and we remain agnostic about their origin. Finally, our model contains additional parameters $\frac{F_{X'}}{M}$, which sets the scale for the tree level contribution to A_t, and the coupling κ (see (3.1.9)).

A low messenger scale $M = 250$ TeV and a large messenger number $N_m = 3$ are motivated by the simultaneous requirements of reducing the tuning from the RG while allowing a large enough SUSY scale to be achieved for the Higgs mass. (A different choice of messenger number does not alter the phenomenology heavily, for reasons that will be explained later.) We take $\tan\beta = 20$ to saturate the tree level bound of the Higgs mass and $\kappa = 1$ for simplicity and perturbativity. With these choices, the parameter space of our models reduces to $(\frac{F_{X'}}{M}, \frac{F_X}{M})$. (Recall that we must take $\frac{F_{X'}}{M} \sim \frac{1}{16\pi^2}\frac{F_X}{M}$ to achieve A-terms comparable to the GMSB soft masses.) To make contact with the IR observables, we can trade $(\frac{F_{X'}}{M}, \frac{F_X}{M})$ by the IR values of A_t and the mass of the lightest stop $m_{\tilde{t}_1}$ or the mass of the lightest stau $m_{\tilde{\tau}_1}$. This parametrization is especially relevant for the LHC phenomenology, since $\tilde{t}_1$ and $\tilde{\tau}_1$ are the lightest colored particle and the NLSP respectively, as will be seen shortly.

To generate the IR spectrum we use `SOFTSUSY 3.5.1` [82]. Fine tuning Δ_{FT} is calculated according to the measure introduced in [63], given by

$$\begin{aligned} &\Delta_i \equiv \frac{\partial \log m_z^2}{\partial \log \Lambda_i^2} \qquad \Lambda_i \in \{g_1^2\frac{F_X}{M}, g_2^2\frac{F_X}{M}, g_3^2\frac{F_X}{M}, \frac{F_{X'}}{M}, \kappa\frac{F_{X'}}{M}, \mu\} \\ &\Delta_{FT} \equiv \max \Delta_i. \end{aligned} \tag{3.2.3}$$

The results are presented in figure 3.1 where we show contours of the Higgs mass, tuning and M_{SUSY}, both in the $(A_t, m_{\tilde{t}_1})$ and $(A_t, m_{\tilde{\tau}_1})$ planes. Note that M_{SUSY} is significantly larger than $m_{\tilde{t}_1}$. This is because the two stop soft masses are split due to the negative contribution to $m_{\tilde{u}_3}^2$ in (3.2.2). In the gray shaded region the GMSB contribution is insufficient to cancel this negative contribution, and the spectrum is invalidated by a stop tachyon. The main source of tuning in this model is the running effect due to the colored spectrum or the A-term. From the Higgs and tuning contour lines in both figures, we see that the model is able to reproduce the Higgs mass, while keeping fine tuning to the percent level (which is basically the best that can be achieved in the MSSM). Moreover, the

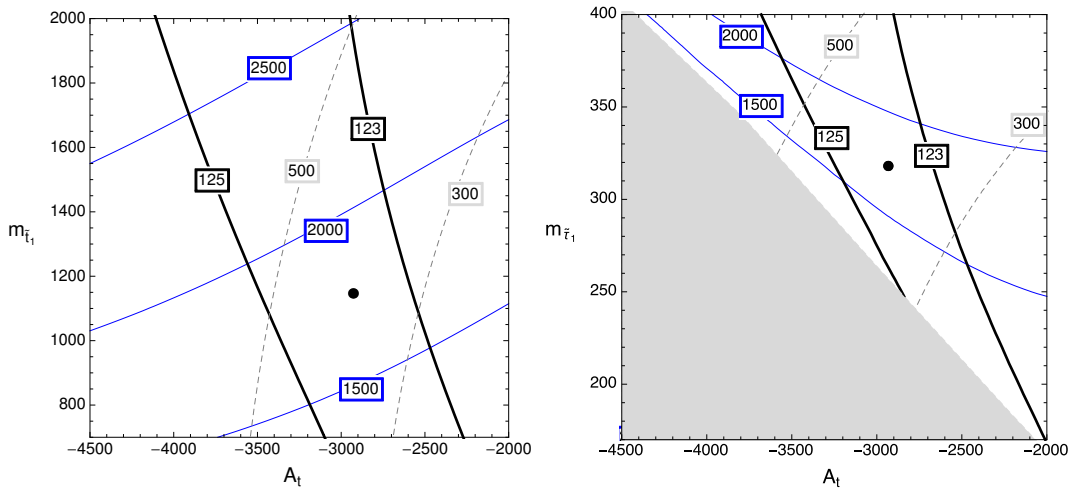

Figure 3.1: Contours of the Higgs mass (black), geometric mean of the stop masses (blue) and tuning (dashed), in the $(A_t, m_{\tilde{t}_1})$ (left) and $(A_t, m_{\tilde{\tau}_1})$ (right) planes. The shaded region on the $(A_t, m_{\tilde{\tau}_1})$ plane corresponds to points with tachyonic stops. The black dot on both figures corresponds to the same point in parameter space, with a spectrum presented in figure 3.2. All quantities are evaluated at M_{SUSY}.

Higgs mass can be reproduced in interesting parts of parameter space, where there is both a light colored particle $m_{\tilde{t}_1}$ and a light slepton $m_{\tilde{\tau}_1}$.

A typical spectrum for the model is presented in figure 3.2, which corresponds to the black dot indicated in the two different planes presented in figure 3.1.[3] In general, the spectrum across the parameter space of our model is basically that of MGM with $N_{mess} = 3$ (gaugino unification, colored sparticles heavier than electroweak sparticles, right-handed stau NLSP, etc.). There are, however, two key differences. First, in order to counteract the large negative contribution (3.2.2) to the right-handed stop, the MGM scale $\frac{F_X}{M}$ is considerably larger than would otherwise be the case. This results in the other colored sparticles being essentially decoupled. It also results in a higher gravitino mass, which explains [83] why slepton co-NLSPs do not occur in figure 3.1. Second, the right-handed sleptons are a bit lighter than in MGM due to the effects of running induced by the split stops. Amusingly, this effect of running means that the stau is the NLSP even for lower N_{mess}, unlike in MGM, where lowering N_{mess} leads to bino NLSP.[4]

Due to the split spectrum, the largest sparticle pair production cross sections at LHC correspond to $\tilde{t}_1$ and the right-handed sleptons. Pair production of stops leads to a decay chain with jets, leptons

[3] We choose our benchmark point here and in the next subsection to have $m_h = 124$ GeV in order to account optimistically for the theory uncertainty on the Higgs mass calculation.

[4] Note that if we exchange the roles of $\overline{u}_3$ and Q_3 in (3.1.9), a negative soft mass for Q_3 would be induced instead, leading to a heavier $\tilde{\tau}_1$ through running. In this case, it could be possible to have a bino NLSP even for $N_m > 1$.

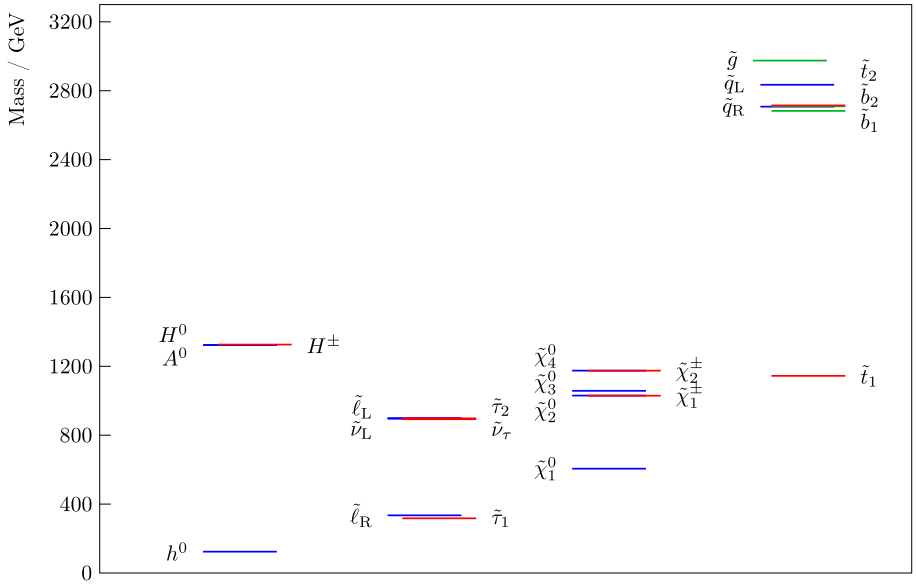

Figure 3.2: Spectrum for the point marked with the dot in figure 3.1. The Higgs mass is $m_h = 124$ GeV, with $A_t = -2.9$ TeV. $\tilde{\tau}_1$ is 17 GeV lighter than the right handed sleptons. The Higgsino mass is $\mu = 1.05$ TeV. Fine tuning is $\sim 1/400$.

and missing energy. When right handed sleptons are directly pair produced, the decay chain will include relatively soft leptons (due to the moderate splitting of the right handed sleptons and the stau), taus and missing energy. Of course the direct pair production of staus will lead to taus and missing energy.

Of the above signatures, the most spectacular one is given by the decay of pair produced stops, which can contain two jets, 4 leptons (from the decay of the bino to RH sleptons and RH sleptons to stau), and two τ jets plus missing energy. A search with a similar topology was carried out in [84], where a limit on the total strong production cross section of ~ 1 fb was obtained. This limit can be used to set an approximate bound on our parameter space, by comparing with our model's tree level total strong production cross section, which we obtain using MadGraph [85]. This leads to excluding stops roughly below 800 GeV in the parameter space presented in figure 3.1, which corresponds to staus heavier than 150 GeV.

The spectrum presented in figure 3.2 is inaccessible to the LHC run at 8 TeV, but it will become accessible at 14 TeV. The total SUSY cross section of such point at the 14 TeV LHC is 8 fb, while the total tree level colored production cross section is 2 fb. Relevant searches will be the updated versions of multilepton or GMSB-inspired searches as [86] and [84].

	X'	$Q, \overline{u}, \overline{d}, L, \overline{e}$	H_u	H_d	ϕ	$\tilde{\phi}$
$\mathbb{Z}_3$	1/3	2/3	1/3	2/3	2/3	1/3

Table 3.1: Charge assignments securing (3.3.1) and (3.3.2).

3.3 An MFV model

Next we will turn to the MFV model (3.1.3). Apart from the issues of UV completions to be discussed in the next section, this model is slightly more complicated than the non-MFV model because here we would like to generate the MSSM up-type Yukawas and the A-terms from the same operator. To achieve this, it is necessary to turn on a lowest component vev for X', which implies that one must re-diagonalize the messenger mass matrix prior to integrating out the messengers. For later convenience, we will redefine X' so that its lowest component vev is separated out and denoted by X'_0. Then (3.1.3) becomes

$$W = (X'_0 + X')H_u\tilde{\phi} + \lambda_u^{ij}\phi Q_i\overline{u}_j + M\phi\tilde{\phi} \tag{3.3.1}$$

with $\langle X' \rangle = F_{X'}\theta^2$. The form of (3.3.1) is the most general allowed by a $\mathbb{Z}_3$ symmetry, as detailed in table 3.1, which also allows for a μ-term and down type Yukawas,

$$\delta W = \mu' H_u H_d + \lambda_d^{ij} H_d Q_i \overline{d}_j + \lambda_e^{ij} H_d L_i \overline{e}_j \tag{3.3.2}$$

We will not discuss the down sector Yukawas any further.

After diagonalizing the mass matrix and integrating out the heavy messenger states, we are left with the supersymmetric effective action:

$$\begin{aligned} W_{eff} &\supset y_u^{ij}\left(1 + \cot\theta_H \cos\theta_H \frac{X'}{M'}\right) H_u Q_i \overline{u}_j + \mu\left(1 + \sin\theta_H \frac{X'}{M'}\right) H_u H_d \\ K_{eff} &\supset \frac{\cos^2\theta_H}{M'^2} X'^{\dagger} X' H_u^{\dagger} H_u + \frac{\cot^2\theta_H}{M'^2} y_u^{il} y_u^{jk*} Q_i^{\dagger} u_l^{\dagger} Q_j u_k \end{aligned} \tag{3.3.3}$$

where

$$M' = \sqrt{X_0'^2 + M^2}, \qquad \sin\theta_H = \frac{X'_0}{M'}, \qquad y_u^{ij} = -\lambda_u^{ij}\sin\theta_H, \qquad \mu = \mu'\cos\theta_H \tag{3.3.4}$$

and we have everywhere expanded in $\mu' \ll M, X_0$, keeping only the lowest nonzero order. In (3.3.3), the first term in the effective superpotential leads to an A-term proportional to the up-type Yukawas. The second term in the effective Kähler potential is an MFV interaction suppressed by the messenger scale, so it is safe from flavor constraints [87]. Meanwhile, the first term in K_{eff}

represents a contribution to the soft mass of H_u:[5]

$$\delta m_{H_u}^2 = -|A_t|^2 \tan^2\theta_H \tag{3.3.5}$$

This is a manifestation of the little A/m_H^2 problem. Note that this contribution is negative, so it is not dangerous for electroweak symmetry breaking, unlike what was found in the Kähler potential models [62]. However, if $\tan\theta_H \gtrsim 1$ it still represents a major contribution to fine-tuning. Taking $\tan\theta_H \ll 1$ would alleviate this fine-tuning problem, but at the cost of enlarging the underlying coupling λ_u^{33} according to (3.3.4). This leads to a Landau pole at low scales and a UV completion becomes necessary. Such a UV completion is the subject of section 3.4, in which we use Seiberg duality [76, 77] to realize the large coupling λ_u^{33}.

As in the previous section, to generate the rest of the soft masses we specialize to the case of MGM. The parameter space is essentially the same as before, namely the MGM sector is described by N_m, $\tan\beta$, M and $\frac{F_X}{M}$, while our effective theory contains $\frac{F_{X'}}{M}$ which sets the scale for the tree level contribution to A_t, and a coupling λ_u^{33}. Again, we consider μ and B_μ to be determined by the EWSB conditions. We fix most of the parameters to the same values as before – $N_m = 3$, $\tan\beta = 20$ and $M = 250$ TeV – for essentially the same reasons. Finally, we consider two values for λ_u^{33}: $\lambda_u^{33} = 1$ is chosen to illustrate the perturbative case, while $\lambda_u^{33} = 3$ is studied since it has a beneficial effect on decreasing tuning. With these choices, the parameter space of our model reduces to $(\frac{F_{X'}}{M}, \frac{F_X}{M})$, which we can trade for the IR values of the A-term A_t and the gluino mass $M_{\tilde{g}}$.

In figure 3.3 we show contours of the Higgs mass, tuning and M_{SUSY} in the $(M_{\tilde{g}}, A_t)$ plane for the two choices of λ_u^{33}. In both figures **??** and 3.3 a large Higgs mass can be achieved with moderate values of M_{SUSY} thanks to the large A-terms. In figure **??** however, the μ-term is very large and induces sizable negative contributions to m_h through the stau and sbottom sectors. This implies that a higher M_{SUSY} is needed to obtain the correct Higgs mass. (see e.g. [88].) The main source of tuning can be either the large induced Higgs soft mass from (3.3.5) or, for large M_{SUSY}, the running effect. We immediately see from figure **??** that the first of these sources represents a serious tuning problem for $\lambda_u^{33} = 1$, in which case for a 125 GeV Higgs we obtain a typical tuning of $\sim 10^{-4}$. In figure 3.3 we see the beneficial effect of considering a larger value for λ_u^{33}. This choice suppresses the fine tuning induced by (3.3.5), in such a way that a 125 GeV Higgs can be achieved while keeping tuning to the one part in ~ 500 level.

[5]The second term in the effective superpotential (3.3.3) gives rise to $B_\mu = \mu A_t \tan^2\theta_H$ at the messenger scale. While this is parametrically of the right size for EWSB, it has the incorrect sign to lead to the large $\tan\beta$ EWSB condition $B_\mu \approx 0$ at the weak scale. Thus a more complete model that also aspires to explain the origin of μ and B_μ must include additional contributions to these parameters.

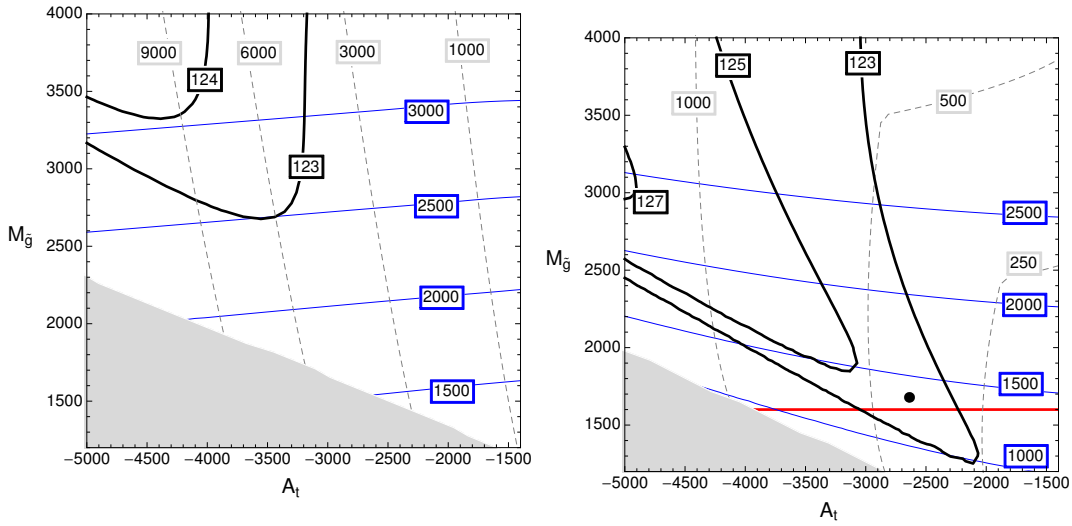

Figure 3.3: Contours of the Higgs mass (black), geometric mean of the stop masses (blue) and tuning (dashed), for $\lambda_u^{33} = 1$ (left) and $\lambda_u^{33} = 3$ (right) with $N_m = 3$, $\tan\beta = 20$, $M = 250$ TeV. Different Higgs mass contours are presented to account for the uncertainty in the theoretical Higgs mass calculation. The shaded region corresponds to tachyonic stops/staus. The dot on the figure on the right corresponds to the point in parameter space with the spectrum presented in figure 3.4. The parameter space below the red line on the same figure is excluded by [84]. All quantities are evaluated at M_{SUSY}.

In figure 3.4 we present a typical spectrum for the model with $\lambda_u^{33} = 3$, which corresponds to the black dot in figure 3.3. This model is even more similar to MGM with stau NLSP than the one presented in the previous subsection, since there is no negative contribution to the right-handed stop to counteract. The only difference now with MGM is the large A-term, which has a minor effect on the rest of the spectrum primarily through the RG. The MGM collider signatures here are potentially spectacular. If colored superpartners are accessible to collider experiments they will lead to a long decay chain including jets, leptons and missing energy. As in our non-MFV model, searches that look for jets, tau final states and large missing energy can be sensitive to this spectrum when the strong production is accessible. In particular ATLAS search [84] analyses a similar spectrum and their results apply directly to our case, setting strong bounds on parts of the parameter space. For $\tan\beta = 20$, gluinos of up to 1.6 TeV are excluded, which corresponds to a total strong production cross section of ~ 1.5 fb at tree level [85].

Multilepton searches could also be a leading probe of this model, especially when the colored sparticles are too heavy to be produced. The stau NLSP scenario considered in [86] can be sensitive to our case, but since in our spectrum $\tilde{m}_{e_R} - \tilde{m}_{\tau_1} \sim 20$ GeV and 150 GeV $< \tilde{m}_{\tau_1}$, the obtained bounds are not currently relevant for us. However, updates of these searches in Run II of the LHC

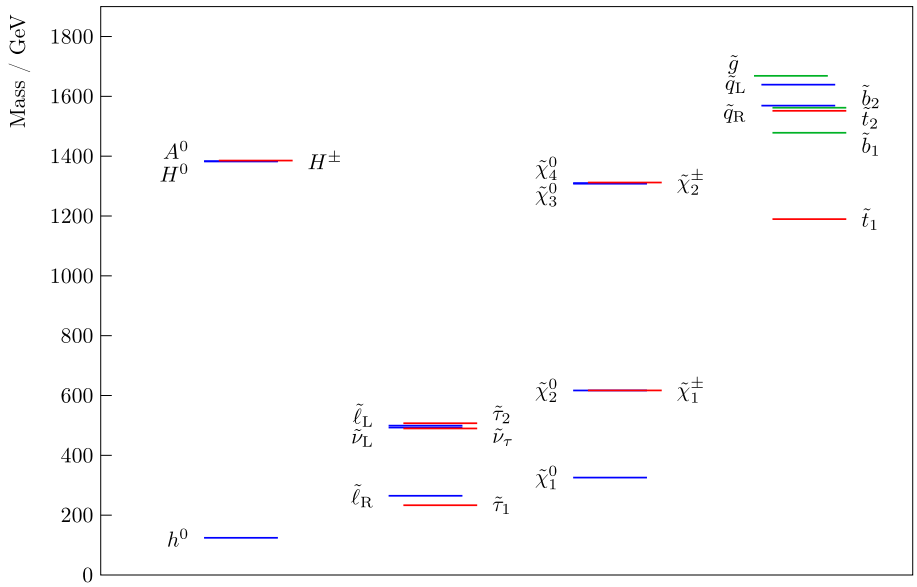

Figure 3.4: Spectrum for the point shown in figure 3.3. The Higgs mass is $m_h = 124$ GeV, with $A_t = -2.7$ TeV. $\tilde{\tau}_1$ is 32 GeV lighter than the right handed sleptons. The Higgsino mass is $\mu = 1.3$ TeV. Fine tuning is $\sim 1/400$.

can be very interesting for our models.

3.4 A composite model from Seiberg duality

As discussed in the previous section, the little A/m_H^2 problem in the MFV model (3.3.5) necessitates a large value for λ_u^{33}, and the theory has a Landau pole at a low scale. One way to explain physics above the Landau pole is to build composite models that naturally provide $|\lambda_u^{33}| \gg 1$ due to the underlying strong interactions. In general, characterizing such a strongly coupled UV completion is challenging at best, however in the context of supersymmetric gauge theories we can make use of Seiberg duality [76, 77]. We embed the model of section 3.3 in the magnetic side of the duality, where the fields $Q_3, \overline{u}_3$ and ϕ will be composite degrees of freedom. Since it is conceptually simpler, we first discuss the electric side of the duality. In a second stage we discuss the mapping to the composite degrees of freedom on the magnetic side, and we complete the model by adding in a number of spectator fields.

3.4.1 Electric theory

The electric theory is defined by SQCD with $N_c = 2$ colors and $N_f = 3$ flavors. Since the fundamental of the electric gauge group $SU(2)_E$ is pseudo-real, this theory is invariant under an $SU(6)$ global

GUT	field	$SU(2)_E$	$SU(3)_c$	$SU(2)_L$	$U(1)_Y$	$\mathbb{Z}_3$	B
5	q_c	$\square$	$\square$	1	$-\frac{1}{3}$	$\frac{1}{3}$	$-\frac{1}{6}$
	q_L	$\square$	1	$\square$	$\frac{1}{2}$	$\frac{1}{3}$	$\frac{1}{2}$
1	q_S	$\square$	1	1	0	$\frac{1}{3}$	$-\frac{1}{2}$

Table 3.2: Matter content of the electric theory. $q = q_c \oplus q_L \oplus q_S$ form a fundamental of the $SU(6)$ global symmetry.

symmetry. It is therefore convenient to parametrize its degrees of freedom with a single matter field q_a^i in the fundamental of $SU(2)_E$ and $SU(6)$. The standard model gauge group can be embedded in the global symmetry as follows

$$SU(6) \supset SU(5) \supset SU(3)_c \times SU(2)_L \times U(1)_Y \tag{3.4.1}$$

With this matter content, the global symmetry is anomalous. In section 3.4.3 we will introduce some spectator fields to cancel the gauge anomalies and give vector-like masses to some exotics. Note that because the global symmetry contains $SU(5)$, grand unification is manifest in this model from the outset. Concretely, the fundamental of $SU(6)$ trivially decomposes as

$$\mathbf{6} = \mathbf{5} \oplus \mathbf{1} \tag{3.4.2}$$

where the **5** further decomposes into standard model representations in the conventional way. The quantum numbers of q_a^i are summarized in table 3.2.

In addition to hypercharge $U(1)_Y$, the breaking pattern in (3.4.1) allows for an additional global symmetry which we will denote by $U(1)_G$. As will be seen in section 3.4.2, it is necessary to consider the MSSM baryon number to be part of the global symmetries for proton stability. It will also be seen that baryon number has a unique embedding in $U(1)_G$ and $U(1)_Y$ given by:

$$B = \frac{4}{5}Y + \frac{1}{10}G \qquad \text{with} \qquad \begin{aligned} Y &= \text{diag}(-\tfrac{1}{3}, -\tfrac{1}{3}, -\tfrac{1}{3}, \tfrac{1}{2}, \tfrac{1}{2}, 0) \\ G &= \text{diag}(1, 1, 1, 1, 1, -5) \end{aligned} \tag{3.4.3}$$

Note that both the electric and magnetic theories have a $\mathbb{Z}_{N_f}$ discrete symmetry that is leftover from the anomalous global $U(1)$ symmetry. As we will discuss in the next subsection, we will identify this $\mathbb{Z}_3$ with the one of table 3.1.

3.4.2 Magnetic theory

This theory s-confines in the IR and has a weakly-coupled magnetic dual description in terms of the mesons and baryons of the electric theory as described in table 3.3. These gauge invariants $q^i q^j$

GUT	field	$SU(3)_c$	$SU(2)_L$	$U(1)_Y$	composite	$\mathbb{Z}_3$	B
10	Q_3	$\square$	$\square$	$1/6$	$q_c q_L$	2/3	1/3
	$\overline{u}_3$	$\overline{\square}$	1	$-2/3$	$q_c q_c$	2/3	-1/3
	E'	1	1	1	$q_L q_L$	2/3	1
5	ϕ	1	$\square$	$1/2$	$q_L q_S$	2/3	0
	d'	$\square$	1	$-1/3$	$q_c q_S$	2/3	-2/3

Table 3.3: Matter content of the magnetic side of the duality. All fields fill out complete GUT multiplets. Since E' carries baryon number, it cannot be identified with a right handed lepton.

transform as the antisymmetric tensor $\mathbf{15}_A$ of the global $SU(6)$. Under $SU(5)$ this decomposes as

$$\mathbf{15}_A = \mathbf{10}_A \oplus \mathbf{5}. \tag{3.4.4}$$

The resulting $SU(5)$ representations allow us to identify Q_3, $\overline{u}_3$ and ϕ with composite degrees of freedom. Note that the baryon numbers of Q_3 and $\overline{u}_3$ uniquely determined the coefficients of $U(1)_Y$ and $U(1)_G$ in (3.4.3). The rest of the composite fields are E' and d', of which E' has the same gauge quantum numbers as right handed leptons, but non-zero baryon number.

The confining electric gauge group dynamically generates a superpotential in the magnetic dual, given by

$$\begin{aligned} W_{\text{mag}} &= \frac{1}{\Lambda^3}\text{Pf}(q^i q^j) \\ &= \kappa(\phi Q_3 \overline{u}_3 - Q_3 Q_3 d' + d' \overline{u}_3 E') \end{aligned} \tag{3.4.5}$$

where Pf is the Pfaffian of the antisymmetric matrix $q^i q^j$, and we used the mapping to the magnetic theory in the second line. The coupling κ descends from the strong dynamics in the electric theory and can be large (for concreteness we assumed $\kappa \sim 3$ in section 3.3). From the last two operators in (3.4.5) it should also be clear that rapid, dimension 6 proton decay would be introduced if one were to identify E' with one of the MSSM leptons. The B and $\mathbb{Z}_3$ charges for the composite fields are fixed by those of the electric quarks in table 3.2.

3.4.3 Complete model with spectators

Let us now weakly gauge a $SU(3)_c \times SU(2)_L \times U(1)_Y$ subgroup of the global symmetry. To cancel anomalies, fill out complete GUT multiplets, and match the field content of the magnetic theory to the model of section 3.3, we add a number of fundamental fields, which are all spectators as far as the Seiberg duality is concerned. Among these spectators are all three $\overline{d}$, L and $\overline{e}$ generations of the MSSM, as well as the first two generations of the Q and $\overline{u}$ sectors. Finally, the H_u and H_d are

GUT	field	$SU(3)_c$	$SU(2)_L$	$U(1)_Y$	$\mathbb{Z}_3$	B
$\overline{\mathbf{5}}$	$\tilde{\phi}$	1	$\square$	$-1/2$	1/3	0
	$\overline{d}'$	$\overline{\square}$	1	1/3	1/3	2/3
$\overline{\mathbf{5}}$	L_3	1	$\square$	$-1/2$	2/3	0
	$\overline{d}_3$	$\overline{\square}$	1	1/3	2/3	-1/3
10	Q'	$\square$	$\square$	1/6	1/3	1/3
	$\overline{U}'$	$\overline{\square}$	1	$-2/3$	1/3	-1/3
	$\overline{e}_3$	1	1	1	2/3	0
$\overline{\mathbf{10}}$	$\overline{Q}'$	$\overline{\square}$	$\square$	$-1/6$	2/3	-1/3
	U'	$\square$	1	2/3	2/3	1/3
	$\overline{E}'$	1	1	-1	1/3	-1
	H_u	1	$\square$	1/2	1/3	0
	H_d	1	$\square$	$-1/2$	2/3	0

Table 3.4: Spectators of the Seiberg duality required to cancel anomalies and fill out complete GUT multiplets. Primed fields have heavy vector-like masses and are integrated out at the duality scale. The first two generations are also spectators but are not shown here for simplicity.

spectators as well, but do not come in complete GUT multiplets. This is nothing other than the usual doublet-triplet splitting problem in models with grand unification. The spectators and their quantum numbers are introduced in table 3.4. Aside from the usual baryon number, we also assign the $\mathbb{Z}_3$ charges for the spectator fields such that the symmetry in table 3.1 is realized. In addition to the fields we introduced so far, one may choose to add up to three pairs of conventional, **5**-$\overline{\mathbf{5}}$ gauge mediation messengers without spoiling perturbative gauge coupling unification.[6]

All the non-MSSM fields have vector-like masses. Some arise from Yukawa interactions in the electric theory, while others are mass terms:

$$\begin{aligned} W_{\text{elec}} &\supset y_{d'} q_c q_S \overline{d}' + y_{E'} q_L q_L \overline{E}' + M_{Q'} Q' \overline{Q}' + M_{U'} U' \overline{U}' \\ &\to W_{\text{mag}} \supset y_{d'} \Lambda d' \overline{d}' + y_{E'} \Lambda E' \overline{E}' + M_{Q'} Q' \overline{Q}' + M_{U'} U' \overline{U}' \end{aligned} \tag{3.4.6}$$

Those that are Yukawas in the electric theory are naturally of the same size as the compositeness scale Λ, and so for unification we must also take $M_{Q'} \sim M_{U'} \sim \Lambda$.

We can see that it is possible to reproduce the model in (3.3.1) by adding interactions between spectators and the composites and between spectators themselves if we allow the following interactions

$$\delta W = (X_0' + X') H_u \tilde{\phi} + \tilde{\lambda}_u^{ij} \phi Q_i \overline{u}_j + M \phi \tilde{\phi} \tag{3.4.7}$$

[6]We hereby assume that any uncalculable threshold corrections at the compositeness scale are negligible.

where i, j identify quark fields in the gauge eigenbasis. To avoid clutter, we suppressed the mass terms that are introduced in (3.4.6), as well as the μ-term and the down and lepton Yukawas. This superpotential is generic if we impose the $\mathbb{Z}_3$ symmetry of tables 3.3 and 3.4.

As noted earlier, the first and second generations of the MSSM matter fields are all elementary and spectators as far as the Seiberg duality is concerned. Since ϕ is a composite operator in the electric theory, all up-type Yukawa couplings (other than the top Yukawa) must arise from irrelevant operators in the electric theory. (Recall that the $\mathbb{Z}_3$ symmetry of table 3.1 forbids the usual up-type Yukawa couplings $H_u Q \overline{u}$.) For instance

$$\begin{aligned} \frac{1}{\Lambda_{UV}^2}(q_L q_S)(q_c q_L)\overline{u}_2 &\rightarrow \frac{\Lambda^2}{\Lambda_{UV}^2}\phi Q_3 \overline{u}_2 \\ \frac{1}{\Lambda_{UV}}(q_L q_S) Q_2 \overline{u}_2 &\rightarrow \frac{\Lambda}{\Lambda_{UV}}\phi Q_2 \overline{u}_2 \end{aligned} \tag{3.4.8}$$

where Λ_{UV} is a cut-off scale of the electric theory. In the notation of section 3.3 this yields:

$$\lambda_u^{ij} = \kappa \delta^{i3}\delta^{3j} + \tilde{\lambda}_u^{ij} \sim \begin{pmatrix} 0 & 0 & 0 \\ 0 & 0 & 0 \\ 0 & 0 & \kappa \end{pmatrix} + \begin{pmatrix} \epsilon & \epsilon & \epsilon^2 \\ \epsilon & \epsilon & \epsilon^2 \\ \epsilon^2 & \epsilon^2 & \epsilon^3 \end{pmatrix} \tag{3.4.9}$$

with $\epsilon \sim \Lambda/\Lambda_{UV} \ll 1$. The composite sector therefore naturally provides a partial explanation of the texture of the up-type Yukawa matrix. Since Q_3 is a composite degree of freedom, it also predicts $\epsilon \sim y_b \sim 0.1$, but the rest of the hierarchies in y_d and y_ℓ are not explained.

Upon integrating out the messenger fields, the analysis further reduces to what was presented in section 3.3. There is one exception, in the sense that the model is no longer manifestly MFV since the third generation was given a special treatment. In particular a non-MFV dimension six operator is generated in the Kähler potential from integrating out d' in (3.4.5)

$$\delta K_{\text{eff}} \sim \frac{1}{\Lambda^2}(Q_3 Q_3)^\dagger (Q_3 Q_3) \sim \frac{1}{\Lambda^2}(u_3 d_3)^\dagger (u_3 d_3). \tag{3.4.10}$$

By rotating Q_3 to the mass eigenbasis, this operator can in principle couple quarks of different generations. However note that this operator does not introduce any new CP phase into the model and it does not contribute to FCNC processes at tree level. Moreover it is suppressed by the duality scale that is above the messenger scale $\gtrsim 100$ TeV. The effects in the first two generation quarks are further suppressed by powers of ϵ coming from (3.4.9). For instance, the operator contributing to K-$\overline{K}$ mixing receives an additional suppression of $\sim \epsilon^8$. Therefore we conclude that it is consistent with the bounds from flavor observables [87].

3.5 Conclusions of this chapter

In this chapter, we presented a new mechanism to generate large A-terms through tree-level superpotential operators. We provided explicit examples of both MFV and non-MFV models. In contrast to the conventional setups with one-loop A-terms through Kähler potential operators, our tree-level mechanism does not induce any dangerously large soft masses and is therefore manifestly free from the A/m^2 problem. Generically, a soft mass of the same order as the A-term is nevertheless still generated. For the non-MFV example this contribution greatly increases the splitting between the stop mass eigenstates, but otherwise does not significantly impact the phenomenology or the fine tuning. For the MFV case, the soft mass could potentially lead to disastrous levels of fine tuning, but it can be brought under control by the existence of strong dynamics near the messenger scale. We provide an example of such a composite sector which has a description in terms of Seiberg duality and which explicitly allows for gauge coupling unification.

Some potential future directions suggested by this work include:

- An interesting avenue to pursue, is to study if these particular models of GMSB are absolutely consistent with supersymmetric Barr-Nelson mechanisms, as the one presented in chapter 2, such that they do not spoil the solution to the strong CP problem.

- For concreteness, we focused on an MGM setup as a first example, but we emphasize that tree-level A-terms are merely a module that can be added to any mechanism for mediating SUSY breaking. In particular, it would be interesting to study whether the mechanism can naturally be embedded in more realistic models of dynamical supersymmetry breaking. In addition one could generalize X' beyond the spurion limit, and study the effects of its dynamics on the phenomenology.

- In the non-MFV case it may be interesting to embed the tree-level A-term into a full fledged theory of flavor.

- In the MFV case, we saw that the A-term module generated a contribution to B_μ which unfortunately was of the wrong sign for EWSB. An interesting opportunity here would be to construct a complete model that produces both tree-level A-terms and B_μ, perhaps along the lines of the models constructed in [75].

- Finally, the emergence of large A-terms from a composite sector in the MFV case may open a new avenue towards constructing a realistic model where large A-terms are generated at the TeV scale, hence further reducing the fine-tuning.

Chapter 4

Effective Theory of Higgs Sector Vacuum States

4.1 Introduction

In chapter 3 we analyzed part of the low energy phenomenology of supersymmetric models with soft gauge mediated supersymmetry breaking, and we postponed the discussion of the phenomenology of the Higgs sector of supersymmetric models to this chapter. All supersymmetric models, as well as many extensions of the Standard Model contain extended Higgs sectors. The observation of a Higgs-like boson at the LHC [1, 2] opened a new era for discovery in this regard. The Higgs sector must now be probed, and it must be determined if it corresponds to the one of the Standard Model (SM), or if evidence of extended models such as supersymmetry can be found in data. In this chapter, we study the phenomenology of such extended Higgs sectors in a very general framework, which includes but is not limited to, the Higgs sector of the MSSM.

The Higgs sector of the SM has a very particular phenomenology. In the SM there is a single vacuum state responsible for giving mass to all elementary fields, and its couplings are determined entirely by these masses and gauge invariance. Both ATLAS and CMS have an extensive program to search for scalar states that might be new vacuum states [89–93] and to test if Higgs couplings are SM like [94–96].

From the theory perspective, the interpretation of any deviation in the SM Higgs sector predictions requires an organization of the phenomenology of the possible extensions. This exercise cannot be done in full generality, but existing experimental data can provide strong motivation in favor of particular models. First, no significant deviations from the SM predictions for any of the Higgs

couplings that have been measured at LHC have been found [94–96]. In the SM, the Higgs particle couples to fermions and gauge bosons with the same strength than the Higgs condensate itself. This property is called alignment, and it is not automatically fulfilled in extended Higgs sectors with multiple vacuum states, but it is recovered in the limit in which all the beyond the SM field content is decoupled [97]. A second strong limitation comes from the ρ parameter ($\rho = m_W^2/(m_Z^2 \cos^2\theta_W)$), which is measured in EW precision experiments to be very close to one [41], as predicted in the SM or in extensions with an arbitrary number of Higgs doublets and/or singlets [26]. Extensions with more complicated $SU(2)$ representations generally break this relation at tree level[1].

The above considerations provide a strong motivation to study the low energy phenomenology of Higgs sectors extended only with heavy singlets and doublets. The main features of such extensions can be studied by considering the most general extension with a real singlet [99, 100] or a second doublet [101–104]. These models are referred as the Singlet Higgs Standard Model (SHSM, also dubbed xSM) and the two Higgs doublet model (2HDM). Extensions with singlets arise in the NMSSM [105] and in models of EW baryogenesis [106]. Theories with two Higgs doublets arise in different BSM scenarios and in particular, they are a fundamental part of all supersymmetric models [22] including the models studied in the previous chapters. The theory and phenomenology of both the SHSM [107–109] and the 2HDM [26–29, 110, 111] have been studied extensively in the literature in the so called mixing language, which relies in finding the vacuum mass eigenstates and its couplings using the full microscopic theories.

In this work we follow an alternative approach to study the SHSM and 2HDM: we derive their tree level Wilsonian low energy effective theories (EFT)[7] by integrating out the heavy SU(2) singlet or doublet. Near the decoupling limit, EFT is the most powerful available tool to study the low energy observables, since it automatically includes all the effects of UV physics and organizes them hierarchically in an expansion in terms suppressed by the heavy mass scale. This allows us to find patterns of deviations from the SM Higgs couplings for the different UV completions, and to clearly organize flavor and T violating effects. In order to get a consistent expansion, it is important to identify which operators must be kept in the EFT, and this is done by finding the correct concept of effective operator dimension.

We start by studying the SHSM. We first review the phenomenology in the mixing language and then we follow the alternative method using EFT. The correct concept of effective operator dimension in the SHSM EFT corresponds to just naive operator dimension. We work up to effective dimension six and we give only one example of an operator at effective dimension eight. We find

[1] For an example of an exception see [98].

that all the couplings of the Higgs are modified at effective dimension six with respect to their SM counterparts. We also find that all the couplings of the Higgs to massive gauge bosons and fermions are generically smaller in magnitude than in the SM, while self couplings may be larger. When comparing with the results obtained using the mixing language, we find that all trilinear couplings in the EFT and mixing languages coincide, but no coupling with more than three legs does. For instance, the coupling of two Higgses to two gauge bosons obtained in the EFT language differs from the one obtained in the mixing language. We provide a precise explanation on why this is the case - trilinear couplings in both languages must coincide, since they control long distance pieces of scattering amplitudes which cannot be modified by threshold corrections. This is a generic feature of EFT, and it is also valid in the UV completion with an SU(2) doublet. We also perform a thorough check of the EFT by comparing scattering amplitudes calculated in the mixing and EFT languages and we correct previous results in the literature [112].

We then study the SM completed in the UV with an SU(2) doublet. Without loss of generality in this chapter we work in the so called Higgs basis [113], which is particularly useful near the alignment limit. In this basis, only one of the doublets contains the Higgs vacuum expectation value (vev), so in the exact alignment limit it must also contain the Higgs particle. The doublet with no vev must be interpreted as the doublet that is decoupled. We begin by reviewing the mixing language from a somewhat unconventional perspective, which relies on the use of the Higgs basis and background symmetry invariant eigenvectors and eigenstates of the mass matrix. These eigenvectors allow us to introduce a notion of complex alignment parameter, which is invariant under background symmetries, is a straightforward generalization of the alignment parameter of the T conserving 2HDM, and simplifies the analysis of the general T violating 2HDM in the mixing language. We then present the tree level low energy effective theory. We identify a concept of operator effective dimension, which *differs from naive operator dimension*. We work up to effective dimension six in operators involving fermions, and up to effective dimension eight in purely bosonic interactions. We find that operators of effective dimension six modify Higgs self-couplings, couplings to fermions and also lead to four fermion interactions, while Higgs interactions with massive gauge bosons are only modified by operators of effective dimension eight. We also find that all the self-couplings of the Higgs and the couplings to massive gauge bosons are generically smaller in magnitude than the ones of the SM, while the couplings to fermions can be larger in magnitude. Regarding flavor violation, Higgs Yukawas allow for $\Delta F = 1$ chirality violating processes, while both $\Delta F = 1$ and $\Delta F = 2$, chirality preserving and chirality violating processes are allowed in four fermion operators. Regarding T violation, we find that at effective dimension six it only arises in Higgs interactions

with fermions. The T violating phases that can be associated exclusively with couplings in the 2HDM potential [114], including the one in the complex alignment parameter, are not relevant up to at least effective dimension eight. The consistency of the EFT is checked by comparing with scattering amplitudes calculated in the mixing language. We finally perform a detailed analysis of the 2HDM with Glashow-Weinberg conditions [30], namely the types I-IV 2HDM. We comment on the different $\tan\beta$ dependence on different types, and we find that at effective dimension six, there is a single universal T violating phase contained exclusively in the interactions of the Higgs boson with fermions.

The chapter is organized as follows. In section 4.2 we present the Standard Model extended with a real singlet. We first study the model using the mixing language, and then we derive the EFT and reinterpret all the results from this perspective. In section 4.3 we present the most general extension of the Standard Model with an SU(2) doublet and derive the couplings of the Higgs in the decoupling limit using the mixing language. In section 4.4 we present the corresponding effective field theory. In section 4.5 we study the effective theories of the 2HDM with Glashow-Weinberg conditions in generality, allowing for CP violation. In section (4.7) we study the constraints on CP violation of such 2HDM with GW conditions from electric dipole moment experiments. We conclude with comments on the phenomenology and a summary table of properties of the SHSM and 2HDM effective field theories.

4.2 A Higgs and a heavy real scalar singlet

4.2.1 The model

We begin by describing a Higgs sector containing a Higgs doublet H and a real scalar gauge singlet S. H is taken to have hypercharge $Y = 1$. We consider canonically normalized fields and the most general potential. The Lagrangian density is given by

$$D_\mu H^\dagger D^\mu H - V(H) - \left[\lambda^u_{ij}\ Q_i H \overline{u}_j - \lambda^d_{ij} Q_i H^c \overline{d}_j - \lambda^\ell_{ij} L_i H^c \overline{\ell}_j + \text{h.c.} \right] \tag{4.2.1}$$

the covariant derivative acting on the doublet is

$$D_\mu H = \left[\partial_\mu - i \left(g_2 W_{a\mu} T_a + \frac{1}{2} g_1 B_\mu \right) \right] H \tag{4.2.2}$$

In the potential, any linear term in S can be absorbed in a shift of S, so the most general potential at the renormalizable level is

$$V(H) = \frac{\mu^2}{2} S^2 + \frac{\zeta}{3} S^3 + \frac{\lambda_S}{8} S^4 + m^2 H^\dagger H + \frac{\lambda}{2} (H^\dagger H)^2 + \xi S H^\dagger H + \frac{\lambda'}{2} S^2 H^\dagger H \tag{4.2.3}$$

The potential is invariant under the $\mathbb{Z}_2$ background symmetry specified in table 4.1. All measurable quantities must be invariant under the background symmetry. Note that the $\mathbb{Z}_2$ symmetry is explicitly broken by ξ and ζ.

	$\mathbb{Z}_2$
H	$+$
S	$-$
$m^2, \mu^2, \lambda, \lambda', \lambda_S$	$+$
ξ, ζ	$-$

Table 4.1: Charge assignments for the background $\mathbb{Z}_2$ symmetry of the potential (4.2.3).

We consider perturbative marginal couplings. Stability of the potential requires $\lambda_S > 0, \lambda > 0, \lambda' > -\sqrt{\lambda\lambda_S}$. By redefining the sign of the singlet we can make either ξ or ζ positive. We also consider a non tachyonic singlet mass $\mu^2 > 0$. For $H = 0$ the potential is a quartic polynomial in S, with a stable and a metastable minimum and an unstable maximum. Without loss of generality we define the global minimum to be at $S = 0$. In order for the minimum away from the origin to be the metastable minimum the potential parameters fulfill

$$\zeta^2 < \frac{9}{4}\lambda_S \mu^2 \tag{4.2.4}$$

The gauge invariant combination characterizing the Higgs condensate with symmetry breaking pattern $SU(2)_L \times U(1)_Y \to U(1)_Q$, and the $\mathbb{Z}_2$ invariant combination characterizing the singlet condensate are

$$\frac{v^2}{2} = \langle H^\dagger H \rangle \qquad \frac{v_s^2}{2} = \langle S^2 \rangle \tag{4.2.5}$$

The vacuum states s, h are defined as

$$S = v_s + s \qquad H_0 = \frac{1}{\sqrt{2}}(v + h) \tag{4.2.6}$$

where H_0 is the neutral component of the doublet. Gauge invariance ensures $v \geq 0$. The Higgs vev is $v = 246$ GeV. v_s has negative charge under the $\mathbb{Z}_2$ background symmetry of table 4.1.

The Higgs condensate gives mass to the gauge bosons corresponding to the broken gauge symmetries. The W and Z boson masses are

$$m_W = \frac{g_2 v}{2} \qquad m_Z = \frac{m_W}{\cos\,\theta_W} \qquad \tan\,\theta_W = \frac{g_1}{g_2} \tag{4.2.7}$$

Fermions are defined in the mass eigenbasis so λ^f_{ij} ($f = u, d, \ell$) are diagonal matrices in flavor space. The Yukawa matrices in terms of the fermion masses are

$$\lambda^f_{ij} = \frac{\sqrt{2}m^f_{ij}}{v} = \frac{\sqrt{2}m^f_i}{v}\ \delta_{ij} \tag{4.2.8}$$

We are interested in the case in which there is a separation of scales $\mu^2 \gg \left|m^2\right|$, which corresponds to the limit in which the mass of the singlet is much heavier than the EW scale. In the EFT language, μ will be the cutoff of the low energy theory. We allow the remaining two mass scales in the theory, ξ and ζ, to be as large as the cutoff

$$\xi, \zeta \lesssim \mu \tag{4.2.9}$$

Finally, the decoupling limit is defined as

$$\lambda\frac{v^2}{\mu^2}\ ,\ \lambda'\frac{v^2}{\mu^2}\ ,\ \lambda_S\frac{v^2}{\mu^2}\ ,\ \frac{\xi^2}{\mu^2}\frac{v^2}{\mu^2}\ ,\ \frac{\zeta^2}{\mu^2}\frac{v^2}{\mu^2}\ ,\ \frac{\xi\zeta}{\mu^2}\frac{v^2}{\mu^2} \ll 1 \tag{4.2.10}$$

4.2.2 Mass eigenstates and couplings in the mixing language

In the mixing language, the couplings of the Higgs particle are found by identifying the mass eigenstates of the scalar potential (4.2.3) in the Higgs-singlet condensate. The minimization conditions of the potential specify the Higgs and singlet vevs in terms of Lagrangian parameters

$$\frac{\partial V}{\partial H}\Big|_{H=v/\sqrt{2}} = \sqrt{2}m^2 v + \frac{\lambda}{\sqrt{2}}v^3 + \frac{\lambda'}{\sqrt{2}}v v_s^2 + \sqrt{2}\xi v v_s = 0 \tag{4.2.11}$$

$$\frac{\partial V}{\partial S}\Big|_{S=v_s} = \mu^2 v_s + \frac{\xi}{2}v^2 + \frac{\lambda'}{2}v^2 v_s + \zeta v_s^2 + \frac{\lambda_s}{2}v_s^3 = 0 \tag{4.2.12}$$

We consider $\mu > 0$, so the minimum at the origin of field space can be destabilized only by the Higgs mass at zero Higgs vev. From (4.2.12), the extrema for the Higgs are at

$$v = 0 \quad \text{and} \quad v^2 = -\frac{2}{\lambda}\left(m^2 + \frac{1}{2}\lambda' v_s^2 + \xi v_s\right) \tag{4.2.13}$$

The term in parenthesis in the second expression is the Higgs mass at the origin. When positive, the potential has a global minimum at $v = 0, v_s = 0$. When negative, the global minimum is away from the origin and is a solution of the second expression in (4.2.13). The Higgs condensate induces a tadpole for the singlet, destabilizing the global minimum at the origin of the singlet field space and inducing a singlet condensate. The tadpole vanishes when $\xi \to 0$. The singlet vev is given by

(4.2.12)

$$
\begin{aligned}
v_s &= -\frac{2\zeta^2 - 3\lambda_S\left(\mu^2 + \frac{1}{2}\lambda' v^2\right) + 2A^2 + 2\zeta A}{3\lambda_S A} \\
A &= \left[\zeta^3 - \frac{9}{4}\zeta\lambda_S\left(\mu^2 + \frac{1}{2}\lambda' v^2\right) + \frac{27}{16}\lambda_S^2\xi v^2\right. \\
&\quad \left. + \sqrt{\left(\zeta^3 - \frac{9}{4}\zeta\lambda_S\left(\mu^2 + \frac{1}{2}\lambda' v^2\right) + \frac{27}{16}\lambda_S^2\xi v^2\right)^2 - \left(\zeta^2 - \frac{3}{2}\lambda_S\left(\mu^2 + \frac{1}{2}\lambda' v^2\right)\right)^3}\right]^{1/3}
\end{aligned}
\tag{4.2.14}
$$

which is the solution of the cubic equation (4.2.12) that vanishes at $\xi \to 0$. The remaining two solutions are the unstable maximum and the metastable minimum which we do not study here. The factor $\mu^2 + \frac{1}{2}\lambda' v^2$ is the heavy singlet mass for a non-zero Higgs vev at the origin of the singlet field space. Expanding in $v^2/\left(\mu^2 + \frac{1}{2}\lambda' v^2\right)$ we get

$$
\begin{aligned}
v_s &= -\frac{\xi v^2}{2\mu^2 + \lambda' v^2}\left[1 + \frac{\zeta\xi}{2\left(\mu^2 + \frac{1}{2}\lambda' v^2\right)}\left(\frac{v^2}{\mu^2 + \frac{\lambda' v^2}{2}}\right)\right. \\
&\quad \left. + \left(\frac{\zeta^2\xi^2}{2\left(\mu^2 + \frac{1}{2}\lambda' v^2\right)^2} - \frac{\lambda_S\xi^2}{8\left(\mu^2 + \frac{1}{2}\lambda' v^2\right)}\right)\left(\frac{v^2}{\mu^2 + \frac{\lambda' v^2}{2}}\right)^2 + \mathcal{O}\left(\frac{v^2}{\mu^2 + \frac{\lambda' v^2}{2}}\right)^3\right]
\end{aligned}
\tag{4.2.15}
$$

Note that v_s vanishes in the limit $\xi \to 0$, as expected. Since near the decoupling limit $v \ll \mu$, we further expand the above expression in (v/μ),

$$
\begin{aligned}
v_s &= -\frac{\xi}{2}\left(\frac{v}{\mu}\right)^2\left[1 + \left(\frac{\zeta\xi}{2\mu^2} - \frac{\lambda'}{2}\right)\left(\frac{v}{\mu}\right)^2\right. \\
&\quad \left. + \left(\frac{\zeta^2\xi^2}{2\mu^4} - \frac{3\zeta\lambda'\xi}{4\mu^2} + \frac{\lambda'^2}{4} - \frac{\lambda_S\xi^2}{8\mu^2}\right)\left(\frac{v}{\mu}\right)^4 + \mathcal{O}\left(\frac{v^6}{\mu^6}\right)\right]
\end{aligned}
\tag{4.2.16}
$$

The mass matrix for the vacuum states is specified by the second derivatives of the potential at the stable minimum. They are

$$
\begin{aligned}
\frac{\partial^2 V}{\partial h^2} &= m_{hh}^2 = m^2 + \frac{3}{2}\lambda v^2 + \frac{1}{2}\lambda' v_s^2 + \xi v_s \\
\frac{\partial^2 V}{\partial h \partial s} &= m_{hs}^2 = \lambda' v v_s + \xi v \\
\frac{\partial^2 V}{\partial s^2} &= m_{ss}^2 = \mu^2 + \frac{3}{2}\lambda_S v_s^2 + \frac{1}{2}\lambda' v^2 + 2\zeta v_s
\end{aligned}
\tag{4.2.17}
$$

Mixing is introduced between the singlet field and the Higgs in the mass matrix (4.2.17) due to the

condensates. The mixing matrix is

$$\begin{pmatrix} \varphi_1 \\ \varphi_2 \end{pmatrix} = \begin{pmatrix} \cos\gamma & \sin\gamma \\ -\sin\gamma & \cos\gamma \end{pmatrix} \begin{pmatrix} h \\ s \end{pmatrix} \tag{4.2.18}$$

where φ_1 is the lightest mass eigenstate and will be identified with the physical Higgs. The mixing angle is

$$\tan 2\gamma = \frac{-2m_{hs}^2}{m_{ss}^2 - m_{hh}^2} \tag{4.2.19}$$

or

$$\sin 2\gamma = \frac{-2m_{hs}^2}{m_{+}^2 - m_{-}^2} \tag{4.2.20}$$

where m_+^2, m_-^2 are the eigenvalues of the mass matrix. Using (4.2.17) in (4.2.19) we find

$$\tan 2\gamma = \frac{-2(\lambda' v v_s + \xi v)}{\mu^2 - m^2 + \frac{3}{2}(\lambda_S v_s^2 - \lambda v^2) + (2\zeta - \xi)v_s + \frac{1}{2}\lambda'(v^2 - v_s^2)} \tag{4.2.21}$$

From (4.2.13), the soft mass is

$$m^2 = -\frac{1}{2}\lambda v^2 - \frac{1}{2}\lambda' v_s^2 - \xi v_s \tag{4.2.22}$$

so (4.2.22) in (4.2.21) we express the mixing angle as

$$\tan 2\gamma = \frac{-2(\lambda' v v_s + \xi v)}{\mu^2 - \lambda v^2 + 2\zeta v_s + \frac{3}{2}\lambda_S v_s^2 + \frac{1}{2}\lambda' v^2} \tag{4.2.23}$$

A convenient expansion near the decoupling limit can be found for $\tan 2\gamma$ using the expansion for the singlet condensate (4.2.16) in (4.2.23)

$$\tan 2\gamma = -\frac{2\xi}{\mu}\left(\frac{v}{\mu}\right) + \left(-\frac{2\lambda\xi}{\mu} + \frac{2\lambda'\xi}{\mu} - \frac{2\zeta\xi^2}{\mu^3}\right)\left(\frac{v}{\mu}\right)^3 + \mathcal{O}\left(\frac{v^5}{\mu^5}\right) \tag{4.2.24}$$

or, in terms of $\cos\gamma$ and $\sin\gamma$

$$\begin{aligned} \cos\gamma &= 1 - \frac{\xi^2}{2\mu^2}\left(\frac{v}{\mu}\right)^2 + \left(-\frac{\lambda\xi^2}{\mu^2} + \frac{\lambda'\xi^2}{\mu^2} - \frac{\zeta\xi^3}{\mu^4} + \frac{11\xi^4}{8\mu^4}\right)\left(\frac{v}{\mu}\right)^4 + \mathcal{O}\left(\frac{v^6}{\mu^6}\right) \\ \sin\gamma &= -\frac{\xi}{\mu}\left(\frac{v}{\mu}\right) + \left(-\frac{\lambda\xi}{\mu} + \frac{\lambda'\xi}{\mu} - \frac{\zeta\xi^2}{\mu^3} + \frac{3\xi^3}{2\mu^3}\right)\left(\frac{v}{\mu}\right)^3 + \mathcal{O}\left(\frac{v^5}{\mu^5}\right) \end{aligned} \tag{4.2.25}$$

On the other hand, the two mass eigenvalues of the mass matrix (4.2.17) are

$$m_{\pm}^2 = \frac{1}{2}\Big(m_{hh}^2 + m_{ss}^2 \pm \sqrt{(m_{ss}^2 - m_{hh}^2)^2 + 4m_{hs}^2}\Big) \tag{4.2.26}$$

We identify the Higgs with the lightest mass eigenstate φ_1. Using (4.2.16) and (4.2.17) in (4.2.26) we get the Higgs mass near the decoupling limit

$$\begin{aligned} m_{\varphi_1}^2 &= v^2\Bigg[\left(\lambda - \frac{\xi^2}{\mu^2}\right) + \left(\frac{3\lambda'\xi^2}{2\mu^2} - \frac{\lambda\xi^2}{\mu^2} - \frac{\zeta\xi^3}{\mu^4} + \frac{\xi^4}{\mu^4}\right)\frac{v^2}{\mu^2} \\ &\quad + \left(-\frac{3\zeta^2\xi^4}{2\mu^6} - \frac{2\zeta\lambda\xi^3}{\mu^4} + \frac{3\zeta\lambda'\xi^3}{\mu^4} + \frac{3\zeta\xi^5}{\mu^6} - \frac{\lambda^2\xi^2}{\mu^2} + \frac{2\lambda\lambda'\xi^2}{\mu^2}\right. \\ &\quad \left. + \frac{3\lambda\xi^4}{\mu^4} - \frac{3\lambda'^2\xi^2}{2\mu^2} - \frac{7\lambda'\xi^4}{2\mu^4} + \frac{3\lambda_S\xi^4}{8\mu^4} - \frac{2\xi^6}{\mu^6}\right)\frac{v^4}{\mu^4} + \mathcal{O}\left(\frac{v^6}{\mu^6}\right)\Bigg] \end{aligned} \tag{4.2.27}$$

while the mass of the heavy eigenstate is

$$\begin{aligned} m_{\varphi_2}^2 \;=\; \mu^2\Bigg[1 + \bigg(-\frac{\zeta\xi}{\mu^2} + \frac{\lambda'}{2} + \frac{\xi^2}{\mu^2}\bigg)\frac{v^2}{\mu^2} \\ + \bigg(-\frac{\zeta^2\xi^2}{2\mu^4} + \frac{\zeta\lambda'\xi}{2\mu^2} + \frac{\zeta\xi^3}{\mu^4} + \frac{\lambda\xi^2}{\mu^2} - \frac{3\lambda'\xi^2}{2\mu^2} \\ + \frac{3\lambda_S\xi^2}{8\mu^2} - \frac{\xi^4}{\mu^4}\bigg)\frac{v^4}{\mu^4} + \mathcal{O}\bigg(\frac{v^6}{\mu^6}\bigg)\Bigg] \end{aligned} \tag{4.2.28}$$

We are now ready to study the couplings of the mass eigenstates. The Lagrangian for the mass eigenstates is obtained from (4.2.1) and (4.2.18) and it is given by

$$\begin{aligned} &\frac{1}{2}\partial\varphi_a\partial\varphi_a + \frac{1}{2}Z^\mu Z_\mu\left(m_Z^2 + g_{\varphi_a ZZ}\;\varphi_a + \frac{1}{2}g_{\varphi_a^2 ZZ}\;\varphi_a^2 + g_{\varphi_1\varphi_2 ZZ}\,\varphi_1\varphi_2\right) \\ &+W^{+\mu}W_\mu^-\left(m_W^2 + g_{\varphi_a WW}\;\varphi_a + \frac{1}{2}g_{\varphi_a^2 WW}\;\varphi_a^2 + g_{\varphi_1\varphi_2 WW}\,\varphi_1\varphi_2\right) \\ &-(m_i^f f_i\overline{f}_j\;\delta_{ij} + \lambda_{\varphi_a ij}^f\;f_i\varphi_a\overline{f}_j + \text{h.c.}) - V(\varphi_1,\varphi_2) \end{aligned} \tag{4.2.29}$$

where we sum over repeated indices and

$$\begin{aligned} V(\varphi_1,\varphi_2) \;=\; &\frac{1}{2}m_{\varphi_a}^2\varphi_a^2 - \sum_{n=0}^{n=3}\frac{1}{n!(3-n)!}g_{\varphi_1^n\varphi_2^{3-n}}\;\varphi_1^n\varphi_2^{3-n} \\ &- \sum_{n=0}^{n=4}\frac{1}{n!(4-n)!}g_{\varphi_1^n\varphi_2^{4-n}}\;\varphi_1^n\varphi_2^{4-n} \end{aligned} \tag{4.2.30}$$

We give explicit expressions for all couplings in (4.2.29) and (4.2.30) below. As a consequence of mixing with the singlet the couplings of the Higgs are modified with respect to their SM expressions. We begin with the Higgs couplings to massive gauge bosons and fermions. Couplings of the Higgs to gauge bosons $V = Z, W$ and fermions $f = u, d, \ell$ are simply diluted by a factor of $\cos\gamma$ for each Higgs field,

$$\begin{aligned} g_{\varphi_1 VV} \;&=\; \frac{2m_V^2}{v}\cos\gamma \\ g_{\varphi_1^2 VV} \;&=\; \frac{2m_V^2}{v^2}\cos^2\gamma \\ \lambda_{\varphi_1 ij}^f \;&=\; \frac{m_i^f}{v}\cos\gamma\;\delta_{ij} \end{aligned} \tag{4.2.31}$$

The expressions for these couplings near the decoupling limit can be easily obtained using (4.2.25). We omit the explicit expressions for brevity. The couplings of φ_2 to fermions and gauge bosons are inherited from the mixing between h and s

$$\begin{aligned} g_{\varphi_2 VV} \;&=\; -\frac{2m_V^2}{v}\sin\gamma \\ g_{\varphi_2^2 VV} \;&=\; \frac{2m_V^2}{v^2}\sin^2\gamma \\ \lambda_{\varphi_2 ij}^f \;&=\; -\frac{m_i^f}{v}\sin\gamma\;\delta_{ij} \end{aligned} \tag{4.2.32}$$

The couplings of $\varphi_1\varphi_2$ to massive gauge bosons are also inherited from mixing

$$g_{\varphi_1\varphi_2 VV} \;=\; -\frac{2m_V^2}{v}\sin\gamma\cos\gamma \tag{4.2.33}$$

Self couplings and Higgs-singlet couplings are given by using (4.2.18) and the Higgs potential (4.2.3)

$$\begin{aligned}
g_{\varphi_1^3} &= -3\lambda v\cos^3\gamma - 3\xi\cos^2\gamma\sin\gamma - 3\lambda' v_s\cos^2\gamma\sin\gamma \\
&\quad -3\lambda' v\cos\gamma\sin^2\gamma - 2\zeta\sin^3\gamma - 3\lambda_S v_s\sin^3\gamma \\
g_{\varphi_1^2\varphi_2} &= -\xi\cos^3\gamma - \lambda' v_s\cos^3\gamma + 3\lambda v\cos^2\gamma\sin\gamma - 2\lambda' v\cos^2\gamma\sin\gamma - 2\zeta\cos\gamma\sin^2\gamma \\
&\quad +2\xi\cos\gamma\sin^2\gamma + 2\lambda' v_s\cos\gamma\sin^2\gamma - 3\lambda_S v_s\cos\gamma\sin^2\gamma + \lambda' v\sin^3\gamma \\
g_{\varphi_1\varphi_2^2} &= -v\lambda'\cos^3\gamma - 2\zeta\cos^2\gamma\sin\gamma + 2\xi\cos^2\gamma\sin\gamma + 2\lambda' v_s\cos^2\gamma\sin\gamma \\
&\quad -3\lambda_S v_s\cos^2\gamma\sin\gamma - 3\lambda v\cos\gamma\sin^2\gamma + 2\lambda' v\cos\gamma\sin^2\gamma - \xi\sin^3\gamma - \lambda' v_s\sin^3\gamma \\
g_{\varphi_2^3} &= -2\zeta\cos^3\gamma - 3\lambda_S v_s\cos^3\gamma + 3\lambda' v\cos^2\gamma\sin\gamma \\
&\quad -3\xi\cos\gamma\sin^2\gamma - 3\lambda' v_s\cos\gamma\sin^2\gamma + 3\lambda v\sin^3\gamma \\
g_{\varphi_1^4} &= -3\lambda\cos\gamma^4 - 6\lambda'\cos^2\gamma\sin^2\gamma - 3\lambda_S\sin\gamma^4 \\
g_{\varphi_1^3\varphi_2} &= 3\lambda\cos^3\gamma\sin\gamma - 3\lambda'\cos^3\gamma\sin\gamma + 3\lambda'\cos\gamma\sin^3\gamma - 3\lambda_S\cos\gamma\sin^3\gamma \\
g_{\varphi_1^2\varphi_2^2} &= -\lambda'\cos\gamma^4 - 3\lambda\cos^2\gamma\sin^2\gamma + 4\lambda'\cos^2\gamma\sin^2\gamma - 3\lambda_S\cos^2\gamma\sin^2\gamma - \lambda'\sin\gamma^4 \\
g_{\varphi_1\varphi_2^3} &= 3\lambda'\cos^3\gamma\sin\gamma - 3\lambda_S\cos^3\gamma\sin\gamma + 3\lambda\cos\gamma\sin^3\gamma - 3\lambda'\cos\gamma\sin^3\gamma \\
g_{\varphi_2^4} &= -3\lambda_S\cos\gamma^4 - 6\lambda'\cos^2\gamma\sin^2\gamma - 3\lambda\sin\gamma^4
\end{aligned}$$

The expressions for these couplings near the decoupling limit are obtained using (4.2.16) and (4.2.25). Here for convenience we present the expansion for the Higgs self couplings

$$\begin{aligned}
\frac{g_{\varphi_1^3}}{v} &= -\frac{3m_{\varphi_1}^2}{v^2} + \left(\frac{9\lambda\xi^2}{2\mu^2} - \frac{3\lambda'\xi^2}{\mu^2} - \frac{9\xi^4}{2\mu^4} + \frac{2\zeta\xi^3}{\mu^4}\right)\frac{v^2}{\mu^2} + \mathcal{O}\left(\frac{v^4}{\mu^4}\right) \\
g_{\varphi_1^4} &= -\frac{3m_{\varphi_1}^2}{v^2} - \frac{3\xi^2}{\mu^2} + \left(-\frac{3\zeta\xi^3}{\mu^4} + \frac{3\lambda\xi^2}{\mu^2} - \frac{3\lambda'\xi^2}{2\mu^2} + \frac{3\xi^4}{\mu^4}\right)\frac{v^2}{\mu^2} + \mathcal{O}\left(\frac{v^4}{\mu^4}\right)
\end{aligned} \tag{4.2.34}$$

We will also make use of the coupling of two Higgses to a heavy mass eigenstate when calculating scattering amplitudes. Near the decoupling limit we get

$$g_{\varphi_1^2\varphi_2} \;=\; -\xi + \left(-3\lambda\xi - \frac{2\zeta\xi^2}{\mu^2} + \frac{5\lambda'\xi}{2} + \frac{7\xi^3}{2\mu^2}\right)\frac{v^2}{\mu^2} + \mathcal{O}\left(\frac{v^4}{\mu^4}\right) \tag{4.2.35}$$

4.2.2.1 Scattering amplitudes

As an application of the results of the previous section we obtain some selected Higgs scattering amplitudes. This will prove to be useful as a consistency check of the EFT description, to be

presented in section 4.2.3, and to understand the difference between couplings in the mixing language and the effective theory language. All the scattering amplitudes are modified with respect to their SM values. The SM amplitudes can be read from this section by taking the limit $\xi \to 0$. We omit spinors in all amplitudes.

The dihiggs scattering amplitude to two W bosons is given by the tree level coupling plus the contribution of diagrams with internal φ_1, φ_2 and W boson propagators,

$$\mathcal{A}\left(\varphi_1\varphi_1 \to W^+W^-\right) \;=\; g_{\mu\nu}\left[g_{\varphi_1^2WW} - \frac{g_{\varphi_1^2\varphi_a}g_{\varphi_a WW}}{s-m^2_{\varphi_a}} - g^2_{\varphi_1 WW}\left(\frac{1}{t-m_W^2}+\frac{1}{u-m_W^2}\right)\right] \tag{4.2.36}$$

where we sum over a. Using the couplings (4.2.31), (4.2.32) and (4.2.34) in (4.2.36) we get

$$\begin{aligned}\mathcal{A}\left(\varphi_1\varphi_1 \to W^+W^-\right) \;=\; g_{\mu\nu}\Bigg[&\frac{2m_W^2}{v^2}\left(1-\frac{\xi^2v^2}{\mu^4}\right)+\frac{2m_W^2}{v^2}\left[\frac{3m^2_{\varphi_1}}{v^2}+\left(-\frac{2\zeta\xi^3}{\mu^4}\right.\right.\\
&\left.\left.-\frac{6\lambda\xi^2}{\mu^2}+\frac{3\lambda'\xi^2}{\mu^2}+\frac{6\xi^4}{\mu^4}\right)\frac{v^2}{\mu^2}\right]\left(\frac{v^2}{s-m^2_{\varphi_1}}\right)-\frac{2m_W^2\xi^2}{v^2\mu^2}\left(\frac{v^2}{\mu^2}\right)\\
&-\frac{4m_W^4}{v^4}\left[1-\frac{\xi^2v^2}{\mu^4}\right]\left(\frac{v^2}{t-m_W^2}+\frac{v^2}{u-m_W^2}\right)\\
&+\mathcal{O}\left(\frac{sv^2}{\mu^4},\frac{s^2v^2}{\mu^6},\frac{v^4}{\mu^4}\right)\Bigg]\end{aligned} \tag{4.2.37}$$

The first term is the contact interaction. The second term is the long distance s-channel contribution mediated by the light mass eigenstate. The third term comes from an s-channel diagram mediated by the heavy state. The last term is the long distance contribution mediated by the W boson. Note that all the long distance contributions are controlled by the trilinear couplings $g_{\varphi_1^3}$ and $g_{\varphi_1 WW}$. In general, all the long distance pieces of the amplitudes in this section are controlled exclusively by trilinear couplings. We will make use of this observation in section 4.2.3.

The dihiggs to difermion chirality violating scattering amplitude is

$$\mathcal{A}\left(\varphi_1\varphi_1 \to f_i\overline{f}_j\right) \;=\; \frac{g_{\varphi_1^2\varphi_a}\lambda^f_{\varphi_a ij}}{s-m^2_{\varphi_a}} \tag{4.2.38}$$

where we sum over a. Using the couplings (4.2.31), (4.2.32) and (4.2.34) in (4.2.38) we get

$$\begin{aligned}\mathcal{A}\left(\varphi_1\varphi_1 \to f_i\overline{f}_j\right) \;=\; \frac{m_i^f\,\delta_{ij}}{v^2}\Bigg[&\left(-\frac{3m^2_{\varphi_1}}{v^2}+\left[\frac{2\zeta\xi^3}{\mu^4}-\frac{3\lambda'\xi^2}{\mu^2}-\frac{6\xi^4}{\mu^4}\right.\right.\\
&\left.\left.+\frac{6\lambda\xi^2}{\mu^2}\right]\frac{v^2}{\mu^2}\right)\left(\frac{v^2}{s-m^2_{\varphi_1}}\right)+\frac{\xi^2v^2}{\mu^4}+\mathcal{O}\left(\frac{sv^2}{\mu^4},\frac{s^2v^2}{\mu^6},\frac{v^4}{\mu^4},\frac{m_i^{f\,2}}{v^2}\right)\Bigg]\end{aligned} \tag{4.2.39}$$

The last term in the above expression comes from the s-channel amplitude mediated by the heavy state. The rest is the long distance contribution mediated by the light mass eigenstate. Note that the long distance contribution is controlled by the trilinear couplings $g_{\varphi_1^3}$ and $\lambda^f_{\varphi_1 ij}$

The dihiggs to dihiggs scattering amplitude is

$$\mathcal{A}\left(\varphi_1\varphi_1 \to \varphi_1\varphi_1\right) \;=\; g_{\varphi_1^4} - g^2_{\varphi_1^2\varphi_a}\left(\frac{1}{s-m^2_{\varphi_a}} + \frac{1}{t-m^2_{\varphi_a}} + \frac{1}{u-m^2_{\varphi_a}}\right) \tag{4.2.40}$$

where we sum over a. Using the couplings (4.2.34) in (4.2.40) we get

$$\begin{aligned}\mathcal{A}\left(\varphi_1\varphi_1 \to \varphi_1\varphi_1\right) \;=\; & -\frac{3m^2_{\varphi_1}}{v^2} - \left[\frac{9m^4_{\varphi_1}}{v^4} + \left(-\frac{12\zeta\lambda\xi^3}{\mu^4} + \frac{12\zeta\xi^5}{\mu^6} - \frac{27\lambda^2\xi^2}{\mu^2} + \frac{18\lambda\lambda'\xi^2}{\mu^2}\right.\right. \\ & \left.\left. + \frac{54\lambda\xi^4}{\mu^4} - \frac{18\lambda'\xi^4}{\mu^4} - \frac{27\xi^6}{\mu^6}\right)\frac{v^2}{\mu^2}\right]\left(\frac{v^2}{s-m^2_{\varphi_1}} + \frac{v^2}{t-m^2_{\varphi_1}} + \frac{v^2}{u-m^2_{\varphi_1}}\right) \\ & + \left(\frac{12\zeta\xi^3}{\mu^4} + \frac{21\lambda\xi^2}{\mu^2} - \frac{18\lambda'\xi^2}{\mu^2} - \frac{21\xi^4}{\mu^4}\right)\frac{v^2}{\mu^2} \\ & + \frac{\xi^2}{\mu^2}\left(\frac{s+t+u}{\mu^2}\right) + \mathcal{O}\left(\frac{x^2}{\mu^4}, \frac{xv^2}{\mu^4}, \frac{v^4}{\mu^4}\right)\end{aligned} \tag{4.2.41}$$

where $x = s, t, u$. On shell we get

$$\begin{aligned}\mathcal{A}\left(\varphi_1\varphi_1 \to \varphi_1\varphi_1\right) \;=\; & -\frac{3m^2_{\varphi_1}}{v^2} + \left(\frac{12\zeta\xi^3}{\mu^4} + \frac{25\lambda\xi^2}{\mu^2} - \frac{18\lambda'\xi^2}{\mu^2} - \frac{25\xi^4}{\mu^4}\right)\left(\frac{v}{\mu}\right)^2 \\ & - \left[\frac{9m^4_{\varphi_1}}{v^4} + \left(-\frac{12\zeta\lambda\xi^3}{\mu^4} + \frac{12\zeta\xi^5}{\mu^6} - \frac{27\lambda^2\xi^2}{\mu^2} + \frac{18\lambda\lambda'\xi^2}{\mu^2}\right.\right. \\ & \left.\left. + \frac{54\lambda\xi^4}{\mu^4} - \frac{18\lambda'\xi^4}{\mu^4} - \frac{27\xi^6}{\mu^6}\right)\frac{v^2}{\mu^2}\right]\left(\frac{v^2}{s-m^2_{\varphi_1}} + \frac{v^2}{t-m^2_{\varphi_1}} + \frac{v^2}{u-m^2_{\varphi_1}}\right) \\ & + \mathcal{O}\left(\frac{x^2}{m^4_{\varphi_2}}, \frac{v^4}{\mu^4}\right)\end{aligned} \tag{4.2.42}$$

Note that the long distance contribution to the amplitude is controlled by the trilinear coupling $g_{\varphi_1^3}$.

4.2.3 The low energy effective theory

The mixing language presented in the last section provides a complete description of the Higgs particle in the SHSM. In this section we are interested in following an alternative approach in terms of EFT by integrating out the singlet. This approach is valid near the decoupling limit defined in (4.2.10). The cutoff of the EFT is the singlet mass μ. No reference to mixing between the singlet and the Higgs is needed in the EFT approach to describe the properties of the Higgs boson, all the effects of mixing are automatically encoded in the low energy theory. In deriving the low energy theory we work at tree level. All the corrections to the SM Lagrangian in this case are threshold effects. This is enough to reproduce the tree level mixing effects presented in the last section.

EFT organizes the corrections to the SM properties hierarchically in terms of the small expansion parameter v^2/μ^2. In order to work consistently up to a particular order in the small expansion parameter, we must define a concept of *effective operator dimension* which allows us to identify the operators that must be kept in the low energy theory. In the SHSM, the correct concept of effective

dimension is just naive operator dimension. For instance, we will see that the effective Lagrangian contains a threshold correction to the quartic

$$\frac{\xi^2}{\mu^2}(H^\dagger H)^2 \tag{4.2.43}$$

The coefficient of this operator contains a power of the heavy singlet mass in the denominator, but it must not be considered to be suppressed, since ξ^2 in the numerator is allowed to be as large as μ^2, so this operator is of effective dimension four. In section 4.4 we will see that in the case of the effective field theory of the 2HDM, we will need to define a concept of effective dimension which does not coincide with naive operator dimension. In this chapter, we build the low energy theory of the SHSM up to effective dimension six. Just for illustrative purposes, we also keep the leading effects in λ_S at effective dimension eight.

The tree level low energy effective theory of the SHSM can be obtained by computing the diagrams of figures 4.1-4.4. Diagrams 4.1-4.3 give all the effective dimension six threshold corrections, and diagram 4.4 gives the leading correction in λ_S at effective dimension eight. The resulting effective Lagrangian is

$$\begin{aligned} &Z_H\, D_\mu H^\dagger D^\mu H + \frac{1}{2}\zeta_H\, \partial_\mu (H^\dagger H)\partial^\mu (H^\dagger H) - V(H) \\ &-\Big[\ \lambda^u_{ij}\ Q_i H \overline{u}_j - \lambda^d_{ij} Q_i H^c \overline{d}_j - \lambda^\ell_{ij} L_i H^c \overline{\ell}_j + \text{h.c.}\ \Big] \end{aligned} \tag{4.2.44}$$

where

$$V(H) = m_H^2 H^\dagger H + \frac{1}{2}\lambda_H (H^\dagger H)^2 + \frac{1}{3}\eta_6 (H^\dagger H)^3 + \frac{1}{4}\eta_8 (H^\dagger H)^4 \tag{4.2.45}$$

with

$$Z_H = 1 \qquad \zeta_H = \frac{\xi^2}{\mu^4} \qquad m_H^2 = m^2$$

$$\lambda_H = \lambda - \frac{\xi^2}{\mu^2} \qquad \eta_6 = \frac{3\lambda'\xi^2}{2\mu^4} - \frac{\xi^3\zeta}{\mu^6} \qquad \eta_8 = \frac{\lambda_S \xi^4}{2\mu^8} \qquad \lambda^f_{ij} = \frac{\sqrt{2}m^f_{ij}}{v} = \frac{\sqrt{2}m^f_i}{v}\ \delta^f_{ij}$$

The Higgs quartic in the low energy $\lambda_H = \lambda - \xi^2/\mu^2$ can be negative, since ξ^2/μ^2 can be of order one. In that case, the Higgs potential can still be stabilized by the $(H^\dagger H)^3$ operator, as needed in some models of baryogenesis [106]. Note that the coupling λ_S is irrelevant at effective dimension six: it first enters as a coefficient of a dimension eight operator. As a consequence, its effects in the low energy theory are always subleading in the expansion in the small parameter v^2/μ^2. The effective theory (4.2.44) has the particularity that it does not contain operators with gauge boson or fermion fields beyond the ones already present in the SM, since the particle that is being integrated out is a singlet. All the modifications of the Higgs couplings to fermions and massive gauge bosons with respect to their SM values come from the operator $\partial_\mu (H^\dagger H)\partial^\mu (H^\dagger H)$, as we will see shortly.

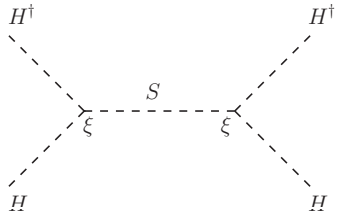

Figure 4.1: At dimension four and six generates the operators $(H^\dagger H)^2$ and $\partial_\mu(H^\dagger H)\partial^\mu(H^\dagger H)$.

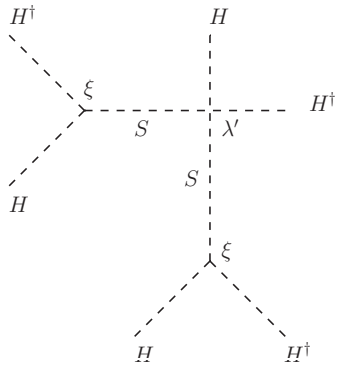

Figure 4.2: At dimension six generates the operator $(H^\dagger H)^3$.

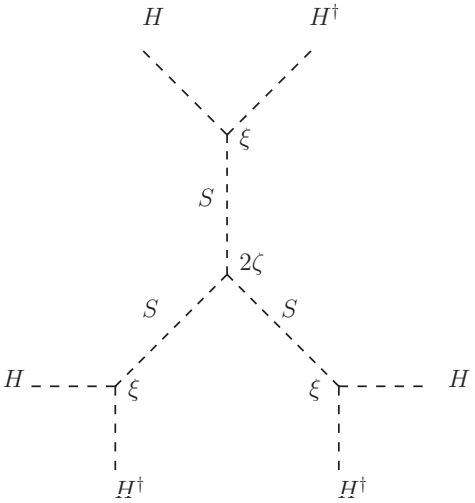

Figure 4.3: At dimension six generates the operator $(H^\dagger H)^3$.

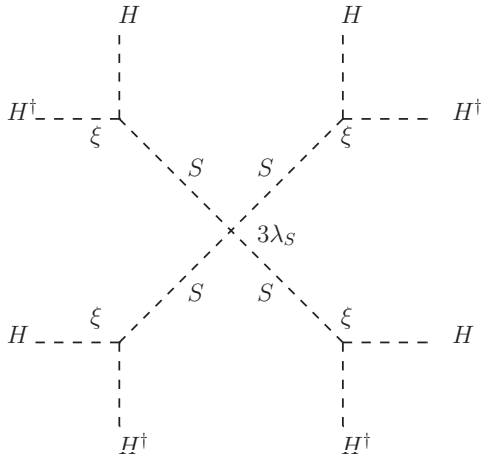

Figure 4.4: At dimension eight generates the operator $(H^\dagger H)^4$. This diagrams represents the leading order correction in λ_S, and is considered only for illustrative purposes.

We now proceed to write the effective theory for the neutral component of the doublet in the unitary gauge, which corresponds to the Higgs in the EFT description. The extremum condition for the potential is

$$\frac{\partial V}{\partial v}\Big|_{h=0} = v\Big(m_H^2 + \frac{1}{2}\lambda_H v^2 + \frac{1}{4}\eta_6 v^4 + \frac{1}{8}\eta_8 v^6\Big) = 0 \tag{4.2.46}$$

For a non-zero vev, the soft mass can be expressed in terms of the vev and couplings

$$m_H^2 = -\frac{1}{2}\lambda_H v^2 - \frac{1}{4}\eta_6 v^4 - \frac{1}{8}\eta_8 v^6 \tag{4.2.47}$$

The low energy Lagrangian density for the Higgs is

$$\begin{aligned}\frac{1}{2}Z_H\,\partial_\mu h\,\partial^\mu h+\zeta_H\left(\frac{1}{2}v^2\,\partial_\mu h\,\partial^\mu h+vh\,\partial_\mu h\,\partial^\mu h+\frac{1}{2}h^2\,\partial_\mu h\,\partial^\mu h\right)-V(h)\\ +\frac{1}{2}m_Z^2\left(1+\frac{2h}{v}+\frac{h^2}{v^2}\right)Z^\mu Z_\mu+m_W^2\left(1+\frac{2h}{v}+\frac{h^2}{v^2}\right)W^{+\mu}W^-_\mu\\ -\left(1+\frac{h}{v}\right)m^f_{ij}\,f_i\overline{f}_j+\text{h.c.}\end{aligned}\tag{4.2.48}$$

where

$$\begin{aligned}V(h)\;=\;&\frac{1}{2}\,m_H^2h^2+\frac{1}{2}\,\lambda_H\left(\frac{3}{2}v^2h^2+vh^3+\frac{1}{4}h^4\right)\\ &+\frac{1}{3}\,\eta_6\left(\frac{15v^4}{8}h^2+\frac{5v^3}{2}h^3+\frac{15v^2}{8}h^4+\frac{3v}{4}h^5+\frac{1}{8}h^6\right)\\ &+\frac{1}{4}\,\eta_8\left(\frac{7v^6}{4}h^2+\frac{7v^5}{2}h^3+\frac{35v^4}{8}h^4+\frac{7v^3}{2}h^5+\frac{7v^2}{4}h^6+\frac{v}{2}h^7+\frac{1}{16}h^8\right)\end{aligned}\tag{4.2.49}$$

The lowest order equation of motion for the Higgs field is

$$\begin{aligned}Z_H\Box h\;=\;&-m_H^2h-\frac{1}{2}\lambda_H(3v^2h+3vh^2+h^3)\\ &+\left(\frac{m_Z^2}{v}Z^\mu Z_\mu+\frac{2m_W^2}{v}W^{+\mu}W^-_\mu\right)\left(1+\frac{h}{v}\right)-\left(\frac{m^f_{ij}}{v}f_i\overline{f_j}+\text{h.c.}\right)+\dots\end{aligned}\tag{4.2.50}$$

where the dots represent terms of higher effective dimension. From now on we commit to $Z_H=1$.

The operator $\partial_\mu(H^\dagger H)\partial^\mu(H^\dagger H)$ leading to the non canonical kinetic terms in (4.2.48) has two effects in the couplings of the Higgs. First, it leads to wave function renormalization which dilutes all couplings. Second it gives additional irrelevant operators with derivatives which further modify the Higgs couplings, once they are replaced in favor of operators with no derivatives using integration by parts and the Higgs equation of motion. This second effect is usually not considered in the literature [112], but it is important to obtain the correct couplings in the low energy theory. We start by discussing these irrelevant operators. First, using integration by parts, the operator $\partial_\mu(H^\dagger H)\partial^\mu(H^\dagger H)$ can be rewritten as

$$\begin{aligned}\frac{1}{2}\zeta_H\partial_\mu(H^\dagger H)\partial^\mu(H^\dagger H)\;&=\;\zeta_H\left(\frac{1}{2}v^2\,\partial_\mu h\,\partial^\mu h+vh\,\partial_\mu h\,\partial^\mu h+\frac{1}{2}h^2\,\partial_\mu h\,\partial^\mu h\right)\\ &=\;\zeta_H\left(\frac{1}{2}v^2\,\partial_\mu h\,\partial^\mu h-\frac{1}{2}vh^2\,\Box h-\frac{1}{6}h^3\,\Box h\right)\end{aligned}\tag{4.2.51}$$

The lowest order equation of motion (4.2.50) can be used in (4.2.51) to replace the operator $\Box h$ in

favor of operators with no derivatives. The resulting Lagrangian is

$$\begin{aligned}
&\frac{1}{2}\,\partial_\mu h\,\partial^\mu h + \zeta_H\Bigg(\frac{1}{2}v^2\,\partial_\mu h\,\partial^\mu h - \left(\frac{1}{2}vh^2\ +\frac{1}{6}h^3\right)\Bigg[-m_H^2 h\\
&-\frac{1}{2}\lambda_H(3v^2h+3vh^2+h^3)+\left(\frac{m_Z^2}{v}Z^\mu Z_\mu+\frac{2m_W^2}{v}W^{+\mu}W^-_\mu\right)\left(1+\frac{h}{v}\right)\\
&-\left(\frac{m_{ij}^f}{v}f_i\overline{f_j}+\text{h.c.}\right)\Bigg]\Bigg)-V(h)\\
&+\frac{1}{2}m_Z^2\left(1+\frac{2h}{v}+\frac{h^2}{v^2}\right)Z^\mu Z_\mu+m_W^2\left(1+\frac{2h}{v}+\frac{h^2}{v^2}\right)W^{+\mu}W^-_\mu\\
&-\left(1+\frac{h}{v}\right)m_{ij}^f\,f_i\overline{f}_j+\text{h.c.}
\end{aligned}\tag{4.2.52}$$

We now discuss the wave function renormalization term $\zeta_H v^2\,\partial_\mu h\,\partial^\mu h$ in (4.2.52). To canonicalize the kinetic Lagrangian, we perform a field redefinition

$$\varphi=(1+\zeta_H v^2)^{1/2}h=\left[1+\frac{\xi^2v^2}{\mu^4}\right]^{1/2}h=\left[1+\sin^2\gamma+\mathcal{O}\left(\frac{v^4}{\mu^4}\right)\right]^{1/2}h \tag{4.2.53}$$

where using (4.2.25) we expressed the result in terms of $\sin^2\gamma$ to point out the close relation between mixing and wave function renormalization. In the mixing language, all Higgs couplings are diluted democratically due to mixing with the singlet. In the EFT language, this dilution is represented as wave function renormalization of the Higgs field: the wave function renormalization constant is equal to $\cos^{-1}\gamma$ up to corrections that in principle could come from higher order derivative interactions. Note that in the SHSM EFT wave function renormalization is an effective dimension six effect. The full Lagrangian in its final form is

$$\begin{aligned}
\mathcal{L}\ =\ &\frac{1}{2}\partial_\mu\varphi\partial^\mu\varphi-\frac{1}{2}m_\varphi^2\varphi^2+\sum_{n=3}^{n=8}\frac{1}{n!}g_{\varphi^n}\varphi^n+\frac{1}{2}m_Z^2Z^\mu Z_\mu+m_W^2W^{+\mu}W^-_\mu\\
&+\sum_{n=1}^{n=4}\frac{\varphi^n}{n!}\left[g_{\varphi^nZZ}\ \frac{1}{2}Z^\mu Z_\mu+g_{\varphi^nWW}\ W^{+\mu}W^-_\mu\right]\\
&-m_{ij}^f f_i\overline{f}_j-\sum_{n=1}^{n=3}\frac{\varphi^n}{n!}\left[\lambda^f_{\varphi^nij}\ f_i\overline{f}_j+\text{h.c.}\right]
\end{aligned}\tag{4.2.54}$$

where all the Higgs couplings can be expressed in terms of couplings of the UV completion using (4.2.52) and (4.2.53), and are written down explicitly below. We start with the Higgs mass, which is given by

$$\begin{aligned}
m_\varphi^2\ =\ v^2\Bigg[&\left(\lambda-\frac{\xi^2}{\mu^2}\right)+\left(\frac{3\lambda'\xi^2}{2\mu^2}-\frac{\lambda\xi^2}{\mu^2}-\frac{\zeta\xi^3}{\mu^4}+\frac{\xi^4}{\mu^4}\right)\frac{v^2}{\mu^2}\\
&+\frac{3\lambda_S\xi^4}{8\mu^4}\frac{v^4}{\mu^4}+\mathcal{O}\left(\frac{v^4}{\mu^4},\lambda_S^2\frac{v^6}{\mu^6}\right)\Bigg]
\end{aligned}\tag{4.2.55}$$

where we used (4.2.47) to replace the Lagrangian mass m_H in favor of the vacuum expectation value v. The term linear in λ_S in (4.2.55) comes from our example of an effective dimension eight effect.

We only keep this term for illustrative purposes for the Higgs mass, and we drop it from now on for the rest of the calculations.

The couplings of the Higgs to gauge bosons are given by

$$\begin{aligned} g_{\varphi VV} &= \frac{2m_V^2}{v}\left[1-\frac{\xi^2}{2\mu^2}\frac{v^2}{\mu^2}+\mathcal{O}\left(\frac{v^4}{\mu^4}\right)\right] \\ g_{\varphi^2 VV} &= \frac{2m_V^2}{v^2}\left[1-2\frac{\xi^2}{\mu^2}\frac{v^2}{\mu^2}+\mathcal{O}\left(\frac{v^4}{\mu^4}\right)\right] \end{aligned} \tag{4.2.56}$$

The modification of $g_{\varphi VV}$ with respect to its SM value comes exclusively from wave function renormalization as defined in (4.2.53). The modification of $g_{\varphi^2 VV}$ with respect to its SM value comes from wave function renormalization and from the additional interaction terms obtained from using the Higgs equation of motion in going from (4.2.51) to (4.2.52). For completeness, the rest of the couplings to gauge bosons are

$$v g_{\varphi^3 VV} = v^2 g_{\varphi^4 VV} = -\frac{m_V^2}{v^2}\left[\frac{8\xi^2 v^2}{\mu^4}+\mathcal{O}\left(\frac{v^4}{\mu^4}\right)\right] \tag{4.2.57}$$

$g_{\varphi^3 VV}$ and $g_{\varphi^4 VV}$ are irrelevant couplings, and they vanish in the decoupling limit. They come from using the Higgs equation of motion in (4.2.51).

The couplings to fermions are

$$\begin{aligned} \lambda^f_{\varphi ij} &= \frac{m_i^f}{v}\left[1-\frac{\xi^2}{2\mu^2}\frac{v^2}{\mu^2}+\mathcal{O}\left(\frac{v^4}{\mu^4}\right)\right]\delta_{ij} \\ v\lambda^f_{\varphi^2 ij} &= v^2\lambda^f_{\varphi^3 ij} = -\frac{m_i^f}{v}\left[\frac{\xi^2 v^2}{\mu^4}+\mathcal{O}\left(\frac{v^4}{\mu^4}\right)\right]\delta_{ij} \end{aligned} \tag{4.2.58}$$

The modification of $\lambda^f_{\varphi ij}$ with respect to its SM value comes exclusively from wave function renormalization. $\lambda^f_{\varphi^2 ij}, \lambda^f_{\varphi^3 ij}$ are irrelevant couplings which come from using the Higgs equation of motion in (4.2.51). They vanish in the decoupling limit.

The Higgs cubic and quartic self-couplings are modified by wave function renormalization and extra contributions from the rest of the irrelevant operators of the effective potential

$$\begin{aligned} \frac{g_{\varphi^3}}{v} &= -\frac{3m_\varphi^2}{v^2}+\left(\frac{9\lambda\xi^2}{2\mu^2}-\frac{3\lambda'\xi^2}{\mu^2}-\frac{9\xi^4}{2\mu^4}+\frac{2\zeta\xi^3}{\mu^4}\right)\frac{v^2}{\mu^2}+\mathcal{O}\left(\frac{v^4}{\mu^4}\right) \\ g_{\varphi^4} &= -\frac{3m_\varphi^2}{v^2}+\left(\frac{12\zeta\xi^3}{\mu^4}+\frac{25\lambda\xi^2}{\mu^2}-\frac{18\lambda'\xi^2}{\mu^2}-\frac{25\xi^4}{\mu^4}\right)\frac{v^2}{\mu^2}+\mathcal{O}\left(\frac{v^4}{\mu^4}\right) \end{aligned} \tag{4.2.59}$$

The rest of the self-couplings are all irrelevant couplings, and they vanish in the decoupling limit.

They are given by

$$\begin{aligned}
v g_{\varphi^5} &= \left(\frac{30\zeta\xi^3}{\mu^4} - \frac{45\lambda'\xi^2}{\mu^2} + \frac{60\lambda\xi^2}{\mu^2} - \frac{60\xi^4}{\mu^4}\right)\frac{v^2}{\mu^2} - \frac{105\lambda_S\xi^4}{2\mu^4}\,\frac{v^4}{\mu^4} + \mathcal{O}\left(\frac{v^4}{\mu^4}, \lambda_S^2\frac{v^6}{\mu^6}\right) \\
v^2 g_{\varphi^6} &= \left(\frac{30\zeta\xi^3}{\mu^4} - \frac{45\lambda'\xi^2}{\mu^2} + \frac{60\lambda\xi^2}{\mu^2} - \frac{60\xi^4}{\mu^4}\right)\frac{v^2}{\mu^2} - \frac{315\lambda_S\xi^4}{2\mu^4}\,\frac{v^4}{\mu^4} + \mathcal{O}\left(\frac{v^4}{\mu^4}, \lambda_S^2\frac{v^6}{\mu^6}\right) \\
v^3 g_{\varphi^7} &= -\frac{315\lambda_S\xi^4}{\mu^4}\,\frac{v^4}{\mu^4} + \mathcal{O}\left(\frac{v^4}{\mu^4}, \lambda_S^2\frac{v^6}{\mu^6}\right) \\
v^4 g_{\varphi^8} &= -\frac{315\lambda_S\xi^4}{\mu^4}\,\frac{v^4}{\mu^4} + \mathcal{O}\left(\frac{v^4}{\mu^4}, \lambda_S^2\frac{v^6}{\mu^6}\right)
\end{aligned} \tag{4.2.60}$$

Note that in the SHSM EFT, all the modifications to Higgs couplings come at effective dimension six. Also, all the couplings of the Higgs to fermions and gauge bosons are reduced at leading order with respect to their SM counterparts, but Higgs self couplings may be larger. These features, together with the absence of novel flavor and T violating effects, are the main phenomenological features of the EFT of a Higgs sector completed in the UV with a real singlet.

We conclude this section by pointing out that all trilinear couplings involving at least one Higgs are the same in the EFT and in the mixing language. Integrating out heavy fields does not modify cubic interactions. The reason is that cubic interactions control the *long distance* (non analytic) pieces of the tree level four linear scattering amplitudes, which do not receive contributions from diagrams mediated by heavy fields. The equality of the cubic interactions in the EFT and mixing languages ensures the equality between the long distance pieces of these amplitudes in both languages. We give examples of calculations of these type of amplitudes in section 4.2.2.1 in the mixing language and in section 4.2.3.1 in the EFT language. This logic can be run backwards: the equality between the non analytic scattering amplitudes enforces that the trilinear couplings in both languages must match. The four linear couplings are not the same in the mixing and EFT languages. Integrating out heavy fields in general modifies quartic (and higher order) interactions. These couplings control *short distance* pieces of the tree level four linear amplitudes, which do get contributions from diagrams mediated by the heavy mass eigenstate. In any case, even though couplings in general do not coincide in the mixing and EFT languages, the scattering amplitudes must coincide. Scattering amplitudes using the EFT language are obtained in the following section.

4.2.3.1 Scattering amplitudes

In this section we obtain the scattering amplitudes which were already computed in section 4.2.2.1 using the mixing language, now using the low energy EFT summarized in equation (4.2.54). This serves as a consistency check of the EFT, all amplitudes in the EFT and mixing language must match. We omit spinors in all amplitudes.

The dihiggs scattering amplitude to two W bosons is

$$\mathcal{A}\left(\varphi\varphi \to W^+W^-\right) \;=\; g_{\mu\nu}\left[g_{\varphi^2WW} - \frac{g_{\varphi^3}g_{\varphi WW}}{s-m_\varphi^2} - g^2_{\varphi WW}\left(\frac{1}{t-m_W^2}+\frac{1}{u-m_W^2}\right)\right] \tag{4.2.61}$$

Note that the same amplitude calculated in the mixing language (see (4.2.36)) also contains a contribution from a diagram mediated by the heavy mass eigenstate. In the EFT language the heavy state has already been integrated out, so its contribution is already included in the low energy effective couplings. Using the couplings of the effective theory (4.2.56) and (4.2.59) in (4.2.61), we get

$$\begin{aligned}\mathcal{A}\left(\varphi\varphi \to W^+W^-\right) \;=\; g_{\mu\nu}\Bigg[&\frac{2m_W^2}{v^2}\left(1-\frac{2\xi^2v^2}{\mu^4}\right)+\frac{2m_W^2}{v^2}\left[\frac{3m_\varphi^2}{v^2}+\left(-\frac{2\zeta\xi^3}{\mu^4}\right.\right.\\ &\left.\left.-\frac{6\lambda\xi^2}{\mu^2}+\frac{3\lambda'\xi^2}{\mu^2}+\frac{6\xi^4}{\mu^4}\right)\frac{v^2}{\mu^2}\right]\left(\frac{v^2}{s-m_\varphi^2}\right)\\ &-\frac{4m_W^4}{v^4}\left[1-\frac{\xi^2v^2}{\mu^4}\right]\left(\frac{v^2}{t-m_W^2}+\frac{v^2}{u-m_W^2}\right)+\mathcal{O}\left(\frac{v^4}{\mu^4}\right)\Bigg]\end{aligned} \tag{4.2.62}$$

which coincides with the corresponding calculation in the mixing language (4.2.37).

The chirality violating dihiggs to difermion scattering amplitude is

$$\mathcal{A}\left(\varphi\varphi \to f_i\overline{f}_j\right) \;=\; -\lambda^f_{\varphi^2 ij} + \frac{g_{\varphi^3}\lambda^f_{\varphi ij}}{s-m_\varphi^2} \tag{4.2.63}$$

The same amplitude calculated in the mixing language (4.2.38) also contains a diagram mediated by the heavy mass eigenstates, which in the EFT is already included in the low energy effective couplings. Note that in the EFT language there is a four linear effective coupling $\lambda^f_{\varphi^2 ij}$ that contributes to the amplitude. Using the effective couplings of the EFT (4.2.58) and (4.2.59) in (4.2.63) we get

$$\begin{aligned}\mathcal{A}\left(\varphi\varphi \to f_i\overline{f}_j\right) \;=\; \frac{m_i^f\;\delta_{ij}}{v^2}\Bigg[&\left(-\frac{3m_\varphi^2}{v^2}+\left[\frac{2\zeta\xi^3}{\mu^4}-\frac{3\lambda'\xi^2}{\mu^2}-\frac{6\xi^4}{\mu^4}\right.\right.\\ &\left.\left.+\frac{6\lambda\xi^2}{\mu^2}\right]\frac{v^2}{\mu^2}\right)\left(\frac{v^2}{s-m_\varphi^2}\right)+\frac{\xi^2v^2}{\mu^4}+\mathcal{O}\left(\frac{v^4}{\mu^4},\frac{m_i^{f\,2}}{v^2}\right)\Bigg]\end{aligned} \tag{4.2.64}$$

which coincides with the result obtained using the mixing language (4.2.39).

The dihiggs to dihiggs amplitude is

$$\mathcal{A}\left(\varphi\varphi \to \varphi\varphi\right) \;=\; g_{\varphi^4} - g^2_{\varphi^3}\left(\frac{1}{s-m_\varphi^2}+\frac{1}{t-m_\varphi^2}+\frac{1}{u-m_\varphi^2}\right) \tag{4.2.65}$$

This amplitude calculated in the mixing language (4.2.40) also contains a diagram mediated by the heavy mass eigenstates, which in the EFT are already included in the low energy effective couplings.

Using the couplings of the effective theory (4.2.59) in (4.2.65) and expanding in v^2/μ^2 we get

$$\begin{aligned}\mathcal{A}(\varphi\varphi\to\varphi\varphi) \;=\; & -\frac{3m_\varphi^2}{v^2}+\left(\frac{12\zeta\xi^3}{\mu^4}+\frac{25\lambda\xi^2}{\mu^2}-\frac{18\lambda'\xi^2}{\mu^2}-\frac{25\xi^4}{\mu^4}\right)\frac{v^2}{\mu^2}\\ & -\left[\frac{9m_\varphi^4}{v^4}+\left(-\frac{12\zeta\lambda\xi^3}{\mu^4}+\frac{12\zeta\xi^5}{\mu^6}-\frac{27\lambda^2\xi^2}{\mu^2}+\frac{18\lambda\lambda'\xi^2}{\mu^2}\right.\right.\\ & \left.\left.+\frac{54\lambda\xi^4}{\mu^4}-\frac{18\lambda'\xi^4}{\mu^4}-\frac{27\xi^6}{\mu^6}\right)\frac{v^2}{\mu^2}\right]\left(\frac{v^2}{s-m_\varphi^2}+\frac{v^2}{t-m_\varphi^2}+\frac{v^2}{u-m_\varphi^2}\right)\\ & +\mathcal{O}\left(\frac{v^4}{\mu^4}\right)\end{aligned} \tag{4.2.66}$$

Note that the equivalence between this result and the corresponding amplitude calculated in the mixing language (4.2.42) is only on-shell, since we used equations of motion to write our EFT in its final form.

4.3 The two Higgs doublet model

The 2HDM is a theory with a Higgs sector composed by two identical complex scalar fields Φ_a, $a=1,2$, charged under $SU(2)_L\times U(1)_Y$, with hypercharge one. The two Higgs doublets span a two dimensional complex plane. A $U(2)$ rotation in this complex plane does not affect the canonically normalized kinetic terms and leads to a different choice of Higgs fields, which we call the choice of basis. The ungauged $SU(2)=U(2)/U(1)_Y$ subgroup of the $U(2)$ is the full background symmetry of the model [114, 115]. The Lagrangian density of the Higgs doublets in a generic basis is

$$D_\mu\Phi_a^\dagger D^\mu\Phi_a - V(\Phi_1,\Phi_2) - \left[\;\lambda^u_{aij}\;Q_i\Phi_a\overline{u}_j - \lambda^{d\dagger}_{aij}Q_i\Phi_a^c\overline{d}_j - \lambda^{\ell\dagger}_{aij}L_i\Phi_a^c\overline{\ell}_j + \text{h.c.}\right] \tag{4.3.1}$$

where we sum over repeated indices and the covariant derivative acting on the doublets is

$$D_\mu\Phi_{1,2} = \left[\partial_\mu - i\left(g_2W_{a\mu}T_a+\frac{1}{2}g_1B_\mu\right)\right]H_{1,2} \tag{4.3.2}$$

The most general potential at the renormalizable level is given by

$$\begin{aligned}V(\Phi_1,\Phi_2) \;=\; & m_1^2\Phi_1^\dagger\Phi_1+m_2^2\Phi_2^\dagger\Phi_2-\left(m_{12}^2\Phi_1^\dagger\Phi_2+\text{h.c.}\right)+\frac{1}{2}\lambda_1(\Phi_1^\dagger\Phi_1)^2\\ + \;& \frac{1}{2}\lambda_2(\Phi_2^\dagger\Phi_2)^2+\lambda_3(\Phi_1^\dagger\Phi_1)(\Phi_2^\dagger\Phi_2)+\lambda_4(\Phi_1^\dagger\Phi_2)(\Phi_2^\dagger\Phi_1)\\ + \;& \left[\;\frac{1}{2}\lambda_5(\Phi_1^\dagger\Phi_2)^2+\lambda_6(\Phi_1^\dagger\Phi_1)(\Phi_1^\dagger\Phi_2)+\lambda_7(\Phi_2^\dagger\Phi_2)(\Phi_1^\dagger\Phi_2)+\text{h.c.}\;\right]\end{aligned} \tag{4.3.3}$$

The parameters $m_1^2, m_2^2, \lambda_1, \lambda_2, \lambda_3, \lambda_4$ are real, while $m_{12}^2, \lambda_5, \lambda_6, \lambda_7$ are in general complex.

The gauge invariant combinations of the fields that characterize the Higgs condensate with $SU(2)_L\times U(1)_Y\to U(1)_Q$ are

$$\frac{v_1^2}{2}=\langle\Phi_1^\dagger\Phi_1\rangle \qquad \frac{v_2^2}{2}=\langle\Phi_2^\dagger\Phi_2\rangle \qquad v_1^2+v_2^2=v^2 \tag{4.3.4}$$

$$\frac{v_{12}^2}{2} = \langle \Phi_1^\dagger \Phi_2 \rangle$$

while the gauge invariant combination that measures charge breaking is

$$\frac{v_c^2}{2} = \langle \Phi_1^c \Phi_2 \rangle$$

v_1 and v_2 are real, while v_{12} and v_c are in general complex. The Higgs vacuum expectation value takes the value $v = 246$ GeV. We also define the ratio of the vacuum expectation values $\tan\beta$ and the relative phase of the condensate ξ

$$\tan\beta = \frac{v_2}{v_1} \qquad\qquad \xi = \mathrm{Arg}\langle \Phi_1^\dagger \Phi_2 \rangle \tag{4.3.5}$$

The $U(1)_{\rm PQ}$ invariant potential for the Higgs condensate in terms gauge invariant quantities is

$$\begin{aligned} V(v_1, v_2, \xi) \;=\; & \frac{1}{2}m_1^2 v_1^2 + \frac{1}{2}m_2^2 v_2^2 + \frac{1}{8}\lambda_1 v_1^4 + \frac{1}{8}\lambda_2 v_2^4 + \frac{1}{4}\big(\lambda_3 + \lambda_4\big) v_1^2 v_2^2 \\ & + \mathrm{Re}\Big(- v_1 v_2 m_{12}^2 e^{i\xi} + \frac{1}{4} v_1^2 v_2^2 \lambda_5 e^{2i\xi} + \frac{1}{2} v_1^3 v_2 \lambda_6 e^{i\xi} + \frac{1}{2} v_1 v_2^3 \lambda_7 e^{i\xi} \Big) \end{aligned} \tag{4.3.6}$$

The condensate in terms of Lagrangian parameters is given by the minimization equations

$$\begin{aligned} \frac{\partial V}{\partial \xi} \;=\; 0 \;=\; & \frac{1}{2} v^2 \sin 2\beta \,\big[\, \mathrm{Im}(m_{12}^2 e^{i\xi}) - \frac{1}{4} v^2 \sin 2\beta\, \mathrm{Im}(\lambda_5 e^{2i\xi}) \\ & - \frac{1}{2} v^2 \cos^2\beta\, \mathrm{Im}(\lambda_6 e^{i\xi}) - \frac{1}{2} v^2 \sin^2\beta\, \mathrm{Im}(\lambda_7 e^{i\xi}) \,\big] \end{aligned} \tag{4.3.7}$$

$$\begin{aligned} \frac{\partial V}{\partial v_1} \;=\; 0 \;=\; & m_1^2 v \cos\beta + \frac{1}{2}\lambda_1\, v^3 \cos^3\beta + \frac{1}{2}(\lambda_3 + \lambda_4) v^3 \sin^2\beta \cos\beta \\ & - v \sin\beta\, \mathrm{Re}(m_{12}^2 e^{i\xi}) + \frac{1}{2} v^3 \sin^2\beta \cos\beta\, \mathrm{Re}(\lambda_5 e^{2i\xi}) \\ & + \frac{3}{2} v^3 \sin\beta \cos^2\beta\, \mathrm{Re}(\lambda_6 e^{i\xi}) + \frac{1}{2} v^3 \sin^3\beta\, \mathrm{Re}(\lambda_7 e^{i\xi}) \end{aligned} \tag{4.3.8}$$

$$\begin{aligned} \frac{\partial V}{\partial v_2} \;=\; 0 \;=\; & m_2^2 v \sin\beta + \frac{1}{2}\lambda_2\, v^3 \sin^3\beta + \frac{1}{2}(\lambda_3 + \lambda_4) v^3 \sin\beta \cos^2\beta \\ & - v \cos\beta\, \mathrm{Re}(m_{12}^2 e^{i\xi}) + \frac{1}{2} v^3 \sin\beta \cos^2\beta\, \mathrm{Re}(\lambda_5 e^{2i\xi}) \\ & + \frac{1}{2} v^3 \cos^3\beta\, \mathrm{Re}(\lambda_6 e^{i\xi}) + \frac{3}{2} v^3 \sin^2\beta \cos\beta\, \mathrm{Re}(\lambda_7 e^{i\xi}) \end{aligned} \tag{4.3.9}$$

The Higgs condensate gives mass to the gauge bosons corresponding to the broken gauge symmetries. The W and Z boson masses are

$$m_W = \frac{g_2 v}{2} \qquad m_Z = \frac{m_W}{\cos\,\theta_W} \qquad \tan\,\theta_W = \frac{g_1}{g_2} \tag{4.3.10}$$

The magnitudes of the Higgs condensates v_1, v_2 break the $SU(2)$ background symmetry down to a $U(1)_{\rm PQ}$ subset. The $U(1)_{\rm PQ}$ charges of fields and couplings are specified in table 4.2.

	$U(1)_{\rm PQ}$
Φ_1	$+1$
Φ_2	-1
$m_1^2, m_2^2, \lambda_1, \lambda_2, \lambda_3, \lambda_4$	0
$m_{12}^2, \lambda_6, \lambda_7$	$+2$
λ_5	$+4$
v_1, v_2	0
$e^{i\xi}$	-2
λ^f_{1ij}	-1
λ^f_{2ij}	$+1$

Table 4.2: $U(1)_{\rm PQ}$ charges. v_1, v_2 and ξ specify the Higgs condensate as defined in (4.3.4) and (4.3.5). The $U(1)_{\rm PQ}$ is the part of the background symmetry that is left unbroken by v_1 and v_2. The label f in the Yukawa couplings corresponds to u, d or ℓ. Fermions and gauge bosons are $U(1)_{\rm PQ}$ invariant fields.

In a general 2HDM with the EWSB pattern (4.3.4), the only feature that allows us to distinguish between the two doublets is the direction of the vev in the space of the neutral components of the doublets. This motivates the introduction of the *Higgs basis*, in which the vev is contained exclusively in one of the doublets. The Higgs basis is obtained by a rotation in the doublet space into a new set of doublets H_a, $a = 1, 2$

$$\begin{aligned} e^{-i\xi/2} H_1 &= \cos\beta\ \Phi_1 + \sin\beta\ e^{-i\xi}\ \Phi_2 \\ H_2 &= -\sin\beta\ e^{i\xi}\ \Phi_1 + \cos\beta\ \Phi_2 \end{aligned} \tag{4.3.11}$$

such that in the new basis, only one of the doublets is responsible for EWSB

$$\frac{v^2}{2} = \langle H_1^\dagger H_1 \rangle \qquad 0 = \langle H_2^\dagger H_2 \rangle \tag{4.3.12}$$

Note that the Higgs basis is not unique. A $U(1)_{\rm PQ}$ transformation leaves the magnitudes of the Higgs condensates invariant. As a consequence, the condition (4.3.12) is $U(1)_{\rm PQ}$ invariant, and different Higgs basis can be obtained by performing a $U(1)_{\rm PQ}$ transformation on the doublets H_a.

We now describe the 2HDM in the Higgs basis. The Lagrangian density in the Higgs basis is

$$D_\mu H_a^\dagger D^\mu H_a - V(H_1, H_2) - \left[\ \tilde\lambda^u_{aij}\ Q_i H_a \overline{u}_j - \tilde\lambda^{d\dagger}_{aij} Q_i H_a^c \overline{d}_j - \tilde\lambda^{\ell\dagger}_{aij} L_i H_a^c \overline{\ell}_j + \text{h.c.} \right] \tag{4.3.13}$$

Since only H_1 carries a vev, the quark mass matrices are given by

$$\tilde\lambda^f_{1ij} = \frac{\sqrt{2} m^f_{ij}}{v} \tag{4.3.14}$$

where the mass matrices for the quarks and leptons are defined in the Lagrangian as

$$- m^f_{ij} u_i \overline{u}_j - m^{d\dagger}_{ij} d_i \overline{d}_j - m^{\ell\dagger}_{ij} \ell_i \overline{\ell}_j + \text{h.c.} \tag{4.3.15}$$

In the above definition and for the rest of this chapter, note that there is a dagger in the definition of the down type mass matrices with respect to the up type mass matrix.

The potential in (4.3.13) is given by

$$\begin{aligned} V(H_1,H_2) &= \tilde{m}_1^2 H_1^\dagger H_1 + \tilde{m}_2^2 H_2^\dagger H_2 + \left(\tilde{m}_{12}^2 H_1^\dagger H_2 + \text{h.c.}\right) \\ &+ \frac{1}{2}\tilde{\lambda}_1 (H_1^\dagger H_1)^2 + \frac{1}{2}\tilde{\lambda}_2 (H_2^\dagger H_2)^2 + \tilde{\lambda}_3 (H_2^\dagger H_2)(H_1^\dagger H_1) + \tilde{\lambda}_4 (H_2^\dagger H_1)(H_1^\dagger H_2) \\ &+ \left[\frac{1}{2}\tilde{\lambda}_5 (H_1^\dagger H_2)^2 + \tilde{\lambda}_6 H_1^\dagger H_1 H_1^\dagger H_2 + \tilde{\lambda}_7 (H_2^\dagger H_2)(H_1^\dagger H_2) + \text{h.c.} \right] \end{aligned} \tag{4.3.16}$$

The parameters $\tilde{m}_1^2, \tilde{m}_2^2, \tilde{\lambda}_1, \tilde{\lambda}_2, \tilde{\lambda}_3, \tilde{\lambda}_4$ are real, while $\tilde{m}_{12}^2, \tilde{\lambda}_5, \tilde{\lambda}_6, \tilde{\lambda}_7$ are in general complex. The relations between the couplings in the Higgs basis and the generic basis are [115]

$$\begin{aligned} \tilde{\lambda}^f_{1ij} &= e^{-i\xi/2}\lambda^f_{1ij}\cos\beta + e^{i\xi/2}\lambda^f_{2ij}\sin\beta \\ \tilde{\lambda}^f_{2ij} &= -e^{-i\xi}\lambda^f_{1ij}\sin\beta + \lambda^f_{2ij}\cos\beta \end{aligned} \tag{4.3.17}$$

$$\begin{aligned} \tilde{m}_1^2 &= m_1^2 c_\beta^2 + m_2^2 s_\beta^2 - \text{Re}(m_{12}^2 e^{i\xi}) s_{2\beta} \\ \tilde{m}_2^2 &= m_1^2 s_\beta^2 + m_2^2 c_\beta^2 + \text{Re}(m_{12}^2 e^{i\xi}) s_{2\beta} \\ \tilde{m}_{12}^2 e^{i\xi/2} &= -\frac{1}{2}(m_1^2 - m_2^2) s_{2\beta} - \text{Re}(m_{12}^2 e^{i\xi}) c_{2\beta} - i\text{Im}(m_{12}^2 e^{i\xi}) \end{aligned} \tag{4.3.18}$$

$$\begin{aligned} \tilde{\lambda}_1 &= \lambda_1 c_\beta^4 + \lambda_2 s_\beta^4 + \frac{1}{2}\lambda_{345} s_{2\beta}^2 + 2 s_{2\beta}\left(c_\beta^2 \text{Re}(\lambda_6 e^{i\xi}) + s_\beta^2 \text{Re}(\lambda_7 e^{i\xi})\right) \\ \tilde{\lambda}_2 &= \lambda_1 s_\beta^4 + \lambda_2 c_\beta^4 + \frac{1}{2}\lambda_{345} s_{2\beta}^2 - 2 s_{2\beta}\left(s_\beta^2 \text{Re}(\lambda_6 e^{i\xi}) + c_\beta^2 \text{Re}(\lambda_7 e^{i\xi})\right) \\ \tilde{\lambda}_3 &= \frac{1}{4} s_{2\beta}^2 (\lambda_1 + \lambda_2 - 2\lambda_{345}) + \lambda_3 - s_{2\beta} c_{2\beta} \text{Re}((\lambda_6 - \lambda_7) e^{i\xi}) \\ \tilde{\lambda}_4 &= \frac{1}{4} s_{2\beta}^2 (\lambda_1 + \lambda_2 - 2\lambda_{345}) + \lambda_4 - s_{2\beta} c_{2\beta} \text{Re}((\lambda_6 - \lambda_7) e^{i\xi}) \\ \tilde{\lambda}_5 e^{i\xi} &= \frac{1}{4} s_{2\beta}^2 (\lambda_1 + \lambda_2 - 2\lambda_{345}) + \text{Re}(\lambda_5 e^{2i\xi}) + i c_{2\beta} \text{Im}(\lambda_5 e^{2i\xi}) \\ &- s_{2\beta} c_{2\beta} \text{Re}\left((\lambda_6 - \lambda_7) e^{i\xi}\right) - i s_{2\beta} \text{Im}\left((\lambda_6 - \lambda_7) e^{i\xi}\right) \\ \tilde{\lambda}_6 e^{i\xi/2} &= -\frac{1}{2} s_{2\beta}\left(\lambda_1 c_\beta^2 - \lambda_2 s_\beta^2 - \lambda_{345} c_{2\beta} - i\text{Im}(\lambda_5 e^{2i\xi})\right) \\ &+ c_\beta c_{3\beta} \text{Re}(\lambda_6 e^{i\xi}) + s_\beta s_{3\beta} \text{Re}(\lambda_7 e^{i\xi}) + i c_\beta^2 \text{Im}(\lambda_6 e^{i\xi}) + i s_\beta^2 \text{Im}(\lambda_7 e^{i\xi}) \\ \tilde{\lambda}_7 e^{i\xi/2} &= -\frac{1}{2} s_{2\beta}\left(\lambda_1 s_\beta^2 - \lambda_2 c_\beta^2 + \lambda_{345} c_{2\beta} + i\text{Im}(\lambda_5 e^{2i\xi})\right) \\ &+ s_\beta s_{3\beta} \text{Re}(\lambda_6 e^{i\xi}) + c_\beta c_{3\beta} \text{Re}(\lambda_7 e^{i\xi}) + i s_\beta^2 \text{Im}(\lambda_6 e^{i\xi}) + i c_\beta^2 \text{Im}(\lambda_7 e^{i\xi}) \end{aligned} \tag{4.3.19}$$

where $c_{n\beta} \equiv \cos n\beta$ and $s_{n\beta} \equiv \sin n\beta$ and we defined

$$\lambda_{345} \equiv \lambda_3 + \lambda_4 + \text{Re}(\lambda_5 e^{2i\xi}) \tag{4.3.20}$$

In a general 2HDM, $\tan\beta$ is only required to map between couplings in the original generic basis and the Higgs basis, but it is irrelevant for any calculation, since the generic basis is arbitrary. In other words, $\tan\beta$ is a parameter that contains no physical information in a general 2HDM, since there is no feature in the model that allows us to distinguish the direction of the doublets Φ_1, Φ_2 as special directions in field space. For this reason, we will make no further reference to $\tan\beta$ until section 4.5, where we study particular cases of 2HDM with features that allow us to specify a preferred basis which is different from the Higgs basis. The fields and couplings in the Higgs basis are charged under a $U(1)_{\rm PQ}$ background symmetry as specified in table 4.3. Note that all the relations (4.3.17), (4.3.18) and (4.3.19) are covariant under the $U(1)_{\rm PQ}$.

The decoupling limit in the Higgs basis can be very simple defined as the limit in which

$$\tilde{m}_2^2 \gg \left|\tilde{\lambda}_i\right| v^2 \tag{4.3.21}$$

where $i = 1..7$. This definition is motivated by the fact that in the decoupling limit, the Higgs aligns with the vacuum expectation value which is contained entirely in H_1, so H_2 must be the decoupled doublet. Near the decoupling limit alignment is not exact, and there are corrections that can be understood in two ways. In the mixing language, corrections arise due to mixing between the neutral components of H_1 and H_2, which is suppressed by powers of the electrosheep scale over the heavy mass of H_2, as we will see in section 4.3.1. In the effective field theory language, corrections arise in the form of higher dimensional operators that modify the SM Lagrangian, which are induced when H_2 is integrated out, as we will see in section 4.4.

	$U(1)_{\rm PQ}$
H_1	0
H_2	-1
$\tilde{m}_1^2, \tilde{m}_2^2, \tilde{\lambda}_1, \tilde{\lambda}_2, \tilde{\lambda}_3, \tilde{\lambda}_4$	0
$\tilde{m}_{12}^2, \tilde{\lambda}_6, \tilde{\lambda}_7$	$+1$
$\tilde{\lambda}_5$	$+2$
v	0
$\tilde{\lambda}_{1ij}^f$	0
$\tilde{\lambda}_{2ij}^f$	$+1$

Table 4.3: $U(1)_{\rm PQ}$ charges in the Higgs basis. The label f in the Yukawa couplings corresponds to u, d or ℓ. Fermions and gauge bosons are $U(1)_{\rm PQ}$ invariant fields.

The EWSB conditions in the Higgs basis are simplified by the fact that only one of the doublets

contains a vev. They are given by

$$\begin{aligned}\frac{\partial V}{\partial H_1}\Big|_{H_1=v/\sqrt{2},H_2=0} &= \frac{1}{\sqrt{2}}\tilde{m}_1^2 v + \frac{1}{2\sqrt{2}}\tilde{\lambda}_1 v^3 = 0 \\ \frac{\partial V}{\partial H_2}\Big|_{H_1=v/\sqrt{2},H_2=0} &= \frac{1}{\sqrt{2}}\tilde{m}_{12}^2 v + \frac{1}{2\sqrt{2}}\tilde{\lambda}_6 v^3 = 0\end{aligned} \tag{4.3.22}$$

These conditions can be rewritten as

$$v^2 = -2\frac{\tilde{m}_1^2}{\tilde{\lambda}_1} \tag{4.3.23}$$

$$\tilde{m}_{12}^2 = -\frac{1}{2}\tilde{\lambda}_6 v^2 \tag{4.3.24}$$

where (4.3.23) involves only real parameters and (4.3.24) is a complex equation. The expressions (4.3.23) and (4.3.24) relate $\tilde{m}_1$ and $\tilde{m}_{12}$ with the electroweak scale. The relation (4.3.24) can be interpreted as a no tadpole condition for the H_2 doublet.

The Higgs potential (4.3.16) contains fourteen parameters. However, not all of these parameters are physical or independent of each other. Only thirteen of the parameters are invariants under the background $U(1)_{\rm PQ}$, namely the six real couplings, the four magnitudes of the complex couplings and $\mathrm{Arg}(\tilde{m}_{12}^4\tilde{\lambda}_5^*), \mathrm{Arg}(\tilde{m}_{12}^2\tilde{\lambda}_6^*), \mathrm{Arg}(\tilde{m}_{12}^2\tilde{\lambda}_7^*)$. On the other hand, the EWSB relations (4.3.23) and (4.3.24) impose three conditions on the couplings, so the final number of physical and independent invariants in the potential is eleven. One of the invariants can be chosen to be the Higgs vev. Some of the parameters specifying the Higgs potential and Yukawa interactions in a general 2HDM are complex, and allow for T violation. There are two independent physical T violating phases in the bosonic sector in the case in which $\tilde{\lambda}_5 \neq 0$ [114]. We take them to be the $U(1)_{\rm PQ}$ invariant combinations

$$\begin{aligned}\theta_1 &= \frac{1}{2}\mathrm{Arg}\big(\tilde{\lambda}_6^2\tilde{\lambda}_5^*\big) = \frac{1}{2}\mathrm{Arg}\big(\tilde{m}_{12}^4\tilde{\lambda}_5^*\big) \\ \theta_2 &= \frac{1}{2}\mathrm{Arg}\big(\tilde{\lambda}_7^2\tilde{\lambda}_5^*\big)\end{aligned} \tag{4.3.25}$$

where in the first line we made use of (4.3.24). In the case in which $\tilde{\lambda}_5 = 0$, there is only one independent T violating phase given by $\theta_3 = \mathrm{Arg}\big(\tilde{\lambda}_7\tilde{\lambda}_6^*\big)$. When considering also fermionic interactions, there are several additional T violating phases. The $U(1)_{\rm PQ}$ invariant phases are

$$\tilde{\lambda}_5^*(\tilde{\lambda}_{2ij}^f)^2 \qquad \tilde{\lambda}_6^*\tilde{\lambda}_{2ij}^f \qquad \tilde{\lambda}_7^*\tilde{\lambda}_{2ij}^f \tag{4.3.26}$$

All the $U(1)_{\rm PQ}$ invariant phases in the most general 2HDM can be expressed in terms of the complete set of independent phases

$$\theta_1(\text{or } \theta_3 \text{ if } \tilde{\lambda}_5 \text{ vanishes}) \qquad \theta_2 \qquad \mathrm{Arg}\big(\tilde{\lambda}_6^*\tilde{\lambda}_{2ij}^f\big) \quad , \quad f = u, d, \ell \tag{4.3.27}$$

In this work we allow for T violation both in the bosonic sector and the fermionic interactions, and we will specify when we specialize to the T conserving case. In this chapter we assume that there is a low energy solution for the strong CP problem and we do not worry about possible contributions from complex phases to θ_{QCD}.

We now turn to the components of the Higgs doublets. The neutral and charged components of the Higgs basis doublets are

$$\begin{aligned} H_1^0 &= \frac{1}{\sqrt{2}}\Big(v + h_1 + iG^0\Big) \\ H_2^0 &= \frac{1}{\sqrt{2}}\, e^{i\,\mathrm{Arg}(\tilde{\lambda}_5^*)/2}\Big(h_2 + ih_3\Big) \\ H_1^+ &= G^+ \\ H_2^+ &= e^{i\,\mathrm{Arg}(\tilde{\lambda}_5^*)/2}\, H^+ \end{aligned} \tag{4.3.28}$$

where gauge invariance ensures $v \geq 0$. As advertised, the second doublet H_2 in the Higgs basis does not participate in EWSB. The phase $e^{i\,\mathrm{Arg}(\tilde{\lambda}_5^*)/2}$ is added in the definition of the components of H_2 because it makes the mass matrix automatically block diagonal in the T conserving case, as we will see in section 4.3.1. In this case the fields h_1 and h_2 do not mix with h_3, which will automatically be a T odd eigenstate. Note that the fields h_1, h_2 and h_3 are invariant under the $U(1)_{\rm PQ}$ background symmetry. G^0, G^+ are Goldstone bosons. From now on we work in the unitary gauge.

4.3.1 Mass eigenstates

In the unitary gauge, the two doublets contain four Higgs particles, three of which are neutral and one is charged. The charged Higgs boson is a mass eigenstate with mass

$$m_{H\pm}^2 = \tilde{m}_2^2 + \frac{1}{2}\tilde{\lambda}_3 v^2 \tag{4.3.29}$$

The three neutral states mix in the mass matrix

$$V \supset \frac{1}{2}\mathcal{M}_{ij}^2 h_i h_j \tag{4.3.30}$$

where we sum over $i, j = 1, 2, 3$. This mass matrix is $U(1)_{\rm PQ}$ invariant, real and symmetric. It is specified by five real numbers and it is given by

$$\mathcal{M}^2 = \begin{pmatrix} v^2\tilde{\lambda}_1 & v^2\left|\tilde{\lambda}_6\right|\cos\theta_1 & -v^2\left|\tilde{\lambda}_6\right|\sin\theta_1 \\ v^2\left|\tilde{\lambda}_6\right|\cos\theta_1 & \tilde{m}_2^2 + \frac{1}{2}v^2\Big(\tilde{\lambda}_3 + \tilde{\lambda}_4 + \left|\tilde{\lambda}_5\right|\Big) & 0 \\ -v^2\left|\tilde{\lambda}_6\right|\sin\theta_1 & 0 & \tilde{m}_2^2 + \frac{1}{2}v^2\Big(\tilde{\lambda}_3 + \tilde{\lambda}_4 - \left|\tilde{\lambda}_5\right|\Big) \end{pmatrix} \tag{4.3.31}$$

where θ_1 is one of the bosonic CP violating phases defined in (4.3.25). In this chapter we identify the Higgs particle with the lightest of the three neutral mass eigenstates, which are labeled in increasing order by their mass as $(\varphi_1, \varphi_2, \varphi_3)$. We are interested in analyzing the decoupling limit (4.3.21), in which mixing in the mass matrix is suppressed.

The time reversal transformation properties of the mass eigenstates can be derived by inspecting their couplings to gauge bosons and fermions. In general we expect the mass eigenstates to be fields with indefinite T properties, due to the T violating phases (4.3.25) and (4.3.26) of the 2HDM. Note that the T violating effect of θ_1 is encoded in mixing of h_1 with h_3. On the other hand, the T violating phase θ_2 does not appear in the mass matrix. Note that the phase $e^{i\,\mathrm{Arg}(\tilde{\lambda}_5^*)/2}$ in the definition (4.3.28) guarantees that the mass matrix is automatically block diagonal in the T conserving case.

The mass matrix has two zeroes, which have their origin in the underlying $U(1)_{\rm PQ}$ background symmetry. To understand the zeroes, consider the limit in which we suppress the mixing between h_1 and h_2 by taking $\tilde{\lambda}_6$ and $\tilde{m}_{12}^2$ equal to zero. In this case, the only $U(1)_{\rm PQ}$ breaking term that enters in the mass matrix is $\tilde{\lambda}_5$, which breaks the mass degeneracy of the two heavy eigenstates. The phase $e^{i\,\mathrm{Arg}(\tilde{\lambda}_5^*)/2}$ included in our choice of component fields h_2, h_3 in (4.3.28), makes sure that h_2 and h_3 do not mix in the mass matrix, giving rise to the aforementioned zeroes. In this case, h_2 and h_3 are the heavy neutral mass eigenstates, with mass splitting controlled by $\left|\tilde{\lambda}_5\right|$.

4.3.1.1 The T conserving case

Before analyzing the neutral mass matrix in generality, let us start by studying the mass eigenstates in the simpler, T conserving case. This is defined as the case in which all the T violating phases (4.3.25) and (4.3.26) vanish [114]. In the case that $\tilde{\lambda}_5 = 0$, one must also check that $\mathrm{Arg}\big(\tilde{\lambda}_7\tilde{\lambda}_6^*\big)$ vanishes. In this section we can take all couplings to be real. In the T conserving case the mass matrix simplifies to a block diagonal form, mixing only the fields h_1 and h_2, which are now T even. The field h_3 is T odd and corresponds to the mass eigenstate φ_2

$$m_{\varphi_2}^2 = \mathcal{M}_{33}^2 = \tilde{m}_2^2 + \frac{1}{2}v^2\Big(\tilde{\lambda}_3 + \tilde{\lambda}_4 - \left|\tilde{\lambda}_5\right|\Big) \tag{4.3.32}$$

The masses of the remaining neutral eigenstates are

$$m_{\varphi_1,\varphi_3}^2 = \frac{1}{2}\left(\mathcal{M}_{11}^2 + \mathcal{M}_{22}^2 \pm \sqrt{(\mathcal{M}_{22}^2 - \mathcal{M}_{11}^2)^2 + 4\mathcal{M}_{12}^2}\right) \tag{4.3.33}$$

In terms of couplings in the potential, the Higgs mass near the decoupling limit is given by

$$m_{\varphi_1}^2 \;=\; v^2\left[\tilde{\lambda}_1 - \tilde{\lambda}_6^2\,\frac{v^2}{\tilde{m}_2^2} - \frac{1}{2}\tilde{\lambda}_6^2\left[2\tilde{\lambda}_1 - \tilde{\lambda}_3 - \tilde{\lambda}_4 - \tilde{\lambda}_5\right]\frac{v^4}{\tilde{m}_2^4} + \mathcal{O}\left(\frac{v^6}{\tilde{m}_2^6}\right)\right] \tag{4.3.34}$$

For completeness, the mass of the remaining neutral eigenstate is

$$m^2_{\varphi_2} = \tilde{m}_2^2\left[1 + \frac{1}{2}\left(\tilde{\lambda}_3 + \tilde{\lambda}_4 + \left|\tilde{\lambda}_5\right|\right)\frac{v^2}{\tilde{m}_2^2} + \tilde{\lambda}_6^2\,\frac{v^4}{\tilde{m}_2^4} + \mathcal{O}\left(\frac{v^6}{\tilde{m}_2^6}\right)\right] \tag{4.3.35}$$

Note that the splitting between the two heavy neutral eigenstates is

$$m^2_{\varphi_3} - m^2_{\varphi_2} = v^2\left[\left|\tilde{\lambda}_5\right| + \tilde{\lambda}_6^2\,\frac{v^2}{\tilde{m}_2^2} + \mathcal{O}\left(\frac{v^4}{\tilde{m}_2^4}\right)\right] \tag{4.3.36}$$

The mixing angle between the h_1 and h_2 is generally named in the literature $\beta - \alpha$, where α is the rotation angle that diagonalizes the T even part of the mass matrix in the generic basis [26]. The relation between the mass eigenstates and h_1 and h_2 is given by

$$\begin{pmatrix} \varphi_1 \\ \varphi_3 \end{pmatrix} = \begin{pmatrix} \sin(\beta-\alpha) & \cos(\beta-\alpha) \\ -\cos(\beta-\alpha) & \sin(\beta-\alpha) \end{pmatrix}\begin{pmatrix} h_1 \\ h_2 \end{pmatrix} \tag{4.3.37}$$

$\cos(\beta-\alpha)$ is called the alignment parameter [28], and the alignment limit is defined as the limit in which $\cos(\beta-\alpha) = 0$. In this limit, the Higgs lies along the direction of h_1, which by definition of the Higgs basis is the direction of the vev in field space. The alignment parameter controls the couplings of the Higgs to gauge bosons and fermions [26]. In the alignment limit the couplings of the Higgs are Standard Model like. The alignment parameter is given by

$$\cos(\beta-\alpha) = \frac{-2\mathcal{M}_{12}^2}{\sqrt{4\left(\mathcal{M}_{12}^2\right)^2 + \left[\mathcal{M}_{22}^2 - \mathcal{M}_{11}^2 + \sqrt{\left(\mathcal{M}_{22}^2 - \mathcal{M}_{11}^2\right)^2 + 4\mathcal{M}_{12}^2}\right]^2}} \tag{4.3.38}$$

which at first order in $v^2/\tilde{m}_2^2$ is

$$\cos(\beta-\alpha) = -\left|\tilde{\lambda}_6\right|\,\frac{v^2}{\tilde{m}_2^2} + \mathcal{O}\left(\frac{v^4}{\tilde{m}_2^4}\right) \tag{4.3.39}$$

4.3.1.2 The general T violating case

We now proceed to study the neutral mass eigenstates in the general T violating case, in which all three fields h_1, h_2 and h_3 mix in the mass matrix. Phases must now be included in the mixing discussion [116]. The characteristic equation of the mass matrix is

$$-\det(\mathcal{M}^2 - xI) = x^3 + ax^2 + bx + c = 0 \tag{4.3.40}$$

with

$$\begin{aligned}
a &= -2\tilde{m}_2^2 - v^2(\tilde{\lambda}_1 + \tilde{\lambda}_3 + \tilde{\lambda}_4) \\
b &= \tilde{m}_2^4 + v^2\tilde{m}_2^2(2\tilde{\lambda}_1 + \tilde{\lambda}_3 + \tilde{\lambda}_4) + v^4\left[\tilde{\lambda}_1(\tilde{\lambda}_3 + \tilde{\lambda}_4) + \frac{1}{4}(\tilde{\lambda}_3 + \tilde{\lambda}_4)^2 - \frac{1}{4}\tilde{\lambda}_5\tilde{\lambda}_5^* - \tilde{\lambda}_6\tilde{\lambda}_6^*\right] \\
c &= -v^2\tilde{m}_2^4\tilde{\lambda}_1 + v^4\tilde{m}_2^2\left[\tilde{\lambda}_6\tilde{\lambda}_6^* - \tilde{\lambda}_1(\tilde{\lambda}_3 + \tilde{\lambda}_4)\right] \\
&\quad - \frac{1}{4}v^6\left[\tilde{\lambda}_1(\tilde{\lambda}_3 + \tilde{\lambda}_4)^2 - \tilde{\lambda}_1\tilde{\lambda}_5\tilde{\lambda}_5^* - 2\tilde{\lambda}_6\tilde{\lambda}_6^*(\tilde{\lambda}_3 + \tilde{\lambda}_4) + (\tilde{\lambda}_5\tilde{\lambda}_6^{*2} + \text{h.c.})\right]
\end{aligned} \tag{4.3.41}$$

The three solutions to the characteristic equation are the masses of the neutral Higgs particles, and they are given by

$$\begin{aligned} m^2_{\varphi_a} &= -\frac{1}{3C}\left[aC + \omega_a C^2 + \frac{A}{\omega_a} \right] \\ A &= a^2 - 3b \\ B &= 2a^3 - 9ab + 27c \\ C &= \left[\frac{B}{2} + \frac{1}{2}\sqrt{B^2 - 4A^3} \right]^{1/3} \\ \omega_1 &= 1 \quad , \quad \omega_2 = -\frac{1}{2} + i\frac{\sqrt{3}}{2} \quad , \quad \omega_3 = \omega_2^* \end{aligned} \tag{4.3.42}$$

We identify the smallest root of the characteristic polynomial with the Higgs mass.

Near the decoupling limit, the mass eigenstates (4.3.42) have simple expressions in terms of expansions in $v^2/\tilde{m}_2^2$. In this case, the Higgs mass is given by

$$m^2_{\varphi_1} = v^2\left[\tilde{\lambda}_1 - \tilde{\lambda}_6^*\tilde{\lambda}_6 \frac{v^2}{\tilde{m}_2^2} - \frac{1}{2}\Big[(2\tilde{\lambda}_1 - \tilde{\lambda}_3 - \tilde{\lambda}_4)\tilde{\lambda}_6^*\tilde{\lambda}_6 - \frac{1}{2}(\tilde{\lambda}_5^*\tilde{\lambda}_6^2 + \text{h.c}) \Big] \frac{v^4}{\tilde{m}_2^4} + \mathcal{O}\left(\frac{v^6}{\tilde{m}_2^6} \right) \right] \tag{4.3.43}$$

while the masses of the heavy eigenstates are

$$m^2_{\varphi_2,\varphi_3} = \tilde{m}_2^2\left[1 + \frac{1}{2}\big(\tilde{\lambda}_3 + \tilde{\lambda}_4 \pm \left|\tilde{\lambda}_5\right| \big) \frac{v^2}{\tilde{m}_2^2} + \frac{1}{2}\tilde{\lambda}_6^*\tilde{\lambda}_6 \big[1 \pm \cos 2\theta_1 \big] \frac{v^4}{\tilde{m}_2^4} + \mathcal{O}\left(\frac{v^6}{\tilde{m}_2^6} \right) \right] \tag{4.3.44}$$

Note that the mass splitting between the heavy states is

$$m^2_{\varphi_3} - m^2_{\varphi_2} = v^2\left[\left|\tilde{\lambda}_5\right| + \tilde{\lambda}_6^*\tilde{\lambda}_6 \cos 2\theta_1 \frac{v^2}{\tilde{m}_2^2} + \mathcal{O}\left(\frac{v^4}{\tilde{m}_2^4} \right) \right] \tag{4.3.45}$$

The eigenvectors V^a corresponding to the three mass eigenvalues $m^2_{\varphi_a}$ characterize the mixing and satisfy

$$\mathcal{M}^2_{ij} V^a_j = m^2_{\varphi_a} V^a_i \tag{4.3.46}$$

where only a sum over j is intended. The eigenvectors can be chosen to be real, and they are given by [117][2]

$$V^a_i = \varepsilon_{ijk}(\mathcal{M}^2_{Aj} - m^2_{\varphi_a}\delta_{Aj})(\mathcal{M}^2_{Bk} - m^2_{\varphi_a}\delta_{Bk}) \tag{4.3.47}$$

where we sum over j, k. A and B can take the values $1, 2$ or 3 subject to $A \neq B$. Different choices lead to different sign conventions for the eigenvectors. We commit to the choice $A = 2, B = 3$ for the rest of this chapter. The eigenvectors are invariant under the $U(1)_{\text{PQ}}$ background symmetry, so they are physical, measurable quantities. The normalized eigenvectors are defined as

$$\widehat{V}^a_i = \frac{V^a_i}{|V^a|} \tag{4.3.48}$$

[2]This expression is not valid when the eigenvalues are not degenerate. In practice, we will use it only for the Higgs eigenstate, which in the decoupling limit is not degenerate. For the degenerate case, see [117].

The normalized eigenvectors can be used to diagonalize the mass matrix

$$\widehat{V}_i^a \mathcal{M}_{ij}^2 \widehat{V}_j^b = \delta_{ab} m_{\varphi_a}^2 \tag{4.3.49}$$

Each normalized eigenvector has only two independent real components due to the normalization condition

$$\left(\widehat{V}_1^a\right)^2 + \left(\widehat{V}_2^a\right)^2 + \left(\widehat{V}_3^a\right)^2 = 1 \tag{4.3.50}$$

Furthermore, the three eigenvectors are orthogonal to each other for non degenerate mass eigenvalues, so all together they can be specified by three real numbers. Now, using (4.3.47), the normalized eigenvectors are

$$\begin{aligned}
\widehat{V}_1^a &= \frac{(\mathcal{M}_{22}^2 - m_{\varphi_a}^2)(\mathcal{M}_{33}^2 - m_{\varphi_a}^2)}{\sqrt{(\mathcal{M}_{33}^2 - m_{\varphi_a}^2)^2 \left(\mathcal{M}_{12}^4 + (\mathcal{M}_{22}^2 - m_{\varphi_a}^2)^2\right) + \mathcal{M}_{13}^4 (\mathcal{M}_{22}^2 - m_{\varphi_a}^2)^2}} \\
\widehat{V}_2^a &= -\frac{\mathcal{M}_{12}^2(\mathcal{M}_{33}^2 - m_{\varphi_a}^2)}{\sqrt{(\mathcal{M}_{33}^2 - m_{\varphi_a}^2)^2 \left(\mathcal{M}_{12}^4 + (\mathcal{M}_{22}^2 - m_{\varphi_a}^2)^2\right) + \mathcal{M}_{13}^4 (\mathcal{M}_{22}^2 - m_{\varphi_a}^2)^2}} \\
\widehat{V}_3^a &= -\frac{\mathcal{M}_{13}^2(\mathcal{M}_{22}^2 - m_{\varphi_a}^2)}{\sqrt{(\mathcal{M}_{33}^2 - m_{\varphi_a}^2)^2 \left(\mathcal{M}_{12}^4 + (\mathcal{M}_{22}^2 - m_{\varphi_a}^2)^2\right) + \mathcal{M}_{13}^4 (\mathcal{M}_{22}^2 - m_{\varphi_a}^2)^2}}
\end{aligned} \tag{4.3.51}$$

$\widehat{V}_1^1$ can always be chosen to be positive by a sign redefinition of the eigenvector. The definition chosen in (4.3.51) leads to $\widehat{V}_1^1 > 0$ near the decoupling limit, since in that case $\mathcal{M}_{22}^2$ and $\mathcal{M}_{33}^2$ are of order $\tilde{m}_2^2 \gg m_{\varphi_1}^2$. Without loss of generality we can write the normalized eigenvector corresponding to the Higgs in terms of a *complex alignment parameter* Ξ

$$\widehat{V}_1^1 = \sqrt{1 - |\Xi|^2} \qquad \widehat{V}_2^1 = \mathrm{Re}\,\Xi \qquad \widehat{V}_3^1 = \mathrm{Im}\,\Xi \quad , \quad \Xi \in \mathbb{C}^1 \tag{4.3.52}$$

Ξ specifies the projections of the Higgs particle φ_1 along h_1, h_2 and h_3. Note that $\sqrt{1 - |\Xi|^2}$ gives the component of the Higgs in the direction of h_1, which by definition in the Higgs basis is the direction of the vev in field space. Ξ is the complex generalization of the alignment parameter $\cos(\beta - \alpha)$ for the general T violating 2HDM. In the T conserving case, $\mathrm{Im}\,\Xi = 0$ and Ξ reduces to $\cos(\beta - \alpha)$. We will see in the next section that Ξ controls the deviations of the Higgs couplings to fermions and gauge bosons from their SM counterparts. In the alignment limit, $\Xi = 0$, and the couplings of the Higgs are SM like. The complex alignment parameter is invariant under the $U(1)_{\mathrm{PQ}}$ background symmetry and both its magnitude and its phase are physical, measurable quantities.

Near the decoupling limit it is useful to find the complex alignment parameter as an expansion in $v^2/\tilde{m}_2^2$ in terms of parameters of the Higgs potential. The real and imaginary components of the complex alignment parameter can be obtained using (4.3.51). The calculation is straightforward,

using the elements of the mass matrix (4.3.31) and the expression for the Higgs mass (4.3.43) we get

$$\Xi = -\left|\tilde{\lambda}_6\right| e^{-i\theta_1}\,\frac{v^2}{\tilde{m}_2^2}\left[1-\frac{1}{2}\big(2\tilde{\lambda}_1-\tilde{\lambda}_3-\tilde{\lambda}_4-\left|\tilde{\lambda}_5\right|\big)\,\frac{v^2}{\tilde{m}_2^2}+\mathcal{O}\!\left(\frac{v^4}{\tilde{m}_2^4}\right)\right] \tag{4.3.53}$$

where $\theta_1 = 1/2\,\mathrm{Arg}\big(\tilde{\lambda}_6^2\tilde{\lambda}_5^*\big)$ is one of the CP violating phases defined in (4.3.25). In calculating the couplings of the light Higgs, an important combination will be

$$\Xi\, e^{i\,\mathrm{Arg}(\tilde{\lambda}_5^*)/2} = -\tilde{\lambda}_6^*\,\frac{v^2}{\tilde{m}_2^2}+\mathcal{O}\!\left(\frac{v^4}{\tilde{m}_2^4}\right) \tag{4.3.54}$$

Also, note from (4.3.44) that at first order, $\tilde{m}_2$ corresponds to the mass of the heavy mass eigenstates, so we can write

$$\Xi\, e^{i\,\mathrm{Arg}(\tilde{\lambda}_5^*)/2} = -\tilde{\lambda}_6^*\,\frac{v^2}{m_{\varphi_{2,3}}^2}+\mathcal{O}\!\left(\frac{v^4}{\tilde{m}_2^4}\right) \tag{4.3.55}$$

In the next section we will also make use of the projection of the heavy neutral mass eigenstates in the direction of the vev, which are given by $\widehat{V}_1^2$ and $\widehat{V}_1^3$. Using the mass matrix elements (4.3.31) and the expression for the mass of the heavy eigenstates (4.3.44) in (4.3.51), to first order in $v^2/\tilde{m}_2^2$ we get

$$\begin{aligned}
\widehat{V}_1^2 &= -\mathrm{Im}\,\Xi\left[1+\mathrm{Re}\,\Xi\,\mathcal{O}\!\left(\frac{v^2}{\tilde{m}_2^2}\right)\right] = -\left|\tilde{\lambda}_6\right|\sin\,\theta_1\,\frac{v^2}{\tilde{m}_2^2}\left[1+\,\mathcal{O}\!\left(\frac{v^2}{\tilde{m}_2^2}\right)\right]\\
\widehat{V}_1^3 &= -\mathrm{Re}\,\Xi\left[1+\mathrm{Im}\,\Xi\,\mathcal{O}\!\left(\frac{v^2}{\tilde{m}_2^2}\right)\right] = \left|\tilde{\lambda}_6\right|\cos\,\theta_1\,\frac{v^2}{\tilde{m}_2^2}\left[1+\mathcal{O}\!\left(\frac{v^2}{\tilde{m}_2^2}\right)\right]
\end{aligned} \tag{4.3.56}$$

Note that in the T conserving limit, $\mathrm{Im}\,\Xi = 0$ and $\varphi_2 = h_3$ is a pseudoscalar mass eigenstate that does not mix with the CP even fields h_1 or h_2, so $\widehat{V}_1^2$ vanishes and $\widehat{V}_1^3$ reduces to the usual alignment parameter $-\cos(\beta-\alpha)$.

4.3.2 Couplings of the Higgs boson

We now study the couplings of the Higgs particle φ_1 in the 2HDM. In this section, the complex alignment parameter (4.3.53) is used extensively. Working near the decoupling limit is not a necessary condition to make use of the complex alignment parameter.

In this section, when working near the decoupling limit, we express the deviations from the SM couplings of the light Higgs as an expansion in $v^2/\tilde{m}_2^2$. We work up to first order in $v^2/\tilde{m}_2^2$ for the fermionic interactions, and second order in the bosonic interactions. We will see that this captures all the leading order deviations from the SM predictions near the decoupling limit.

We start by defining the Lagrangian density for the light Higgs

$$\begin{aligned}
&\frac{1}{2}\partial\varphi_1\partial\varphi_1 + \frac{1}{2}Z^\mu Z_\mu \left(m_Z^2 + g_{\varphi_a ZZ}\ \varphi_a + \frac{1}{2}g_{\varphi_1^2 ZZ}\ \varphi_1^2\right) \\
&+W^{+\mu}W^-_\mu \left(m_W^2 + g_{\varphi_a WW}\ \varphi_a + \frac{1}{2}g_{\varphi_1^2 WW}\ \varphi_1^2\right) \\
&+\Big[g_{\varphi_1 H^\pm W}(W^{+\mu}\partial_\mu H^- \varphi_1 - W^{+\mu}H^-\partial_\mu\varphi_1) + \text{h.c.}\Big] \\
&+(g_{\varphi_1\varphi_2 Z}Z^\mu\partial_\mu\varphi_2\,\varphi_1 - Z^\mu\varphi_2\partial_\mu\varphi_1) + g_{\varphi_1\varphi_3 Z}(Z^\mu\partial_\mu\varphi_3\,\varphi_1 - Z^\mu\varphi_3\partial_\mu\varphi_1) \\
&-(m^f_{ij}f_i\overline{f}_j + \lambda^f_{\varphi_a ij}\ f_i\varphi_a\overline{f}_j + \text{h.c.}) - V(\varphi_1,\varphi_2,\varphi_3)
\end{aligned} \tag{4.3.57}$$

where we sum over repeated indices and we included the Yukawa and gauge couplings involving one heavy Higgs, for later use. We leave out interactions with more than one heavy Higgs, which will not be used in this chapter. The potential for the light Higgs is

$$\begin{aligned}
V(\varphi_1,\varphi_2,\varphi_3) \ =\ & \frac{1}{2}m^2_{\varphi_1}\varphi_1^2 - \frac{1}{3!}g_{\varphi_1^3}\varphi_1^3 - \frac{1}{4!}g_{\varphi_1^4}\varphi_1^4 - \frac{1}{2}g_{\varphi_1^2\varphi_2}\varphi_1^2\varphi_2 \\
& - \frac{1}{2}g_{\varphi_1^2\varphi_3}\varphi_1^2\varphi_3 - \frac{1}{3!}g_{\varphi_1^3\varphi_2}\varphi_1^3\varphi_2 - \frac{1}{3!}g_{\varphi_1^3\varphi_3}\varphi_1^3\varphi_3
\end{aligned} \tag{4.3.58}$$

where again we included the couplings involving at most one heavy Higgs.

Due to mixing of the doublets, the couplings of the Higgs are modified with respect to their SM values. An exception is the coupling between two Higgses and two gauge bosons since it is determined by gauge invariance and both H_1 and H_2 have the same quantum numbers. This coupling is given by

$$g_{\varphi_1^2 VV} = \frac{2m_V^2}{v^2} \tag{4.3.59}$$

The coupling of one Higgs to two gauge bosons comes exclusively from the projection of the Higgs into the direction of the vev in field space $\widehat{V}_1^1 = \sqrt{1-|\Xi|^2}$, so it is diluted with respect to its SM value by the complex alignment parameter as

$$g_{\varphi_1 VV} = \frac{2m_V^2}{v}\sqrt{1-|\Xi|^2} \tag{4.3.60}$$

Note that when the Higgs potential is T conserving, this leads to the familiar relation $g_{\varphi_1 VV} = 2m_V^2/v\,\sin(\beta-\alpha)$ [26]. Near the decoupling limit, using the complex alignment parameter to lowest order in $v^2/\tilde{m}_2^2$ given in (4.3.53), we get

$$g_{\varphi_1 VV} = \frac{2m_V^2}{v}\left[1 - \frac{1}{2}\tilde{\lambda}_6^*\tilde{\lambda}_6\,\frac{v^4}{\tilde{m}_2^4} + \mathcal{O}\left(\frac{v^6}{\tilde{m}_2^6}\right)\right] \tag{4.3.61}$$

Yukawa couplings to up and down type fermions can be found by using the Higgs doublet Yukawa couplings defined in (4.3.13) and the projections of the Higgs into the neutral components of the

doublets (4.3.52). They are given by

$$\lambda^f_{\varphi_1 ij} = \delta_{ij}\,\frac{m_i^f}{v}\sqrt{1-|\Xi|^2} + \frac{1}{\sqrt{2}}\tilde{\lambda}^f_{2ij}\,\Xi\,e^{i\,\mathrm{Arg}(\tilde{\lambda}_5^*)/2} \tag{4.3.62}$$

This coupling violates the flavor and T symmetries due to the correction proportional to $\tilde{\lambda}^f_{2ij}\,\Xi$, which is inherited from the mixing with the heavy doublet. Near the decoupling limit, using (4.3.53) we get

$$\lambda^f_{\varphi_1 ij} = \delta_{ij}\,\frac{m_i^f}{v} - \frac{1}{\sqrt{2}}\tilde{\lambda}^f_{2ij}\tilde{\lambda}_6^*\,\frac{v^2}{\tilde{m}_2^2} + \mathcal{O}\!\left(\frac{v^4}{\tilde{m}_2^4}\right) \tag{4.3.63}$$

Note that if the Yukawa of the heavy doublet vanishes $\tilde{\lambda}^f_{2ij} = 0$, the Higgs Yukawas are not modified with respect to their SM values at first order in $v^2/\tilde{m}_2^2$. In this case, the modifications come exclusively from dilution due to the complex alignment parameter in (4.3.62), which is a second order effect. Note that in this case, the modifications to the SM predictions for the Higgs Yukawas and to the coupling of a Higgs to two gauge bosons are identical: both couplings are diluted by $\sqrt{1-|\Xi|^2}$. This limit resembles the results of the SHSM studied in section 4.2.

The Higgs self-couplings are obtained from the 2HDM potential (4.3.16) and the projections of the Higgs into the neutral components of the doublets (4.3.52). They are given by

$$\begin{aligned}\frac{1}{v}g_{\varphi_1^3} \;=\; & -3\tilde{\lambda}_1\left(1-|\Xi|^2\right)^{3/2} - 3(\tilde{\lambda}_3+\tilde{\lambda}_4)\,|\Xi|^2\left(1-|\Xi|^2\right)^{1/2} \\ & - 3\left|\tilde{\lambda}_5\right|\mathrm{Re}\,\Xi^2\left(1-|\Xi|^2\right)^{1/2} - \frac{9}{2}\Big[\,\left|\tilde{\lambda}_6\right| e^{i\theta_1}\,\Xi(1-|\Xi|^2) + \mathrm{h.c.}\Big] \\ & - \frac{3}{2}\Big[\,\left|\tilde{\lambda}_7\right| e^{i\theta_2}\,\Xi\,|\Xi|^2 + \mathrm{h.c.}\Big]\end{aligned} \tag{4.3.64}$$

$$\begin{aligned}g_{\varphi_1^4} \;=\; & -3\tilde{\lambda}_1\left(1-|\Xi|^2\right)^2 - 3\tilde{\lambda}_2\,|\Xi|^4 - 6(\tilde{\lambda}_3+\tilde{\lambda}_4)\,|\Xi|^2\left(1-|\Xi|^2\right) \\ & - 6\left|\tilde{\lambda}_5\right|\mathrm{Re}\,\Xi^2\left(1-|\Xi|^2\right) - 6\Big[\,\left|\tilde{\lambda}_6\right| e^{i\theta_1}\,\Xi\left(1-|\Xi|^2\right)^{3/2} + \mathrm{h.c.}\Big] \\ & - 6\Big[\,\left|\tilde{\lambda}_7\right| e^{i\theta_2}\,\Xi\,|\Xi|^2\left(1-|\Xi|^2\right)^{1/2} + \mathrm{h.c.}\Big]\end{aligned} \tag{4.3.65}$$

Using (4.3.53) in the exact expression for the cubic Higgs self-coupling (4.3.65), we get

$$\begin{aligned}\frac{1}{v}g_{\varphi_1^3} \;=\; & -\frac{3m^2_{\varphi_1}}{v^2} + 6\tilde{\lambda}_6^*\tilde{\lambda}_6\,\frac{v^2}{\tilde{m}_2^2} \\ & + \frac{1}{2}\Big[\,\big[21\tilde{\lambda}_1 - 12(\tilde{\lambda}_3+\tilde{\lambda}_4)\big]\tilde{\lambda}_6^*\tilde{\lambda}_6 - \big(6\tilde{\lambda}_5\tilde{\lambda}_6^{*2} + \mathrm{h.c.}\big)\Big]\,\frac{v^4}{\tilde{m}_2^4} + \mathcal{O}\!\left(\frac{v^6}{\tilde{m}_2^6}\right)\end{aligned} \tag{4.3.66}$$

$$\begin{aligned}g_{\varphi_1^4} \;=\; & -\frac{3m^2_{\varphi_1}}{v^2} + 9\tilde{\lambda}_6^*\tilde{\lambda}_6\,\frac{v^2}{\tilde{m}_2^2} \\ & + \frac{1}{4}\Big[\,\big[60\tilde{\lambda}_1 - 42(\tilde{\lambda}_3+\tilde{\lambda}_4)\big]\tilde{\lambda}_6^*\tilde{\lambda}_6 - \big(21\tilde{\lambda}_5\tilde{\lambda}_6^{*2} + \mathrm{h.c.}\big)\Big]\,\frac{v^4}{\tilde{m}_2^4} + \mathcal{O}\!\left(\frac{v^6}{\tilde{m}_2^6}\right)\end{aligned} \tag{4.3.67}$$

Note that all the deviations from the SM values of the Higgs couplings are parametrized by the complex alignment parameter, such that if $\Xi = 0$ all the coupling of the Higgs are SM like.

Let us now consider couplings involving also one heavy Higgs state. They will be used in the next section to calculate scattering amplitudes of the Higgs to gauge bosons, fermions and Higgses. The couplings of one neutral heavy Higgs to two gauge bosons are obtained from the projection of these states into the field direction of the vev

$$\begin{aligned}\frac{1}{v}g_{\varphi_2 VV} &= \frac{2m_V^2}{v^2}\widehat{V}_1^2 = -\frac{2m_V^2}{v^2}\left|\tilde{\lambda}_6\right|\sin\theta_1\,\frac{v^2}{\tilde{m}_2^2}+\mathcal{O}\left(\frac{v^4}{\tilde{m}_2^4}\right)\\ \frac{1}{v}g_{\varphi_3 VV} &= \frac{2m_V^2}{v^2}\widehat{V}_1^3 = \frac{2m_V^2}{v^2}\left|\tilde{\lambda}_6\right|\cos\theta_1\,\frac{v^2}{\tilde{m}_2^2}+\mathcal{O}\left(\frac{v^4}{\tilde{m}_2^4}\right)\end{aligned} \tag{4.3.68}$$

where we used (4.3.56) . The $g_{\varphi_1 H^\pm W}$ coupling is obtained from the projection of the Higgs into the neutral components of the heavy doublet H_2, since the charged Higgs resides entirely in H_2, so its couplings to gauge bosons come exclusively from the kinetic term $D_\mu H_2^\dagger\, D^\mu H_2$. In terms of the complex alignment parameter this coupling can be expressed in a remarkably simple way

$$g_{\varphi_1 H^\pm W} = -\frac{im_W}{v}\,\Xi \tag{4.3.69}$$

Using (4.3.53), to lowest order in $v^2/\tilde{m}_2^2$ we get

$$g_{\varphi_1 H^\pm W} = \frac{im_W}{v}\left|\tilde{\lambda}_6\right| e^{-i\theta_1}\,\frac{v^2}{\tilde{m}_2^2}+\mathcal{O}\left(\frac{v^4}{\tilde{m}_2^4}\right) \tag{4.3.70}$$

The couplings involving a light Higgs, a heavy Higgs and the Z boson come exclusively from the kinetic term of the second doublet $D_\mu H_2^\dagger\, D^\mu H_2$. They are given by

$$\begin{aligned}g_{\varphi_1\varphi_2 Z} &= \frac{m_Z}{v}\mathrm{Re}\,\Xi\left[1+\mathrm{Im}\,\Xi\,\mathcal{O}\left(\frac{v^2}{\tilde{m}_2^2}\right)\right] = -\frac{m_Z}{v}\left|\tilde{\lambda}_6\right|\cos\theta_1\,\frac{v^2}{\tilde{m}_2^2}+\mathcal{O}\left(\frac{v^4}{\tilde{m}_2^4}\right)\\ g_{\varphi_1\varphi_3 Z} &= -\frac{m_Z}{v}\mathrm{Im}\,\Xi\left[1+\mathrm{Re}\,\Xi\,\mathcal{O}\left(\frac{v^2}{\tilde{m}_2^2}\right)\right] = -\frac{m_Z}{v}\left|\tilde{\lambda}_6\right|\sin\theta_1\,\frac{v^2}{\tilde{m}_2^2}+\mathcal{O}\left(\frac{v^4}{\tilde{m}_2^4}\right)\end{aligned} \tag{4.3.71}$$

The couplings of the heavy neutral states to fermions are to lowest order in $v^2/\tilde{m}_2^2$ given by the Yukawas of the heavy doublet,

$$\lambda^f_{\varphi_2 ij} = \frac{1}{\sqrt{2}}\,i\,\tilde{\lambda}^f_{2ij}e^{i\mathrm{Arg}(\tilde{\lambda}_5^*)/2}+\mathcal{O}\left(\frac{v^2}{\tilde{m}_2^2}\right) \tag{4.3.72}$$

$$\lambda^f_{\varphi_3 ij} = \frac{1}{\sqrt{2}}\tilde{\lambda}^f_{2ij}e^{i\mathrm{Arg}(\tilde{\lambda}_5^*)/2}+\mathcal{O}\left(\frac{v^2}{\tilde{m}_2^2}\right) \tag{4.3.73}$$

where the factor $e^{i\mathrm{Arg}(\tilde{\lambda}_5^*)/2}$ comes from the definition of the component fields (4.3.28). Note that these couplings are not controlled by the complex alignment parameter Ξ, and do not vanish in the alignment limit.

The dihiggs couplings to one heavy Higgs are obtained from the Higgs potential, and they are

$$\begin{aligned}\frac{1}{v}g^2_{\varphi_1^2\varphi_2} &= 3\left|\tilde{\lambda}_6\right|\sin\theta_1 + \mathcal{O}\left(\frac{v^2}{\tilde{m}_2^2}\right)\\ \frac{1}{v}g^2_{\varphi_1^2\varphi_3} &= -3\left|\tilde{\lambda}_6\right|\cos\theta_1 + \mathcal{O}\left(\frac{v^2}{\tilde{m}_2^2}\right)\end{aligned} \tag{4.3.74}$$

Note that these couplings are not controlled by the complex alignment parameter. In particular, Ξ could be small due to a large separation of scales $v^2/\tilde{m}_2^2 \ll 1$, while $g^2_{\varphi_1^2\varphi_2}, g^2_{\varphi_1^2\varphi_3}$ could be of order v, if $\left|\tilde{\lambda}_6\right|$ is not small.

4.3.3 Scattering amplitudes

We now work out some examples of tree level dihiggs scattering amplitudes. They will be used as a consistency check for the 2HDM low energy EFT that will be presented in section 4.4.3 and to compare couplings in the EFT and mixing languages. The Standard Model results for the amplitudes can be read from this section by taking the limit $\tilde{\lambda}_6 \to 0$. We omit spinors in all amplitudes.

The tree level dihiggs to di-W boson scattering amplitude is

$$\begin{aligned}\mathcal{A}\left(\varphi_1\varphi_1 \to W^+W^-\right) &= g_{\mu\nu}\left[g_{\varphi_1^2 W^2} - \frac{g_{\varphi_1^2\varphi_a}g_{\varphi_a W^2}}{s-m^2_{\varphi_a}} - g^2_{\varphi_1 W^2}\left(\frac{1}{t-m_W^2}+\frac{1}{u-m_W^2}\right)\right]\\ &- \left|g_{\varphi_1 H^\pm W}\right|^2\left[\frac{(2p_1-p_+)_\mu(p_1+p_2+p_+)_\nu}{t-m^2_{H^\pm}} + \ (p_+ \leftrightarrow p_-)\right]\end{aligned} \tag{4.3.75}$$

where we sum over a and $p_\pm$ are the momenta of the $W^\pm$ bosons. In the last line, exchanging p_+ with p_- changes the Mandelstam variable t to u. Using the expressions for the couplings (4.3.59), (4.3.61), (4.3.67), (4.3.68) (4.3.70) and (4.3.74), we get

$$\begin{aligned}\mathcal{A}\left(\varphi_1\varphi_1 \to W^+W^-\right) &= g_{\mu\nu}\left[\frac{2m_W^2}{v^2} - 6\tilde{\lambda}_6\tilde{\lambda}_6^*\frac{m_W^2}{v^2}\frac{v^4}{\tilde{m}_2^4}\right.\\ &- \frac{2m_W^2}{v^2}\left[-\frac{3m^2_{\varphi_1}}{v^2} + 6\tilde{\lambda}_6^*\tilde{\lambda}_6\frac{v^2}{\tilde{m}_2^2} + \frac{1}{2}\Big(\left[21\tilde{\lambda}_1 - 12(\tilde{\lambda}_3+\tilde{\lambda}_4)\right]\tilde{\lambda}_6^*\tilde{\lambda}_6\right.\\ &- \left.\left(6\tilde{\lambda}_5\tilde{\lambda}_6^{*2} + \text{h.c.}\right)\Big)\frac{v^4}{\tilde{m}_2^4} + \frac{3}{2}\tilde{\lambda}_6^*\tilde{\lambda}_6\frac{m^2_{\varphi_1}v^2}{\tilde{m}_2^4}\right]\left(\frac{v^2}{s-m^2_{\varphi_1}}\right)\\ &- \left.\frac{4m_W^4}{v^4}\left[1-\tilde{\lambda}_6^\dagger\tilde{\lambda}_6\frac{v^4}{\tilde{m}_2^4}\right]\left(\frac{v^2}{t-m_W^2}+\frac{v^2}{u-m_W^2}\right) + \mathcal{O}\left(\frac{sv^2}{\tilde{m}_2^4}, \frac{v^6}{\tilde{m}_2^6}\right)\right]\end{aligned} \tag{4.3.76}$$

where the first term is the contact interaction, the second term comes from the short distance contribution of the heavy neutral states, and the two last terms are the long distance contributions from Higgs and W boson mediated diagrams. Note that the contributions mediated by the charged

Higgs written in the last line of (4.3.75) drop out of the calculations - they do not contribute to the order we work to.

The dihiggs to difermion chirality violating scattering amplitude is

$$\mathcal{A}\left(\varphi_1\varphi_1 \to f_i\overline{f}_j\right) \;=\; \frac{g_{\varphi_1^2\varphi_a}\lambda^f_{\varphi_a ij}}{s-m^2_{\varphi_a}} \tag{4.3.77}$$

where we sum over a. Using the expressions for the couplings (4.3.63), (4.3.67), (4.3.72), (4.3.73) and (4.3.74) we get

$$\begin{aligned}
\mathcal{A}\left(\varphi_1\varphi_1 \to f_i\overline{f}_j\right) \;&=\; \frac{1}{v}\Bigg[\left[\delta_{ij}\frac{m_i^f}{v}\left(-\frac{3m^2_{\varphi_1}}{v^2}+6\tilde{\lambda}_6\tilde{\lambda}_6^*\,\frac{v^2}{\tilde{m}_2^2}\right)+\frac{3}{\sqrt{2}}\,\tilde{\lambda}^f_{2ij}\tilde{\lambda}_6^*\,\frac{m^2_{\varphi_1}}{\tilde{m}_2^2}\right]\left(\frac{v^2}{s-m^2_{\varphi_1}}\right)\\
&\quad+\left[\frac{3}{\sqrt{2}}\tilde{\lambda}^f_{2ij}e^{i\mathrm{Arg}(\tilde{\lambda}_5^*)/2}\left|\tilde{\lambda}_6\right|e^{-i\theta_1}\,\frac{v^2}{\tilde{m}_2^2}\right]+\mathcal{O}\left(\frac{sv^2}{\tilde{m}_2^4},\frac{v^4}{\tilde{m}_2^4},\frac{m_i^{f\,2}}{v^2}\right)\Bigg]\\
&=\; \frac{1}{v}\Bigg[\left[\delta_{ij}\frac{m_i^f}{v}\left(-\frac{3m^2_{\varphi_1}}{v^2}+6\tilde{\lambda}_6\tilde{\lambda}_6^*\,\frac{v^2}{\tilde{m}_2^2}\right)+\frac{3}{\sqrt{2}}\,\tilde{\lambda}^f_{2ij}\tilde{\lambda}_6^*\,\frac{m^2_{\varphi_1}}{\tilde{m}_2^2}\right]\left(\frac{v^2}{s-m^2_{\varphi_1}}\right)\\
&\quad+\frac{3}{\sqrt{2}}\tilde{\lambda}^f_{2ij}\tilde{\lambda}_6^*\,\frac{v^2}{\tilde{m}_2^2}+\mathcal{O}\left(\frac{sv^2}{\tilde{m}_2^4},\frac{v^4}{\tilde{m}_2^4},\frac{m_i^{f\,2}}{v^2}\right)\Bigg]
\end{aligned} \tag{4.3.78}$$

where in the last step we made use of the definition of the CP violating phase $\theta_1 = \frac{1}{2}\mathrm{Arg}\left(\tilde{\lambda}_6^2\tilde{\lambda}_5^*\right)$ (see (4.3.25)). The first term in square brackets is the long distance contribution mediated by the Higgs, and the last term corresponds to the short distance contributions mediated by the heavy Higgses. Note that this amplitude has a flavor and T violating term both in the long and short distance pieces, inherited from $\tilde{\lambda}^f_{2ij}$, the coupling of the heavy doublet to the fermions.

The four Higgs scattering amplitude is

$$\mathcal{A}\left(\varphi_1\varphi_1 \to \varphi_1\varphi_1\right) \;=\; g_{\varphi_1^4}-g^2_{\varphi_1^2\varphi_a}\left(\frac{1}{s-m^2_{\varphi_a}}+\frac{1}{t-m^2_{\varphi_a}}+\frac{1}{u-m^2_{\varphi_a}}\right) \tag{4.3.79}$$

where we sum over a. Using (4.3.67) and (4.3.74) we get

$$\begin{aligned}
\mathcal{A}\left(\varphi_1\varphi_1 \to \varphi_1\varphi_1\right) \;&=\; g_{\varphi_1^4}-\frac{g^2_{\varphi_1^2\varphi_2}}{v^2}\left[-\frac{3v^2}{m^2_{\varphi_2}}+\mathcal{O}\left(\frac{xv^2}{\tilde{m}^4_{\varphi_2}}\right)\right]-\frac{g^2_{\varphi_1^2\varphi_3}}{v^2}\left[-\frac{3v^2}{m^2_{\varphi_3}}+\mathcal{O}\left(\frac{xv^2}{\tilde{m}^4_{\varphi_3}}\right)\right]\\
&\quad-\frac{g^2_{\varphi_1^3}}{v^2}\left(\frac{v^2}{s-m^2_{\varphi_1}}+\frac{v^2}{t-m^2_{\varphi_1}}+\frac{v^2}{u-m^2_{\varphi_1}}\right)\\
&=\; -\frac{3m^2_{\varphi_1}}{v^2}+9\tilde{\lambda}_6^*\tilde{\lambda}_6\,\frac{v^2}{\tilde{m}_2^2}+27\tilde{\lambda}_6\tilde{\lambda}_6^*\cos^2\theta_1\,\frac{v^2}{\tilde{m}_2^2}+27\tilde{\lambda}_6\tilde{\lambda}_6^*\sin^2\theta_1\,\frac{v^2}{\tilde{m}_2^2}\\
&\quad-\left(\frac{9m^4_{\varphi_1}}{v^4}-36\tilde{\lambda}_1\tilde{\lambda}_6^*\tilde{\lambda}_6\,\frac{v^2}{\tilde{m}_2^2}\right)\left(\frac{v^2}{s-m^2_{\varphi_1}}+\frac{v^2}{t-m^2_{\varphi_1}}+\frac{v^2}{u-m^2_{\varphi_1}}\right)\\
&\quad+\mathcal{O}\left(\frac{v^4}{\tilde{m}_2^4},\frac{xv^2}{\tilde{m}_2^4}\right)\\
&=\; -\frac{3m^2_{\varphi_1}}{v^2}+36\tilde{\lambda}_6^*\tilde{\lambda}_6\left(\frac{v^2}{\tilde{m}_2^2}\right)-\left(\frac{9m^2_{\varphi_1}}{v^4}-36\tilde{\lambda}_1\tilde{\lambda}_6^*\tilde{\lambda}_6\,\frac{v^2}{\tilde{m}_2^2}\right)\\
&\quad\left(\frac{v^2}{s-m^2_{\varphi_1}}+\frac{v^2}{t-m^2_{\varphi_1}}+\frac{v^2}{u-m^2_{\varphi_1}}\right)+\mathcal{O}\left(\frac{xv^2}{\tilde{m}_2^4},\frac{v^4}{\tilde{m}_2^4}\right)
\end{aligned} \tag{4.3.80}$$

where the first two terms come from the contact interaction and the short distance diagrams mediated by the Heavy Higgses, and the last term is the long distance contribution mediated by the Higgs particle.

4.4 The low energy effective theory of the 2HDM

In this section we present the tree level low energy effective theory of the Standard Model extended in the UV with a heavy Higgs doublet. Near the decoupling limit the heavy doublet can be integrated out, and the remaining Higgs doublet in the low energy theory contains the vev and the Higgs particle. The cutoff of the EFT is the heavy doublet mass $\tilde{m}_2$. The EFT description is an alternative to the mixing language, and no reference to mixing between the neutral components of the doublets is needed in deriving the EFT. Working at tree level is enough to reproduce the mixing effects described in the previous section. The effective theory can be derived most easily by working in the Higgs basis. In this basis one of the doublets carries no vev and must be identified with the heavy doublet, as discussed in the previous section. The remaining doublet contains the particle that must be identified with the Higgs in the low energy theory. In the derivation of the EFT we keep track of the $U(1)_{\rm PQ}$ symmetry defined in table 4.3, which can be used at any point of the calculations as a consistency check, since all the fields in the low energy theory (fermions, gauge bosons and the Higgs doublet H_1) are PQ invariants, so no coupling of the low energy theory can be charged under the $U(1)_{\rm PQ}$.

The regime of the 2HDM parameters we work in is the following. We consider all the marginal couplings of the 2HDM in the Higgs basis $\tilde{\lambda}_i$ $i = 1..7$ to be perturbative. The 2HDM has three dimensionful couplings: $\tilde{m}_1, \tilde{m}_2$ and $\tilde{m}_2$. However, there are only two mass scales, $\tilde{m}_1$ $\tilde{m}_2$; due to the no tadpole condition (4.3.24), $\tilde{m}_{12}$ is of the order of $\tilde{m}_1$. Due to the EWSB condition (4.3.23), the mass of the remaining doublet $\tilde{m}_1$ must be identified with the EWSB scale. Near the decoupling limit, $\tilde{m}_2^2 \gg \left|\tilde{\lambda}_i\right| v^2$. Due to the separation of scales, we organize the corrections to the SM predictions as an expansion in the small parameter $v^2/\tilde{m}_2^2$. To obtain a consistent expansion in $v^2/\tilde{m}_2^2$ in the 2HDM EFT, we need to define a concept of effective operator dimension which *differs from naive operator dimension*. The separation of scales motivates us to define our concept of effective operator dimension by counting powers of the heavy scale in the operator's coefficient in the Lagrangian. Since $\tilde{m}_2$ is the only heavy mass term, we define the operator's effective dimension as

$$n_E = 4 - n_{\tilde{m}_2^2} \tag{4.4.1}$$

where $n_{\tilde{m}_2^2}$ is the number of powers of $\tilde{m}_2^2$ in the operator's coefficient. For instance, the operators

$$\frac{\tilde{m}_{12}^2}{\tilde{m}_2^2}(H_1^\dagger H_1)^2 \qquad \frac{1}{\tilde{m}_2^2}(H_1^\dagger H_1)^3 \tag{4.4.2}$$

are both of effective dimension six, even though the first operator is of naive operator dimension four. In this work, we choose to work up to effective dimension eight in the Higgs potential and kinetic terms (including gauge interactions), and up to effective dimension six in operators involving fermions. We will see that this captures all the lowest order deviations to the SM predictions for the Higgs bosonic and fermionic interactions.

4.4.1 Diagrams and derivation of the EFT

In this section we present all the needed diagrams to derive the low energy EFT up to effective dimension eight in the Higgs potential and kinetic terms and up to effective dimension six in operators involving fermions. Since the maximum effective dimension we work up to is eight, all diagrams can have at most two inverse powers of $\tilde{m}_2^2$, *i.e.*, they can have at most two H_2 propagators. Note that of all couplings in the 2HDM Lagrangian (4.3.16), $\tilde{m}_{12}^2$, $(\tilde{m}_{12}^2)^*$, $\tilde{\lambda}_6$, $\tilde{\lambda}_6^*$, $\tilde{\lambda}_{2ij}$ and $\tilde{\lambda}_{2ij}^*$ are the only ones that involve only one heavy doublet H_2, so using these interactions it is possible to draw diagrams with only one H_2 propagator. These will be the diagrams that, at zero momentum, induce the irrelevant operators with the lowest effective dimension (six). As such, leading deviations to the SM predictions will be controlled by this small subset of parameters of the UV completion. We organize the presentation of the diagrams by number of insertions of Higgs potential or fermionic couplings involving the heavy Higgs doublet H_2.

leftmargin=* **Diagrams with two $\tilde{m}_{12}^2$ insertions**:

Let us start with the diagrams of figure 4.5. Up to effective dimension eight they lead to

$$\begin{aligned}&\frac{\left|\tilde{m}_{12}^2\right|^2}{\tilde{m}_2^2}H^\dagger H + \frac{\left|\tilde{m}_{12}^2\right|^2}{\tilde{m}_2^4}\partial_\mu H^\dagger \partial^\mu H + \frac{\left|\tilde{m}_{12}^2\right|^2}{\tilde{m}_2^4}\Big[g_2^2 H_1^\dagger T_a T_b W_{a\mu} W_b^\mu H_1 \\ &- g_2\left(i\partial_\mu H_1^\dagger T_a W_a^\mu H_1 + \text{h.c.}\right) + \frac{1}{4}g_1^2 H_1^\dagger B_\mu B^\mu H_1 - \frac{1}{2}g_1\left(i\partial_\mu H_1^\dagger B^\mu H_1 + \text{h.c.}\right)\Big]\end{aligned} \tag{4.4.3}$$

which can be rearranged into

$$\frac{\left|\tilde{m}_{12}^2\right|^2}{\tilde{m}_2^2}H_1^\dagger H_1 + \frac{\left|\tilde{m}_{12}^2\right|^2}{\tilde{m}_2^4}\left(D_\mu H_1\right)^\dagger \left(D^\mu H_1\right) \tag{4.4.4}$$

leftmargin=* **Diagrams with two $\tilde{\lambda}_6$ insertions:**

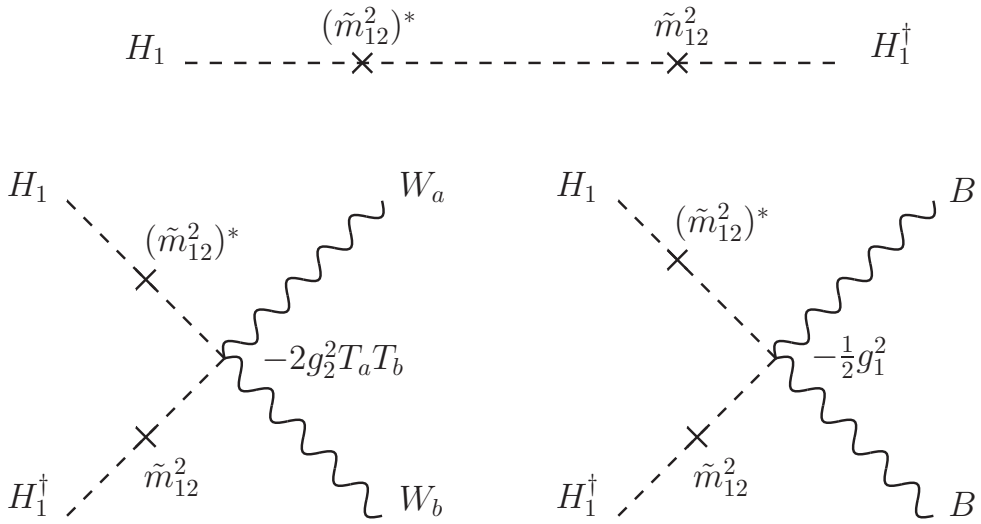

Figure 4.5: Diagrams with two m^2_{12} insertions and gauge boson legs leading to operators up to effective dimension eight. By gauge invariance there are also diagrams with only one gauge boson attached to the internal heavy Higgs propagator, which we do not draw for brevity, but that are considered when deriving the low energy theory. The upper diagram must be expanded up to quadratic order in the momentum of the external leg to work up to effective dimension eight. The upper diagram at zero momentum leads to the operator $H_1^\dagger H_1$. The upper diagram at quadratic order in the momentum expansion, together with the diagrams with gauge bosons lead to the operator $(D_\mu H_1)^\dagger (D^\mu H_1)$.

The diagrams of figure 4.6 lead to

$$\begin{aligned}
&\frac{\tilde{\lambda}_6^*\tilde{\lambda}_6}{\tilde{m}_2^2}(H_1^\dagger H_1)^3 + \frac{\tilde{\lambda}_6^*\tilde{\lambda}_6}{\tilde{m}_2^4}\Bigg[-\frac{3}{2}(H_1^\dagger H_1)^2(\,\Box H_1^\dagger H_1 + \text{h.c}) \\
&- H_1^\dagger H_1\Big(\partial_\mu H_1^\dagger \partial^\mu H_1 H_1^\dagger H_1 + \partial_\mu H_1^\dagger H_1 \partial^\mu H_1^\dagger H_1 + H_1^\dagger \partial_\mu H_1 \partial^\mu H_1^\dagger H_1 + \text{h.c}\Big) \\
&+ (H_1^\dagger H_1)^2\Bigg[g_2^2 H_1^\dagger T_a T_b W_{a\mu} W_b^\mu H_1 - g_2\Big(i\partial_\mu H_1^\dagger T_a W_a^\mu H_1 + \text{h.c.}\Big) \\
&+ \frac{1}{4}g_1^2 H_1^\dagger B_\mu B^\mu H_1 - \frac{1}{2}g_1\Big(i\partial_\mu H_1^\dagger B^\mu H_1 + \text{h.c.}\Big)\Bigg]\Bigg]
\end{aligned} \tag{4.4.5}$$

Rearranging the derivatives and the interactions with gauge bosons into covariant derivatives we get

$$\frac{\tilde{\lambda}_6^*\tilde{\lambda}_6}{\tilde{m}_2^2}(H_1^\dagger H_1)^3 + \frac{\tilde{\lambda}_6^*\tilde{\lambda}_6}{\tilde{m}_2^4}\Big[\,2\,\partial_\mu(H_1^\dagger H_1)\partial^\mu(H_1^\dagger H_1)(H_1^\dagger H_1) + (D_\mu H_1)^\dagger (D^\mu H_1)(H_1^\dagger H_1)^2\Big] \tag{4.4.6}$$

leftmargin=* **Diagrams with one $\tilde{\lambda}_6$ and one $\tilde{m}^2_{12}$ insertions**

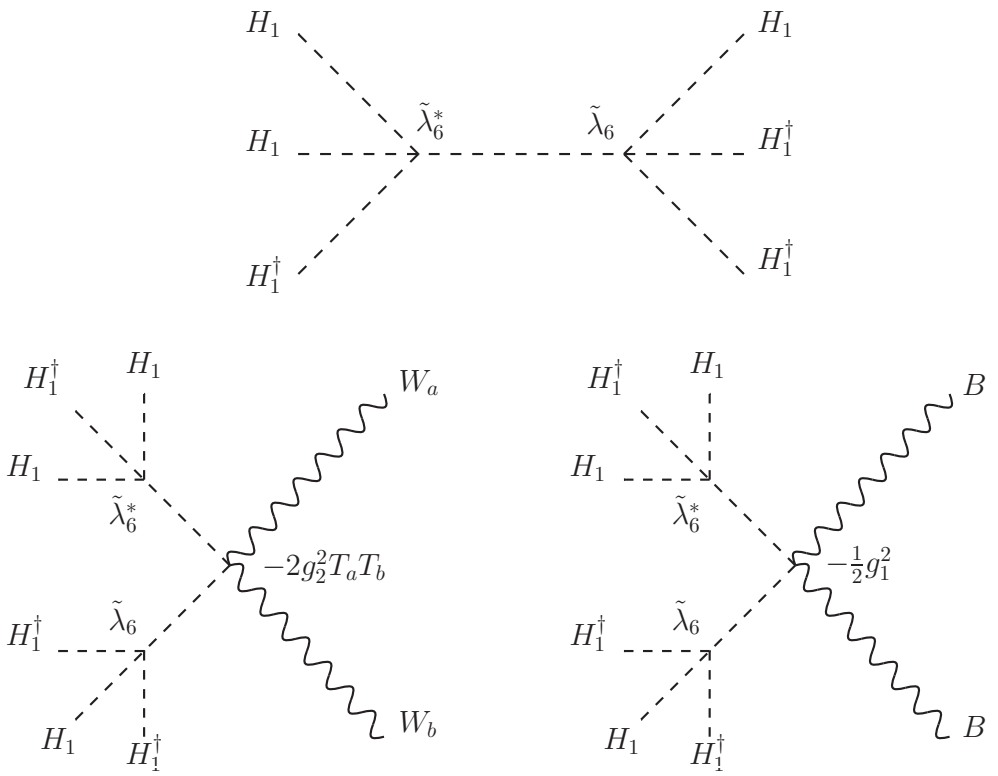

Figure 4.6: Diagrams with two λ_6 insertions and gauge boson legs leading to operators up to effective dimension eight. By gauge invariance there are also diagrams with only one gauge boson attached to the internal heavy Higgs propagator, which we do not draw for brevity, but that are considered when deriving the low energy theory. The upper diagram must be expanded up to quadratic order in the momentum of the external leg to work up to effective dimension eight. The upper diagram at zero momentum leads to the operator $(H_1^\dagger H_1)^3$. The upper diagram at quadratic order in the momentum of the external legs leads to $\partial_\mu(H_1^\dagger H_1)\partial^\mu(H_1^\dagger H_1)(H_1^\dagger H_1)$ and also, together with the diagrams with gauge bosons, to $(D_\mu H_1)^\dagger(D^\mu H_1)(H_1^\dagger H_1)^2$.

The diagrams in figure 4.7 lead to

$$\begin{aligned}
&\frac{\tilde{\lambda}_6(\tilde{m}_{12}^2)^*}{\tilde{m}_2^2}(H_1^\dagger H_1)^2 + \frac{\tilde{\lambda}_6(\tilde{m}_{12}^2)^*}{\tilde{m}_2^4}\Bigg[- H_1^\dagger H_1\, H_1^\dagger \Box H_1 \\
&+ H_1^\dagger H_1 \Bigg[g_2^2 H_1^\dagger T_a T_b W_{a\mu} W_b^\mu H_1 - g_2\Big(i\partial_\mu H_1^\dagger T_a W_a^\mu H_1 + \text{h.c.}\Big) \\
&+ \frac{1}{4} g_1^2 H_1^\dagger B_\mu B^\mu H_1 - \frac{1}{2} g_1 \Big(i\partial_\mu H_1^\dagger B^\mu H_1 + \text{h.c.}\Big) \Bigg] \Bigg] + \text{h.c.}
\end{aligned} \tag{4.4.7}$$

Rearranging the derivatives

$$\frac{2\tilde{\lambda}_6^* \tilde{m}_{12}^2}{\tilde{m}_2^2}(H_1^\dagger H_1)^2 + \frac{\tilde{\lambda}_6^* \tilde{m}_{12}^2}{\tilde{m}_2^4}\Big[\partial_\mu(H_1^\dagger H_1)\partial^\mu(H_1^\dagger H_1) + 2(D_\mu H_1)^\dagger (D^\mu H_1) H_1^\dagger H_1 \Big] \tag{4.4.8}$$

where we used $\tilde{\lambda}_6^* \tilde{m}_{12}^2 = \tilde{\lambda}_6 \tilde{m}_{12}^{2*}$ due to the no tadpole condition (4.3.24).

leftmargin=* **Diagrams with $\tilde{\lambda}_3, \tilde{\lambda}_4$ and $\tilde{\lambda}_5$ insertions**

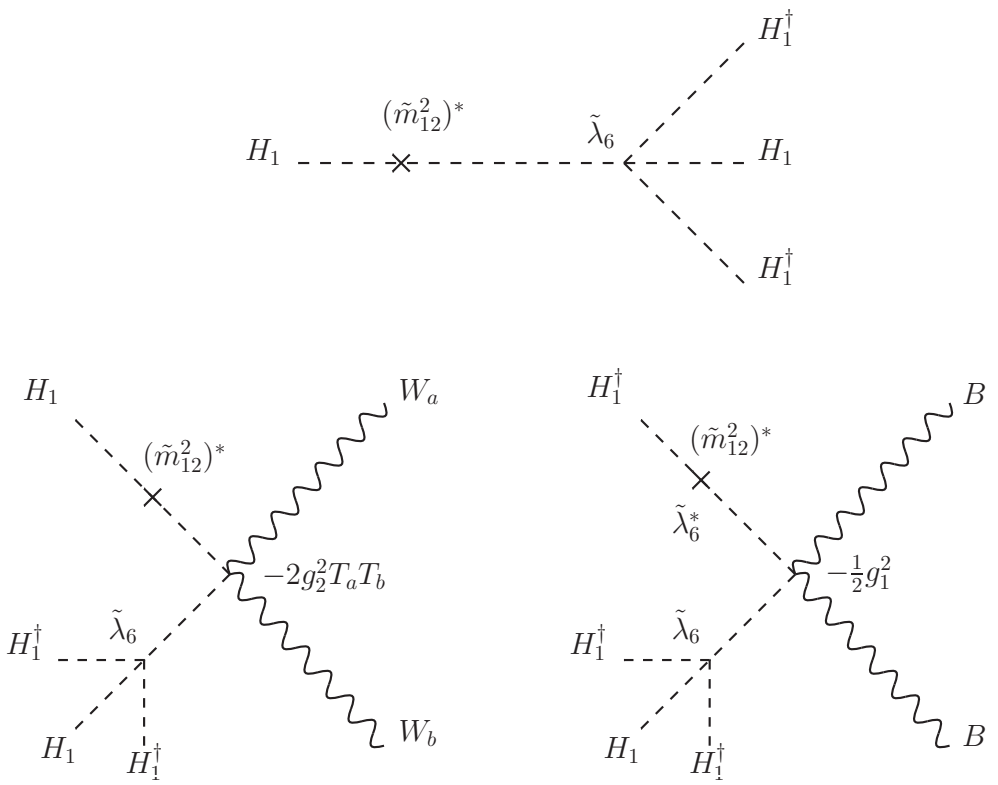

Figure 4.7: Diagrams with one λ_6 and one $(\tilde{m}_{12}^2)^*$ insertion up to effective dimension eight. There are also hermitic conjugate versions of these diagrams and diagrams with only one gauge boson attached to the internal heavy Higgs propagator, which are not drawn for brevity but considered when deriving the low energy theory. The upper diagram must be expanded up to quadratic order in the momentum of the external leg to work up to effective dimension eight. The upper diagram at zero momentum leads to the operator $(H_1^\dagger H_1)^2$. The upper diagram at quadratic order in momentum of the external legs leads to $H_1^\dagger H_1 H_1^\dagger \Box H_1$ and also, together with the diagrams with gauge bosons, to $(D_\mu H_1)^\dagger (D^\mu H_1) H_1^\dagger H_1$.

The diagrams of figure 4.8 lead to

$$\begin{aligned}
&-\frac{\tilde{\lambda}_3 \left|\tilde{m}_{12}^2\right|^2}{\tilde{m}_2^4}(H_1^\dagger H_1)^2 - \frac{2\tilde{\lambda}_3\tilde{\lambda}_6^*\tilde{m}_{12}^2}{\tilde{m}_2^4}(H_1^\dagger H_1)^3 - \frac{\tilde{\lambda}_3\tilde{\lambda}_6^*\tilde{\lambda}_6}{\tilde{m}_2^4}(H_1^\dagger H_1)^4 \\
&- \frac{\tilde{\lambda}_4 \left|\tilde{m}_{12}^2\right|^2}{\tilde{m}_2^4}(H_1^\dagger H_1)^2 - \frac{2\tilde{\lambda}_4\tilde{\lambda}_6^*\tilde{m}_{12}^2}{\tilde{m}_2^4}(H_1^\dagger H_1)^3 - \frac{\tilde{\lambda}_4\tilde{\lambda}_6^*\tilde{\lambda}_6}{\tilde{m}_2^4}(H_1^\dagger H_1)^4 \\
&- \frac{(\tilde{\lambda}_5^*\tilde{m}_{12}^4 + \text{h.c.})}{2\tilde{m}_2^4}(H_1^\dagger H_1)^2 - \frac{(\tilde{\lambda}_5^*\tilde{\lambda}_6\tilde{m}_{12}^2 + \text{h.c.})}{\tilde{m}_2^4}(H_1^\dagger H_1)^3 - \frac{(\tilde{\lambda}_5^*\tilde{\lambda}_6^2 + \text{h.c.})}{2\tilde{m}_2^4}(H_1^\dagger H_1)^4
\end{aligned} \tag{4.4.9}$$

where we used $\tilde{\lambda}_6^*\tilde{m}_{12}^2 = \tilde{\lambda}_6\tilde{m}_{12}^{2*}$ due to the no tadpole condition (4.3.24).

leftmargin=* **Diagrams with Yukawas and an $\tilde{m}_{12}^2$ or $\tilde{\lambda}_6$ insertion:**

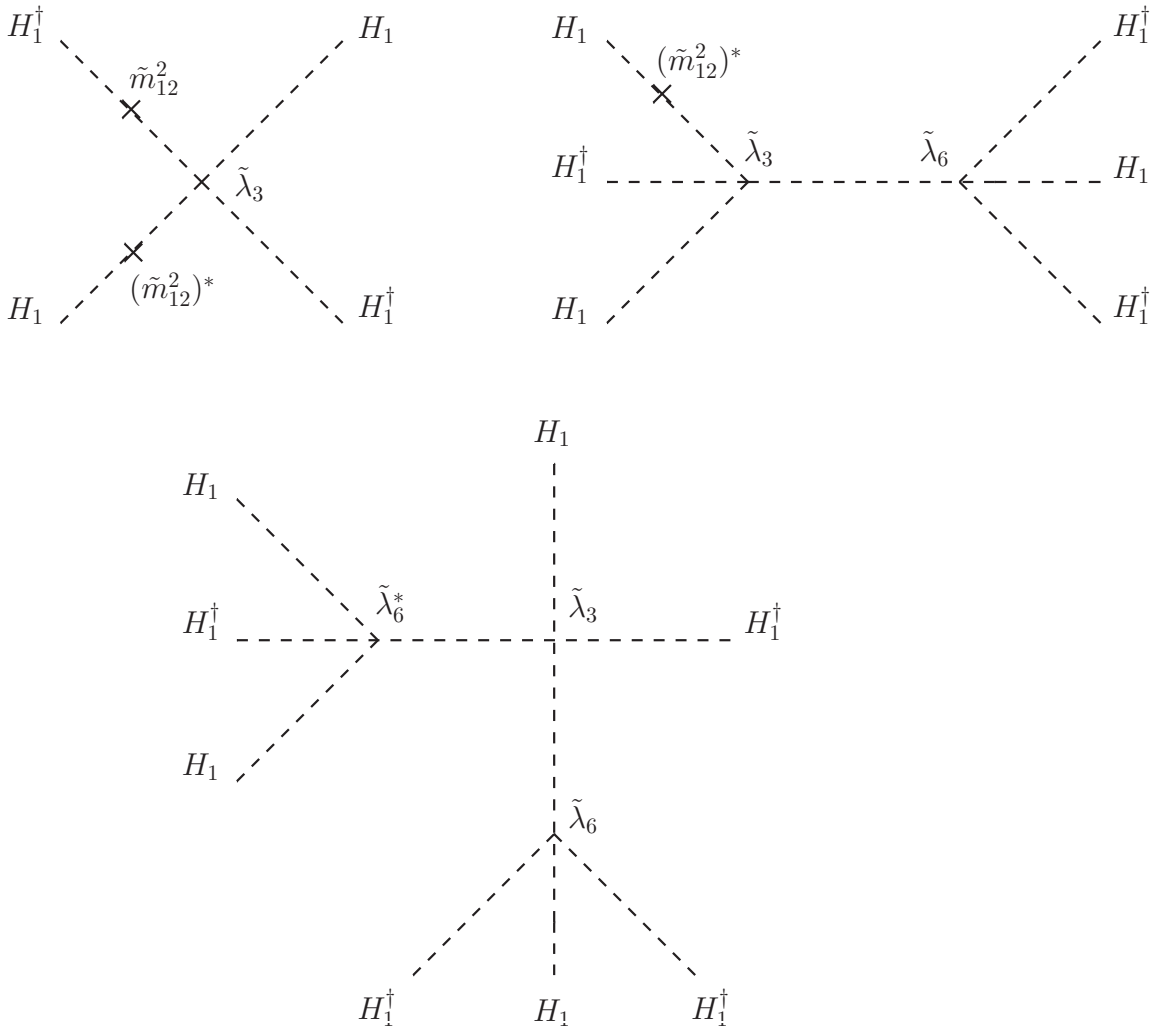

Figure 4.8: Diagrams with a $\tilde{\lambda}_3$ vertex up to effective dimension eight. All diagrams are at zero momentum. There are similar diagrams replacing the $\tilde{\lambda}_3$ vertex with $\tilde{\lambda}_4$ and $\tilde{\lambda}_5$, which are also considered to derive the low energy EFT. The diagrams with a $\tilde{\lambda}_5$ vertex are slightly different, they contain two $\tilde{m}_{12}^2$ vertices instead of one $\tilde{m}_{12}^2$ and one $(\tilde{m}_{12}^2)^*$ vertex. The upper left diagram leads to the operator $(H_1^\dagger H_1)^2$. The upper right diagram leads to the operator $(H_1^\dagger H_1)^3$. The lower diagram leads to the operator $(H_1^\dagger H_1)^4$.

The diagrams of figure 4.9 lead to

$$\frac{\tilde{\lambda}_{2ij}^u}{\tilde{m}_2^2} Q_i H_1 \overline{u}_j \left[(\tilde{m}_{12}^2)^* + \tilde{\lambda}_6^* H_1^\dagger H_1 \right] - \frac{\tilde{\lambda}_{2ij}^{d\dagger}}{\tilde{m}_2^2} Q_i H_1^c \overline{d}_j \left[\tilde{m}_{12}^2 + \tilde{\lambda}_6 H_1^\dagger H_1 \right]$$
$$- \frac{\tilde{\lambda}_{2ij}^{\ell\dagger}}{\tilde{m}_2^2} L_i H_1^c \overline{\ell}_j \left[\tilde{m}_{12}^2 + \tilde{\lambda}_6 H_1^\dagger H_1 \right] + \text{h.c.} \tag{4.4.10}$$

We do not present the operators at effective dimension 8 that modify the Yukawas.

leftmargin=* **Diagrams with Yukawas only (four fermion operators):**

The diagrams of figure 4.10 lead to

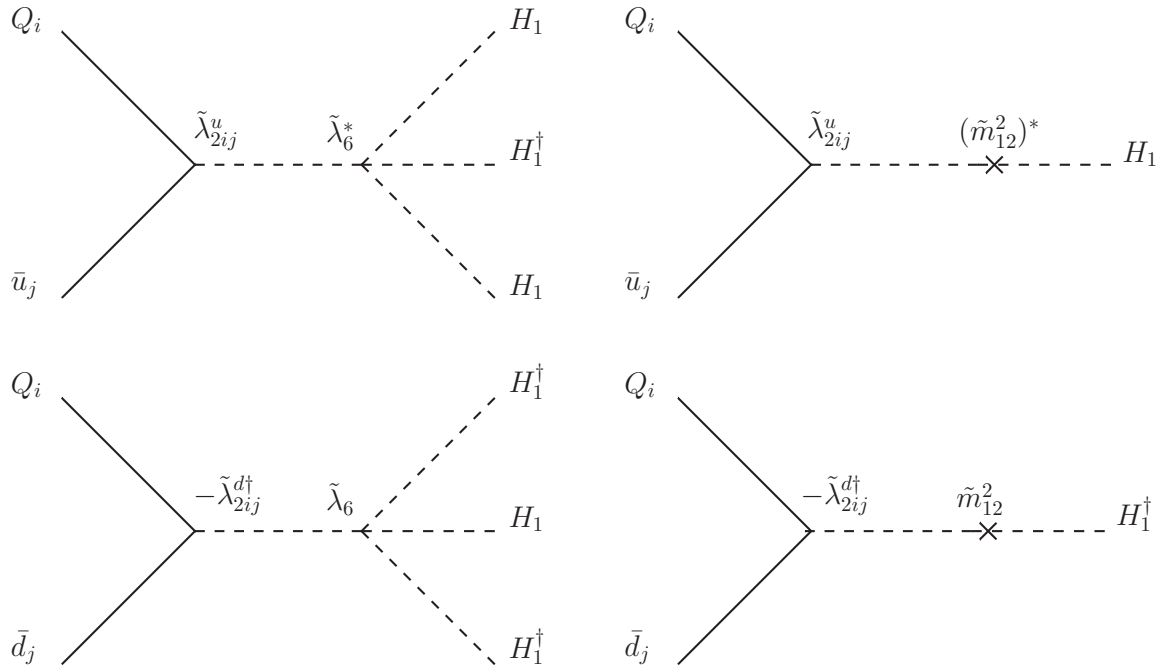

Figure 4.9: Diagrams with one Yukawa and one $\tilde{\lambda}_6$ or $\tilde{m}^2_{12}$ coupling up to effective dimension six. All diagrams are at zero momentum. There are also complex conjugate versions of these diagrams and diagrams with leptonic Yukawas, which are also considered to derive the low energy EFT. The upper left diagram leads to the operator $Q_i H_1 \overline{u}_j$. The upper right diagram leads to the operator $Q_i H_1 \overline{u}_j\, H_1^\dagger H_1$. The lower left diagram leads to the operator $Q_i H_1^c \overline{d}_j$. The lower right diagram leads to the operator $Q_i H_1^c \overline{d}_j\, H_1^\dagger H_1$.

$$\begin{aligned}
&\frac{\tilde{\lambda}^u_{2ij}\tilde{\lambda}^{u\dagger}_{2mn}}{\tilde{m}_2^2}(Q_i\overline{u}_j)(\overline{u}^\dagger_m Q^\dagger_n) + \frac{\tilde{\lambda}^{d\dagger}_{2ij}\tilde{\lambda}^{d}_{2mn}}{\tilde{m}_2^2}(Q_i\overline{d}_j)(\overline{d}^\dagger_m Q^\dagger_n) + \frac{\tilde{\lambda}^{\ell\dagger}_{2ij}\tilde{\lambda}^{\ell}_{2mn}}{\tilde{m}_2^2}(L_i\overline{\ell}_j)(\overline{\ell}^\dagger_m L^\dagger_n) \\
+ &\left[\frac{\tilde{\lambda}^{d\dagger}_{2ij}\tilde{\lambda}^{\ell}_{2mn}}{\tilde{m}_2^2}(Q_i\overline{d}_j)(\overline{\ell}^\dagger_m L^\dagger_n) + \frac{\tilde{\lambda}^{u}_{2ij}\tilde{\lambda}^{d\dagger}_{2mn}}{\tilde{m}_2^2}(Q_i\overline{u}_j)(Q_m\overline{d}_n) + \frac{\tilde{\lambda}^{u}_{2ij}\tilde{\lambda}^{\ell\dagger}_{2mn}}{\tilde{m}_2^2}(Q_i\overline{u}_j)(L_m\overline{\ell}_n) + \text{h.c.}\right]
\end{aligned} \tag{4.4.11}$$

4.4.2 The low energy theory of the Higgs doublet

Collecting the results (4.4.4), (4.4.6), (4.4.8), (4.4.9), (4.4.10) and (4.4.11) we are ready to write down the low energy theory. For the remainder of this chapter we drop the subscripts in the doublet of the low energy theory H_1 and its neutral component h_1. The effective Lagrangian density for the

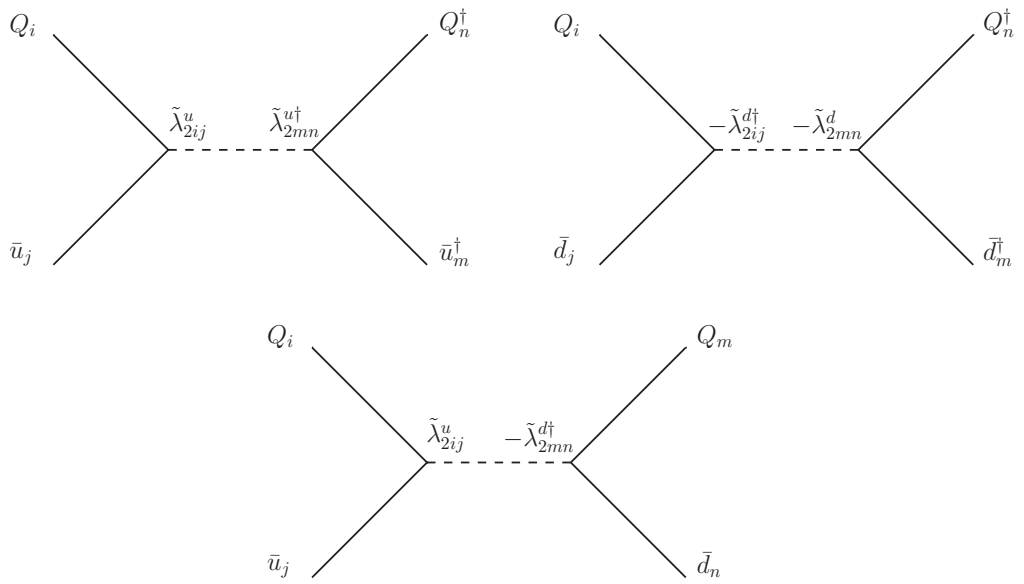

Figure 4.10: Diagrams with two Yukawas up to effective dimension six. The lower diagram also has a complex conjugate version. There are also diagrams with leptonic Yukawas. The upper left diagram leads to the operator $(Q_i\overline{u}_j)(\overline{u}^\dagger_m Q^\dagger_n)$. The upper right diagram leads to the operator $(Q_i\overline{d}_j)(\overline{d}^\dagger_m Q^\dagger_n)$. The lower diagram leads to the operator $-(Q_i\overline{u}_j)(Q_i\overline{d}_j)$, where the minus sign comes from reordering the contraction of fields charged under $SU(2)$.

Higgs doublet is

$$\begin{aligned}\mathcal{L} \;=\; & Z_H\, D_\mu H^\dagger D^\mu H + \zeta_H\left[\frac{1}{2}\partial_\mu(H^\dagger H)\partial^\mu(H^\dagger H) + H^\dagger H\, D_\mu H^\dagger D^\mu H\right] \\ & + \zeta'_H\left[2H^\dagger H\,\partial_\mu(H^\dagger H)\partial^\mu(H^\dagger H) + (H^\dagger H)^2\, D_\mu H^\dagger D^\mu H\right] - V(H) \\ & - \left[Q_i H\big(\lambda^u_{ij} + \eta^u_{ij} H^\dagger H\big)\overline{u}_j - Q_i H^c\big(\lambda^{d\dagger}_{ij} + \eta^{d\dagger}_{ij} H^\dagger H\big)\overline{d}_j - L_i H^c\big(\lambda^{\ell\dagger}_{ij} + \eta^{\ell\dagger}_{ij} H^\dagger H\big)\overline{\ell}_j + \text{h.c.}\right]\end{aligned} \tag{4.4.12}$$

$$V(H) = m_H^2 H^\dagger H + \frac{1}{2}\lambda_H (H^\dagger H)^2 + \frac{1}{3}\eta_6 (H^\dagger H)^3 + \frac{1}{4}\eta_8 (H^\dagger H)^4 \tag{4.4.13}$$

where

$$\begin{aligned}\zeta'_H &= \frac{\tilde{\lambda}^*_6 \tilde{\lambda}_6}{\tilde{m}_2^4} \\ Z_H &= 1 + \Delta_{Z_H} = 1 + \frac{\left|\tilde{m}^2_{12}\right|^2}{\tilde{m}_2^4} \\ \zeta_H &= \frac{2\tilde{m}^2_{12}\tilde{\lambda}^*_6}{\tilde{m}_2^4} \\ \Delta_{Z_H} &= \frac{1}{4}\zeta'_H v^4 = -\frac{1}{4}\zeta_H v^2\end{aligned} \tag{4.4.14}$$

$$
\begin{aligned}
m_H^2 &= \tilde{m}_1^2 - \frac{\left|\tilde{m}_{12}^2\right|^2}{\tilde{m}_2^2} \\
\lambda_H &= \tilde{\lambda}_1 - \frac{4\tilde{m}_{12}^2\tilde{\lambda}_6^*}{\tilde{m}_2^2} + \frac{2(\tilde{\lambda}_3+\tilde{\lambda}_4)\left|\tilde{m}_{12}^2\right|^2}{\tilde{m}_2^4} + \frac{(\tilde{\lambda}_5^*\tilde{m}_{12}^4 + \text{h.c.})}{\tilde{m}_2^4} \\
\eta_6 &= -\frac{3\tilde{\lambda}_6^\dagger\tilde{\lambda}_6}{\tilde{m}_2^2} + \frac{6(\tilde{\lambda}_3+\tilde{\lambda}_4)\tilde{m}_{12}^2\tilde{\lambda}_6^*}{\tilde{m}_2^4} + \frac{3(\tilde{\lambda}_5^*\tilde{\lambda}_6\tilde{m}_{12}^2 + \text{h.c})}{\tilde{m}_2^4} \\
\eta_8 &= \frac{4(\tilde{\lambda}_3+\tilde{\lambda}_4)\tilde{\lambda}_6^*\tilde{\lambda}_6}{\tilde{m}_2^4} + \frac{2(\tilde{\lambda}_5^*\tilde{\lambda}_6^2 + \text{h.c.})}{\tilde{m}_2^4}
\end{aligned}
\tag{4.4.15}
$$

$$
\begin{aligned}
\eta_{ij}^f &= -\frac{\tilde{\lambda}_{2ij}^f\tilde{\lambda}_6^*}{\tilde{m}_2^2} \\
\lambda_{ij}^f &= \tilde{\lambda}_{1ij}^f - \frac{\tilde{\lambda}_{2ij}^f\tilde{m}_{12}^{*2}}{\tilde{m}_2^2} \qquad\qquad f = u, d, \ell
\end{aligned}
$$

Note that due to the no tadpole condition (4.3.24), the operator coefficients Δ_{Z_H}, ζ_H' and ζ_H are not independent, as we see in the last lines of (4.4.14). Note also that in the effective theory there are no threshold corrections to the Higgs kinetic Lagrangian at effective dimension six, the first corrections are of effective dimension eight. The Higgs potential is modified at effective dimension six. The EFT contains cubic Yukawa operators at effective dimension six, for all types of SM fermions. We do not present operators with naive dimension six and eight involving the Higgs and gauge field strength tensors since they come at effective dimension higher than eight. We also drop all operator dimension six Higgs-fermion interactions with derivatives since they come at effective dimension eight. Note that T violation in purely bosonic operators (operators involving no SM fermions) is irrelevant to the effective dimension we work to; all the bosonic operators in (4.4.12) are T conserving. Up to the order we work to, T violation only arises in the Higgs-fermion interactions. The fermion mass matrices are given by the linear and cubic Yukawas by

$$
\frac{\lambda_{ij}^f v}{\sqrt{2}} + \frac{\eta_{ij}^f v^3}{2\sqrt{2}} = m_{ij}^f \tag{4.4.16}
$$

The four fermion operators of the low energy theory are given by (4.4.11). Here we write them as

$$
\begin{aligned}
&\Omega_{ijmn}^{uu(0)}(Q_i\overline{u}_j)(\overline{u}_m^\dagger Q_n^\dagger) + \Omega_{ijmn}^{dd(0)}(Q_i\overline{d}_j)(\overline{d}_m^\dagger Q_n^\dagger) + \Omega_{ijmn}^{\ell\ell(0)}(L_i\overline{\ell}_j)(\overline{\ell}_m^\dagger L_n^\dagger) \\
+ &\left[\Omega_{ijmn}^{d\ell(0)}(Q_i\overline{d}_j)(\overline{\ell}_m^\dagger L_n^\dagger) + \Omega_{ijmn}^{ud(2)}(Q_i\overline{u}_j)(Q_m\overline{d}_n) + \Omega_{ijmn}^{u\ell(2)}(Q_i\overline{u}_j)(L_m\overline{\ell}_n) + \text{h.c.}\right]
\end{aligned}
\tag{4.4.17}
$$

or, expanding in components of the fermion doublets

$$\begin{aligned}
&\Omega^{uu(0)}_{ijmn}\Big[(u_i\overline{u}_j)(\overline{u}^\dagger_m u^\dagger_n)+(d_i\overline{u}_j)(\overline{u}^\dagger_m d^\dagger_n)\Big]+\Omega^{dd(0)}_{ijmn}\Big[(u_i\overline{d}_j)(\overline{d}^\dagger_m u^\dagger_n)+(d_i\overline{d}_j)(\overline{d}^\dagger_m d^\dagger_n)\Big]\\
&+\Omega^{\ell\ell(0)}_{ijmn}\Big[(\nu_i\overline{\ell}_j)(\overline{\ell}^\dagger_m\nu^\dagger_n)+(\ell_i\overline{\ell}_j)(\overline{\ell}^\dagger_m\ell^\dagger_n)\Big]\\
&+\Bigg[\ \Omega^{d\ell(0)}_{ijmn}\Big[(u_i\overline{d}_j)(\overline{\ell}^\dagger_m\nu^\dagger_n)+(d_i\overline{d}_j)(\overline{\ell}^\dagger_m\ell^\dagger_n)\Big]+\Omega^{ud(2)}_{ijmn}\Big[(u_i\overline{u}_j)(d_m\overline{d}_n)-(d_i\overline{u}_j)(u_m\overline{d}_n)\Big]\\
&+\Omega^{u\ell(2)}_{ijmn}\Big[(u_i\overline{u}_j)(\ell_m\overline{\ell}_n)-(d_i\overline{u}_j)(\nu_m\overline{\ell}_n)\Big]+\text{h.c.}\ \Bigg]
\end{aligned}\tag{4.4.18}$$

These are all the four fermion operators that are obtained at effective dimension six. The superindices (0) and (2) represent operators that violate chirality by zero or two units respectively. The labels $uu, dd, \ell\ell, d\ell, ud, u\ell$ label the right handed quarks appearing in the four fermion operator. The coefficients of the operators are

$$\begin{aligned}
&\Omega^{uu(0)}_{ijmn}=\frac{\tilde\lambda^u_{2ij}\tilde\lambda^{u\dagger}_{2mn}}{\tilde m_2^2}\quad,\quad \Omega^{dd(0)}_{ijmn}=\frac{\tilde\lambda^{d\dagger}_{2ij}\tilde\lambda^{d}_{2mn}}{\tilde m_2^2}\quad,\quad \Omega^{\ell\ell(0)}_{ijmn}=\frac{\tilde\lambda^{\ell\dagger}_{2ij}\tilde\lambda^{\ell}_{2mn}}{\tilde m_2^2}\\
&\Omega^{d\ell(0)}_{ijmn}=\frac{\tilde\lambda^{d\dagger}_{2ij}\tilde\lambda^{\ell}_{2mn}}{\tilde m_2^2}\quad,\quad \Omega^{ud(2)}_{ijmn}=\frac{\tilde\lambda^{u}_{2ij}\tilde\lambda^{d\dagger}_{2mn}}{\tilde m_2^2}\quad,\quad \Omega^{u\ell(2)}_{ijmn}=\frac{\tilde\lambda^{u}_{2ij}\tilde\lambda^{\ell\dagger}_{2mn}}{\tilde m_2^2}
\end{aligned}\tag{4.4.19}$$

For general $\tilde\lambda^f_{2ij}$ matrices, these four fermion interactions are flavor and T violating.

4.4.3 The Low energy theory of the Higgs boson

We now write down the effective theory for the neutral component of the Higgs doublet in the unitary gauge. The no tadpole condition (4.3.24) will be used extensively in the rest of the discussion.

Writing the Lagrangian density (4.4.12) in terms of h we get

$$
\begin{aligned}
& Z_H\left[\frac{1}{2}\partial_\mu h\partial^\mu h+\frac{1}{2}m_Z^2Z^\mu Z_\mu\Big(1+\frac{2h}{v}+\frac{h^2}{v^2}\Big)+m_W^2W^{+\mu}W_\mu^-\Big(1+\frac{2h}{v}+\frac{h^2}{v^2}\Big)\right]\\
& +\zeta_H\left[\frac{1}{2}\partial_\mu h\partial^\mu h\Big(\frac{3}{2}v^2+3vh+\frac{3}{2}h^2\Big)+\right.\\
& \left.+\Big(\frac{1}{2}m_Z^2Z^\mu Z_\mu+m_W^2W^{+\mu}W_\mu^-\Big)\Big(\frac{1}{2}v^2+2vh+3h^2+\frac{2h^3}{v}+\frac{1}{2}\frac{h^4}{v^2}\Big)\right]\\
& +\zeta_H'\left[\frac{1}{2}\partial_\mu h\partial^\mu h\Big(\frac{9}{4}v^4+9v^3h+\frac{27}{2}v^2h^2+9vh^3+\frac{9}{4}h^4\Big)\right.\\
& \left.+\Big(\frac{1}{2}m_Z^2Z^\mu Z_\mu+m_W^2W^{+\mu}W_\mu^-\Big)\Big(\frac{1}{4}v^4+\frac{3}{2}v^3h+\frac{15}{4}v^2h^2+5vh^3+\frac{15}{4}h^4+\frac{3}{2}\frac{h^5}{v}+\frac{1}{4}\frac{h^6}{v^2}\Big)\right]\\
& -V(h)-\left[u_i\overline{u}_j\left[m_{ij}^u+\Big(\frac{m_{ij}^u}{v}+2\Big(\frac{\eta_{ij}^uv^2}{2\sqrt{2}}\Big)\Big)h+3\Big(\frac{\eta_{ij}^uv}{2\sqrt{2}}\Big)h^2+\Big(\frac{\eta_{ij}^u}{2\sqrt{2}}\Big)h^3\right]\right.\\
& -d_i\overline{d}_j\left[m_{ij}^{d\dagger}+\Big(\frac{m_{ij}^{d\dagger}}{v}+2\Big(\frac{\eta_{ij}^{d\dagger}v^2}{2\sqrt{2}}\Big)\Big)h+3\Big(\frac{\eta_{ij}^{d\dagger}v}{2\sqrt{2}}\Big)h^2+\Big(\frac{\eta_{ij}^{d\dagger}}{2\sqrt{2}}\Big)h^3\right]\\
& \left.-\ell_i\overline{\ell}_j\left[m_{ij}^{\ell\dagger}+\Big(\frac{m_{ij}^{\ell\dagger}}{v}+2\Big(\frac{\eta_{ij}^{\ell\dagger}v^2}{2\sqrt{2}}\Big)\Big)h+3\Big(\frac{\eta_{ij}^{\ell\dagger}v}{2\sqrt{2}}\Big)h^2+\Big(\frac{\eta_{ij}^{\ell\dagger}}{2\sqrt{2}}\Big)h^3\right]+\text{h.c.}\right]
\end{aligned}
\tag{4.4.20}
$$

The cubic Yukawa for the doublet contributes a term $3\eta_{ij}^fv^2/(2\sqrt{2})$ to the linear Yukawas of the Higgs $f_i\overline{f}_jh$, but one factor of $\eta_{ij}^fv^2/(2\sqrt{2})$ is already included in the definition of the fermion mass matrix m_{ij}^f/v, Eq. (4.4.16). The Higgs potential is given by

$$
\begin{aligned}
V(h) \;=\; & \frac{1}{2}\,m_H^2h^2+\frac{1}{2}\,\lambda_H\Big(\frac{3}{2}v^2h^2+vh^3+\frac{1}{4}h^4\Big)\\
& +\frac{1}{3}\,\eta_6\Big(\frac{15v^4}{8}h^2+\frac{5v^3}{2}h^3+\frac{15v^2}{8}h^4+\frac{3v}{4}h^5+\frac{1}{8}h^6\Big)\\
& +\frac{1}{4}\,\eta_8\Big(\frac{7v^6}{4}h^2+\frac{7v^5}{2}h^3+\frac{35v^4}{8}h^4+\frac{7v^3}{2}h^5+\frac{7v^2}{4}h^6+\frac{v}{2}h^7+\frac{1}{16}h^8\Big)
\end{aligned}
\tag{4.4.21}
$$

The irrelevant kinetic operators in (4.4.20) can be replaced in favor of operators with no derivatives using integration by parts and equations of motion. We first use integration by parts to rewrite the kinetic terms proportional to ζ_H as

$$
\begin{aligned}
& \frac{1}{2}\partial_\mu(H^\dagger H)\partial^\mu(H^\dagger H)+H^\dagger H\,D_\mu H^\dagger D^\mu H\\
& =\frac{3}{4}v^2\,\partial_\mu h\partial^\mu h+\frac{3}{2}vh\,\partial_\mu h\partial^\mu h+\frac{3}{4}h^2\,\partial_\mu h\partial^\mu h+\\
& +\Big(\frac{1}{2}m_Z^2Z^\mu Z_\mu+m_W^2W^{+\mu}W_\mu^-\Big)\Big(\frac{1}{2}v^2+2vh+3h^2+\frac{2h^3}{v}+\frac{1}{2}\frac{h^4}{v^2}\Big)\\
& =\frac{3}{4}\partial_\mu h\partial^\mu h\,v^2-\frac{3}{4}vh^2\,\Box h-\frac{1}{4}h^3\,\Box h+\\
& +\Big(\frac{1}{2}m_Z^2Z^\mu Z_\mu+m_W^2W^{+\mu}W_\mu^-\Big)\Big(\frac{1}{2}v^2+2vh+3h^2+\frac{2h^3}{v}+\frac{1}{2}\frac{h^4}{v^2}\Big)
\end{aligned}
\tag{4.4.22}
$$

We also use integration by parts to rewrite the kinetic terms proportional to ζ'_H,

$$
\begin{aligned}
&2H^\dagger H\,\partial_\mu(H^\dagger H)\partial^\mu(H^\dagger H) + (H^\dagger H)^2\,D_\mu H^\dagger D^\mu H \\
&= \frac{9}{8}v^4\,\partial_\mu h\partial^\mu h + \frac{9}{2}v^3 h\,\partial_\mu h\partial^\mu h + \frac{27}{4}v^2h^2\,\partial_\mu h\partial^\mu h + \frac{9}{2}vh^3\,\partial_\mu h\partial^\mu h + \frac{9}{8}h^4\,\partial_\mu h\partial^\mu h \\
&+ \left(\frac{1}{2}m_Z^2 Z^\mu Z_\mu + m_W^2 W^{+\mu}W^-_\mu\right)\left(\frac{1}{4}v^4 + \frac{3}{2}v^3h + \frac{15}{4}v^2h^2 + 5vh^3 + \frac{15}{4}h^4 + \frac{3}{2}\frac{h^5}{v} + \frac{1}{4}\frac{h^6}{v^2}\right) \\
&= \frac{9}{8}\partial_\mu h\partial^\mu h\,v^4 - \frac{9}{4}v^3h^2\,\Box h - \frac{9}{4}v^2h^3\,\Box h - \frac{9}{8}vh^4\,\Box h - \frac{9}{40}h^5\,\Box h \\
&+ \left(\frac{1}{2}m_Z^2 Z^\mu Z_\mu + m_W^2 W^{+\mu}W^-_\mu\right)\left(\frac{1}{4}v^4 + \frac{3}{2}v^3h + \frac{15}{4}v^2h^2 + 5vh^3 + \frac{15}{4}h^4 + \frac{3}{2}\frac{h^5}{v} + \frac{1}{4}\frac{h^6}{v^2}\right)
\end{aligned}
\tag{4.4.23}
$$

The lowest order (effective dimension four) equation of motion for the Higgs field is

$$
\begin{aligned}
\Box h \;=\; & -m_H^2 h - \frac{1}{2}\lambda_H(3v^2h + 3vh^2 + h^3) \\
& + \left(\frac{m_Z^2}{v}Z^\mu Z_\mu + \frac{2m_W^2}{v}W^{+\mu}W^-_\mu\right)\left(1 + \frac{h}{v}\right) \\
& - \left(\frac{m^u_{ij}}{v}u_i\overline{u}_j + \frac{m^{d\dagger}_{ij}}{v}d_i\overline{d}_j + \frac{m^{\ell\dagger}_{ij}}{v}\ell_i\overline{\ell}_j + \text{h.c.}\right) + \ldots
\end{aligned}
\tag{4.4.24}
$$

where the dots represent terms of higher effective dimension. Using (4.4.24) in (4.4.22) and in (4.4.23), we can rewrite the Higgs Lagrangian (4.4.20) with no irrelevant operators with derivatives

$$
\begin{aligned}
& Z_H\left[\frac{1}{2}\partial_\mu h\partial^\mu h + \frac{1}{2}m_Z^2\left(1 + \frac{2h}{v} + \frac{h^2}{v^2}\right)Z^\mu Z_\mu + m_W^2\left(1 + \frac{2h}{v} + \frac{h^2}{v^2}\right)W^{+\mu}W^-_\mu\right] \\
& + \zeta_H\left[\frac{3}{4}\partial_\mu h\partial^\mu h\,v^2 - \left(\frac{3}{4}vh^2 + \frac{1}{4}h^3\right)\left[-m_H^2 h - \frac{1}{2}\lambda_H(3v^2h + 3vh^2 + h^3)\right.\right. \\
& \left. + \left(\frac{m_Z^2}{v}Z^\mu Z_\mu + \frac{2m_W^2}{v}W^{+\mu}W^-_\mu\right)\left(1 + \frac{h}{v}\right) - \left(\frac{m^u_{ij}}{v}u_i\overline{u}_j + \frac{m^{d\dagger}_{ij}}{v}d_i\overline{d}_j + \frac{m^{\ell\dagger}_{ij}}{v}\ell_i\overline{\ell}_j + \text{h.c.}\right)\right] \\
& \left. + \left(\frac{1}{2}m_Z^2 Z^\mu Z_\mu + m_W^2 W^{+\mu}W^-_\mu\right)\left(\frac{1}{2}v^2 + 2vh + 3h^2 + \frac{2h^3}{v} + \frac{1}{2}\frac{h^4}{v^2}\right)\right] \\
& + \zeta'_H\left[\frac{9}{8}\partial_\mu h\partial^\mu h\,v^4 - \left(\frac{9}{4}v^3h^2 + \frac{9}{4}v^2h^3 + \frac{9}{8}vh^4 + \frac{9}{40}h^5\right)\left[-m_H^2 h - \frac{1}{2}\lambda_H(3v^2h + 3vh^2 + h^3)\right.\right. \\
& \left. + \left(\frac{m_Z^2}{v}Z^\mu Z_\mu + \frac{2m_W^2}{v}W^{+\mu}W^-_\mu\right)\left(1 + \frac{h}{v}\right) - \left(\frac{m^u_{ij}}{v}u_i\overline{u}_j + \frac{m^{d\dagger}_{ij}}{v}d_i\overline{d}_j + \frac{m^{\ell\dagger}_{ij}}{v}\ell_i\overline{\ell}_j + \text{h.c.}\right)\right] \\
& \left. + \left(\frac{1}{2}m_Z^2 Z^\mu Z_\mu + m_W^2 W^{+\mu}W^-_\mu\right)\left(\frac{1}{4}v^4 + \frac{3}{2}v^3h + \frac{15}{4}v^2h^2 + 5vh^3 + \frac{15}{4}h^4 + \frac{3}{2}\frac{h^5}{v} + \frac{1}{4}\frac{h^6}{v^2}\right)\right] \\
& - V(h) - \left[u_i\overline{u}_j\left[m^u_{ij} + \left(\frac{m^u_{ij}}{v} + 2\left(\frac{\eta^u_{ij}v^2}{2\sqrt{2}}\right)\right)h + 3\left(\frac{\eta^u_{ij}v}{2\sqrt{2}}\right)h^2 + \left(\frac{\eta^u_{ij}}{2\sqrt{2}}\right)h^3\right]\right. \\
& - d_i\overline{d}_j\left[m^{d\dagger}_{ij} + \left(\frac{m^{d\dagger}_{ij}}{v} + 2\left(\frac{\eta^{d\dagger}_{ij}v^2}{2\sqrt{2}}\right)\right)h + 3\left(\frac{\eta^{d\dagger}_{ij}v}{2\sqrt{2}}\right)h^2 + \left(\frac{\eta^{d\dagger}_{ij}}{2\sqrt{2}}\right)h^3\right] \\
& \left. - \ell_i\overline{\ell}_j\left[m^{\ell\dagger}_{ij} + \left(\frac{m^{\ell\dagger}_{ij}}{v} + 2\left(\frac{\eta^{\ell\dagger}_{ij}v^2}{2\sqrt{2}}\right)\right)h + 3\left(\frac{\eta^{\ell\dagger}_{ij}v}{2\sqrt{2}}\right)h^2 + \left(\frac{\eta^{\ell\dagger}_{ij}}{2\sqrt{2}}\right)h^3\right] + \text{h.c.}\right]
\end{aligned}
\tag{4.4.25}
$$

Note that using equations of motion leads to new interaction terms for the Higgs with fermions and gauge bosons - irrelevant operators involving derivatives of the Higgs cannot be neglected when studying Higgs couplings. The wave function renormalization term in (4.4.25) can be made canonical by performing a field redefinition

$$\begin{aligned}\varphi &= \left(1+\Delta Z_H+\frac{3}{2}\zeta_H v^2+\frac{9}{4}\zeta'_H v^4\right)^{1/2} h \\ &= \left[1+\tilde{\lambda}_6^\dagger\tilde{\lambda}_6\left(\frac{v^2}{\tilde{m}_2^2}\right)^2\right]^{1/2} h = \left[1+|\Xi|^2+\mathcal{O}\left(\frac{v^6}{\tilde{m}_2^6}\right)\right]^{1/2} h \end{aligned} \tag{4.4.26}$$

where in going from the first to the second line we made use of (4.4.14). As in section 4.2.3, we see that there is a close relation between the mixing parameter (in this case, the complex alignment parameter Ξ) in the mixing language and wave function renormalization in the EFT language.

Finally, note that the extremum condition for the potential is

$$\frac{\partial V}{\partial v}\Big|_{h=0} = v\Big(m_H^2+\frac{1}{2}\lambda_H v^2+\frac{1}{4}\eta_6 v^4+\frac{1}{8}\eta_8 v^6\Big)=0 \tag{4.4.27}$$

so the Lagrangian mass parameter m_H can be expressed in terms of Higgs potential couplings and the vev

$$m_H^2 = -\frac{1}{2}\lambda_H v^2-\frac{1}{4}\eta_6 v^4-\frac{1}{8}\eta_8 v^6 \tag{4.4.28}$$

Using (4.4.26) and (4.4.28) in (4.4.25) we write the effective field theory for the Higgs boson in its final form

$$\begin{aligned}\mathcal{L} &= \frac{1}{2}\partial_\mu\varphi\partial^\mu\varphi-\frac{1}{2}m_\varphi^2\varphi^2+\sum_{n=3}^{n=8}\frac{1}{n!}g_{\varphi^n}\varphi^n+\frac{1}{2}m_Z^2 Z^\mu Z_\mu+m_W^2 W^{+\mu}W^-_\mu \\ &+\sum_{n=1}^{n=6}\frac{\varphi^n}{n!}\left[g_{\varphi^n ZZ}\ \frac{1}{2}Z^\mu Z_\mu+g_{\varphi^n WW}\ W^{+\mu}W^-_\mu\right] \\ &-m^u_{ij}u_i\overline{u}_j-m^{d\dagger}_{ij}d_i\overline{d}_j-m^{\ell\dagger}_{ij}\ell_i\overline{\ell}_j \\ &-\sum_{n=1}^{n=3}\frac{\varphi^n}{n!}\left[\lambda^u_{\varphi^n ij}\ u_i\overline{u}_j+\lambda^{d\dagger}_{\varphi^n ij}\ d_i\overline{d}_j+\lambda^{\ell\dagger}_{\varphi^n ij}\ \ell_i\overline{\ell}_j+\text{h.c.}\right]\end{aligned} \tag{4.4.29}$$

We now give explicit expressions for all the couplings of the effective theory. All the SM values of the couplings of the Higgs can be read from this section by taking the limit $\tilde{\lambda}_6\to 0$. The no tadpole condition is crucial for the final results. For instance, note that in (4.4.25) there are several mass terms for the W and Z bosons at effective dimension eight. The no tadpole condition imposes conditions between the coefficients of these operators, Eq. (4.4.14). These conditions ensure that all the effective dimension eight mass terms cancel out, such that the mass of the W and Z boson coincide with their values in the renormalizable SM, $m_W=g_2 v/2$ and $m_Z=g_2 v/(2\cos\theta_W)$. Note that this ensures that $\rho=m_W^2/(m_Z^2\cos^2\theta_W)=1$.

We start by the Higgs mass, which is given by

$$m_\varphi^2 \;=\; v^2\left[\tilde\lambda_1-\tilde\lambda_6^*\tilde\lambda_6\,\frac{v^2}{\tilde m_2^2}-\frac{1}{2}\Big[(2\tilde\lambda_1-\tilde\lambda_3-\tilde\lambda_4)\tilde\lambda_6^*\tilde\lambda_6-\frac{1}{2}(\tilde\lambda_5^*\tilde\lambda_6^2+\text{h.c})\Big]\frac{v^4}{\tilde m_2^4}+\mathcal{O}\bigg(\frac{v^6}{\tilde m_2^6}\bigg)\right] \tag{4.4.30}$$

The second term in (4.4.30) comes from the threshold correction to the operators $(H^\dagger H)^2$ and $(H^\dagger H)^3$ at effective dimension six. The rest of the corrections come from operators of effective dimension eight: the term proportional to $\tilde\lambda_1\tilde\lambda_6^*\tilde\lambda_6$ is due to wave function renormalization (4.4.25), and the rest of the terms come from threshold corrections to the operators $(H^\dagger H)^n$, $n=2,3,4$ at effective dimension eight.

The couplings of one Higgs to two massive gauge bosons $V=W,Z$ are

$$g_{\varphi VV}=\frac{2m_V^2}{v}\left[1-\frac{1}{2}\tilde\lambda_6^*\tilde\lambda_6\,\frac{v^4}{\tilde m_2^4}+\mathcal{O}\bigg(\frac{v^6}{\tilde m_2^6}\bigg)\right] \tag{4.4.31}$$

The difference with respect to the SM values comes exclusively from dilution by wave function renormalization (4.4.26) at effective dimension eight. The rest of the contributions to these couplings coming from the terms with covariant derivatives proportional to ζ_H and ζ_H' in (4.4.12) cancel out, thanks to (4.4.14). The result (4.4.31) coincides with the corresponding couplings obtained in the mixing language (4.3.61). The couplings of two Higgses to two massive gauge bosons are

$$g_{\varphi^2VV}=\frac{2m_V^2}{v^2}\left[1-3\tilde\lambda_6^*\tilde\lambda_6\,\frac{v^4}{\tilde m_2^4}+\mathcal{O}\bigg(\frac{v^6}{\tilde m_2^6}\bigg)\right] \tag{4.4.32}$$

The difference with respect to the SM prediction comes exclusively from the terms that were generated by using the equations of motion in (4.4.25). This is an effective dimension eight effect. The rest of the effective dimension eight terms cancel out. Note that (4.4.32) does not coincide with the result in the mixing language (4.3.59). As discussed in the SHSM EFT, four linear couplings in general do not coincide in the mixing and EFT languages, we comment on the difference in the end of this section. For completeness, the irrelevant couplings to gauge bosons come at effective dimension eight and are given by

$$\begin{aligned}
v g_{\varphi^3VV} &= -\frac{m_V^2}{v^2}\left[24\tilde\lambda_6^*\tilde\lambda_6\,\frac{v^4}{\tilde m_2^4}+\mathcal{O}\bigg(\frac{v^6}{\tilde m_2^6}\bigg)\right]\\
v^2 g_{\varphi^4VV} &= -\frac{m_V^2}{v^2}\left[72\tilde\lambda_6^*\tilde\lambda_6\,\frac{v^4}{\tilde m_2^4}+\mathcal{O}\bigg(\frac{v^6}{\tilde m_2^6}\bigg)\right]\\
v^3 g_{\varphi^5VV} &= -\frac{m_V^2}{v^2}\left[144\tilde\lambda_6^*\tilde\lambda_6\,\frac{v^4}{\tilde m_2^4}+\mathcal{O}\bigg(\frac{v^6}{\tilde m_2^6}\bigg)\right]\\
v^4 g_{\varphi^6VV} &= -\frac{m_V^2}{v^2}\left[144\tilde\lambda_6^*\tilde\lambda_6\,\frac{v^4}{\tilde m_2^4}+\mathcal{O}\bigg(\frac{v^6}{\tilde m_2^6}\bigg)\right]
\end{aligned} \tag{4.4.33}$$

These couplings vanish in the decoupling limit.

Higgs-fermion interactions are modified by the cubic Yukawas of the Higgs doublet, which come at effective dimension six. They are given by

$$\begin{aligned}
\lambda^f_{\varphi ij} &= \frac{m_i^f}{v}\,\delta_{ij} - 2\left(\frac{\tilde\lambda^f_{2ij}\tilde\lambda^*_6}{2\sqrt{2}}\right)\left(\frac{v^2}{\tilde m_2^2}\right) + \mathcal{O}\left(\frac{v^4}{\tilde m_2^4}\right)\\
v\lambda^f_{\varphi^2 ij} &= -3\left(\frac{\tilde\lambda^f_{2ij}\tilde\lambda^*_6}{\sqrt{2}}\right)\left(\frac{v^2}{\tilde m_2^2}\right) + \mathcal{O}\left(\frac{v^4}{\tilde m_2^4}\right)\\
v^2\lambda^f_{\varphi^3 ij} &= -3\left(\frac{\tilde\lambda^f_{2ij}\tilde\lambda^*_6}{\sqrt{2}}\right)\left(\frac{v^2}{\tilde m_2^2}\right) + \mathcal{O}\left(\frac{v^4}{\tilde m_2^4}\right)
\end{aligned} \tag{4.4.34}$$

Note that we neglect the effective dimension eight terms coming from wave function renormalization (4.4.26) and from the use of the equations of motion in (4.4.23), since we only work up to effective dimension six in interactions involving fermions. All the flavor violating terms in the fermionic couplings (4.4.34) are inherited from the heavy doublet Yukawa matrix, $\tilde\lambda^f_{2ij}$. Non zero phases in $\tilde\lambda^f_{2ij}\tilde\lambda^*_6$ lead to T violating processes mediated by Higgs boson exchange, since they induce a relative phase between the Yukawas and the quark mass matrices. Note that the irrelevant couplings $\lambda^f_{\varphi^2 ij}$ and $\lambda^f_{\varphi^3 ij}$ vanish in the decoupling limit.

Higgs self couplings are modified by the operators of effective dimension six and eight in (4.4.12). They are given by

$$\begin{aligned}
\frac{1}{v}g_{\varphi_1^3} \;=\; & -\frac{3m^2_{\varphi_1}}{v^2} + 6\tilde\lambda^*_6\tilde\lambda_6\,\frac{v^2}{\tilde m_2^2}\\
& + \frac{1}{2}\left[\left[21\tilde\lambda_1 - 12(\tilde\lambda_3+\tilde\lambda_4)\right]\tilde\lambda^*_6\tilde\lambda_6 - \left(6\tilde\lambda_5\tilde\lambda^{*2}_6 + \text{h.c.}\right)\right]\frac{v^4}{\tilde m_2^4} + \mathcal{O}\left(\frac{v^6}{\tilde m_2^6}\right)
\end{aligned} \tag{4.4.35}$$

$$\begin{aligned}
g_{\varphi_1^4} \;=\; & -\frac{3m^2_{\varphi_1}}{v^2} + 36\tilde\lambda^*_6\tilde\lambda_6\,\frac{v^2}{\tilde m_2^2}\\
& + \left[\left[105\tilde\lambda_1 - 60(\tilde\lambda_3+\tilde\lambda_4)\right]\tilde\lambda^*_6\tilde\lambda_6 - \left(30\tilde\lambda_5\tilde\lambda^{*2}_6 + \text{h.c.}\right)\right]\frac{v^4}{\tilde m_2^4} + \mathcal{O}\left(\frac{v^6}{\tilde m_2^6}\right)
\end{aligned} \tag{4.4.36}$$

For completeness, the irrelevant self couplings are given by

$$\begin{aligned}
v g_{\varphi^5} &= 90\tilde\lambda_6\tilde\lambda^*_6\,\frac{v^2}{\tilde m_2^2} + \left(\left[585\tilde\lambda_1 - 330(\tilde\lambda_3+\tilde\lambda_4)\right]\tilde\lambda^*_6\tilde\lambda_6 - \left(165\tilde\lambda_5\tilde\lambda^{*2}_6 + \text{h.c.}\right)\right)\frac{v^4}{\tilde m_2^4} + \mathcal{O}\left(\frac{v^6}{\tilde m_2^6}\right)\\
v^2 g_{\varphi^6} &= 90\tilde\lambda_6\tilde\lambda^*_6\,\frac{v^2}{\tilde m_2^2} + \left(\left[2097\tilde\lambda_1 - 1170(\tilde\lambda_3+\tilde\lambda_4)\right]\tilde\lambda^*_6\tilde\lambda_6 - \left(585\tilde\lambda_5\tilde\lambda^{*2}_6 + \text{h.c.}\right)\right)\frac{v^4}{\tilde m_2^4} + \mathcal{O}\left(\frac{v^6}{\tilde m_2^6}\right)\\
v^3 g_{\varphi^7} &= \left(\left[4536\tilde\lambda_1 - 2520(\tilde\lambda_3+\tilde\lambda_4)\right]\tilde\lambda^*_6\tilde\lambda_6 - \left(1260\tilde\lambda_5\tilde\lambda^{*2}_6 + \text{h.c.}\right)\right)\frac{v^4}{\tilde m_2^4} + \mathcal{O}\left(\frac{v^6}{\tilde m_2^6}\right)\\
v^4 g_{\varphi^8} &= \left(\left[4536\tilde\lambda_1 - 2520(\tilde\lambda_3+\tilde\lambda_4)\right]\tilde\lambda^*_6\tilde\lambda_6 - \left(1260\tilde\lambda_5\tilde\lambda^{*2}_6 + \text{h.c.}\right)\right)\frac{v^4}{\tilde m_2^4} + \mathcal{O}\left(\frac{v^6}{\tilde m_2^6}\right)
\end{aligned} \tag{4.4.37}$$

All these irrelevant self couplings vanish in the decoupling limit.

Note that all trilinear couplings coincide in the EFT and mixing languages, while four-linear interactions do not coincide, as already discussed in section 4.2.3 for the case of the SM extended

with a heavy singlet. The equality of the trilinear couplings in the EFT and mixing languages ensures the equality between the non analytic (long distance) physical scattering amplitudes in the EFT and mixing languages. Integrating out heavy fields cannot modify cubic interactions. Four-linear interactions can be different in both languages, since four linear couplings in the mixing language do not contain all the short distance pieces of the corresponding amplitudes, but EFT couplings do. Scattering amplitudes calculated in both languages coincide, as we will see in section 4.4.4.

We conclude this section emphasizing a series of particular phenomenological characteristics of the 2HDM EFT. First, deviations to the SM predictions of the Higgs-fermion couplings come at effective dimension six, while deviations to the Higgs-gauge boson couplings come first at effective dimension eight. This hierarchy is one of the main features of the 2HDM EFT. Deviations from the SM predictions in a measurement of fermionic Higgs couplings at colliders, together with no corresponding modifications to the Higgs-gauge boson couplings, would be a possible indication of a Higgs sector completed with a second doublet in the UV. Second, all the deviations to the SM predictions for the couplings of the Higgs at effective dimension six are controlled exclusively by a small subset of the couplings of the UV completion: the PQ invariant combinations $\tilde{\lambda}^f_{2ij}\tilde{\lambda}_6$ and $\tilde{\lambda}^*_6\tilde{\lambda}_6$. This significantly reduces the complexity of the analysis of the most general 2HDM. In the mixing language, $\tilde{\lambda}_6$ is related to the complex alignment parameter through (4.3.53). The modifications to Higgs-gauge boson couplings with respect to their SM predictions at effective dimension eight, are also controlled by $\tilde{\lambda}^*_6\tilde{\lambda}_6$. Another special characteristic of the 2HDM EFT is that *all* the bosonic couplings of the Higgs are smaller in magnitude than their SM counterparts. This is evident in the EFT, but less obvious in the mixing language, where the coupling of two Higgses to two gauge bosons is left unmodified with respect to its SM value.

T violation has a particular structure in the 2HDM EFT. All T violation at effective dimension six comes exclusively from the PQ invariant phases in the fermionic interactions proportional to $\tilde{\lambda}^f_{2ij}\tilde{\lambda}_6$. The T violating phases θ_1 and θ_2 defined in (4.3.25) which come from the 2HDM potential do not show up at effective dimension six. Note that θ_1 is the phase of the complex alignment parameter (4.3.53). As a consequence, measuring the phase of the complex alignment parameter is challenging for a 2HDM near the decoupling limit, since the T violating effects of θ_1 are subleading. The T violating effects of θ_1 might first appear in fermionic interactions involving an insertion of the coupling $\tilde{\lambda}_5$ at effective dimension eight. Finally, there is no CP violation in purely bosonic interactions up to at least effective dimension ten in the 2HDM EFT. For instance, the operator $H^\dagger H F_{\mu\nu}\tilde{F}^{\mu\nu}$ is not induced up to at least effective dimension ten.

Regarding the four fermion operators (4.4.17), note that they are the only operators which are not controlled by $\tilde{\lambda}_6$, and they are the only operators at effective dimension six which do not vanish in the exact alignment limit, when $\Xi \propto \tilde{\lambda}_6 = 0$. In the exact alignment limit and near the decoupling limit, the only hope to get hints of a second doublet would be at flavor experiments sensitive to flavor violation in the four fermion operators (4.4.17).

Finally, note that in our results there is no reference to $\tan\beta$ anywhere, since in a general 2HDM, $\tan\beta$ has no physical meaning.

4.4.4 Scattering amplitudes

As a consistency check of the EFT we compute scattering amplitudes, and compare with the corresponding results obtained in the mixing language in section 4.3.3. We omit spinors in the amplitudes.

The dihiggs to di-W boson scattering amplitude is

$$\mathcal{A}\left(\varphi_1\varphi_1 \to W^+W^-\right) \;=\; g_{\mu\nu}\left[g_{\varphi^2W^2} - \frac{g_{\varphi^3}g_{\varphi W^2}}{s-m_\varphi^2} - g_{\varphi W^2}^2\left(\frac{1}{t-m_W^2}+\frac{1}{u-m_W^2}\right)\right] \tag{4.4.38}$$

Using the EFT couplings (4.4.31), (4.4.32) and (4.4.35) the resulting amplitude is

$$\begin{aligned}\mathcal{A}\left(\varphi\varphi \to W^+W^-\right) \;=\;& g_{\mu\nu}\left[\frac{2m_W^2}{v^2} - 6\tilde{\lambda}_6\tilde{\lambda}_6^*\frac{m_W^2}{v^2}\,\frac{v^4}{\tilde{m}_2^4}\right.\\
&- \frac{2m_W^2}{v^2}\left[-\frac{3m_\varphi^2}{v^2} + 6\tilde{\lambda}_6^*\tilde{\lambda}_6\,\frac{v^2}{\tilde{m}_2^2} + \frac{1}{2}\left(\left[21\tilde{\lambda}_1 - 12(\tilde{\lambda}_3+\tilde{\lambda}_4)\right]\tilde{\lambda}_6^*\tilde{\lambda}_6\right.\right.\\
&\left.\left.- \left(6\tilde{\lambda}_5\tilde{\lambda}_6^{*2} + \text{h.c.}\right)\right)\frac{v^4}{\tilde{m}_2^4} + \frac{3}{2}\tilde{\lambda}_6^*\tilde{\lambda}_6\frac{m_\varphi^2 v^2}{\tilde{m}_2^4}\right]\left(\frac{v^2}{s-m_\varphi^2}\right)\\
&\left.- \frac{4m_W^4}{v^4}\left[1 - \tilde{\lambda}_6^\dagger\tilde{\lambda}_6\,\frac{v^4}{\tilde{m}_2^4}\right]\left(\frac{v^2}{t-m_W^2}+\frac{v^2}{u-m_W^2}\right) + \mathcal{O}\left(\frac{v^6}{\tilde{m}_2^6}\right)\right]\end{aligned} \tag{4.4.39}$$

which coincides with the result obtained in the mixing language (4.3.76). Note that the second term in (4.4.39) comes from the modification to the dihiggs di-W boson coupling with respect to its SM value.

The dihiggs to difermion chirality violating scattering amplitude is

$$\mathcal{A}\left(\varphi\varphi \to f_i\overline{f}_j\right) \;=\; -\lambda^f_{\varphi^2 ij} + \frac{g_{\varphi^3}\lambda^f_{\varphi ij}}{s-m_\varphi^2} \tag{4.4.40}$$

Using the EFT couplings (4.4.34) and (4.4.35) we get

$$\begin{aligned}\mathcal{A}\left(\varphi\varphi \to f_i\overline{f}_j\right) \;=\;& \frac{1}{v}\left[\frac{3}{\sqrt{2}}\tilde{\lambda}^f_{2ij}\tilde{\lambda}_6^*\,\frac{v^2}{\tilde{m}_2^2} + \left[\delta_{ij}\frac{m_i^f}{v}\left(-\frac{3m_\varphi^2}{v^2} + 6\tilde{\lambda}_6\tilde{\lambda}_6^*\,\frac{v^2}{\tilde{m}_2^2}\right)\right.\right.\\
&\left.\left.+ \frac{3}{\sqrt{2}}\,\tilde{\lambda}^f_{2ij}\tilde{\lambda}_6^*\,\frac{m_\varphi^2}{\tilde{m}_2^2}\right]\left(\frac{v^2}{s-m_\varphi^2}\right) + \mathcal{O}\left(\frac{v^4}{\tilde{m}_2^4}\right)\right]\end{aligned} \tag{4.4.41}$$

which coincides with the result obtained in the mixing language (4.3.78). Note that this amplitude has a flavor and T violating term both in the long and short distance pieces, inherited from the Yukawas of the heavy doublet $\tilde{\lambda}^f_{2ij}$.

The dihiggs to dihiggs scattering amplitude is

$$\mathcal{A}(\varphi\varphi \to \varphi\varphi) = g_{\varphi^4} - g^2_{\varphi^3}\left(\frac{1}{s-m^2_\varphi} + \frac{1}{t-m^2_\varphi} + \frac{1}{u-m^2_\varphi}\right) \tag{4.4.42}$$

Using the EFT coupling (4.4.35) we get

$$\begin{aligned}\mathcal{A}(\varphi\varphi \to \varphi\varphi) \;=\; & -\frac{3m^2_\varphi}{v^2} + 36\tilde{\lambda}^*_6\tilde{\lambda}_6\left(\frac{v^2}{\tilde{m}^2_2}\right) - \left(\frac{9m^2_\varphi}{v^4} - 36\tilde{\lambda}_1\tilde{\lambda}^*_6\tilde{\lambda}_6\;\frac{v^2}{\tilde{m}^2_2}\right) \\ & \left(\frac{v^2}{s-m^2_\varphi} + \frac{v^2}{t-m^2_\varphi} + \frac{v^2}{u-m^2_\varphi}\right) + \mathcal{O}\left(\frac{v^4}{\tilde{m}^4_2}\right)\end{aligned} \tag{4.4.43}$$

which coincides with the result obtained in the mixing language (4.3.80).

4.5 The EFT of the 2HDM with Glashow-Weinberg conditions

In the SM, the fermion mass matrices and the Higgs Yukawas are aligned in flavor space, so they can be simultaneously diagonalized by performing quark and lepton field redefinitions. As a consequence, there are no flavor changing neutral currents (FCNC). FCNC are experimentally strongly constrained.

In a general 2HDM, it is not possible to simultaneously diagonalize the fermion mass matrices and the Yukawas of both Higgs doublets simultaneously by performing field redefinitions. This leads to FCNC mediated by neutral Higgs states. In the 2HDM, FCNCs can be avoided by imposing the Glashow-Weinberg (GW) conditions [30]. The conditions consist in giving mass to all fermions in a particular representation by allowing them to couple with only one of the two doublets. These conditions can be imposed by discrete symmetries or supersymmetry. The Glashow-Weinberg (GW) conditions are satisfied by four discrete choices of the Yukawa couplings (4.3.1) of the doublets Φ_1, Φ_2

$$\begin{aligned}\text{Type I: } & \lambda^u_1 = \lambda^d_1 = \lambda^\ell_1 = 0 \\ \text{Type II: } & \lambda^u_1 = \lambda^d_2 = \lambda^\ell_2 = 0 \\ \text{Type III: } & \lambda^u_1 = \lambda^d_1 = \lambda^\ell_2 = 0 \\ \text{Type IV: } & \lambda^u_1 = \lambda^d_2 = \lambda^\ell_1 = 0\end{aligned} \tag{4.5.1}$$

In the 2HDM with GW conditions, the ratio of the vevs of the doublets $v_2/v_1 = \tan\beta$ defined in (4.3.5) contains physical information, since it is the ratio of the vevs in the preferred basis of the

Higgs doublets in which one of the conditions (4.5.1) holds. In other words, in a 2HDM with GW conditions, $\tan\beta$ is physical, since it is the rotation angle relating the preferred basis with the Higgs basis (4.3.11) [3].

The objective of this section is to study the types I-IV 2HDM using the EFT presented in section 4.4. GW conditions impose a particular structure on the Yukawas and four fermion operators of the low energy theory, but we impose no other restrictions in addition to one of the conditions (4.5.1), *i.e.*, we consider the Higgs potential to be the most general one at the renormalizable level, and we allow for all the possible T violating phases. Since the GW conditions only refer to the fermionic interactions, we do not present the bosonic interactions in this section. All the bosonic interactions are the ones of a general 2HDM, and were presented in section 4.4. Each type of 2HDM will be presented in sections 4.5.1, 4.5.2, 4.5.3 and 4.5.4. The detailed discussion of T violation in the types I-IV 2HDM is left to section 4.6.

4.5.1 Type I

In the type I 2HDM the Yukawas of the doublet Φ_1 are set to zero

$$\lambda_1^u = \lambda_1^d = \lambda_1^\ell = 0 \tag{4.5.2}$$

so all the fermions get their mass from their coupling to the second doublet Φ_2.

The Yukawas of the doublets in the Higgs basis are obtained by using (4.5.2) in (4.3.17)

$$\tilde{\lambda}_{1ij}^{u,d,\ell} = e^{\frac{i\xi}{2}} \lambda_{2ij}^{u,d,\ell} \sin\beta \tag{4.5.3}$$

$$\tilde{\lambda}_{2ij}^{u,d,\ell} = \lambda_{2ij}^{u,d,\ell} \cos\beta \tag{4.5.4}$$

The fermion mass matrices are related to $\tilde{\lambda}_{1ij}^{u,d,\ell}$ through (4.3.14), so using (4.5.3) we rewrite $\lambda_{2ij}^{u,d,\ell}$ as

$$\lambda_{2ij}^{u,d,\ell} = e^{\frac{-i\xi}{2}} \frac{\sqrt{2} m_{ij}^{u,d,\ell}}{v} \csc\beta \tag{4.5.5}$$

Using (4.5.5) in (4.5.4), we write the Yukawas of the second doublet in the Higgs basis as

$$\tilde{\lambda}_{2ij}^{u,d,\ell} = \sqrt{2} e^{-\frac{i\xi}{2}} \cot\beta \, \frac{m_{ij}^{u,d,\ell}}{v} \tag{4.5.6}$$

[3] In the MSSM, $\tan\beta$ can be defined independently of the Yukawas, since there is a flat direction $H_u = H_d$ which specifies the preferred basis.

Using (4.5.6) in the Higgs Yukawas (4.4.34), we get

$$\begin{aligned}
\lambda^{u,d,\ell}_{\varphi ij} &= \frac{m^{u,d,\ell}_{ij}}{v}\left[1-\tilde{\lambda}^{*}_{6}e^{-i\xi/2}\cot\beta\,\frac{v^2}{\tilde{m}_2^2}+\mathcal{O}\left(\frac{v^4}{\tilde{m}_2^4}\right)\right]\\
v\lambda^{u,d,\ell}_{\varphi^2 ij} &= -\frac{m^{u,d,\ell}_{ij}}{v}\left[3\tilde{\lambda}^{*}_{6}e^{-\frac{i\xi}{2}}\cot\beta\,\frac{v^2}{\tilde{m}_2^2}+\mathcal{O}\left(\frac{v^4}{\tilde{m}_2^4}\right)\right]\\
v^2\lambda^{u,d,\ell}_{\varphi^3 ij} &= -\frac{m^{u,d,\ell}_{ij}}{v}\left[3\tilde{\lambda}^{*}_{6}e^{-\frac{i\xi}{2}}\cot\beta\,\frac{v^2}{\tilde{m}_2^2}+\mathcal{O}\left(\frac{v^4}{\tilde{m}_2^4}\right)\right]
\end{aligned}\tag{4.5.7}$$

Note that using (4.3.54) the Higgs Yukawas can also be expressed in terms of the complex alignment parameter

$$\begin{aligned}
\lambda^{u,d,\ell}_{\varphi ij} &= \delta_{ij}\,\frac{m^{u,d,\ell}_{ij}}{v}\left[1+e^{i\,\mathrm{Arg}(\tilde{\lambda}^{*}_{5})/2}e^{-\frac{i\xi}{2}}\,\Xi\,\cot\beta+\mathcal{O}\left(\Xi^2\right)\right]\\
v\lambda^{u,d,\ell}_{\varphi^2 ij} &= \frac{m^{u,d,\ell}_{ij}}{v}\left[3e^{i\,\mathrm{Arg}(\tilde{\lambda}^{*}_{5})/2}e^{-\frac{i\xi}{2}}\,\Xi\,\cot\beta+\mathcal{O}\left(\Xi^2\right)\right]\\
v^2\lambda^{u,d,\ell}_{\varphi^3 ij} &= \frac{m^{u,d,\ell}_{ij}}{v}\left[3e^{i\,\mathrm{Arg}(\tilde{\lambda}^{*}_{5})/2}e^{-\frac{i\xi}{2}}\,\Xi\,\cot\beta+\mathcal{O}\left(\Xi^2\right)\right]
\end{aligned}\tag{4.5.8}$$

The coefficients of the four fermion operators are found using (4.5.6) in (4.4.17)

$$\begin{aligned}
\Omega^{uu(0)}_{ijmn} &= 2\,\frac{1}{\tilde{m}_2^2}\frac{m^{u}_{ij}m^{u\dagger}_{mn}}{v^2}\cot^2\beta\\
\Omega^{dd(0)}_{ijmn} &= 2\,\frac{1}{\tilde{m}_2^2}\frac{m^{d\dagger}_{ij}m^{d}_{mn}}{v^2}\cot^2\beta\\
\Omega^{\ell\ell(0)}_{ijmn} &= 2\,\frac{1}{\tilde{m}_2^2}\frac{m^{\ell\dagger}_{ij}m^{\ell}_{mn}}{v^2}\cot^2\beta\\
\Omega^{d\ell(0)}_{ijmn} &= 2\,\frac{1}{\tilde{m}_2^2}\frac{m^{d\dagger}_{ij}m^{\ell}_{mn}}{v^2}\cot^2\beta\\
\Omega^{ud(2)}_{ijmn} &= 2\,\frac{1}{\tilde{m}_2^2}\frac{m^{u}_{ij}m^{d\dagger}_{mn}}{v^2}\cot^2\beta\\
\Omega^{u\ell(2)}_{ijmn} &= 2\,\frac{1}{\tilde{m}_2^2}\frac{m^{u}_{ij}m^{\ell\dagger}_{mn}}{v^2}\cot^2\beta
\end{aligned}\tag{4.5.9}$$

In the EFT of a type I 2HDM at effective dimension six, all the modifications to the SM predictions for the fermionic couplings of the Higgs (4.5.7), and all the four fermion operators (4.5.9) vanish in the large $\tan\beta$ limit. The reason is that in this limit, the doublet H_2 that is integrated out is aligned with the doublet Φ_1, which does not couple to fermions. The leading effects on the Higgs Yukawas in this case are of effective dimension eight, and come from kinetic operators in the effective Lagrangian. Alternatively, in the mixing language, at large $\tan\beta$ the only modifications to the Higgs Yukawa couplings come from dilution due to the complex alignment parameter as discussed in section 4.3.2. In this limit, the modifications to the SM predictions for the Higgs Yukawas and Higgs couplings to gauge bosons are identical: both couplings are diluted by $\sqrt{1-|\Xi|^2}$.

We now perform field redefinitions to present the Yukawa couplings and four fermion operators in the quark mass eigenbasis. Without loss of generality, the quark mass matrices in a general flavor basis are given by

$$m^u = U_{Q_u}\,\mathrm{diag}(m_u, m_c, m_t)\,U_{\overline{u}}^\dagger \tag{4.5.10}$$

$$m^{d\dagger} = U_{Q_d}\,\mathrm{diag}(m_d, m_s, m_b)\,U_{\overline{d}}^\dagger \tag{4.5.11}$$

where all the mass eigenvalues are real and non negative. We define the CKM matrix following the conventions of [41]

$$V = U_{Q_u}^T U_{Q_d}^* \tag{4.5.12}$$

The quark mass matrices are diagonalized by the field redefinitions

$$u_i' = u_j\big[U_{Q_u}\big]_{ji} \qquad d_i' = d_j\big[U_{Q_d}\big]_{ji} \qquad \overline{u}_i' = \big[\,U_{\overline{u}}^\dagger\big]_{ij}\overline{u}_j \qquad \overline{d}_i' = \big[\,U_{\overline{d}}^\dagger\big]_{ij}\overline{d}_j \tag{4.5.13}$$

We drop the primes in the quark fields in the mass eigenbasis for the remainder of this chapter. Using the field redefinitions (4.5.13) in the effective lagrangian (4.4.29) and the Yukawas (4.5.7), we find the Yukawas in the quark mass eigenbasis

$$\begin{aligned}
\lambda_{\varphi ij}^{u,d,\ell} &= \delta_{ij}\,\frac{m_i^{u,d,\ell}}{v}\left[1 - \tilde{\lambda}_6^* e^{-i\xi/2}\cot\beta\,\frac{v^2}{\tilde{m}_2^2} + \mathcal{O}\!\left(\frac{v^4}{\tilde{m}_2^4}\right)\right] \\
v\lambda_{\varphi^2 ij}^{u,d,\ell} &= -\delta_{ij}\,\frac{m_i^{u,d,\ell}}{v}\left[3\tilde{\lambda}_6^* e^{-\frac{i\xi}{2}}\cot\beta\,\frac{v^2}{\tilde{m}_2^2} + \mathcal{O}\!\left(\frac{v^4}{\tilde{m}_2^4}\right)\right] \\
v^2\lambda_{\varphi^3 ij}^{u,d,\ell} &= -\delta_{ij}\,\frac{m_i^{u,d,\ell}}{v}\left[3\tilde{\lambda}_6^* e^{-\frac{i\xi}{2}}\cot\beta\,\frac{v^2}{\tilde{m}_2^2} + \mathcal{O}\!\left(\frac{v^4}{\tilde{m}_2^4}\right)\right]
\end{aligned} \tag{4.5.14}$$

Note that the Yukawas in the mass eigenbasis are diagonal, as expected, since the GW conditions ensure that there are no FCNCs.

We define the coefficients of the four fermion operators for the components of the quark and lepton doublets in the quark mass eigenbasis as

$$\begin{aligned}
&\omega_{ijmn}^{uu(0)}\,(u_i\overline{u}_j)(\overline{u}_m^\dagger u_n^\dagger) + \omega_{ijmn}^{uu\pm(0)}\,(d_i\overline{u}_j)(\overline{u}_m^\dagger d_n^\dagger) \\
&+ \omega_{ijmn}^{dd(0)}\,(d_i\overline{d}_j)(\overline{d}_m^\dagger d_n^\dagger) + \omega_{ijmn}^{dd\pm(0)}\,(u_i\overline{d}_j)(\overline{d}_m^\dagger u_n^\dagger) \\
&+ \omega_{ijmn}^{\ell\ell(0)}\,(\nu_i\overline{\ell}_j)(\overline{\ell}_m^\dagger\nu_n^\dagger) + \omega_{ijmn}^{\ell\ell\pm(0)}\,(\ell_i\overline{\ell}_j)(\overline{\ell}_m^\dagger\ell_n^\dagger) \\
&+ \Big[\omega_{ijmn}^{d\ell(0)}\,(d_i\overline{d}_j)(\overline{\ell}_m^\dagger\ell_n^\dagger) + \omega_{ijmn}^{d\ell\pm(0)}\,(u_i\overline{d}_j)(\overline{\ell}_m^\dagger\nu_n^\dagger) \\
&+ \omega_{ijmn}^{ud(2)}\,(u_i\overline{u}_j)(d_m\overline{d}_n) + \omega_{ijmn}^{ud\pm(2)}\,(d_i\overline{u}_j)(u_m\overline{d}_n) \\
&+ \omega_{ijmn}^{u\ell(2)}\,(u_i\overline{u}_j)(\ell_m\overline{\ell}_n) + \omega_{ijmn}^{u\ell\pm(2)}\,(d_i\overline{u}_j)(\nu_m\overline{\ell}_n) + \mathrm{h.c.}\Big]
\end{aligned} \tag{4.5.15}$$

where the $\pm$ superindex indicates four fermion operators generated by integrating out the charged Higgs, while the operators with no $\pm$ superindex are induced by integrating out neutral heavy Higgs states. In the original gauge interaction basis for the quark fields, the coefficients of these two types of operators are identical, as in (4.4.18), due to gauge invariance of the operators (4.4.17). In the quark mass eigenbasis these two types of operators have different coefficients, since the field redefinitions (4.5.13) act differently on the two components of the quark doublet Q. The coefficients in (4.5.15) are found by using (4.5.9) in (4.4.18), and performing the field redefinitions (4.5.13). We get

$$\begin{aligned}
\omega^{uu(0)}_{ijmn} &= 2\,\frac{1}{\tilde{m}_2^2}\delta_{ij}\delta_{mn}\frac{m_i^u m_m^{u*}}{v^2}\cot^2\beta \qquad \omega^{uu\pm(0)}_{ijmn} = 2\,\frac{1}{\tilde{m}_2^2}\frac{V_{ij}^T m_j^u m_m^{u*} V_{mn}^*}{v^2}\cot^2\beta \\
\omega^{dd(0)}_{ijmn} &= 2\,\frac{1}{\tilde{m}_2^2}\delta_{ij}\delta_{mn}\frac{m_i^{d*} m_m^{d}}{v^2}\cot^2\beta \qquad \omega^{dd\pm(0)}_{ijmn} = 2\,\frac{1}{\tilde{m}_2^2}\frac{V_{ij}^* m_j^{d*} m_m^{d} V_{mn}^T}{v^2}\cot^2\beta \\
\omega^{\ell\ell(0)}_{ijmn} &= \omega^{\ell\ell\pm(0)}_{ijmn} = 2\,\frac{1}{\tilde{m}_2^2}\delta_{ij}\delta_{mn}\frac{m_i^{\ell*} m_m^{\ell}}{v^2}\cot^2\beta \\
\omega^{d\ell(0)}_{ijmn} &= 2\,\frac{1}{\tilde{m}_2^2}\delta_{ij}\delta_{mn}\frac{m_i^{d*} m_m^{\ell}}{v^2}\cot^2\beta \qquad \omega^{d\ell\pm(0)}_{ijmn} = 2\,\frac{1}{\tilde{m}_2^2}\delta_{mn}\frac{V_{ij}^* m_j^{d*} m_m^{\ell}}{v^2}\cot^2\beta \\
\omega^{ud(2)}_{ijmn} &= 2\,\frac{1}{\tilde{m}_2^2}\delta_{ij}\delta_{mn}\frac{m_i^{u} m_m^{d*}}{v^2}\cot^2\beta \qquad \omega^{ud\pm(2)}_{ijmn} = -2\,\frac{1}{\tilde{m}_2^2}\frac{V_{ij}^T m_j^u V_{mn}^* m_n^{d*}}{v^2}\cot^2\beta \\
\omega^{u\ell(2)}_{ijmn} &= 2\,\frac{1}{\tilde{m}_2^2}\delta_{ij}\delta_{mn}\frac{m_i^{u} m_m^{\ell*}}{v^2}\cot^2\beta \qquad \omega^{u\ell\pm(2)}_{ijmn} = -2\,\frac{1}{\tilde{m}_2^2}\delta_{mn}\frac{V_{ij}^T m_j^u m_m^{\ell*}}{v^2}\cot^2\beta
\end{aligned} \tag{4.5.16}$$

where no sum over any index is intended. We keep the stars in the quark mass terms for generality, but in the quark mass eigenbasis they are real. All flavor and T violation in the four fermion operators comes from the CKM matrix, and it is induced by integrating out the charged heavy Higgses. We leave a more detailed discussion of T violation for section 4.6.

4.5.2 Type II: $\lambda_1^u = \lambda_2^d = \lambda_2^\ell = 0$

The type II 2HDM is defined by setting $\lambda_1^u = \lambda_2^d = \lambda_2^\ell = 0$. Here we follow closely the calculations and the discussion performed in section 4.5.1, and we omit repeating some of the details. The Yukawa matrices for the Higgs basis doublets are

$$\begin{aligned}
\tilde{\lambda}^u_{1ij} &= e^{\frac{i\xi}{2}}\lambda^u_{2ij}\sin\beta \\
\tilde{\lambda}^{d,\ell}_{1ij} &= e^{-\frac{i\xi}{2}}\lambda^{d,\ell}_{1ij}\cos\beta
\end{aligned} \tag{4.5.17}$$

$$\begin{aligned}\tilde{\lambda}^{u}_{2ij} &= \lambda^{u}_{2ij}\cos\beta \\ \tilde{\lambda}^{d,\ell}_{2ij} &= -e^{-i\xi}\lambda^{d,\ell}_{1ij}\sin\beta \end{aligned} \tag{4.5.18}$$

Using (4.3.14), (4.5.17) and (4.5.18) we rewrite $\lambda^{u,d,\ell}_{2ij}$ in terms of the fermion mass matrices

$$\begin{aligned}\lambda^{u}_{2ij} &= e^{\frac{-i\xi}{2}}\frac{\sqrt{2}m^{u}_{ij}}{v}\csc\beta \\ \lambda^{d,\ell}_{2ij} &= e^{\frac{i\xi}{2}}\frac{\sqrt{2}m^{d,\ell}_{ij}}{v}\sec\beta \end{aligned} \tag{4.5.19}$$

Using (4.5.19) in (4.5.18), the Yukawas for the heavy doublet can be expressed in terms of the quark mass matrices as

$$\begin{aligned}\tilde{\lambda}^{u}_{2ij} &= \sqrt{2}e^{-\frac{i\xi}{2}}\cot\beta\,\frac{m^{u}_{ij}}{v} \\ \tilde{\lambda}^{d,\ell}_{2ij} &= -\sqrt{2}e^{-\frac{i\xi}{2}}\tan\beta\,\frac{m^{d,\ell}_{ij}}{v} \end{aligned} \tag{4.5.20}$$

Using (4.5.20) in (4.4.34), the resulting couplings of the physical Higgs to up type fermions in the low energy theory are

$$\begin{aligned}\lambda^{u}_{\varphi ij} &= \frac{m^{u}_{ij}}{v}\left[1-\tilde{\lambda}^{*}_{6}e^{-i\xi/2}\cot\beta\,\frac{v^2}{\tilde{m}^2_2}+\mathcal{O}\left(\frac{v^4}{\tilde{m}^4_2}\right)\right] \\ v\lambda^{u}_{\varphi^2 ij} &= -\frac{m^{u}_{ij}}{v}\left[3\tilde{\lambda}^{*}_{6}e^{-\frac{i\xi}{2}}\cot\beta\,\frac{v^2}{\tilde{m}^2_2}+\mathcal{O}\left(\frac{v^4}{\tilde{m}^4_2}\right)\right] \\ v^2\lambda^{u}_{\varphi^3 ij} &= -\frac{m^{u}_{ij}}{v}\left[3\tilde{\lambda}^{*}_{6}e^{-\frac{i\xi}{2}}\cot\beta\,\frac{v^2}{\tilde{m}^2_2}+\mathcal{O}\left(\frac{v^4}{\tilde{m}^4_2}\right)\right] \end{aligned} \tag{4.5.21}$$

while down type quark Yukawas are

$$\begin{aligned}\lambda^{d,\ell}_{\varphi ij} &= \frac{m^{d,\ell}_{ij}}{v}\left[1+\tilde{\lambda}^{*}_{6}e^{-i\xi/2}\tan\beta\,\frac{v^2}{\tilde{m}^2_2}+\mathcal{O}\left(\frac{v^4}{\tilde{m}^4_2}\right)\right] \\ v\lambda^{d,\ell}_{\varphi^2 ij} &= \frac{m^{d,\ell}_{ij}}{v}\left[3\tilde{\lambda}^{*}_{6}e^{-\frac{i\xi}{2}}\tan\beta\,\frac{v^2}{\tilde{m}^2_2}+\mathcal{O}\left(\frac{v^4}{\tilde{m}^4_2}\right)\right] \\ v^2\lambda^{d,\ell}_{\varphi^3 ij} &= \frac{m^{d,\ell}_{ij}}{v}\left[3\tilde{\lambda}^{*}_{6}e^{-\frac{i\xi}{2}}\tan\beta\,\frac{v^2}{\tilde{m}^2_2}+\mathcal{O}\left(\frac{v^4}{\tilde{m}^4_2}\right)\right] \end{aligned} \tag{4.5.22}$$

Note that using (4.3.54) the Higgs Yukawas can be expressed in terms of the complex alignment parameter

$$\begin{aligned}\lambda^{u}_{\varphi ij} &= \delta_{ij}\frac{m^{u}_{ij}}{v}\left[1+e^{i\mathrm{Arg}(\tilde{\lambda}^{*}_{5})/2}e^{-\frac{i\xi}{2}}\,\Xi\,\cot\beta+\mathcal{O}\left(\Xi^2\right)\right] \\ v\lambda^{u}_{\varphi^2 ij} &= \frac{m^{u}_{ij}}{v}\left[3e^{i\mathrm{Arg}(\tilde{\lambda}^{*}_{5})/2}e^{-\frac{i\xi}{2}}\,\Xi\,\cot\beta+\mathcal{O}\left(\Xi^2\right)\right] \\ v^2\lambda^{u}_{\varphi^3 ij} &= \frac{m^{u}_{ij}}{v}\left[3e^{i\mathrm{Arg}(\tilde{\lambda}^{*}_{5})/2}e^{-\frac{i\xi}{2}}\,\Xi\,\cot\beta+\mathcal{O}\left(\Xi^2\right)\right] \end{aligned} \tag{4.5.23}$$

$$\begin{aligned}
\lambda^{d,\ell}_{\varphi ij} &= \delta_{ij}\,\frac{m^{d,\ell}_{ij}}{v}\left[1 - e^{i\,\mathrm{Arg}(\tilde{\lambda}_5^*)/2} e^{-\frac{i\xi}{2}}\,\Xi\,\tan\beta + \mathcal{O}\Big(\Xi^2\Big)\right] \\
v\lambda^{d,\ell}_{\varphi^2 ij} &= -\frac{m^{d,\ell}_{ij}}{v}\left[3e^{i\,\mathrm{Arg}(\tilde{\lambda}_5^*)/2} e^{-\frac{i\xi}{2}}\,\Xi\,\tan\beta + \mathcal{O}\Big(\Xi^2\Big)\right] \\
v^2\lambda^{d,\ell}_{\varphi^3 ij} &= -\frac{m^{d,\ell}_{ij}}{v}\left[3e^{i\,\mathrm{Arg}(\tilde{\lambda}_5^*)/2} e^{-\frac{i\xi}{2}}\,\Xi\,\tan\beta + \mathcal{O}\Big(\Xi^2\Big)\right]
\end{aligned} \tag{4.5.24}$$

In the EFT the type II 2HDM at large $\tan\beta$ the the only modifications to the up type Higgs Yukawas are subleading effects coming from dilution due to the complex alignment parameter by a factor $\sqrt{1-|\Xi|^2}$ as discussed in section 4.3.2. In this limit, the modifications to the SM predictions for the up type Higgs Yukawas and Higgs couplings to gauge bosons are identical: both couplings are diluted by $\sqrt{1-|\Xi|^2}$. In this limit down type Yukawas suffer the largest deviations with respect to their SM values, since they are modified at effective dimension six, and the modifications are enhanced by $\tan\beta$.

The coefficients of the four fermion interactions (4.4.17) are

$$\begin{aligned}
\Omega^{uu(0)}_{ijmn} &= 2\,\frac{1}{\tilde{m}_2^2}\,\frac{m^u_{ij} m^{u\dagger}_{mn}}{v^2}\cot^2\beta \\
\Omega^{dd(0)}_{ijmn} &= 2\,\frac{1}{\tilde{m}_2^2}\,\frac{m^{d\dagger}_{ij} m^{d}_{mn}}{v^2}\tan^2\beta \\
\Omega^{\ell\ell(0)}_{ijmn} &= 2\,\frac{1}{\tilde{m}_2^2}\,\frac{m^{\ell\dagger}_{ij} m^{\ell}_{mn}}{v^2}\tan^2\beta \\
\Omega^{d\ell(0)}_{ijmn} &= 2\,\frac{1}{\tilde{m}_2^2}\,\frac{m^{d\dagger}_{ij} m^{\ell}_{mn}}{v^2}\tan^2\beta \\
\Omega^{ud(2)}_{ijmn} &= -2\,\frac{1}{\tilde{m}_2^2}\,\frac{m^{u}_{ij} m^{d\dagger}_{mn}}{v^2} \\
\Omega^{u\ell(2)}_{ijmn} &= -2\,\frac{1}{\tilde{m}_2^2}\,\frac{m^{u}_{ij} m^{\ell\dagger}_{mn}}{v^2}
\end{aligned} \tag{4.5.25}$$

We now rotate to the quark mass eigenbasis. The up type Yukawas are

$$\begin{aligned}
\lambda^{u}_{\varphi ij} &= \delta_{ij}\,\frac{m^{u}_{i}}{v}\left[1 - \tilde{\lambda}_6^* e^{-i\xi/2}\cot\beta\,\frac{v^2}{\tilde{m}_2^2} + \mathcal{O}\left(\frac{v^4}{\tilde{m}_2^4}\right)\right] \\
v\lambda^{u}_{\varphi^2 ij} &= -\delta_{ij}\,\frac{m^{u}_{i}}{v}\left[3\tilde{\lambda}_6^* e^{-\frac{i\xi}{2}}\cot\beta\,\frac{v^2}{\tilde{m}_2^2} + \mathcal{O}\left(\frac{v^4}{\tilde{m}_2^4}\right)\right] \\
v^2\lambda^{u}_{\varphi^3 ij} &= -\delta_{ij}\,\frac{m^{u}_{i}}{v}\left[3\tilde{\lambda}_6^* e^{-\frac{i\xi}{2}}\cot\beta\,\frac{v^2}{\tilde{m}_2^2} + \mathcal{O}\left(\frac{v^4}{\tilde{m}_2^4}\right)\right]
\end{aligned} \tag{4.5.26}$$

while the down type Yukawas are

$$\begin{aligned}
\lambda^{d,\ell}_{\varphi ij} &= \delta_{ij}\,\frac{m^{d,\ell}_{i}}{v}\left[1 + \tilde{\lambda}_6^* e^{-i\xi/2}\tan\beta\,\frac{v^2}{\tilde{m}_2^2} + \mathcal{O}\left(\frac{v^4}{\tilde{m}_2^4}\right)\right] \\
v\lambda^{d,\ell}_{\varphi^2 ij} &= \delta_{ij}\,\frac{m^{d,\ell}_{i}}{v}\left[3\tilde{\lambda}_6^* e^{-\frac{i\xi}{2}}\tan\beta\,\frac{v^2}{\tilde{m}_2^2} + \mathcal{O}\left(\frac{v^4}{\tilde{m}_2^4}\right)\right] \\
v^2\lambda^{d,\ell}_{\varphi^3 ij} &= \delta_{ij}\,\frac{m^{d,\ell}_{i}}{v}\left[3\tilde{\lambda}_6^* e^{-\frac{i\xi}{2}}\tan\beta\,\frac{v^2}{\tilde{m}_2^2} + \mathcal{O}\left(\frac{v^4}{\tilde{m}_2^4}\right)\right]
\end{aligned} \tag{4.5.27}$$

Note that in a type II 2HDM $\tan\beta$ can be measured from comparing the deviations of up type Yukawas versus down type Yukawas from their SM values. Using (4.5.26) and (4.5.27) we get

$$\tan^2\beta = \left|\frac{m_i^u}{m_i^{d,\ell}}\left(\frac{\lambda_{\varphi ij}^{d,\ell} - m_i^{d,\ell}/v}{\lambda_{\varphi ij}^{u} - m_i^{u}/v}\right)\right| + \mathcal{O}\left(\frac{v^2}{\tilde{m}_2^2}\right) \tag{4.5.28}$$

The four fermion interactions in the quark mass eigenbasis are defined as in (4.5.15). They are given by

$$\begin{aligned}
\omega_{ijmn}^{uu(0)} &= 2\,\frac{1}{\tilde{m}_2^2}\delta_{ij}\delta_{mn}\frac{m_i^u m_m^{u*}}{v^2}\cot^2\beta \qquad \omega_{ijmn}^{uu\pm(0)} = 2\,\frac{1}{\tilde{m}_2^2}\frac{V_{ij}^T m_j^u m_m^{u*} V_{mn}^*}{v^2}\cot^2\beta \\
\omega_{ijmn}^{dd(0)} &= 2\,\frac{1}{\tilde{m}_2^2}\delta_{ij}\delta_{mn}\frac{m_i^{d*} m_m^{d}}{v^2}\tan^2\beta \qquad \omega_{ijmn}^{dd\pm(0)} = 2\,\frac{1}{\tilde{m}_2^2}\frac{V_{ij}^* m_j^{d*} m_m^{d} V_{mn}^T}{v^2}\tan^2\beta \\
\omega_{ijmn}^{\ell\ell(0)} &= \omega_{ijmn}^{\ell\ell\pm(0)} = 2\,\frac{1}{\tilde{m}_2^2}\delta_{ij}\delta_{mn}\frac{m_i^{\ell*} m_m^{\ell}}{v^2}\tan^2\beta \\
\omega_{ijmn}^{d\ell(0)} &= 2\,\frac{1}{\tilde{m}_2^2}\delta_{ij}\delta_{mn}\frac{m_i^{d*} m_m^{\ell}}{v^2}\tan^2\beta \qquad \omega_{ijmn}^{d\ell\pm(0)} = 2\,\frac{1}{\tilde{m}_2^2}\delta_{mn}\frac{V_{ij}^* m_j^{d*} m_m^{\ell}}{v^2}\tan^2\beta \\
\omega_{ijmn}^{ud(2)} &= -2\,\frac{1}{\tilde{m}_2^2}\delta_{ij}\delta_{mn}\frac{m_i^u m_m^{d*}}{v^2} \qquad \omega_{ijmn}^{ud\pm(2)} = 2\,\frac{1}{\tilde{m}_2^2}\frac{V_{ij}^T m_j^u V_{mn}^* m_n^{d*}}{v^2} \\
\omega_{ijmn}^{u\ell(2)} &= -2\,\frac{1}{\tilde{m}_2^2}\delta_{ij}\delta_{mn}\frac{m_i^u m_m^{\ell*}}{v^2} \qquad \omega_{ijmn}^{u\ell\pm(2)} = 2\,\frac{1}{\tilde{m}_2^2}\delta_{mn}\frac{V_{ij}^T m_j^u m_m^{\ell*}}{v^2}
\end{aligned} \tag{4.5.29}$$

where $\pm$ superindex indicates four fermion operators generated by charged Higgs exchange and V is the CKM matrix. Note that some of the four fermion operators in (4.5.29) are $\tan\beta$ independent.

4.5.3 Type III

The type III 2HDM is defined by setting $\lambda_1^u = \lambda_1^d = \lambda_2^\ell = 0$. The Yukawa matrices for the Higgs basis doublets are

$$\begin{aligned}
\tilde{\lambda}_{1ij}^{u,d} &= e^{\frac{i\xi}{2}}\lambda_{2ij}^{u,d}\sin\beta \\
\tilde{\lambda}_{1ij}^{\ell} &= e^{-\frac{i\xi}{2}}\lambda_{1ij}^{\ell}\cos\beta
\end{aligned} \tag{4.5.30}$$

$$\begin{aligned}
\tilde{\lambda}_{2ij}^{u,d} &= \lambda_{2ij}^{u,d}\cos\beta \\
\tilde{\lambda}_{2ij}^{\ell} &= -e^{-i\xi}\lambda_{1ij}^{\ell}\sin\beta
\end{aligned} \tag{4.5.31}$$

Using (4.3.14), (4.5.30) and (4.5.31) we rewrite $\lambda_{2ij}^{u,d,\ell}$ in terms of the fermion mass matrices

$$\begin{aligned}
\lambda_{2ij}^{u,d} &= e^{\frac{-i\xi}{2}}\frac{\sqrt{2}m_{ij}^{u,d}}{v}\csc\beta \\
\lambda_{2ij}^{\ell} &= e^{\frac{i\xi}{2}}\frac{\sqrt{2}m_{ij}^{\ell}}{v}\sec\beta
\end{aligned} \tag{4.5.32}$$

Using (4.5.31) and (4.5.32) the Yukawas for the heavy doublet can be expressed in terms of the quark mass matrices as

$$\begin{aligned}\tilde{\lambda}^{u,d}_{2ij} &= \sqrt{2}e^{-\frac{i\xi}{2}}\cot\beta\,\frac{m^{u,d}_{ij}}{v}\\ \tilde{\lambda}^{\ell}_{2ij} &= -\sqrt{2}e^{-\frac{i\xi}{2}}\tan\beta\,\frac{m^{\ell}_{ij}}{v}\end{aligned} \tag{4.5.33}$$

Using (4.5.33) in (4.4.34), the resulting couplings of the physical Higgs to up and down type quarks in the low energy theory are

$$\begin{aligned}\lambda^{u,d}_{\varphi ij} &= \frac{m^{u,d}_{ij}}{v}\left[1-\tilde{\lambda}^{*}_{6}e^{-i\xi/2}\cot\beta\,\frac{v^2}{\tilde{m}_2^2}+\mathcal{O}\left(\frac{v^4}{\tilde{m}_2^4}\right)\right]\\ v\lambda^{u,d}_{\varphi^2 ij} &= -\frac{m^{u,d}_{ij}}{v}\left[3\tilde{\lambda}^{*}_{6}e^{-\frac{i\xi}{2}}\cot\beta\,\frac{v^2}{\tilde{m}_2^2}+\mathcal{O}\left(\frac{v^4}{\tilde{m}_2^4}\right)\right]\\ v^2\lambda^{u,d}_{\varphi^3 ij} &= -\frac{m^{u,d}_{ij}}{v}\left[3\tilde{\lambda}^{*}_{6}e^{-\frac{i\xi}{2}}\cot\beta\,\frac{v^2}{\tilde{m}_2^2}+\mathcal{O}\left(\frac{v^4}{\tilde{m}_2^4}\right)\right]\end{aligned} \tag{4.5.34}$$

while the lepton Yukawas are

$$\begin{aligned}\lambda^{\ell}_{\varphi ij} &= \frac{m^{\ell}_{ij}}{v}\left[1+\tilde{\lambda}^{*}_{6}e^{-i\xi/2}\tan\beta\,\frac{v^2}{\tilde{m}_2^2}+\mathcal{O}\left(\frac{v^4}{\tilde{m}_2^4}\right)\right]\\ v\lambda^{\ell}_{\varphi^2 ij} &= \frac{m^{\ell}_{ij}}{v}\left[3\tilde{\lambda}^{*}_{6}e^{-\frac{i\xi}{2}}\tan\beta\,\frac{v^2}{\tilde{m}_2^2}+\mathcal{O}\left(\frac{v^4}{\tilde{m}_2^4}\right)\right]\\ v^2\lambda^{\ell}_{\varphi^3 ij} &= \frac{m^{\ell}_{ij}}{v}\left[3\tilde{\lambda}^{*}_{6}e^{-\frac{i\xi}{2}}\tan\beta\,\frac{v^2}{\tilde{m}_2^2}+\mathcal{O}\left(\frac{v^4}{\tilde{m}_2^4}\right)\right]\end{aligned} \tag{4.5.35}$$

The four fermion interactions (4.4.17) are

$$\begin{aligned}\Omega^{uu(0)}_{ijmn} &= 2\,\frac{1}{\tilde{m}_2^2}\frac{m^{u}_{ij}m^{u\dagger}_{mn}}{v^2}\cot^2\beta\\ \Omega^{dd(0)}_{ijmn} &= 2\,\frac{1}{\tilde{m}_2^2}\frac{m^{d\dagger}_{ij}m^{d}_{mn}}{v^2}\cot^2\beta\\ \Omega^{\ell\ell(0)}_{ijmn} &= 2\,\frac{1}{\tilde{m}_2^2}\frac{m^{\ell\dagger}_{ij}m^{\ell}_{mn}}{v^2}\tan^2\beta\\ \Omega^{d\ell(0)}_{ijmn} &= -2\,\frac{1}{\tilde{m}_2^2}\frac{m^{d\dagger}_{ij}m^{\ell}_{mn}}{v^2}\\ \Omega^{ud(2)}_{ijmn} &= 2\,\frac{1}{\tilde{m}_2^2}\frac{m^{u}_{ij}m^{d\dagger}_{mn}}{v^2}\cot^2\beta\\ \Omega^{u\ell(2)}_{ijmn} &= -2\,\frac{1}{\tilde{m}_2^2}\frac{m^{u}_{ij}m^{\ell\dagger}_{mn}}{v^2}\end{aligned} \tag{4.5.36}$$

We now rotate to the quark mass eigenbasis by using (4.5.13). The Yukawas are again diagonal

in flavor space, and given by

$$\begin{aligned}
\lambda^{u,d}_{\varphi ij} &= \delta_{ij}\,\frac{m^{u,d}_i}{v}\left[1-\tilde{\lambda}^*_6 e^{-i\xi/2}\cot\beta\,\frac{v^2}{\tilde{m}_2^2}+\mathcal{O}\left(\frac{v^4}{\tilde{m}_2^4}\right)\right]\\
v\lambda^{u,d}_{\varphi^2 ij} &= -\delta_{ij}\,\frac{m^{u,d}_i}{v}\left[3\tilde{\lambda}^*_6 e^{-\frac{i\xi}{2}}\cot\beta\,\frac{v^2}{\tilde{m}_2^2}+\mathcal{O}\left(\frac{v^4}{\tilde{m}_2^4}\right)\right]\\
v^2\lambda^{u,d}_{\varphi^3 ij} &= -\delta_{ij}\,\frac{m^{u,d}_i}{v}\left[3\tilde{\lambda}^*_6 e^{-\frac{i\xi}{2}}\cot\beta\,\frac{v^2}{\tilde{m}_2^2}+\mathcal{O}\left(\frac{v^4}{\tilde{m}_2^4}\right)\right]
\end{aligned}\tag{4.5.37}$$

$$\begin{aligned}
\lambda^{\ell}_{\varphi ij} &= \delta_{ij}\,\frac{m^{\ell}_i}{v}\left[1+\tilde{\lambda}^*_6 e^{-i\xi/2}\tan\beta\,\frac{v^2}{\tilde{m}_2^2}+\mathcal{O}\left(\frac{v^4}{\tilde{m}_2^4}\right)\right]\\
v\lambda^{\ell}_{\varphi^2 ij} &= \delta_{ij}\,\frac{m^{\ell}_i}{v}\left[3\tilde{\lambda}^*_6 e^{-\frac{i\xi}{2}}\tan\beta\,\frac{v^2}{\tilde{m}_2^2}+\mathcal{O}\left(\frac{v^4}{\tilde{m}_2^4}\right)\right]\\
v^2\lambda^{\ell}_{\varphi^3 ij} &= \delta_{ij}\,\frac{m^{\ell}_i}{v}\left[3\tilde{\lambda}^*_6 e^{-\frac{i\xi}{2}}\tan\beta\,\frac{v^2}{\tilde{m}_2^2}+\mathcal{O}\left(\frac{v^4}{\tilde{m}_2^4}\right)\right]
\end{aligned}\tag{4.5.38}$$

The four fermion interactions in the quark mass eigenbasis are defined as in (4.5.15). They are given by

$$\begin{aligned}
&\omega^{uu(0)}_{ijmn} = 2\,\frac{1}{\tilde{m}_2^2}\delta_{ij}\delta_{mn}\frac{m^u_i m^{u*}_m}{v^2}\cot^2\beta \qquad \omega^{uu\pm(0)}_{ijmn} = 2\,\frac{1}{\tilde{m}_2^2}\frac{V^T_{ij}m^u_j m^{u*}_m V^*_{mn}}{v^2}\cot^2\beta\\
&\omega^{dd(0)}_{ijmn} = 2\,\frac{1}{\tilde{m}_2^2}\delta_{ij}\delta_{mn}\frac{m^{d*}_i m^d_m}{v^2}\cot^2\beta \qquad \omega^{dd\pm(0)}_{ijmn} = 2\,\frac{1}{\tilde{m}_2^2}\frac{V^*_{ij}m^{d*}_j m^d_m V^T_{mn}}{v^2}\cot^2\beta\\
&\omega^{\ell\ell(0)}_{ijmn} = \omega^{\ell\ell\pm(0)}_{ijmn} = 2\,\frac{1}{\tilde{m}_2^2}\delta_{ij}\delta_{mn}\frac{m^{\ell*}_i m^{\ell}_m}{v^2}\tan^2\beta\\
&\omega^{d\ell(0)}_{ijmn} = -2\,\frac{1}{\tilde{m}_2^2}\delta_{ij}\delta_{mn}\frac{m^{d*}_i m^{\ell}_m}{v^2} \qquad \omega^{d\ell\pm(0)}_{ijmn} = -2\,\frac{1}{\tilde{m}_2^2}\delta_{mn}\frac{V^*_{ij}m^{d*}_j m^{\ell}_m}{v^2}\\
&\omega^{ud(2)}_{ijmn} = -2\,\frac{1}{\tilde{m}_2^2}\delta_{ij}\delta_{mn}\frac{m^u_i m^{d*}_m}{v^2}\cot^2\beta \qquad \omega^{ud\pm(2)}_{ijmn} = 2\,\frac{1}{\tilde{m}_2^2}\frac{V^T_{ij}m^u_j V^*_{mn}m^{d*}_n}{v^2}\cot^2\beta\\
&\omega^{u\ell(2)}_{ijmn} = -2\,\frac{1}{\tilde{m}_2^2}\delta_{ij}\delta_{mn}\frac{m^u_i m^{\ell*}_m}{v^2} \qquad \omega^{u\ell\pm(2)}_{ijmn} = 2\,\frac{1}{\tilde{m}_2^2}\delta_{mn}\frac{V^T_{ij}m^u_j m^{\ell*}_m}{v^2}
\end{aligned}\tag{4.5.39}$$

where $\pm$ superindex indicates four fermion operators generated by charged Higgs exchange and V is the CKM matrix.

4.5.4 Type IV

The type IV 2HDM is defined by setting $\lambda^u_1 = \lambda^d_2 = \lambda^\ell_1 = 0$. The Yukawa matrices for the Higgs basis doublets are

$$\begin{aligned}
\tilde{\lambda}^{u,\ell}_{1ij} &= e^{\frac{i\xi}{2}}\lambda^{u,\ell}_{2ij}\sin\beta\\
\tilde{\lambda}^{d}_{1ij} &= e^{-\frac{i\xi}{2}}\lambda^{d}_{1ij}\cos\beta
\end{aligned}\tag{4.5.40}$$

$$\begin{aligned}
\tilde{\lambda}^{u,\ell}_{2ij} &= \lambda^{u,\ell}_{2ij}\cos\beta\\
\tilde{\lambda}^{d}_{2ij} &= -e^{-i\xi}\lambda^{d}_{1ij}\sin\beta
\end{aligned}\tag{4.5.41}$$

Using (4.3.14), (4.5.40) and (4.5.41) we rewrite $\lambda_{2ij}^{u,d,\ell}$ in terms of the fermion mass matrices

$$\begin{aligned}\lambda_{2ij}^{u,d} &= e^{\frac{-i\xi}{2}}\frac{\sqrt{2}m_{ij}^{u,d}}{v}\csc\beta\\ \lambda_{2ij}^{\ell} &= e^{\frac{i\xi}{2}}\frac{\sqrt{2}m_{ij}^{\ell}}{v}\sec\beta\end{aligned}\tag{4.5.42}$$

Using (4.5.41) and (4.5.42), the Yukawas for the heavy doublet can be expressed in terms of the quark mass matrices as

$$\begin{aligned}\tilde{\lambda}_{2ij}^{u,d} &= \sqrt{2}e^{-\frac{i\xi}{2}}\cot\beta\,\frac{m_{ij}^{u,d}}{v}\\ \tilde{\lambda}_{2ij}^{\ell} &= -\sqrt{2}e^{-\frac{i\xi}{2}}\tan\beta\,\frac{m_{ij}^{\ell}}{v}\end{aligned}\tag{4.5.43}$$

Using (4.5.43) in (4.4.34), the resulting couplings of the physical Higgs to up type quarks and leptons in the low energy theory are

$$\begin{aligned}\lambda_{\varphi ij}^{u,\ell} &= \frac{m_{ij}^{u,\ell}}{v}\left[1-\tilde{\lambda}_6^* e^{-i\xi/2}\cot\beta\,\frac{v^2}{\tilde{m}_2^2}+\mathcal{O}\left(\frac{v^4}{\tilde{m}_2^4}\right)\right]\\ v\lambda_{\varphi^2 ij}^{u,\ell} &= -\frac{m_{ij}^{u,\ell}}{v}\left[3\tilde{\lambda}_6^* e^{-\frac{i\xi}{2}}\cot\beta\,\frac{v^2}{\tilde{m}_2^2}+\mathcal{O}\left(\frac{v^4}{\tilde{m}_2^4}\right)\right]\\ v^2\lambda_{\varphi^3 ij}^{u,\ell} &= -\frac{m_{ij}^{u,\ell}}{v}\left[3\tilde{\lambda}_6^* e^{-\frac{i\xi}{2}}\cot\beta\,\frac{v^2}{\tilde{m}_2^2}+\mathcal{O}\left(\frac{v^4}{\tilde{m}_2^4}\right)\right]\end{aligned}\tag{4.5.44}$$

while the down type quark Yukawas are

$$\begin{aligned}\lambda_{\varphi ij}^{d} &= \frac{m_{ij}^{d}}{v}\left[1+\tilde{\lambda}_6^* e^{-i\xi/2}\tan\beta\,\frac{v^2}{\tilde{m}_2^2}+\mathcal{O}\left(\frac{v^4}{\tilde{m}_2^4}\right)\right]\\ v\lambda_{\varphi^2 ij}^{d} &= \frac{m_{ij}^{d}}{v}\left[3\tilde{\lambda}_6^* e^{-\frac{i\xi}{2}}\tan\beta\,\frac{v^2}{\tilde{m}_2^2}+\mathcal{O}\left(\frac{v^4}{\tilde{m}_2^4}\right)\right]\\ v^2\lambda_{\varphi^3 ij}^{d} &= \frac{m_{ij}^{d}}{v}\left[3\tilde{\lambda}_6^* e^{-\frac{i\xi}{2}}\tan\beta\,\frac{v^2}{\tilde{m}_2^2}+\mathcal{O}\left(\frac{v^4}{\tilde{m}_2^4}\right)\right]\end{aligned}\tag{4.5.45}$$

The four fermion interactions (4.4.17) are

$$\begin{aligned}\Omega_{ijmn}^{uu(0)} &= 2\,\frac{1}{\tilde{m}_2^2}\frac{m_{ij}^{u}m_{mn}^{u\dagger}}{v^2}\cot^2\beta\\ \Omega_{ijmn}^{dd(0)} &= 2\,\frac{1}{\tilde{m}_2^2}\frac{m_{ij}^{d\dagger}m_{mn}^{d}}{v^2}\tan^2\beta\\ \Omega_{ijmn}^{\ell\ell(0)} &= 2\,\frac{1}{\tilde{m}_2^2}\frac{m_{ij}^{\ell\dagger}m_{mn}^{\ell}}{v^2}\cot^2\beta\\ \Omega_{ijmn}^{d\ell(0)} &= -2\,\frac{1}{\tilde{m}_2^2}\frac{m_{ij}^{d\dagger}m_{mn}^{\ell}}{v^2}\\ \Omega_{ijmn}^{ud(2)} &= -2\,\frac{1}{\tilde{m}_2^2}\frac{m_{ij}^{u}m_{mn}^{d\dagger}}{v^2}\\ \Omega_{ijmn}^{u\ell(2)} &= 2\,\frac{1}{\tilde{m}_2^2}\frac{m_{ij}^{u}m_{mn}^{\ell\dagger}}{v^2}\cot^2\beta\end{aligned}\tag{4.5.46}$$

We now rotate to the quark mass eigenbasis by using (4.5.13). The Yukawas are again diagonal in flavor space. The up type and lepton Yukawas are

$$\begin{aligned}
\lambda^{u,\ell}_{\varphi ij} &= \delta_{ij}\,\frac{m^{u,\ell}_i}{v}\left[1-\tilde{\lambda}^*_6 e^{-i\xi/2}\cot\beta\,\frac{v^2}{\tilde{m}_2^2}+\mathcal{O}\left(\frac{v^4}{\tilde{m}_2^4}\right)\right]\\
v\lambda^{u,\ell}_{\varphi^2 ij} &= -\delta_{ij}\,\frac{m^{u,\ell}_i}{v}\left[3\tilde{\lambda}^*_6 e^{-\frac{i\xi}{2}}\cot\beta\,\frac{v^2}{\tilde{m}_2^2}+\mathcal{O}\left(\frac{v^4}{\tilde{m}_2^4}\right)\right]\\
v^2\lambda^{u,\ell}_{\varphi^3 ij} &= -\delta_{ij}\,\frac{m^{u,\ell}_i}{v}\left[3\tilde{\lambda}^*_6 e^{-\frac{i\xi}{2}}\cot\beta\,\frac{v^2}{\tilde{m}_2^2}+\mathcal{O}\left(\frac{v^4}{\tilde{m}_2^4}\right)\right]
\end{aligned}\tag{4.5.47}$$

while the down quark Yukawas are

$$\begin{aligned}
\lambda^{d}_{\varphi ij} &= \delta_{ij}\,\frac{m^{d}_i}{v}\left[1+\tilde{\lambda}^*_6 e^{-i\xi/2}\tan\beta\,\frac{v^2}{\tilde{m}_2^2}+\mathcal{O}\left(\frac{v^4}{\tilde{m}_2^4}\right)\right]\\
v\lambda^{d}_{\varphi^2 ij} &= \delta_{ij}\,\frac{m^{d}_i}{v}\left[3\tilde{\lambda}^*_6 e^{-\frac{i\xi}{2}}\tan\beta\,\frac{v^2}{\tilde{m}_2^2}+\mathcal{O}\left(\frac{v^4}{\tilde{m}_2^4}\right)\right]\\
v^2\lambda^{d}_{\varphi^3 ij} &= \delta_{ij}\,\frac{m^{d}_i}{v}\left[3\tilde{\lambda}^*_6 e^{-\frac{i\xi}{2}}\tan\beta\,\frac{v^2}{\tilde{m}_2^2}+\mathcal{O}\left(\frac{v^4}{\tilde{m}_2^4}\right)\right]
\end{aligned}\tag{4.5.48}$$

The four fermion interactions in the quark mass eigenbasis are defined as in (4.5.15). They are given by

$$\begin{aligned}
&\omega^{uu(0)}_{ijmn} = 2\,\frac{1}{\tilde{m}_2^2}\delta_{ij}\delta_{mn}\frac{m^u_i m^{u*}_m}{v^2}\cot^2\beta \qquad \omega^{uu\pm(0)}_{ijmn} = 2\,\frac{1}{\tilde{m}_2^2}\frac{V^T_{ij}m^u_j m^{u*}_m V^*_{mn}}{v^2}\cot^2\beta\\
&\omega^{dd(0)}_{ijmn} = 2\,\frac{1}{\tilde{m}_2^2}\delta_{ij}\delta_{mn}\frac{m^{d*}_i m^{d}_m}{v^2}\tan^2\beta \qquad \omega^{dd\pm(0)}_{ijmn} = 2\,\frac{1}{\tilde{m}_2^2}\frac{V^*_{ij}m^{d*}_j m^{d}_m V^T_{mn}}{v^2}\tan^2\beta\\
&\omega^{\ell\ell(0)}_{ijmn} = \omega^{\ell\ell\pm(0)}_{ijmn} = 2\,\frac{1}{\tilde{m}_2^2}\delta_{ij}\delta_{mn}\frac{m^{\ell*}_i m^{\ell}_m}{v^2}\cot^2\beta\\
&\omega^{d\ell(0)}_{ijmn} = -2\,\frac{1}{\tilde{m}_2^2}\delta_{ij}\delta_{mn}\frac{m^{d*}_i m^{\ell}_m}{v^2} \qquad \omega^{d\ell\pm(0)}_{ijmn} = -2\,\frac{1}{\tilde{m}_2^2}\delta_{mn}\frac{V^*_{ij}m^{d*}_j m^{\ell}_m}{v^2}\\
&\omega^{ud(2)}_{ijmn} = -2\,\frac{1}{\tilde{m}_2^2}\delta_{ij}\delta_{mn}\frac{m^{u}_i m^{d*}_m}{v^2} \qquad \omega^{ud\pm(2)}_{ijmn} = 2\,\frac{1}{\tilde{m}_2^2}\frac{V^T_{ij}m^u_j V^*_{mn} m^{d*}_n}{v^2}\\
&\omega^{u\ell(2)}_{ijmn} = 2\,\frac{1}{\tilde{m}_2^2}\delta_{ij}\delta_{mn}\frac{m^{u}_i m^{\ell*}_m}{v^2}\cot^2\beta \qquad \omega^{u\ell\pm(2)}_{ijmn} = -2\,\frac{1}{\tilde{m}_2^2}\delta_{mn}\frac{V^T_{ij}m^u_j m^{\ell*}_m}{v^2}\cot^2\beta
\end{aligned}\tag{4.5.49}$$

where $\pm$ superindex indicates four fermion operators generated by charged Higgs exchange and V is the CKM matrix.

4.6 T violation in types I-IV 2HDM

In this section we discuss T violation in the types I-IV 2HDM. We restrict ourselves to effective dimension six effects. First, recall that in section 4.4.3 we concluded that at effective dimension six, T violation is contained only in the four fermion operators or in the Higgs Yukawas. In the types I-IV 2HDM, T violation is further restricted.

From equations (4.5.16), (4.5.29), (4.5.39) and (4.5.49), we note that in the types I-IV 2HDM, the only T violation in four fermion operators is due to the known CKM phase. These T violating terms originate from integrating out the charged Higgs, arise only in flavor violating processes with CKM matrix insertions, and are present even if all the T violating phases of the 2HDM vanish. The effects of these T violating terms are heavily suppressed by the Jarlskog invariant.

All non-CKM CP violation at effective dimension six in the low energy theory is contained in the cubic Higgs Yukawa, which modifies the SM like Higgs Yukawa couplings. In the quark mass eigenbasis the Higgs Yukawas can be written as

$$\begin{aligned} \lambda^{u}_{\varphi ij} &= \delta_{ij}\,\frac{m^{u}_{i}}{v}\,(\,1+\kappa_{u}\,) \\ \lambda^{d,\ell\,\dagger}_{\varphi ij} &= \delta_{ij}\,\frac{m^{d,\ell}_{i}}{v}\,(\,1+\kappa_{d,\ell}\,) \end{aligned} \tag{4.6.1}$$

$m_i^{u,d,\ell}$ is the complex quark matrix, and $\kappa_{u,d,\ell}$ is given for each type of 2HDM with Glashow-Weinberg

conditions in section (4.5),

$$
\begin{aligned}
\text{Type I:}\quad & \mathrm{Re}\,\kappa_{u,d,\ell} = -\frac{v^2}{m_H^2}\,\mathrm{Re}\Big[e^{-i\xi/2}\tilde{\lambda}_6^*\Big]\,\cot\,\beta + \mathcal{O}\Big(\frac{v^4}{m_H^4}\Big)\\
& \mathrm{Im}\,\kappa_u = -\mathrm{Im}\,\kappa_{d,\ell} = -\cot\beta\sin\,\delta_{hf\overline{f}} + \mathcal{O}\Big(\frac{v^4}{m_H^4}\Big)\\
\\
\text{Type II:}\quad & \mathrm{Re}\,\kappa_u = -\frac{v^2}{m_H^2}\,\mathrm{Re}\Big[e^{-i\xi/2}\tilde{\lambda}_6^*\Big]\,\cot\,\beta + \mathcal{O}\Big(\frac{v^4}{m_H^4}\Big)\\
& \mathrm{Re}\,\kappa_{d,\ell} = \frac{v^2}{m_H^2}\,\mathrm{Re}\Big[e^{-i\xi/2}\tilde{\lambda}_6^*\Big]\,\tan\,\beta + \mathcal{O}\Big(\frac{v^4}{m_H^4}\Big)\\
& \mathrm{Im}\,\kappa_u = -\,\cot\beta\sin\,\delta_{hf\overline{f}} + \mathcal{O}\Big(\frac{v^4}{m_H^4}\Big)\\
& \mathrm{Im}\,\kappa_{d,\ell} = -\tan\,\beta\,\sin\,\delta_{hf\overline{f}} + \mathcal{O}\Big(\frac{v^4}{m_H^4}\Big)\\
\\
\text{Type III:}\quad & \mathrm{Re}\,\kappa_{u,d} = -\frac{v^2}{m_H^2}\,\mathrm{Re}\Big[e^{-i\xi/2}\tilde{\lambda}_6^*\Big]\,\cot\,\beta + \mathcal{O}\Big(\frac{v^4}{m_H^4}\Big)\\
& \mathrm{Re}\,\kappa_\ell = \frac{v^2}{m_H^2}\,\mathrm{Re}\Big[e^{-i\xi/2}\tilde{\lambda}_6^*\Big]\,\tan\,\beta + \mathcal{O}\Big(\frac{v^4}{m_H^4}\Big)\\
& \mathrm{Im}\,\kappa_u = -\mathrm{Im}\,\kappa_d = -\,\cot\beta\sin\,\delta_{hf\overline{f}} + \mathcal{O}\Big(\frac{v^4}{m_H^4}\Big)\\
& \mathrm{Im}\,\kappa_\ell = -\tan\,\beta\,\sin\,\delta_{hf\overline{f}} + \mathcal{O}\Big(\frac{v^4}{m_H^4}\Big)\\
\\
\text{Type IV:}\quad & \mathrm{Re}\,\kappa_{u,\ell} = -\frac{v^2}{m_H^2}\,\mathrm{Re}\Big[e^{-i\xi/2}\tilde{\lambda}_6^*\Big]\,\cot\,\beta + \mathcal{O}\Big(\frac{v^4}{m_H^4}\Big)\\
& \mathrm{Re}\,\kappa_d = \frac{v^2}{m_H^2}\,\mathrm{Re}\Big[e^{-i\xi/2}\tilde{\lambda}_6^*\Big]\,\tan\,\beta + \mathcal{O}\Big(\frac{v^4}{m_H^4}\Big)\\
& \mathrm{Im}\,\kappa_u = -\mathrm{Im}\,\kappa_\ell = -\,\cot\beta\sin\,\delta_{hf\overline{f}} + \mathcal{O}\Big(\frac{v^4}{m_H^4}\Big)\\
& \mathrm{Im}\,\kappa_d = -\tan\,\beta\,\sin\,\delta_{hf\overline{f}} + \mathcal{O}\Big(\frac{v^4}{m_H^4}\Big)
\end{aligned}
\tag{4.6.2}
$$

where we defined

$$
\begin{aligned}
\sin\delta_{hf\overline{f}} &\equiv \frac{v^2}{m_H^2}\,\Big|\tilde{\lambda}_6\Big|\,\sin\,\mathrm{Arg}\left(\tilde{\lambda}_6^* e^{-i\xi/2}\right)\Big[1+\mathcal{O}\Big(\frac{v^2}{m_H^2}\Big)\Big]\\
&= \frac{v^2}{m_H^2}\,\mathrm{Im}\left(\tilde{\lambda}_6^* e^{-i\xi/2}\right)\Big[1+\mathcal{O}\Big(\frac{v^2}{m_H^2}\Big)\Big]\\
&= -\frac{2}{m_H^2}\,\mathrm{Im}\left(\tilde{m}_{12}^{2\,*} e^{-i\xi/2}\right)\Big[1+\mathcal{O}\Big(\frac{v^2}{m_H^2}\Big)\Big]
\end{aligned}
\tag{4.6.3}
$$

In the last line of (4.6.3) we used the no tadpole condition (4.3.24) to write

$$
\mathrm{Im}\left(\tilde{\lambda}_6^* e^{-i\xi/2}\right) = -2\,\mathrm{Im}\left(\tilde{m}_{12}^{2\,*} e^{-i\xi/2}\right) \tag{4.6.4}
$$

From the effective phase (4.6.2) we see that CP violation at effective dimension six, which is contained in the Higgs Yukawas, can be written in terms of $\sin\delta_{hf\overline{f}}$. Using the relation between Higgs basis parameters and parameters in the original doublet basis, (4.3.18), we obtain the relation

$$\mathrm{Im}\left(\tilde{m}_{12}^{2\,*}e^{-i\xi/2}\right) = -\mathrm{Im}\left(m_{12}^{2\,*}e^{-i\xi}\right) \tag{4.6.5}$$

such that using (4.6.5) we can express the effective dimension six phase $\sin\delta_{hf\overline{f}}$ in terms of potential parameters in the original basis

$$\sin\delta_{hf\overline{f}} = \frac{2}{m_H^2}\,\mathrm{Im}\left(m_{12}^{2\,*}e^{-i\xi}\right)\left[1+\mathcal{O}\left(\frac{v^2}{m_H^2}\right)\right]$$

The quantity $\mathrm{Im}\left(m_{12}^{2\,*}e^{-i\xi}\right)$ depends on the Higgs condensate phase ξ in the original basis. We now solve for the phase in terms of potential parameters. The EWSB condition in the original basis (4.3.7) is

$$\mathrm{Im}\left(m_{12}^{2\,*}e^{-i\xi}\right) \;=\; \frac{1}{4}v^2\sin 2\beta\,\mathrm{Im}(\lambda_5^*e^{-2i\xi}) + \frac{1}{2}v^2\cos^2\beta\,\mathrm{Im}(\lambda_6^*e^{-i\xi}) + \frac{1}{2}v^2\sin^2\beta\,\mathrm{Im}(\lambda_7^*e^{-i\xi}) \tag{4.6.6}$$

Note that from (4.6.6) it is clear that $\mathrm{Im}\left(m_{12}^{2\,*}e^{i\xi}\right)$ is of the order of the electrosheep scale squared. The symmetry protecting the Glashow Weinberg conditions imposes $\lambda_6 = \lambda_7 = 0$, so in this case the EWSB condition (4.6.6) is simplified to

$$\mathrm{Im}\left(m_{12}^{2\,*}e^{-i\xi}\right) \;=\; \frac{1}{4}v^2\sin 2\beta\,\mathrm{Im}(\lambda_5^*e^{-2i\xi}) \tag{4.6.7}$$

Equation (4.6.7) has a simple solution at effective dimension six. We leave the derivation of the solution for an appendix. The solution is given by

$$\mathrm{Im}(m_{12}^{2*}e^{-i\xi}) = \frac{1}{4}v^2\,|\lambda_5|\sin 2\beta\,\sin\mathrm{Arg}\left(m_{12}^4\lambda_5^*\right)\left[1+\mathcal{O}\left(\,|\lambda_5|\,\frac{v^2}{m_H^2}\right)\right] \tag{4.6.8}$$

Using (4.6.8) in the effective dimension six CP violating phase (4.6.6),

$$\begin{aligned}\sin\delta_{hf\overline{f}} \;&=\; \frac{1}{2}\,|\lambda_5|\sin 2\beta\sin\mathrm{Arg}\left(m_{12}^4\lambda_5^*\right)\frac{v^2}{m_H^2}\left[1+\;\mathcal{O}\left(\,|\lambda_5|\,\frac{v^2}{m_H^2}\right)\right] \\ &=\; \frac{\tan\beta}{1+\tan^2\beta}\,|\lambda_5|\sin\mathrm{Arg}\left(m_{12}^4\lambda_5^*\right)\frac{v^2}{m_H^2}\left[1+\;\mathcal{O}\left(\,|\lambda_5|\,\frac{v^2}{m_H^2}\right)\right] \qquad (4.6.9)\end{aligned}$$

(4.6.10)

where in the last line we made use of $\sin 2\beta = 2\tan\beta/(1+\tan^2\beta)$. Note that at large $\tan\beta$ the effective phase $\sin\delta_{hf\overline{f}}$ is suppressed by $1/\tan\beta$,

4.7 The electron EDM

The leading contributions to the electron EDM in terms of the effective Yukawa modifiers κ_u and $\kappa_{d,\ell}$ is given by the sum of terms involving top, bottom, tau and W boson loops []

$$\left.\frac{d_e}{e}\right|_{t\ loop} = -\frac{16}{3}\frac{\sqrt{2}\alpha G_F m_e}{(4\pi)^3}\left[f(m_t^2/m_h^2)\,\mathrm{Im}\,\kappa_\ell + g(m_t^2/m_h^2)\,\mathrm{Im}\,\kappa_u\right] \tag{4.7.1}$$

$$\left.\frac{d_e}{e}\right|_{b\ loop} = -\frac{4}{3}\frac{\sqrt{2}\alpha G_F m_e}{(4\pi)^3}\left[f(m_b^2/m_h^2)\,\mathrm{Im}\,\kappa_\ell + g(m_b^2/m_h^2)\,\mathrm{Im}\,\kappa_b\right] \tag{4.7.2}$$

$$\left.\frac{d_e}{e}\right|_{\tau\ loop} = -\frac{4\sqrt{2}\alpha G_F m_e}{(4\pi)^3}\left[f(m_\tau^2/m_h^2) + g(m_\tau^2/m_h^2)\right]\mathrm{Im}\,\kappa_\ell \tag{4.7.3}$$

$$\begin{aligned}\left.\frac{d_e}{e}\right|_{W\ loop} = {} & \frac{2\sqrt{2}\alpha G_F m_e}{(4\pi)^3}\left[5g(m_W^2/m_h^2) + 3f(m_W^2/m_h^2) + \frac{3}{4}\left[\,g(m_W^2/m_h^2) + h(m_W^2/m_h^2)\,\right]\right. \\ & \left. - \frac{1}{2}\frac{g(m_W^2/m_h^2) - f(m_W^2/m_h^2)}{m_W^2/m_h^2}\right]\mathrm{Im}\,\kappa_\ell\end{aligned} \tag{4.7.4}$$

$$\left.\frac{d_e}{e}\right|_{non\ Barr\text{-}Zee} = \frac{1}{2}\frac{\sqrt{2}\alpha G_F m_e}{(4\pi)^3\,\sin^2\theta_W}\,D(m_W^2/m_h^2)\,\mathrm{Im}\,\kappa_\ell \tag{4.7.5}$$

The corresponding masses are given in table 4.4. We use the $\overline{\mathrm{MS}}$ mass for the bottom quark Yukawa in the calculations. We neglect the renormalization of the rest of the pole masses.

	Pole	$\overline{\mathrm{MS}}\,(m_H)$	$\overline{\mathrm{MS}}\,(m)$
m_t	172.5		163
m_t	172.5		
m_b	3.8	2.8	
m_τ	1.8		
m_W	80.4		
m_h	125		

Table 4.4: Pole and $\overline{\mathrm{MS}}$ masses in GeV.

The functions $f(z), g(z)$ and $D(z)$ are given in appendix C. For reference, the numerical values of the functions are given in table 4.5.

In the absence of additional CP violating operators, the experimental limit on the electron EDM is is [118]

$$d_e < 8.7 \times 10^{-29}\ \text{e cm} \tag{4.7.6}$$

Using the effective Yukawas (4.6.2) in the expression for the electron EDM (4.7.1), (4.7.2), (4.7.3),

z	$f(z)/\sqrt{z}$	$g(z)/\sqrt{z}$	$f(z)/z$	$g(z)/z$	$h(z)/z$	$D(z)/z$
1	0.83	1.17			-0.78	-1.10
m_t^2/m_h^2	0.73	1.04				
m_b^2/m_h^2	0.64	0.79				
m_τ^2/m_h^2	0.45	0.54				
m_W^2/m_h^2			1.47	2.06	-1.25	-2.49

Table 4.5: Reference values of functions $f(z), g(z), h(z)$ and $D(z)$. The functions are defined in appendix C.

(4.7.4) and (4.7.5) we obtain

$$\begin{aligned}
\text{Type I: } d_e &= 7.11\times10^{-27}\cot\beta\sin\delta_{hf\overline{f}}\left[1+\mathcal{O}\left(\frac{v^2}{{m_H}^2}\right)\right]\text{ e cm}\\
\text{Type II: } d_e &= \left[4.56\times10^{-27}\cot\beta-2.56\times10^{-27}\tan\beta\right]\sin\delta_{hf\overline{f}}\left[1+\mathcal{O}\left(\frac{v^2}{{m_H}^2}\right)\right]\text{ e cm}\\
\text{Type III: } d_e &= \left[4.54\times10^{-27}\cot\beta-2.57\times10^{-27}\tan\beta\right]\sin\delta_{hf\overline{f}}\left[1+\mathcal{O}\left(\frac{v^2}{{m_H}^2}\right)\right]\text{ e cm}\\
\text{Type IV: } d_e &= \left[7.12\times10^{-27}\cot\beta-1.38\times10^{-29}\tan\beta\right]\sin\delta_{hf\overline{f}}\left[1+\mathcal{O}\left(\frac{v^2}{{m_H}^2}\right)\right]\text{ e cm}
\end{aligned} \tag{4.7.7}$$

We now make use of the electron EDM's (4.7.7) and the experimental constraint (4.7.6) to set limits on the effective phase $\sin\delta_{hf\overline{f}}$. The limits are shown in figure (4.12) in the plane of the effective phase versus $\tan\beta$. The limits are particularly strong at large values of $\tan\beta$ in the types II and III, since in that case there is a enhancement of the CP violating effective lepton Yukawa, which enhances the EDM diagram with a W boson loop. The weakest limits are for the type I 2HDM, since in that case there is no ehnacement of any of the CP violating effective Yukawas at large $\tan\beta$.

It is also illustrative to express the limits in terms of parameters of the two Higgs doublet model potential (4.3.3) in the original basis using the relation (4.6.9). The relevant combination of potential parameters is $|\lambda_5|\sin\text{Arg}\left(m_{12}^4\lambda_5^*\right)\frac{v^2}{m_H^2}$. The corresponding limits are presented in figure (4.12). In terms of this combination of parameters, there is no $\tan\beta$ enhancement for the limits. The reason is that this combination of perameters enters in the effective phase $\sin\delta_{hf\overline{f}}$ with a power of $\tan\beta$ suppression, which cancels the $\tan\beta$ enhancement of the EDM's (4.7.7) in all cases. Note however that the limits are still considerable in types II and III, in which case most of the parameter space with $|\lambda_5|\sin\text{Arg}\left(m_{12}^4\lambda_5^*\right)\frac{v^2}{m_H^2} > 10^{-1}$ is ruled out. Types I and IV are mostly unconstrained, since in this case the contribution of the combination $|\lambda_5|\sin\text{Arg}\left(m_{12}^4\lambda_5^*\right)\frac{v^2}{m_H^2}$ to the EDM's is heavily suppressed by $\tan\beta$.

Finally, we plot the limits as a function of the imaginary part of the effective top and tau Yukawa

and $\tan\beta$ in 4.13 and 4.14. We

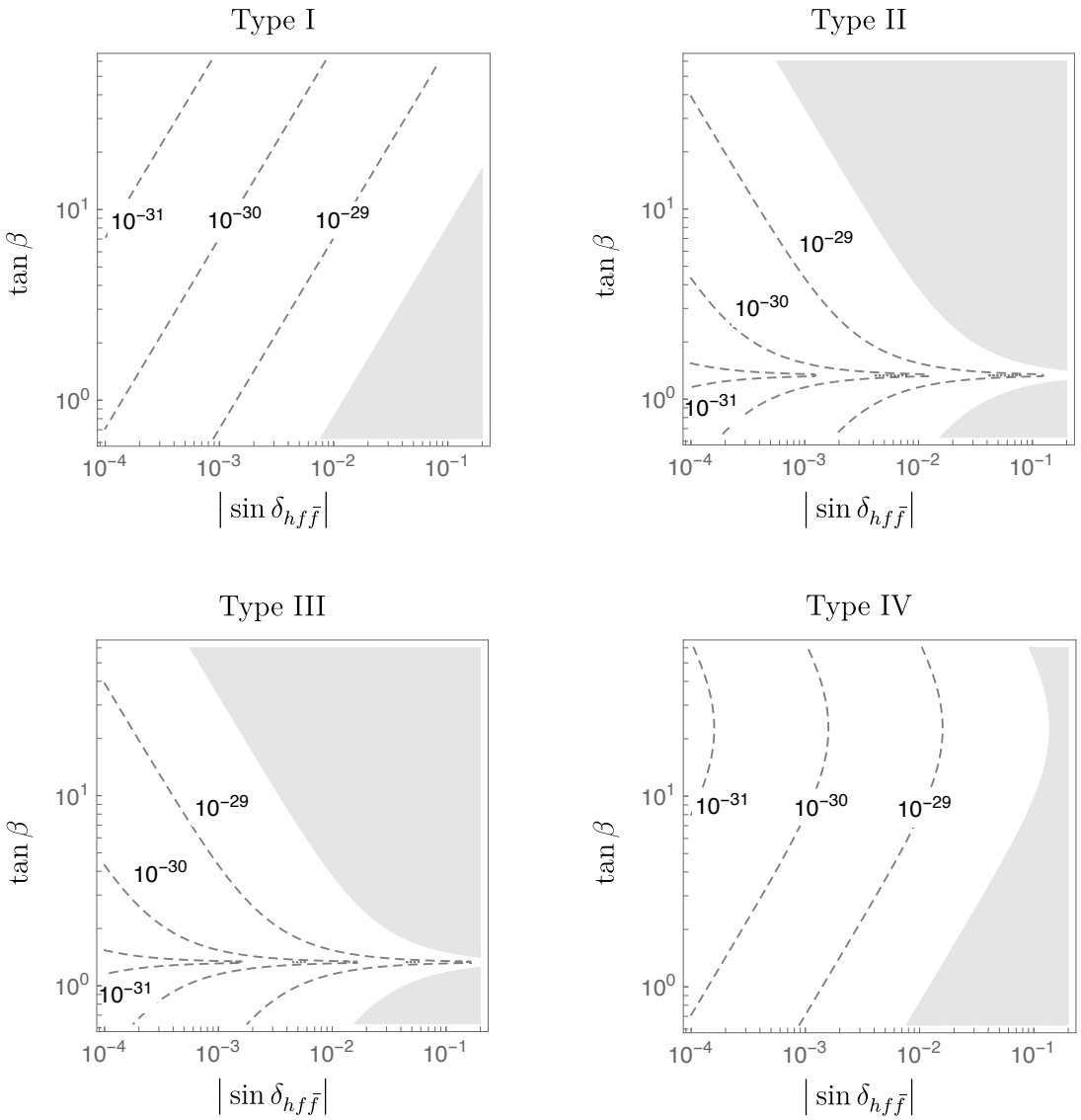

Figure 4.11: Limits on $|\sin\delta_{hf\bar{f}}|$. The shaded region is excluded by the ACME bound $|d_e| < 8.7 \times 10^{-29}$ e cm. Dashed lines correspond to contours of the electron EDM in units of e cm.

4.8 Conclusions of this chapter

In this chapter we studied and organized the low energy phenomenology of the SHSM and 2HDM near the decoupling limit using EFT. We worked at tree level. In the SHSM we worked up to effective dimension six, and in the 2HDM we worked up to effective dimension six in interactions involving fermions, and eight in purely bosonic interactions. The main output of this exercise is a

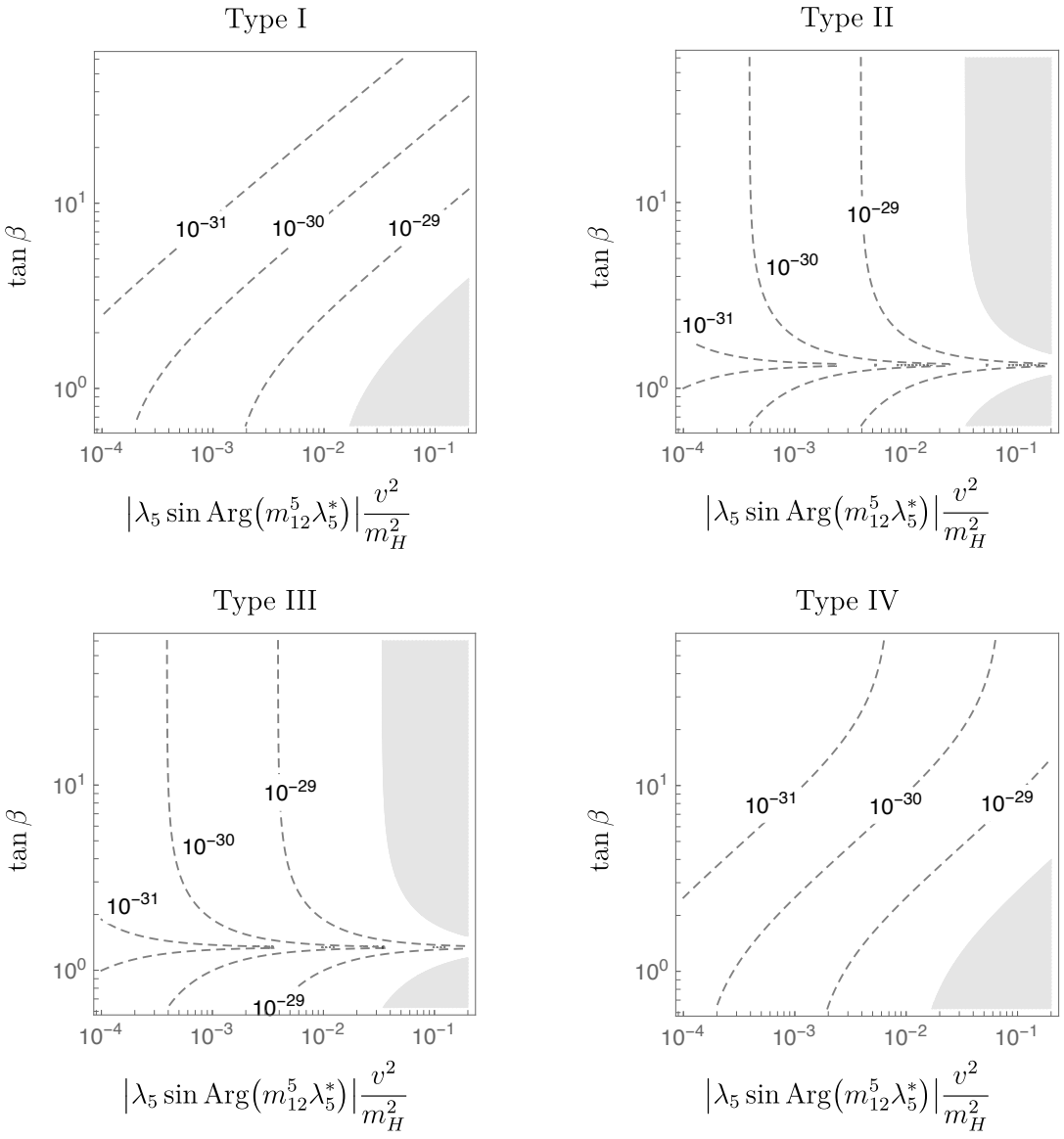

Figure 4.12: Limits on $|\lambda_5| \sin \mathrm{Arg}\left(m_{12}^4 \lambda_5^*\right) \frac{v^2}{m_H^2}$. The shaded region is excluded by the ACME bound $|d_e| < 8.7 \times 10^{-29}$ e cm. Dashed lines correspond to contours of the electron EDM in units of e cm.

general map between experimental signatures and theory. We summarize some of its main features in table 4.6. This map is a valuable, simple tool for interpreting experimental data.

Several observations can be made thanks to the organization of the phenomenology, that will be studied in follow up papers. First, we point out that the main difference of extensions with singlets and doublets, is that couplings of the Higgs to fermions and to massive gauge bosons are modified at different effective dimension. For this reason, a well motivated quantity to study at LHC are ratios

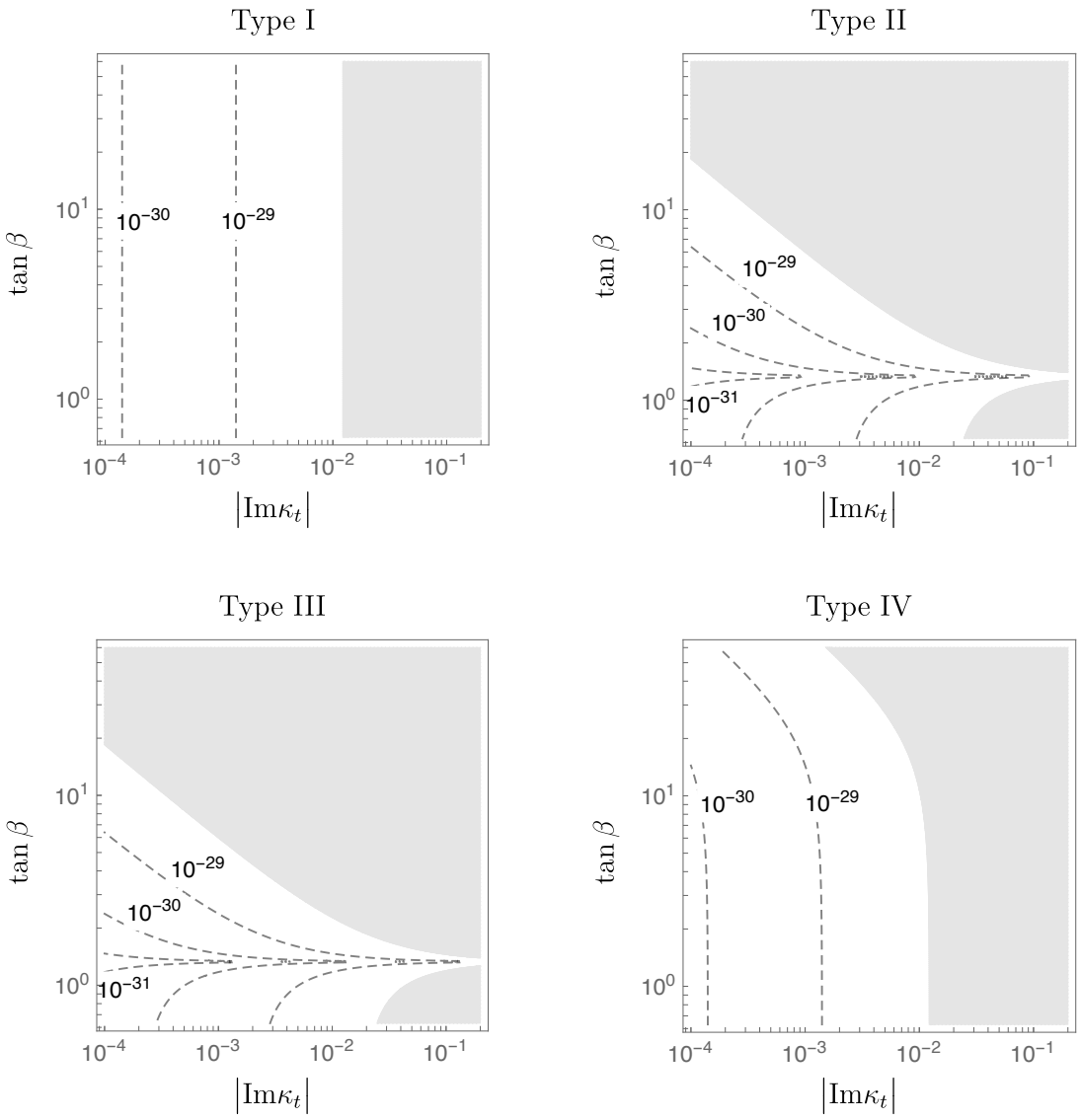

Figure 4.13: Limits the imaginary part of the effective top Yukawas $|\mathrm{Im}\,\kappa_t|$. The shaded region is excluded by the ACME bound $|d_e| < 8.7 \times 10^{-29}$ e cm. Dashed lines correspond to contours of the electron EDM in units of e cm.

of the type

$$\left| \frac{\lambda^f_{\varphi ij}}{g_{\varphi VV}} \frac{g^{\rm SM}_{\varphi VV}}{\lambda^{f\,\rm SM}_{\varphi ij}} \right| \tag{4.8.1}$$

Measurements of these ratios have been recently presented by ATLAS and CMS [96]. In the SHSM these ratios can be obtained from (4.2.56) and (4.2.58), and should be close to one, if radiative effects are small. In the 2HDM they are obtained from (4.4.31) and (4.4.34) and should be generically different from one. These observations remain valid away from the decoupling limit. Ratios of different couplings of the Higgs are one of the main tools to discern between the different extensions

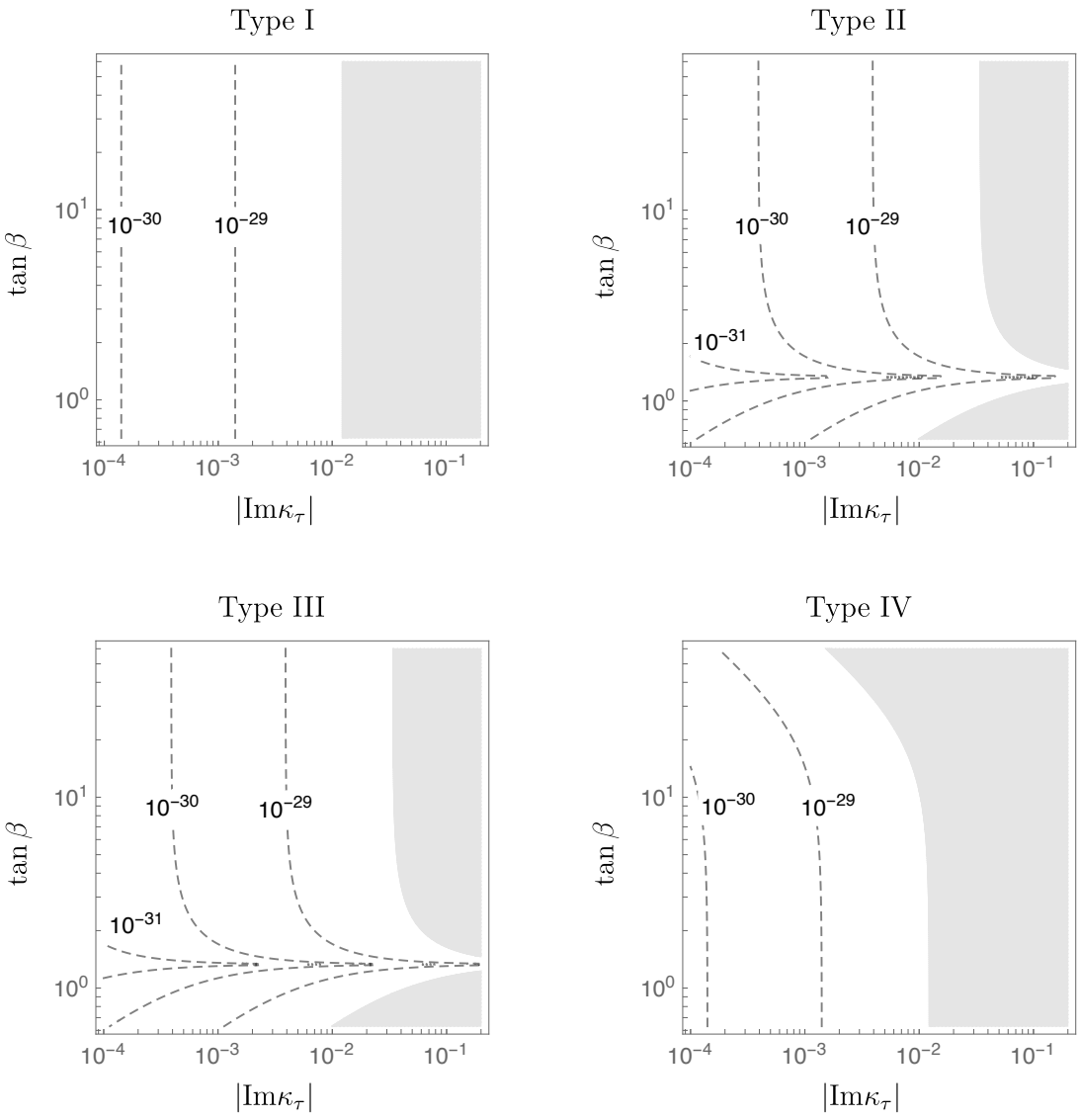

Figure 4.14: Limits the imaginary part of the effective top Yukawas $|\mathrm{Im}\,\kappa_\tau|$. The shaded region is excluded by the ACME bound $|d_e| < 8.7 \times 10^{-29}$ e cm. Dashed lines correspond to contours of the electron EDM in units of e cm.

of the Higgs sector. In the ratios, theoretical and/or experimental uncertainties might cancel. Ratios of Higgs Yukawas or Higgs couplings to massive gauge bosons over Higgs self couplings might also be interesting observables at colliders.

Moreover, the deviations of the couplings with respect to their SM values are controlled by a small subset of parameters of the UV completions. This leads to correlations between the deviations. The simplest case is in the SHSM, where both the Higgs couplings to two massive gauge bosons (4.2.56) and the Higgs Yukawas (4.2.58) suffer the same modification as pointed out above. In the 2HDM,

the deviations of these couplings are not directly correlated in general. However, in the particular limit in which the Yukawas of the heavy doublet vanish, as in the type I 2HDM at large $\tan\beta$, both deviations show up first at effective dimension eight and are equal, mimicking the effective theory of the SHSM. In this case, both deviations can be understood as dilution by the complex alignment parameter.

Regarding T violation, in the 2HDM EFT we identified the $U(1)_{\rm PQ}$ invariant T violating phases of the full 2HDM which are most relevant at low energies. We showed that only relative phases between the Higgs potential coupling $\tilde{\lambda}_6$ and the heavy doublet Yukawas appear at effective dimension six. In particular, in types I-IV 2HDM we showed that there is only one such phase and it appears only in the Higgs Yukawas. This phase can be constrained by EDM experiments.

We also organized all the effective dimension six flavor violating effects in the 2HDM EFT. All the four fermion operators were derived, and the flavor violating Higgs Yukawas were presented. For the general 2HDM, these results are $\tan\beta$ independent. Direct constraints on both the four fermion operator coefficients and on the Higgs Yukawas can be placed, and efforts have already been carried out in the literature [119]. Moreover, recent anomalies on flavor physics [120–126] provide strong motivation to study models with novel sources of flavor violation. These anomalies might be explained with tree level flavor violation [127], and it remains interesting to perform a detailed study of all the alternatives within the 2HDM.

	The SHSM	The 2HDM
Couplings to gauge bosons $g_{\varphi VV}, g_{\varphi^2 VV}$, $V = W, Z$	ED 6 (4.2.56) Always smaller than SM	ED 8 (4.4.31),(4.4.32) Always smaller than SM
Fermionic couplings $\lambda^f_{\varphi ij}$, $f = u, d, \ell$	ED 6 (4.2.58) Always smaller than SM	ED 6 (4.4.34)
Higgs self-couplings $g_{\varphi^3}, g_{\varphi^4}$	ED 6 (4.2.59)	ED 6 (4.4.35), (4.4.36) Always smaller than SM
Flavor violation	✗	ED 6 (4.4.17),(4.4.34) $\Delta F = 1, \Delta F = 2$. Chirality violating and preserving.
T violation	✗	ED 6 (4.4.17),(4.4.34) Only in fermionic interactions. Only one phase δ_{2HDM} (4.6.3) in types I-IV.
Modifications correlated and controlled mostly by	$\frac{\xi^2}{\mu^2}$ (4.2.3) (or $\cos\gamma$ (4.2.18))	$\tilde{\lambda}_6$ (4.3.16) (or Ξ (4.3.52)) and $\tilde{\lambda}^f_{2ij}$(4.3.13) , $f = u, d, \ell$

Table 4.6: Summary table of the main features of the SHSM and 2HDM effective field theories. ED stands for effective dimension. Each equation reference after ED 6 or ED 8 points to the coupling or operator where the corresponding effect can be read off. The rest of the equation references point to definitions of parameters.

Chapter 5

Conclusions and Outlook

In this work we addressed many of the fundamental problems of particle physics. We started by discussing the puzzle of CP violation, which contains four basic moving parts: the strong CP problem, the problem of the origin of the matter-antimatter asymmetry of the universe, the problem of the flavor and CP violating structure of the quark sector, and the problem of the flavor and CP structure of the lepton sector, which includes the issue of the origin of neutrino masses. We provided a full solution to the puzzle of CP violation through a high scale supersymmetric model in which all flavor mixing and CP violation is spontaneously generated through a Nelson-Barr mechanism. We developed powerful analytical tools to study the parameter space of the model, and we were able to conclude that the model not only accommodates all the known flavor and CP structure of the Standard Model, but it accommodates all the required CP violation in nature and included a mechanism for baryogenesis. Moreover, the model provides sharp predictions, making it quite unique. In particular, it provides a strong prediction for the mass of the lightest neutrino, which is below the mass sensitivity of current experiments.

It is exciting to have a well motivated model at disposition which such predictive power. The dark energy survey will reach a bound on the scale of the neutrino masses $\sum m_{\nu i} < 0.1\,\text{eV}$, just above the higher mass range for our prediction. Therefore, our model provides strong motivations to look for alternative ways to lower the bound. On the other hand, better measurements for the mixing angles are crucial to improve the predictions of our model. And finally, measurements of the CP violating phases in the DUNE [48] experiment could rule out or provide evidence in favor of our model.

On the other hand, it is of the greatest importance to have phenomenologically viable mechanisms of supersymmetry breaking. In this work we provided a complete, natural model for gauge

mediated supersymmetry breaking. This model has attracted attention for its simplicity (the model basically rescues a phenomenologically viable versions of minimal gauge mediation), and because it has been shown to be the most natural model available in the literature [16]. The model leads to spectacular experimental signatures at LHC for natural spectra with accessible colored particles (stops or gluinos). The decay chain is long, and includes jets, missing energy and taus in the final state, such that there is discovery potential with only few events. The natural parameter space of this model is being probed at the 13 TeV LHC.

Finally, in this work we carried out a complete and detailed analysis of the Higgs sector of supersymmetric models and of other extensions of the Standard Model. The properties of the Higgs boson are being probed at LHC, and the absence of deviations with respect to the Standard Model predictions lead to strong motivations to consider extended Higgs sector where the additional vacuum states are heavy. Moreover, the possible extensions of the Higgs sector which are compatible with electroweak precision tests are limited. Following these principles, we concentrated in extensions with only a singlet (SHSM) or a heavy second $SU(2)_L$ doublet (2HDM), and we performed a detailed analysis of the phenomenology by using effective field theory. The conclusions are strikingly simple. In the extension with a singlet, we found that only two operators modify the SM lagrangian at leading order in the operator expansion, namely a Higgs sextic interaction and a dimension six kinetic operator, which modifies uniformly the Higgs interactions to fermions and gauge bosons. On the other hand, for any 2HDM near the decoupling limit, we found that the effects on low energy physics are organized by a concept of operator effective dimension, which differs form naive operator dimension. We found that the leading corrections to the SM predictions are exclusively in four fermion operators, a cubic Higgs Yukawa operator and a sextic Higgs potential coupling. The most interesting experimental opportunities arise from the first two types of operators. Four fermion operators and cubic Yukawas may lead to flavor and/or CP violation, and an interesting avenue to pursue is to understand the limits on the flavor structure of such operators. On the other hand, the cubic Yukawa operator modifies the SM like couplings of the Higgs to fermions, and leads to possible deviations that might be found at LHC. The operator analysis shows that in the 2HDM, deviations to the SM like couplings of the Higgs to gauge bosons arise only at higher order in the operator expansion so they are suppressed. The different hierarchy of modifications of the couplings in the SHSM and 2HDM is a powerful tool to distinguish the phenomenology of the different extensions of the SM.

The hierarchical organization of the modification to the Standard Model predictions in each of the models was then used to understand the low energy CP violating effects of first a general 2HDM,

and then of a 2HDM with Glashow Weinberg conditions. In the latter case, it was shown that the observable effects at leading order in an operator expansion come from a single effective dimension six operator, which was constrained using limits on the electric dipole moment of the electron. It is interesting that such limits are most relevant for the 2HDM of types II and III, and constrain the effective phase to be less than one part in ten for most values of $\tan\beta$. Types I and IV are much less constrained, especially at high values of $\tan\beta$, and a large effective CP violating phase may be present. Better limits on the electron EDM will be crucial to probe the remaining parameter space, and if an anomalous result is obtained in the data, it could provide hints for the existence of an extended Higgs sector.

Exciting times are coming for particle physics. All the models discussed in this work are directly targeted to solve the fundamental problems of particle physics, and have phenomenological consequences which are accessible to current or future experiments. Our understanding of the Higgs sector of the SM, of the flavor and CP structure of the quark and lepton sector and of the symmetries underlying our fundamental theories, which have been mostly unaltered in the previous decades, might suffer a drastic change in the next few years. It is of the greatest importance for the theory community to keep working in providing insight to organize and motivate new experimental searches, which may finally lead to the solution of one or more of the current challenges in fundamental physics.

Appendix A

Flavor invariants

A.1 Flavor Invariants in the Standard Model

The dimension five superpotential of the MSSM contains the interactions

$$\begin{aligned} &\lambda^d_{ij}\ Q_i H_d \overline{d}_j - \lambda^u_{ij}\ Q_i H_u \overline{u}_j - \lambda^\ell_{ij}\ L_i H_d \overline{\ell}_j \\ &+ \lambda^\nu_{ij} (L_i H_u)(L_j H_u) \end{aligned} \tag{A.1.1}$$

The MSSM has a $U(3)^5$ background symmetry, which corresponds to its flavor group. The charges of the couplings are specified in table A.1. For convenience, the flavor charges for some combinations of couplings are given in table A.2.

	$U(3)_Q$	$U(3)_{\overline{u}}$	$U(3)_{\overline{d}}$	$U(3)_L$	$U(3)_\ell$
Q	$\mathbf{3}_1$				
$\overline{u}$		$\overline{\mathbf{3}}_1$			
$\overline{d}$			$\overline{\mathbf{3}}_1$		
L				$\mathbf{3}_1$	
$\overline{\ell}$					$\overline{\mathbf{3}}_1$
λ_u	$\overline{\mathbf{3}}_{-1}$	$\mathbf{3}_{-1}$			
λ_d	$\overline{\mathbf{3}}_{-1}$		$\mathbf{3}_{-1}$		
λ_ℓ				$\overline{\mathbf{3}}_{-1}$	$\mathbf{3}_{-1}$
λ^ν				$\overline{\mathbf{6}}_{-2}$	
$e^{i\theta_3}$	$\mathbf{1}_6$	$\mathbf{1}_3$	$\mathbf{1}_3$		
$e^{i\theta_2}$	$\mathbf{1}_9$	$\mathbf{1}_0$	$\mathbf{1}_0$	$\mathbf{1}_3$	$\mathbf{1}_0$
$e^{i\theta_1}$	$\mathbf{1}_2$	$\mathbf{1}_{16}$	$\mathbf{1}_4$	$\mathbf{1}_6$	$\mathbf{1}_{12}$

Table A.1: Flavor symmetries in the Standard model with massive neutrinos. The vacuum angles are defined up to a sign. The subscripts indicate the $U(1) \subset U(3)$ charges.

	$U(3)_Q$	$U(3)_{\overline{u}}$	$U(3)_{\overline{d}}$	$U(3)_L$	$U(3)_\ell$
$\lambda_u\lambda_u^\dagger$	$\mathbf{1}_0 \oplus \mathbf{8}_0$	$\mathbf{1}_0$	$\mathbf{1}_0$		
$\lambda_d\lambda_d^\dagger$	$\mathbf{1}_0 \oplus \mathbf{8}_0$	$\mathbf{1}_0$	$\mathbf{1}_0$		
$\lambda_\ell\lambda_\ell^\dagger$				$\mathbf{1}_0 \oplus \mathbf{8}_0$	$\mathbf{1}_0$
$\lambda_\nu\lambda_\nu^\dagger$				$\mathbf{1}_0 \oplus \mathbf{8}_0 \oplus \mathbf{27}_0$	$\mathbf{1}_0$
$\left[\lambda_u\lambda_u^\dagger, \lambda_d\lambda_d^\dagger\right]$	$\mathbf{8}_{0,A} \oplus \mathbf{10}_{0,A} \oplus \overline{\mathbf{10}}_{0,A}$				
Det λ_u	$\mathbf{1}_{-3}$	$\mathbf{1}_{-3}$	$\mathbf{1}_0$		
Det λ_d	$\mathbf{1}_{-3}$	$\mathbf{1}_0$	$\mathbf{1}_{-3}$		
Det λ_ℓ				$\mathbf{1}_{-3}$	$\mathbf{1}_{-3}$
Det λ_ν				$\mathbf{1}_{-6}$	$\mathbf{1}_0$
$\mathrm{Tr}[(\lambda_u\lambda_u^\dagger)^n]$	$\mathbf{1}_0$				
$\mathrm{Tr}[(\lambda_d\lambda_d^\dagger)^n]$	$\mathbf{1}_0$				
$\mathrm{Tr}[(\lambda_\ell\lambda_\ell^\dagger)^n]$				$\mathbf{1}_0$	
$\mathrm{Tr}[(\lambda_\nu\lambda_\nu^\dagger)^n]$				$\mathbf{1}_0$	

Table A.2: Flavor charges for some combinations of fermionic couplings. The subscripts indicate the $U(1) \subset U(3)$ charges. *This notation could be confusing: for instance $\lambda_u\lambda_u^\dagger$ can be confused with just simple matrix multiplication as in the rest of the paper, but here we mean both the* 8 *that results from matrix multiplication, and the* 1 *that results from the trace of the matrix multiplication. DEU*

All observable quantities must be invariant under flavor transformations. Invariants can be built by taking traces of flavored matrices, as in exemplified in table A.2. Observables that break and do not break CP can be expressed in terms of CP odd and CP even invariants, respectively [128]. A CP odd (even) invariant is defined as a purely imaginary (real) flavor invariant.

In this work we make use of leptonic invariants, which are useful tools to simplify the numerical calculations. Quark invariants are not be used intensively, but they are somewhat simpler and more familiar than the leptonic invariants and they illustrate the ideas of the invariant formalism, so we begin by describing them.

The quark sector contains eleven observable parameters α_i , $i = 1..11$. These parameters are the six masses, three mixing angles, the CKM phase and the strong CP phase. Correspondingly, we must be able to express the eleven observable parameters in terms of eleven independent invariants $\mathcal{I}_j$, $j = 1..11$, nine of which must be CP even and the remaining two must be CP odd. Independence of the invariants is ensured if the Jacobian

$$\det\left(\frac{\partial \mathcal{I}_j}{\partial \alpha_i}\right) \tag{A.1.2}$$

is non zero. In this work we check numerically that this condition is always fulfilled for the set of chosen invariants, but we omit presenting the explicit calculations for brevity.

We now present the independent invariants for the quark sector. *(*maybe just remove the following comment, is not clarifying at all*)* All of them, except the one measuring the strong CP phase, will be built out of traces of matrices that transform only under $U(3)_Q$ to ensure invariance (see table A.2). The magnitude of the six quark masses squared can be expressed in terms of the CP even invariants

$$v_u^{2n}\,\mathrm{Tr}\,\left(\lambda_u\lambda_u^\dagger\right)^n \qquad v_d^{2n}\,\mathrm{Tr}\,\left(\lambda_d\lambda_d^\dagger\right)^n \tag{A.1.3}$$

with $n = 1, 2, 3$. The above invariants are real since the matrices $\lambda_u\lambda_u^\dagger, \lambda_d\lambda_d^\dagger$ are hermitian. The remaining three CP even invariants are related with flavor mixing, and can be chosen to be

$$\begin{aligned}
&\mathrm{Tr}\,\left(\left[\lambda_u\lambda_u^\dagger, \lambda_d\lambda_d^\dagger\right]^2\right)\\
&\mathrm{Tr}\,\left(\left[\lambda_u\lambda_u^\dagger, \lambda_d\lambda_d^\dagger\right]^2\left(\lambda_u\lambda_u^\dagger\right)\right)\\
&\mathrm{Tr}\,\left(\left[\lambda_u\lambda_u^\dagger, \lambda_d\lambda_d^\dagger\right]^2\left(\lambda_d\lambda_d^\dagger\right)\right)
\end{aligned}$$

It can be shown that the above invariants are real by using the cyclic property of the trace and the hermiticity of the matrices $\lambda_u\lambda_u^\dagger$ and $\lambda_d\lambda_d^\dagger$. Note that if the matrices $\lambda_u\lambda_u^\dagger$ and $\lambda_d\lambda_d^\dagger$ can be simultaneously diagonalized by an $SU(3)_Q$ transformation, the invariants in (A.1.4) vanish. This corresponds to the case of no quark mixing.

The CKM phase resides in the CP odd Jarslkog invariant [31], which is conventionally defined as

$$-iJ = \frac{1}{3}v_u^6 v_d^6\,\mathrm{Tr}\,\left(\left[\lambda_u\lambda_u^\dagger, \lambda_d\lambda_d^\dagger\right]^3\right) \tag{A.1.4}$$

The trace in (A.1.4) is purely imaginary since the matrix $\left[\lambda_u\lambda_u^\dagger, \lambda_d\lambda_d^\dagger\right]^3$ is antihermitian. Note that in the case of no quark mixing, the invariant vanishes and the CKM phase is not observable.

We now turn to the strong CP phase. The U(1) charges of $e^{i\theta}$ corresponds to the strength of anomalies. The invariant for the $SU(3)_C$ vacuum angle is given by

$$i\overline{\theta} = i\mathrm{Arg}\big(\, e^{i\theta}\,\mathrm{Det}\lambda_u\,\mathrm{Det}\lambda_d\,\big) \tag{A.1.5}$$

The existence of a basis independent combination of Lagrangian parameters corresponding to the $SU(3)_C$ vacuum angle implies that all of the zero modes of an $SU(3)_C$ instanton can be soaked up by Lagrangian interactions.

Now, without loss of generality the yukawa matrices are given by

$$\begin{aligned}
v_u\lambda_u &= \;\; U_{Q_u}\,\mathrm{diag}(m_u, m_c, m_t)\,U_{\overline{u}}^\dagger\\
v_d\lambda_d &= \;\; U_{Q_d}\,\mathrm{diag}(m_d, m_s, m_b)\,U_{\overline{d}}^\dagger
\end{aligned} \tag{A.1.6}$$

where U_{Q_u}, U_{Q_d}, $U_{\overline{u}}$ and $U_{\overline{d}}$ are basis dependent unitary matrices and the masses are defined to be real and positive. In a given basis, (A.1.6) fixes U_{Q_u}, U_{Q_d}, $U_{\overline{u}}$ and $U_{\overline{d}}$ unambiguously up to

right multiplication by arbitrary diagonal unitary matrices. These diagonal unitary matrices can be seen as the remaining flavor transformation that one can perform in a basis in which λ_u or λ_d are diagonal. Without loss of generality, they can be chosen such that the CKM matrix

$$V_{\rm CKM} = U_{Q_u}^T U_{Q_d}^* \tag{A.1.7}$$

is in its canonical form, as given by [41]

$$V_{\rm CKM} = \begin{pmatrix} c_{12}c_{13} & s_{12}c_{13} & s_{13}e^{-i\delta} \\ -s_{12}c_{23} - c_{12}s_{23}s_{13}e^{i\delta} & c_{12}c_{23} - s_{12}s_{23}s_{13}e^{i\delta} & s_{23}c_{13} \\ s_{12}s_{23} - c_{12}c_{23}s_{13}e^{i\delta} & -c_{12}s_{23} - s_{12}c_{23}s_{13}e^{i\delta} & c_{23}c_{13} \end{pmatrix} \tag{A.1.8}$$

Explicit expressions for the invariants in terms of measurable parameters can be obtained using (A.1.6) and (A.1.7). The results are of course independent of the basis chosen to perform the calculations. As an example, the invariants (A.1.3) are given by

$$\begin{aligned} v_u^{2n}\,{\rm Tr}\,\left(\lambda_u\lambda_u^\dagger\right)^n &= \; m_u^{2n} + m_c^{2n} + m_t^{2n} \\ v_d^{2n}\,{\rm Tr}\,\left(\lambda_d\lambda_d^\dagger\right)^n &= \; m_d^{2n} + m_s^{2n} + m_b^{2n} \end{aligned} \tag{A.1.9}$$

with $n = 1, 2, 3$. Note that these "mass invariants" are independent of the mixing angles and of the CKM phase. The invariants measuring flavor mixing are

$$\begin{aligned} v_u^4 v_d^4\,{\rm Tr}\,\left(\left[\lambda_u\lambda_u^\dagger, \lambda_d\lambda_d^\dagger\right]^2\right) &= 2\,{\rm Tr}\,\Big(M_u^2\, V_{\rm CKM}^*\, M_d^2\, V_{\rm CKM}^T\, M_u^2\, V_{\rm CKM}^*\, M_d^2\, V_{\rm CKM}^T \\ &\quad - M_u^2\, V_{\rm CKM}^*\, M_d^4\, V_{\rm CKM}^T\, M_u^2 \Big) \end{aligned} \tag{A.1.10}$$

$$\begin{aligned} v_u^6 v_d^4\,{\rm Tr}\,\left(\left[\lambda_u\lambda_u^\dagger, \lambda_d\lambda_d^\dagger\right]^2\lambda_u\lambda_u^\dagger\right) &= {\rm Tr}\,\Big(V_{\rm CKM}^*\, M_d^2\, V_{\rm CKM}^T\, M_u^2\, V_{\rm CKM}^*\, M_d^2\, V_{\rm CKM}^T\, M_u^4 \\ &\quad - M_u^6\, V_{\rm CKM}^*\, M_d^4\, V_{\rm CKM}^T \Big) \end{aligned} \tag{A.1.11}$$

$$\begin{aligned} v_u^4 v_d^6\,{\rm Tr}\,\left(\left[\lambda_u\lambda_u^\dagger, \lambda_d\lambda_d^\dagger\right]^2\lambda_d\lambda_d^\dagger\right) &= {\rm Tr}\,\Big(M_d^4\, V_{\rm CKM}^T\, M_u^2\, V_{\rm CKM}^*\, M_d^2\, V_{\rm CKM}^T M_u^2\, V_{\rm CKM}^* \\ &\quad - M_d^6\, V_{\rm CKM}^T\, M_u^4\, V_{\rm CKM}^*\Big) \end{aligned} \tag{A.1.12}$$

The trace for the Jarslkog invariant is given by

$$v_u^6 v_d^6\,{\rm Tr}\,\left(\left[\lambda_u\lambda_u^\dagger, \lambda_d\lambda_d^\dagger\right]^3\right) = {\rm Tr}\,\Big(3M_u^4\, V_{\rm CKM}^*\, M_d^4\, V_{\rm CKM}^T\, M_u^2\, V_{\rm CKM}^*\, M_d^2\, V_{\rm CKM}^T\Big) - {\rm h.c.} \tag{A.1.13}$$

$$\begin{aligned} J &= 2(m_t^2 - m_c^2)(m_t^2 - m_u^2)(m_c^2 - m_u^2)(m_b^2 - m_s^2)(m_b^2 - m_d^2)(m_s^2 - m_d^2) \\ &\quad s_{12}s_{23}s_{31}c_{12}c_{23}c_{31}^2 \sin\delta \end{aligned} \tag{A.1.14}$$

check prefactors The expressions for the flavor mixing CP even invariants (A.1.4) in terms of masses and mixing angles are complicated non-linear expressions, and we choose to omit them. The expressions are complicated since mixing can occur between any two out of the three generations, and the invariants must account for all the possibilities. This is a feature that carries on to the leptonic sector, and in practice disfavors the use of CP even flavor mixing invariants, in the sense that if the numerical values of the flavor mixing invariants are known, it is numerically challenging to extract the values of the mixing angles from them. In this work we do not make use of flavor mixing invariants in the calculations.

The leptonic sector contains twelve observables: the three charged lepton masses, three left handed neutrino masses, three mixing angles and three CP violating phases in the PMNS matrix. One of the CP violating phases is similar to the CKM phase of the quark sector, while the other two are Majorana phases. Correspondingly, there are twelve invariants, nine of which are CP even, and three of which are CP odd. Differently from the quark sector, in this case there is no basis independent combination of quark and lepton Lagrangian interaction parameters that give rise to quark and lepton masses corresponding to the $SU(2)_L$ vacuum angle *does this mean that the $SU(2)_L$ vacuum angle is not observable?*, so the corresponding CP violating phase is not discussed here.

We now present the leptonic invariants. We build them as traces of matrices that transform only under $U(3)_L$ (see table A.2). The magnitude of the three lepton and neutrino masses can be expressed in terms of

$$\mathrm{Tr}[(\lambda_\ell \lambda_\ell^\dagger)^n] \qquad \mathrm{Tr}[(\lambda_\nu \lambda_\nu^\dagger)^n] \tag{A.1.15}$$

for $n = 1, 2, 3$. The above invariants are real since the matrices $\lambda_\ell \lambda_\ell^\dagger, \lambda_\nu \lambda_\nu^\dagger$ are hermitian. The remaining three CP even invariants are related with flavor mixing, and can be chosen to be

$$\begin{aligned} &\mathrm{Tr}\left(\left[\,\lambda_\ell \lambda_\ell^\dagger, \lambda_\nu \lambda_\nu^\dagger\,\right]^2\right) \\ &\mathrm{Tr}\left(\left[\,\lambda_\ell \lambda_\ell^\dagger, \lambda_\nu \lambda_\nu^\dagger\,\right]^2 \left(\lambda_\ell \lambda_\ell^\dagger\right)^2\right) \\ &\mathrm{Tr}\left(\left[\,\lambda_\ell \lambda_\ell^\dagger, \lambda_\nu \lambda_\nu^\dagger\,\right]^2 \left(\lambda_\nu \lambda_\nu^\dagger\right)^2\right) \end{aligned} \tag{A.1.16}$$

The case of commuting $\lambda_\ell \lambda_\ell^\dagger$ and $\lambda_\nu \lambda_\nu^\dagger$ corresponds to the case of no leptonic flavor mixing.

Of the three CP odd invariants for the leptonic sector [128], one is a leptonic Jarlskog invariant

$$-iJ_L = \frac{1}{3} v_d^3 \ \mathrm{Tr}\left(\left[\,\lambda_\ell \lambda_\ell^\dagger\,, \lambda_\nu \lambda_\nu^\dagger\,\right]^3\right) \tag{A.1.17}$$

while the remaining two are related to the Majorana phases

$$\begin{array}{c} \mathrm{Tr}\left(\left[\,\lambda_\ell\lambda_\ell^\dagger\,,\lambda_\nu\big(\lambda_\ell\lambda_\ell^\dagger\big)^*\lambda_\nu^\dagger\,\right]^3\right) \\ \mathrm{Tr}\left(\left[\,\lambda_\ell\lambda_\ell^\dagger\,,\lambda_\nu\lambda_\nu^\dagger\,\right]\left(\lambda_\nu\big(\lambda_\ell\lambda_\ell^\dagger\big)^*\lambda_\nu^\dagger\right)\right) \end{array} \tag{A.1.18}$$

Without loss of generality, the charged lepton Yukawas and the LH neutrino mass matrix are given by

$$\begin{aligned} v_d\,\lambda_\ell &= U_{L_d}\ \mathrm{diag}(m_e,m_\mu,m_\tau)\ U_\ell^\dagger \\ v_u^2\lambda_\nu &= U_{L_u}\ \mathrm{diag}(m_{\nu e},m_{\nu\mu},m_{\nu\tau})\ U_{L_u}^T \end{aligned} \tag{A.1.19}$$

where U_{L_d}, U_{L_u} and U_ℓ are basis dependent unitary matrices and the masses are defined to be real and positive. The PMNS matrix is a unitary, basis independent matrix defined as

$$U_{\mathrm{PMNS}} = U_{L_d}^T U_{L_u}^* \tag{A.1.20}$$

In a given basis, (A.1.19) fixes unambigously U_{L_u}, but U_{L_d} is fixed only up to right multiplication by a diagonal unitary matrix. This diagonal unitary matrix is chosen such that the PMNS matrix is in its canonical form given by

$$U_{\mathrm{PMNS}} = UP \tag{A.1.21}$$

where

$$P = \begin{pmatrix} 1 & 0 & 0 \\ 0 & e^{i\lambda_2} & 0 \\ 0 & 0 & e^{i\lambda_3} \end{pmatrix} \tag{A.1.22}$$

and

$$U = \begin{pmatrix} c_{12}c_{13} & s_{12}c_{13} & s_{13}e^{-i\delta_{13}} \\ -s_{12}c_{23} - c_{12}s_{23}s_{13}e^{i\delta_{13}} & c_{12}c_{23} - s_{12}s_{23}s_{13}e^{i\delta_{13}} & s_{23}c_{13} \\ s_{12}s_{23} - c_{12}c_{23}s_{13}e^{i\delta_{13}} & -c_{12}s_{23} - s_{12}c_{23}s_{13}e^{i\delta_{13}} & c_{23}c_{13} \end{pmatrix} \tag{A.1.23}$$

where we are abusing of the notation by calling the lepton and quark mixing angles in the same way.

Explicit expressions for the invariants in terms of measurable parameters can be obtained using (A.1.19) and (A.1.21). The results are of course independent of the basis chosen to perform the calculations. As an example, the invariants (A.1.15) are given by

$$\begin{aligned} v_d^{2n}\,\mathrm{Tr}\,\left(\lambda_\ell\lambda_\ell^\dagger\right)^n &= m_e^{2n} + m_\mu^{2n} + m_\tau^{2n} \\ v_u^{4n}\,\mathrm{Tr}\,\left(\lambda_\nu\lambda_\nu^\dagger\right)^n &= m_{\nu_1}^{2n} + m_{\nu_2}^{2n} + m_{\nu_3}^{2n} \end{aligned} \tag{A.1.24}$$

with $n = 1, 2, 3$. Note that these "mass invariants" are independent of the mixing angles and CP violating phases.

The flavor mixing invariants (A.1.4) are

$$v_u^8 v_d^4 \,\mathrm{Tr}\left(\left[\,\lambda_\ell\lambda_\ell^\dagger, \lambda_\nu\lambda_\nu^\dagger\,\right]^2\right) = 2\,\mathrm{Tr}\left(\,M_\ell^2\,U_{\rm PMNS}^*\,M_\nu^2\,U_{\rm PMNS}^T\,M_\ell^2\,U_{\rm PMNS}^*\,M_\nu^2\,U_{\rm PMNS}^T - M_\ell^2\,U_{\rm PMNS}^*\,M_\nu^4\,U_{\rm PMNS}^T\,M_\ell^2\,\right) \tag{A.1.25}$$

$$v_u^8 v_d^6 \,\mathrm{Tr}\left(\left[\lambda_\ell\lambda_\ell^\dagger, \lambda_\nu\lambda_\nu^\dagger\right]^2\lambda_\ell\lambda_\ell^\dagger\right) = \mathrm{Tr}\left(U_{\rm PMNS}^*\,M_\nu^2\,U_{\rm PMNS}^T\,M_\ell^2\,U_{\rm PMNS}^*\,M_\nu^2\,U_{\rm PMNS}^T\,M_\ell^4 - M_\ell^6\,U_{\rm PMNS}^*\,M_\nu^4\,U_{\rm PMNS}^T\,\right) \tag{A.1.26}$$

$$v_u^{12} v_d^4 \,\mathrm{Tr}\left(\left[\lambda_\ell\lambda_\ell^\dagger, \lambda_\nu\lambda_\nu^\dagger\right]^2\lambda_\nu\lambda_\nu^\dagger\right) = \mathrm{Tr}\left(M_\nu^4\,U_{\rm PMNS}^T\,M_\ell^2\,U_{\rm PMNS}^*\,M_\nu^2\,U_{\rm PMNS}^T M_\ell^2\,U_{\rm PMNS}^* - M_\nu^6\,U_{\rm PMNS}^T\,M_\ell^4\,U_{\rm PMNS}^*\right) \tag{A.1.27}$$

The trace for the leptonic Jarslkob invariant is

$$v_u^{12} v_d^6 \,\mathrm{Tr}\left(\left[\lambda_\ell\lambda_\ell^\dagger, \lambda_\nu\lambda_\nu^\dagger\right]^3\right) = \mathrm{Tr}\left(3M_\ell^4\,U_{\rm PMNS}^*\,M_\nu^4\,U_{\rm PMNS}^T\,M_\ell^2\,U_{\rm PMNS}^*\,M_\nu^2\,U_{\rm PMNS}^T\right) - \text{h.c.} \tag{A.1.28}$$

We can also evaluate the trace in the leptonic Jarlskob invariant explicitely

$$J_L = -2(m_\mu^2 - m_e^2)(m_\tau^2 - m_e^2)(m_\tau^2 - m_\mu^2)(m_{\nu_2}^2 - m_{\nu_1}^2)(m_{\nu_3}^2 - m_{\nu_1}^2)(m_{\nu_3}^2 - m_{\nu_2}^2) \; s_{12}c_{12}s_{13}c_{13}^2 s_{23}c_{23}\,\sin\,\delta_{13} \tag{A.1.29}$$

Note that this invariant is independent of the Majorana phases of the PMNS matrix.

The CP odd Majorana invariants in terms of masses and the PMNS matrix are

$$v_u^{12} v_d^{12} \,\mathrm{Tr}\left(\left[\,\lambda_\ell\lambda_\ell^\dagger\,, \lambda_\nu\big(\lambda_\ell\lambda_\ell^\dagger\big)^*\lambda_\nu^\dagger\,\right]^3\right) = \mathrm{Tr}\left(3M_\nu^2\,U_{\rm PMNS}^\dagger\,M_\ell^2\,U_{\rm PMNS}\,M_\nu\,U_{\rm PMNS}^T M_\ell^2\,U_{\rm PMNS}^*M_\nu\,U_{\rm PMNS}^\dagger\,M_\ell^2\,U_{\rm PMNS}\,M_\nu\right.$$
$$\left. U_{\rm PMNS}^T\,M_\ell^4\,U_{\rm PMNS}^*M_\nu\,U_{\rm PMNS}^\dagger\,M_\ell^2\,U_{\rm PMNS}\,\right) - \text{h.c.} \tag{A.1.30}$$

$$v_d^4 v_d^8 \,\mathrm{Tr}\left(\left[\,\lambda_\ell\lambda_\ell^\dagger\,, \lambda_\nu\lambda_\nu^\dagger\,\right]\left(\lambda_\nu\big(\lambda_\ell\lambda_\ell^\dagger\big)^*\lambda_\nu^\dagger\right)\right) = \mathrm{Tr}\left(M_\nu^3\,U_{\rm PMNS}^\dagger\,M_\ell^2\,U_{\rm PMNS}\right.$$
$$\left. M_\nu\,U_{\rm PMNS}^T\,M_\ell^2\,U_{\rm PMNS}^*\right) - \text{h.c.} \tag{A.1.31}$$

	$U(3)_N$	$U(3)_L$	$U(3)_\ell$
N	$\mathbf{3}_1$		
L		$\mathbf{3}_1$	
$\bar{\ell}$			$\overline{\mathbf{3}}_1$
λ_N	$\mathbf{3}_1$	$\overline{\mathbf{3}}_{-1}$	
M	$\overline{\mathbf{6}}_{-2}$		
λ_ℓ		$\overline{\mathbf{3}}_{-1}$	$\mathbf{3}_{-1}$
$e^{i\theta_2}$		$\mathbf{1}_3$	$\mathbf{1}_0$
$e^{i\theta_1}$		$\mathbf{1}_6$	$\mathbf{1}_{12}$

Table A.3: Flavor symmetries of a type I seesaw model with leptonic couplings as in (2.2.16). The subscripts indicate the $U(1) \subset U(3)$ charges.

	$U(3)_N$	$U(3)_L$	$U(3)_\ell$
$\lambda_N^\dagger \lambda_N$	$\mathbf{1}_0 \oplus \mathbf{8}_0$	$\mathbf{1}_0$	$\mathbf{1}_0$
$M^* M$	$\mathbf{1}_0 \oplus \mathbf{8}_0 \oplus \mathbf{27}_0$	$\mathbf{1}_0$	$\mathbf{1}_0$

Table A.4: Flavor symmetries of a type I seesaw model for some combinations of fermionic couplings. Couplings are defined as in (2.2.16). The subscripts indicate the $U(1) \subset U(3)$ charges.

A.2 Flavor Invariants in a type I seesaw model

We now consider the leptonic sector of a supersymmetric type I seesaw model. The superpotential contains the interactions

$$\frac{1}{2} M_{ij} N_i N_j - \lambda^\ell_{ij}\ L_i H_d \bar{\ell}_j - \lambda^N_{ij}\ L_i H_u N_j$$

A type I seesaw model has a $U(3)_N \times U(3)_L \times U(3)_\ell$ background symmetry, which corresponds to its flavor symmetries. The flavor symmetries are specified in table A.3. In a type I seesaw model, the RH neutrinos are heavier than the LH leptons. When the RH neutrinos are integrated out, they lead to a low energy effective theory with leptonic flavor symmetry $U(3)_L \times U(3)_\ell$ as in table A.1. For convenience, the transformation properties of some combination of couplings is given in table A.4.

A type I seesaw model has twenty-one independent observables. We separate the observables and invariants in "IR" and "UV" observables and invariants. We define the twelve IR observables ξ_a, $a = 1..12$ to be a minimal set of independent parameters that completely specify all the independent invariants that can be built with the flavor symmetry $U(3)_L \times U(3)_\ell$ of the low energy effective theory. As seen in section A.1, the twelve IR observables can be chosen to be the six LH lepton masses and the six elements of the PMNS matrix.

The remaining nine observables η_b, $b = 1..9$ are defined as the UV observables *maybe the wording "observables" v/s "invariants" is not clear. after all, invariants are also observables.* By definition, the twelve IR invariants $\mathcal{I}_a$ do not depend on the nine UV observables,

$$\frac{\partial \mathcal{I}_a}{\partial \eta_b} = 0 \qquad a = 1..12\ ,\ b = 1..9 \tag{A.2.1}$$

The nine UV invariants $\mathcal{I}_b$ can depend both on the IR and UV observables.

We now identify the nine UV observables. We first note that the RH neutrino mass matrix is, in the most general case

$$M = U_M^T \,\mathrm{diag}(M_1, M_2, M_3)\, U_M \tag{A.2.2}$$

On the other hand, using (2.2.23) and (A.1.19), the neutrino mass matrix must satisfy

$$v_u^2 \lambda_N M^{-1} (\lambda_N)^T = U_{L_u}\ \mathrm{diag}(m_{\nu e}, m_{\nu\mu}, m_{\nu\tau})\ U_{L_u}^T \tag{A.2.3}$$

The most general RH neutrino Yukawa satisfying (A.2.3) is [50]

$$v_u \lambda_N = U_{L_u}\,\mathrm{diag}\Big(\sqrt{m_{\nu e}}, \sqrt{m_{\nu\mu}}, \sqrt{m_{\nu\tau}}\Big)\, R\,\mathrm{diag}\Big(\sqrt{M_1}, \sqrt{M_2}, \sqrt{M_3}\Big)\, U_M \tag{A.2.4}$$

where R is a basis independent, complex orthogonal matrix

$$R R^T = 1 \tag{A.2.5}$$

which we can write as

$$R = \begin{pmatrix} c_2 c_3 & -c_1 s_3 - s_1 s_2 c_3 & s_1 s_3 - c_1 s_2 c_3 \\ c_2 s_3 & c_1 c_3 - s_1 s_2 s_3 & -s_1 c_3 - c_1 s_2 s_3 \\ s_2 & s_1 c_2 & c_1 c_2 \end{pmatrix} \tag{A.2.6}$$

where $s_i = \sin\theta_i, c_i = \cos\theta_1$ and $\theta_1, \theta_2, \theta_3$ are arbitrary complex angles. Since R is basis independent, all of its three real parameters and three phases are observable. They lead to flavor and CP violation in the Yukawa interaction of the RH neutrino. From (A.2.2) and (A.2.4), the nine UV observables η_b can be chosen to be the three RH neutrino masses, and the six elements that specify the matrix R.

We now present the corresponding UV invariants. We build them out of traces of matrices that transform only under $U(3)_N$ as in table A.4. The RH neutrino masses can be expressed in terms of the invariants

$$\mathrm{Tr}\left[\left(M^* M\right)^n\right] \tag{A.2.7}$$

with $n = 1, 2, 3$. The three UV invariants measuring flavor violation are

$$\mathrm{Tr}\left[\lambda_N^\dagger \lambda_N, M^* M\right]^2 \tag{A.2.8}$$

$$\mathrm{Tr}\left[\lambda_N^\dagger \lambda_N, M^* \lambda_N^\dagger \lambda_N M\right]^2 \tag{A.2.9}$$

$$\mathrm{Tr}\left(\left[\lambda_N^\dagger \lambda_N, M^* M\right]^2 \left(M^* \lambda_N^\dagger \lambda_N M\right)^2\right) \tag{A.2.10}$$

The three UV invariants measuring the UV CP violating phases are

$$\mathrm{Tr}\left[\lambda_N^\dagger \lambda_N, M^* M\right]^3 \tag{A.2.11}$$

$$\mathrm{Tr}\left[\lambda_N^\dagger \lambda_N, M^* \lambda_N^\dagger \lambda_N M\right]^3 \tag{A.2.12}$$

$$\mathrm{Tr}\left(\left[\lambda_N^\dagger \lambda_N, M^* M\right] \left(M^* \lambda_N^\dagger \lambda_N M\right)^2\right) \tag{A.2.13}$$

Finally, one must show that the given set of twenty-one invariants is an independent set of invariants. According to (A.2.1), the Jacobian matrix is a block-triangular matrix. This considerably simplifies the calculation of the Jacobian. The determinant of a block triangular matrix is given by the multiplication of the determinants of the diagonal blocks. The determinant of the diagonal block involving only the IR invariants is non-zero, since it corresponds to the condition that the twelve IR invariants are independent. The determinant of the second block is given just by derivatives of the UV invariants with respect to UV parameters

$$\det \frac{\partial \mathcal{I}_b}{\partial \eta_c} \qquad c = 1..9 \tag{A.2.14}$$

Using (A.2.7), (A.2.10) and (A.2.13) we check that (A.2.14) is indeed non-zero numerically. This completes the proof; the twenty-one chosen invariants are independent.

Appendix B

The little A/m^2 problem for arbitrary couplings

In sections 3.2 and 3.3 we concluded that the little A/m^2 tuning problem is most serious when a soft mass for the Higgs field is generated. In this appendix we show that this little A/m^2 problem is generic for our class of models: it cannot be avoided by increasing the messenger number or considering a more general renormalizable superpotential.

Consider the most general renormalizable superpotential coupling the fields $H_u, Q, \overline{u}$ with n pairs of messengers $\phi_k, \tilde{\phi}_k$ $(k = 1 \dots n)$ with the quantum numbers of H_u and its hermitian conjugate

$$W = M_k \phi_k \tilde{\phi}_k + X_k \tilde{\phi}_k H_u + y_t H_u Q \overline{u} + \lambda_k \phi_k Q \overline{u} + \dots \tag{B.0.1}$$

where we sum over repeated indices. Here, differently from section 3.3, we work in a basis in which the supersymmetric mass matrix has already been diagonalized, so X_k have only F-term vevs. The rest of the interactions included in $\dots$ do not matter to derive the induced A-term and soft mass at lowest order, so we neglect them in what follows. Integrating out the messengers in the small SUSY breaking regime $F/M^2 \ll 1$ we get the low energy superpotential and Kähler potential

$$W = y_t H_u Q \overline{u} - \lambda_k \frac{X_k}{M_k} H_u Q \overline{u} \quad , \quad K = \left(1 + \left(\frac{X_k}{M_k}\right)^\dagger \left(\frac{X_k}{M_k}\right)\right) H_u^\dagger H_u + \dots \tag{B.0.2}$$

so the A-term and induced soft mass are

$$y_t A_t = -\frac{\lambda_k X_k}{M_k} \quad , \quad \delta m_{H_u}^2 = -\left(\frac{X_k}{M_k}\right)^\dagger \left(\frac{X_k}{M_k}\right) \tag{B.0.3}$$

To avoid the little A/m^2 problem, we need to maximize the ratio of the A-term over the soft mass. In particular we are interested in knowing if in doing this, the theory remains perturbative, or if it

does not, when does it become strongly coupled. To address this question, note that there is a linear combination of messengers that couples to the light fields with a Yukawa with magnitude given by

$$|\lambda| = \sqrt{\sum_k |\lambda_k|^2} \tag{B.0.4}$$

so that the Yukawa beta functions are, at one loop,

$$\beta_\lambda = \beta^0_\lambda + \frac{6y_t^2\lambda}{16\pi^2} \quad , \quad \beta_{y_t} = \beta^0_{y_t} + \frac{6y_t\lambda^2}{16\pi^2} \tag{B.0.5}$$

where β^0 is a MSSM-like top Yukawa beta function. We immediately see that the parameter that controls the running of the Yukawas is $|\lambda|$. Fixing this parameter, the ratio of the A-term over the soft mass is maximized when λ_k and $\frac{X_k}{M_k}$ are parallel vectors in k space. This leads to the bound

$$\left|\frac{y_t A_t}{\delta m_{H_u}}\right| \leq |\lambda| \tag{B.0.6}$$

where to retain perturbativity λ needs to be of order one or smaller. This bound is valid for the most general renormalizable superpotential that couples messengers with the Higgs at tree level. A similar bound relating the squark mass to the A-term can be obtained for the non-MFV model of section 3.2. Note that the bound is independent of the messenger number. For messengers at 250 TeV and $\lambda = 1$ as considered in section 3.2 a Landau pole is obtained at $\sim 10^{10}$ GeV. A coupling $\lambda = 3$ as considered in section 3.3 leads to a Landau pole less than a decade above the messenger scale.

Appendix C

EDM functions

In this appendix we define the functions needed for the calculation of the electron EDM in section 4.7. The functions are taken from (cite barr and paban) []. The functions $f(z), g(z)$ and $h(z)$ are given by

$$f(z) = \frac{1}{2}z\int_0^1 dx\,\frac{1-2x(1-x)}{x(1-x)-z}\ln\left[\frac{x(1-x)}{z}\right] \tag{C.0.1}$$

$$g(z) = \frac{1}{2}z\int_0^1 dx\,\frac{1}{x(1-x)-z}\ln\left[\frac{x(1-x)}{z}\right] \tag{C.0.2}$$

$$h(z) = \frac{1}{2}z\int_0^1 dx\,\frac{1}{x(1-x)-z}\left(\frac{z}{x(1-x)-z}\ln\left[\frac{x(1-x)}{z}\right]-1\right) \tag{C.0.3}$$

Defining

$$\begin{aligned} a(x) &= x(1-x) \\ A(x,y,z) &= x+y/z \\ B(x,y,z) &= A(x,y,z)-a(x) \\ B'(x,y,z) &= A(x,y,z)-a(y) \\ C(x,y,z) &= \frac{A(x,y,z)}{B(x,y,z)}\ln\left[\frac{A(x,y,z)}{a(x)}\right]-1 \\ C'(x,y,z) &= \frac{a(x)}{B(x,y,z)}\ln\left[\frac{A(x,y,z)}{a(x)}\right]-1 \\ b(x,z) &= \frac{a(x)}{z} \end{aligned} \tag{C.0.4}$$

and

$$D_1(z) = -\frac{1}{2}\int_0^1 dx \int_0^{1-x} dy\, \frac{x}{B(x,y,z)}\left(\frac{2C(x,y,z)}{B(x,y,z)}\left[3A(x,y,z)-2xy\right]-\left[\frac{3a(x)-2xy}{a(x)}\right]\right)$$

$$D_2(z) = \int_0^1 dx \int_0^{1-x} dy\, x\left(C'(x,y,z)\left[\frac{3A(x,y,z)-2xy}{B^2(x,y,z)}+\frac{1+3x(1-2y)/(2a(x))}{B(x,y,z)}+\frac{3}{2a(x)}\right]\right.$$
$$\left.+\ \frac{3A(x,y,z)-2xy}{2a(x)B(x,y,z)}\right)$$

$$D_3(z) = \int_0^1 dx \int_0^{1-x} dy\, \frac{x^2 y}{a(x)(1-y-b)}\left(\frac{b(x,z)}{1-y-b(x,z)}\ln\left[\frac{1-y}{b(x,z)}\right]-1\right)$$

$$D_4(z) = -\frac{1}{8}\int_0^1 dx \int_0^{1-x} dy\left(\frac{1}{zB(x,y,z)}\left[1-\frac{2a(x)C(x,y,z)}{B(x,y,z)}\right]\right.$$
$$\left.+\ \frac{x}{B(x,y,z)}\left[1-\frac{2A(x,y,z)C(x,y,z)}{B(x,y,z)}\right]\right)$$

$$D_5(z) = \frac{1}{8}\int_0^1 dx \int_0^{1-x} dy\, \frac{x}{a(x)}\left(\frac{C'(x,y,z)}{B^2(x,y,z)}\left[x(2x-1)a(x)+x(3x-1)B(x,y,z)\right.\right.$$
$$\left.\left.-\ 2B^2(x,y,z)\right]-2\left[1-\frac{x(2x-1)}{4B(x,y,z)}\right]\right) \tag{C.0.5}$$

the function $D(z)$ is given by

$$D(z) = \sum_{i=1}^{5} D_i(z) \tag{C.0.6}$$

Appendix D

Solution to the EWSB condition for the condensate phase ξ in the $\mathbb{Z}_2$ symmetric limit

Glashow Weinberg conditions may be imposed by a $\mathbb{Z}_2$ symmetry under which the doublets Φ_1, Φ_2 have opposite charges. This symmetry also imposes that the Higgs potential parameters λ_6 and λ_7 defined in (4.3.3) must vanish

$$\lambda_6 = \lambda_7 = 0 \tag{D.0.1}$$

In this appendix we provide the effective dimension six solution to the electroweak symmetry breaking (EWSB) condition (4.3.7) for the gauge invariant condensate parameter ξ defined in (4.3.5) in the $\mathbb{Z}_2$ symmetric limit. In this limit the EWSB condition (4.3.7) is

$$\frac{\partial V}{\partial \xi} \;=\; 0 \;=\; \frac{1}{2}v^2 \sin 2\beta \,\left[\,\mathrm{Im}(m_{12}^2 e^{i\xi}) - \frac{1}{4}v^2 \sin 2\beta\, \mathrm{Im}(\lambda_5 e^{2i\xi})\right] \tag{D.0.2}$$

For $\sin 2\beta \neq 0$ and dividing by $|m_{12}|^2$ we can rewrite the EWSB condition (D.0.2) as

$$\mathrm{Im}\big(e^{i\mathrm{Arg}\, m_{12}^2} e^{i\xi}\big) = \frac{1}{4}\frac{v^2}{|m_{12}|^2}\, \mathrm{Im}(\lambda_5 e^{2i\xi})\, \sin 2\beta \tag{D.0.3}$$

The PQ violating mass term $\left|m_{12}^2\right|$ is related to the heavy Higgs masses through

$$\left|m_{12}^2\right| = \frac{1}{2}\sin 2\beta\, m_H^2 \left[1 + \mathcal{O}\left(\frac{v^2}{m_H^2}\right)\right] \tag{D.0.4}$$

so to lowest order in v^2/m_H^2 the EWSB condition (D.0.3) may be rewritten as

$$\mathrm{Im}\big(e^{i\mathrm{Arg}\, m_{12}^2} e^{i\xi}\big) = \frac{1}{2}\frac{v^2}{m_H^2}\, \mathrm{Im}\big(\lambda_5 e^{2i\xi}\big) + \mathcal{O}\left(\,|\lambda_5|\,\frac{v^4}{m_H^4}\right) \tag{D.0.5}$$

The first step to find the solution to the equation (D.0.5) is to rewrite it as a complex quadratic equation for $e^{i\mathrm{Arg}\, m_{12}^2} e^{i\xi}$

$$e^{i\mathrm{Arg}\, m_{12}^2} e^{i\xi} = \frac{1}{2}\frac{v^2}{m_H^2}\left(\lambda_5 e^{-i\mathrm{Arg}\, m_{12}^4}\right)\left(e^{i\mathrm{Arg}\, m_{12}^2} e^{i\xi}\right)^2 + \gamma + \mathcal{O}\left(|\lambda_5|\,\frac{v^4}{m_H^4}\right) \tag{D.0.6}$$

where γ is a real constant. γ is not an arbitrary constant, since the left hand side of (D.0.6) has unit norm $\left|e^{i\mathrm{Arg}\, m_{12}^2} e^{i\xi}\right| = 1$. Taking the norm of (D.0.6), we find an equation for γ

$$1 = \left|\frac{1}{2}\frac{v^2}{m_H^2}\,\lambda_5 e^{2i\xi} + \gamma + \mathcal{O}\left(|\lambda_5|\,\frac{v^4}{m_H^4}\right)\right| \tag{D.0.7}$$

The solution to the equation (D.0.7) for the constant γ is, at lowest order in v^2/m_H^2

$$\gamma = 1 + \mathcal{O}\left(|\lambda_5|\,\frac{v^2}{m_H^2}\right) \tag{D.0.8}$$

We now solve the complex quadratic equation (D.0.6) for $e^{i\mathrm{Arg}\, m_{12}^2} e^{i\xi}$. Only one of the two solutions to the quadratic equation (D.0.6) remains finite in the limit of vanishing v^2/m_H^2. The solution is

$$e^{i\mathrm{Arg}\, m_{12}^2} e^{i\xi} = \frac{1}{\frac{v^2}{m_H^2}\,\lambda_5 e^{-i\mathrm{Arg}\, m_{12}^4}}\left[1 - \left(1 - 2\gamma\,\frac{v^2}{m_H^2}\,\lambda_5 e^{-i\mathrm{Arg}\, m_{12}^4}\right)^{-1/2}\right] + \mathcal{O}\left(|\lambda_5|\,\frac{v^4}{m_H^4}\right) \tag{D.0.9}$$

Expanding (D.0.9) in v^2/m_H^2, we obtain

$$e^{i\mathrm{Arg}\, m_{12}^2} e^{i\xi} = \gamma + \gamma^2\frac{v^2}{m_H^2}\,\lambda_5 e^{-i\mathrm{Arg}\, m_{12}^4} + \mathcal{O}\left(|\lambda_5|\,\frac{v^4}{m_H^4}\right) \tag{D.0.10}$$

We are only interested in the imaginary part of $e^{i\mathrm{Arg}\, m_{12}^2} e^{i\xi}$. When taking the imaginary part of (D.0.10), the first term on the right hand side vanishes since the constant γ is real, so we obtain

$$\mathrm{Im}\left(e^{i\mathrm{Arg}\, m_{12}^2} e^{i\xi}\right) = \gamma^2\frac{v^2}{m_H^2}\mathrm{Im}\left(\,\lambda_5 e^{-i\mathrm{Arg}\, m_{12}^4}\right) + \mathcal{O}\left(|\lambda_5|\,\frac{v^4}{m_H^4}\right) \tag{D.0.11}$$

Using the solution (D.0.8) for the real constant γ in (D.0.11) we obtain

$$\mathrm{Im}\left(e^{i\mathrm{Arg}\, m_{12}^2} e^{i\xi}\right) = \frac{1}{2}\frac{v^2}{m_H^2}\mathrm{Im}\left(\lambda_5 e^{-i\mathrm{Arg}\, m_{12}^4}\right) + \mathcal{O}\left(|\lambda_5|\,\frac{v^4}{m_H^4}\right) \tag{D.0.12}$$

Inverting equation (D.0.4) to express the heavy Higgs mass m_H^2 as a function of $m_{12}^2/\sin 2\beta$, equation (D.0.12) may be rewritten as

$$\mathrm{Im}(m_{12}^2 e^{i\xi}) = -\frac{1}{4}v^2\,|\lambda_5|\sin 2\beta\,\sin\mathrm{Arg}\left(m_{12}^4\lambda_5^*\right)\left[1 + \mathcal{O}\left(|\lambda_5|\,\frac{v^2}{m_H^2}\right)\right] \tag{D.0.13}$$

Equation (D.0.13) is the solution to the electroweak symmetry breaking condition (D.0.2) for the condensate phase ξ in terms of lagrangian parameters, and is the final result of this appendix.

Bibliography

[1] Georges Aad et al. "Observation of a new particle in the search for the Standard Model Higgs boson with the ATLAS detector at the LHC". In: *Phys.Lett.* B716 (2012), pp. 1–29. DOI: 10.1016/j.physletb.2012.08.020. arXiv: 1207.7214 [hep-ex].

[2] Serguei Chatrchyan et al. "Observation of a new boson at a mass of 125 GeV with the CMS experiment at the LHC". In: *Phys.Lett.* B716 (2012), pp. 30–61. DOI: 10.1016/j.physletb.2012.08.021. arXiv: 1207.7235 [hep-ex].

[3] Vardan Khachatryan et al. "Observation of the rare $B_s^0 \to \mu^+\mu^-$ decay from the combined analysis of CMS and LHCb data". In: *Nature* 522 (2015), pp. 68–72. DOI: 10.1038/nature14474. arXiv: 1411.4413 [hep-ex].

[4] Tatsumi Aoyama et al. "Tenth-Order Electron Anomalous Magnetic Moment — Contribution of Diagrams without Closed Lepton Loops". In: *Phys. Rev.* D91.3 (2015), p. 033006. DOI: 10.1103/PhysRevD.91.033006. arXiv: 1412.8284 [hep-ph].

[5] D. Hanneke, S. Fogwell, and G. Gabrielse. "New Measurement of the Electron Magnetic Moment and the Fine Structure Constant". In: *Phys. Rev. Lett.* 100 (2008), p. 120801. DOI: 10.1103/PhysRevLett.100.120801. arXiv: 0801.1134 [physics.atom-ph].

[6] Brian Fields and Subir Sarkar. "Big-Bang nucleosynthesis (2006 Particle Data Group mini-review)". In: (2006). arXiv: astro-ph/0601514 [astro-ph].

[7] K. G. Wilson. "The renormalization group and critical phenomena". In: *Rev. Mod. Phys.* 55 (1983), pp. 583–600. DOI: 10.1103/RevModPhys.55.583.

[8] Gerard 't Hooft et al. "Recent Developments in Gauge Theories. Proceedings, Nato Advanced Study Institute, Cargese, France, August 26 - September 8, 1979". In: *NATO Sci. Ser. B* 59 (1980), pp.1–438.

[9] Yu. A. Golfand and E. P. Likhtman. "Extension of the Algebra of Poincare Group Generators and Violation of p Invariance". In: *JETP Lett.* 13 (1971). [Pisma Zh. Eksp. Teor. Fiz.13,452(1971)], pp. 323–326.

[10] J. Wess and B. Zumino. "Supergauge Transformations in Four-Dimensions". In: *Nucl. Phys.* B70 (1974), pp. 39–50. DOI: 10.1016/0550-3213(74)90355-1.

[11] Marcus T. Grisaru, W. Siegel, and M. Rocek. "Improved Methods for Supergraphs". In: *Nucl. Phys.* B159 (1979), p. 429. DOI: 10.1016/0550-3213(79)90344-4.

[12] Nathan Seiberg. "Naturalness versus supersymmetric nonrenormalization theorems". In: *Phys. Lett.* B318 (1993), pp. 469–475. DOI: 10.1016/0370-2693(93)91541-T. arXiv: hep-ph/9309335 [hep-ph].

[13] G.F. Giudice and R. Rattazzi. "Theories with gauge mediated supersymmetry breaking". In: *Phys.Rept.* 322 (1999), pp. 419–499. DOI: 10.1016/S0370-1573(99)00042-3. arXiv: hep-ph/9801271 [hep-ph].

[14] Patrick Draper et al. "Implications of a 125 GeV Higgs for the MSSM and Low-Scale SUSY Breaking". In: *Phys. Rev.* D85 (2012), p. 095007. DOI: 10.1103/PhysRevD.85.095007. arXiv: 1112.3068 [hep-ph].

[15] Aria Basirnia et al. "125 GeV Higgs from Tree-Level A-terms". In: *JHEP* 06 (2015), p. 144. DOI: 10.1007/JHEP06(2015)144. arXiv: 1501.00997 [hep-ph].

[16] J. Alberto Casas et al. "Reducing the Fine-Tuning of Gauge-Mediated SUSY Breaking". In: (2016). arXiv: 1602.06892 [hep-ph].

[17] Nicola Cabibbo. "Unitary Symmetry and Leptonic Decays". In: *Phys. Rev. Lett.* 10 (1963). [,648(1963)], pp. 531–533. DOI: 10.1103/PhysRevLett.10.531.

[18] Makoto Kobayashi and Toshihide Maskawa. "CP Violation in the Renormalizable Theory of Weak Interaction". In: *Prog. Theor. Phys.* 49 (1973), pp. 652–657. DOI: 10.1143/PTP.49.652.

[19] B. Pontecorvo. "Neutrino Experiments and the Problem of Conservation of Leptonic Charge". In: *Sov. Phys. JETP* 26 (1968). [Zh. Eksp. Teor. Fiz.53,1717(1967)], pp. 984–988.

[20] Ziro Maki, Masami Nakagawa, and Shoichi Sakata. "Remarks on the unified model of elementary particles". In: *Prog. Theor. Phys.* 28 (1962), pp. 870–880. DOI: 10.1143/PTP.28.870.

[21] C. A. Baker et al. "An Improved experimental limit on the electric dipole moment of the neutron". In: *Phys. Rev. Lett.* 97 (2006), p. 131801. DOI: 10.1103/PhysRevLett.97.131801. arXiv: hep-ex/0602020 [hep-ex].

[22] Savas Dimopoulos and Howard Georgi. "Softly Broken Supersymmetry and SU(5)". In: *Nucl.Phys.* B193 (1981), p. 150. DOI: 10.1016/0550-3213(81)90522-8.

[23] Neil Turok and John Zadrozny. "Electroweak baryogenesis in the two doublet model". In: *Nucl. Phys.* B358 (1991), pp. 471–493. DOI: 10.1016/0550-3213(91)90356-3.

[24] R. D. Peccei and Helen R. Quinn. "CP Conservation in the Presence of Instantons". In: *Phys. Rev. Lett.* 38 (1977), pp. 1440–1443. DOI: 10.1103/PhysRevLett.38.1440.

[25] R. D. Peccei and Helen R. Quinn. "Constraints Imposed by CP Conservation in the Presence of Instantons". In: *Phys. Rev.* D16 (1977), pp. 1791–1797. DOI: 10.1103/PhysRevD.16.1791.

[26] John F. Gunion et al. "The Higgs Hunter's Guide". In: *Front.Phys.* 80 (2000), pp. 1–448.

[27] Nathaniel Craig and Scott Thomas. "Exclusive Signals of an Extended Higgs Sector". In: *JHEP* 1211 (2012), p. 083. DOI: 10.1007/JHEP11(2012)083. arXiv: 1207.4835 [hep-ph].

[28] Nathaniel Craig, Jamison Galloway, and Scott Thomas. "Searching for Signs of the Second Higgs Doublet". In: (2013). arXiv: 1305.2424 [hep-ph].

[29] Nathaniel Craig et al. "The Hunt for the Rest of the Higgs Bosons". In: *JHEP* 06 (2015), p. 137. DOI: 10.1007/JHEP06(2015)137. arXiv: 1504.04630 [hep-ph].

[30] Sheldon L. Glashow and Steven Weinberg. "Natural Conservation Laws for Neutral Currents". In: *Phys.Rev.* D15 (1977), p. 1958. DOI: 10.1103/PhysRevD.15.1958.

[31] C. Jarlskog. "Commutator of the Quark Mass Matrices in the Standard Electroweak Model and a Measure of Maximal CP Violation". In: *Phys. Rev. Lett.* 55 (1985), p. 1039. DOI: 10.1103/PhysRevLett.55.1039.

[32] A. D. Sakharov. "Violation of CP Invariance, c Asymmetry, and Baryon Asymmetry of the Universe". In: *Pisma Zh. Eksp. Teor. Fiz.* 5 (1967). [Usp. Fiz. Nauk161,61(1991)], pp. 32–35. DOI: 10.1070/PU1991v034n05ABEH002497.

[33] Ann E. Nelson. "Naturally Weak CP Violation". In: *Phys. Lett.* B136 (1984), p. 387. DOI: 10.1016/0370-2693(84)92025-2.

[34] Stephen M. Barr. "Solving the Strong CP Problem Without the Peccei-Quinn Symmetry". In: *Phys. Rev. Lett.* 53 (1984), p. 329. DOI: 10.1103/PhysRevLett.53.329.

[35] Luis Bento, Gustavo C. Branco, and Paulo A. Parada. "A Minimal model with natural suppression of strong CP violation". In: *Phys. Lett.* B267 (1991), pp. 95–99. DOI: 10.1016/0370-2693(91)90530-4.

[36] Michael Dine, Robert G. Leigh, and Alex Kagan. "Supersymmetry and the Nelson-Barr mechanism". In: *Phys. Rev.* D48 (1993), pp. 2214–2223. DOI: 10.1103/PhysRevD.48.2214. arXiv: hep-ph/9303296 [hep-ph].

[37] Gudrun Hiller and Martin Schmaltz. "Solving the strong CP problem with supersymmetry". In: *Phys. Lett.* B514 (2001), pp. 263–268. DOI: 10.1016/S0370-2693(01)00814-0. arXiv: hep-ph/0105254 [hep-ph].

[38] Gudrun Hiller and Martin Schmaltz. "Strong weak CP hierarchy from nonrenormalization theorems". In: *Phys. Rev.* D65 (2002), p. 096009. DOI: 10.1103/PhysRevD.65.096009. arXiv: hep-ph/0201251 [hep-ph].

[39] Stephen M. Barr. "A Natural Class of Nonpeccei-quinn Models". In: *Phys. Rev.* D30 (1984), p. 1805. DOI: 10.1103/PhysRevD.30.1805.

[40] M. Fukugita and T. Yanagida. "Baryogenesis Without Grand Unification". In: *Phys. Lett.* B174 (1986), p. 45. DOI: 10.1016/0370-2693(86)91126-3.

[41] K.A. Olive et al. "Review of Particle Physics". In: *Chin.Phys.* C38 (2014), p. 090001. DOI: 10.1088/1674-1137/38/9/090001.

[42] Zhi-zhong Xing, He Zhang, and Shun Zhou. "Updated Values of Running Quark and Lepton Masses". In: *Phys. Rev.* D77 (2008), p. 113016. DOI: 10.1103/PhysRevD.77.113016. arXiv: 0712.1419 [hep-ph].

[43] Jian-wei Mei. "Running neutrino masses, leptonic mixing angles and CP-violating phases: From M(Z) to Lambda(GUT)". In: *Phys. Rev.* D71 (2005), p. 073012. DOI: 10.1103/PhysRevD.71.073012. arXiv: hep-ph/0502015 [hep-ph].

[44] A. Gando et al. "Reactor On-Off Antineutrino Measurement with KamLAND". In: *Phys. Rev.* D88.3 (2013), p. 033001. DOI: 10.1103/PhysRevD.88.033001. arXiv: 1303.4667 [hep-ex].

[45] K. Abe et al. "Precise Measurement of the Neutrino Mixing Parameter θ_{23} from Muon Neutrino Disappearance in an Off-Axis Beam". In: *Phys. Rev. Lett.* 112.18 (2014), p. 181801. DOI: 10.1103/PhysRevLett.112.181801. arXiv: 1403.1532 [hep-ex].

[46] F. P. An et al. "Spectral measurement of electron antineutrino oscillation amplitude and frequency at Daya Bay". In: *Phys. Rev. Lett.* 112 (2014), p. 061801. DOI: 10.1103/PhysRevLett.112.061801. arXiv: 1310.6732 [hep-ex].

[47] P. A. R. Ade et al. "Planck 2015 results. XIII. Cosmological parameters". In: (2015). arXiv: 1502.01589 [astro-ph.CO].

[48] A. de Gouvea et al. "Working Group Report: Neutrinos". In: *Community Summer Study 2013: Snowmass on the Mississippi (CSS2013) Minneapolis, MN, USA, July 29-August 6, 2013*. 2013. arXiv: 1310.4340 [hep-ex]. URL: http://inspirehep.net/record/1260555/files/arXiv:1310.4340.pdf.

[49] Sacha Davidson, Enrico Nardi, and Yosef Nir. "Leptogenesis". In: *Phys. Rept.* 466 (2008), pp. 105–177. DOI: 10.1016/j.physrep.2008.06.002. arXiv: 0802.2962 [hep-ph].

[50] J. A. Casas and A. Ibarra. "Oscillating neutrinos and muon —¿ e, gamma". In: *Nucl. Phys.* B618 (2001), pp. 171–204. DOI: 10.1016/S0550-3213(01)00475-8. arXiv: hep-ph/0103065 [hep-ph].

[51] JiJi Fan, Matthew Reece, and Lian-Tao Wang. "Mitigating Moduli Messes in Low-Scale SUSY Breaking". In: *JHEP* 09 (2011), p. 126. DOI: 10.1007/JHEP09(2011)126. arXiv: 1106.6044 [hep-ph].

[52] Lawrence J. Hall, David Pinner, and Joshua T. Ruderman. "A Natural SUSY Higgs Near 126 GeV". In: *JHEP* 1204 (2012), p. 131. arXiv: 1112.2703 [hep-ph].

[53] S. Heinemeyer, O. Stal, and G. Weiglein. "Interpreting the LHC Higgs Search Results in the MSSM". In: *Phys.Lett.* B710 (2012), pp. 201–206. DOI: 10.1016/j.physletb.2012.02.084. arXiv: 1112.3026 [hep-ph].

[54] A. Arbey et al. "Implications of a 125 GeV Higgs for supersymmetric models". In: *Phys.Lett.* B708 (2012), pp. 162–169. DOI: 10.1016/j.physletb.2012.01.053. arXiv: 1112.3028 [hep-ph].

[55] A. Arbey, M. Battaglia, and F. Mahmoudi. "Constraints on the MSSM from the Higgs Sector". In: *Eur.Phys.J.* C72 (2012), p. 1906. DOI: 10.1140/epjc/s10052-012-1906-4. arXiv: 1112.3032 [hep-ph].

[56] Marcela Carena et al. "A 125 GeV SM-like Higgs in the MSSM and the $\gamma\gamma$ rate". In: *JHEP* 1203 (2012), p. 014. DOI: 10.1007/JHEP03(2012)014. arXiv: 1112.3336 [hep-ph].

[57] Junjie Cao et al. "A SM-like Higgs near 125 GeV in low energy SUSY: a comparative study for MSSM and NMSSM". In: *JHEP* 1203 (2012), p. 086. arXiv: 1202.5821 [hep-ph].

[58] Neil D. Christensen, Tao Han, and Shufang Su. "MSSM Higgs Bosons at The LHC". In: *Phys.Rev.* D85 (2012), p. 115018. DOI: 10.1103/PhysRevD.85.115018. arXiv: 1203.3207 [hep-ph].

[59] Felix Brummer, Sabine Kraml, and Suchita Kulkarni. "Anatomy of maximal stop mixing in the MSSM". In: *JHEP* 1208 (2012), p. 089. DOI: 10.1007/JHEP08(2012)089. arXiv: 1204.5977 [hep-ph].

[60] Simon Knapen, Diego Redigolo, and David Shih. "Work in progress". In: ().

[61] Zhaofeng Kang et al. "A Heavy SM-like Higgs and a Light Stop from Yukawa-Deflected Gauge Mediation". In: *Phys.Rev.* D86 (2012), p. 095020. DOI: 10.1103/PhysRevD.86.095020. arXiv: 1203.2336 [hep-ph].

[62] Nathaniel Craig et al. "A Complete Model of Low-Scale Gauge Mediation". In: *JHEP* 1303 (2013), p. 154. DOI: 10.1007/JHEP03(2013)154. arXiv: 1206.4086 [hep-ph].

[63] Jared A. Evans and David Shih. "Surveying Extended GMSB Models with m_h=125 GeV". In: *JHEP* 1308 (2013), p. 093. DOI: 10.1007/JHEP08(2013)093. arXiv: 1303.0228 [hep-ph].

[64] Nathaniel Craig, Simon Knapen, and David Shih. "General Messenger Higgs Mediation". In: *JHEP* 1308 (2013), p. 118. DOI: 10.1007/JHEP08(2013)118. arXiv: 1302.2642.

[65] Simon Knapen and David Shih. "Higgs Mediation with Strong Hidden Sector Dynamics". In: *JHEP* 1408 (2014), p. 136. DOI: 10.1007/JHEP08(2014)136. arXiv: 1311.7107 [hep-ph].

[66] Mohammad Abdullah et al. "Flavored Gauge Mediation, A Heavy Higgs, and Supersymmetric Alignment". In: *JHEP* 1306 (2013), p. 057. DOI: 10.1007/JHEP06(2013)057. arXiv: 1209.4904 [hep-ph].

[67] Hyung Do Kim, Doh Young Mo, and Min-Seok Seo. "Neutrino Assisted Gauge Mediation". In: *Eur.Phys.J.* C73 (2013), p. 2449. DOI: 10.1140/epjc/s10052-013-2449-z. arXiv: 1211.6479 [hep-ph].

[68] Pritibhajan Byakti and Tirtha Sankar Ray. "Burgeoning the Higgs mass to 125 GeV through messenger-matter interactions in GMSB models". In: *JHEP* 1305 (2013), p. 055. DOI: 10.1007/JHEP05(2013)055. arXiv: 1301.7605 [hep-ph].

[69] Lorenzo Calibbi, Paride Paradisi, and Robert Ziegler. "Gauge Mediation beyond Minimal Flavor Violation". In: *JHEP* 1306 (2013), p. 052. DOI: 10.1007/JHEP06(2013)052. arXiv: 1304.1453 [hep-ph].

[70] Tomasz Jeliński. "On messengers couplings in extended GMSB models". In: *JHEP* 1309 (2013), p. 107. DOI: 10.1007/JHEP09(2013)107. arXiv: 1305.6277 [hep-ph].

[71] Iftah Galon, Gilad Perez, and Yael Shadmi. "Non-Degenerate Squarks from Flavored Gauge Mediation". In: *JHEP* 1309 (2013), p. 117. DOI: 10.1007/JHEP09(2013)117. arXiv: 1306.6631 [hep-ph].

[72] Willy Fischler and Walter Tangarife. "Vector-like Fields, Messenger Mixing and the Higgs mass in Gauge Mediation". In: *JHEP* 1405 (2014), p. 151. DOI: 10.1007/JHEP05(2014)151. arXiv: 1310.6369 [hep-ph].

[73] Ran Ding et al. "Focus Point Supersymmetry in Extended Gauge Mediation". In: *JHEP* 1403 (2014), p. 130. DOI: 10.1007/JHEP03(2014)130. arXiv: 1312.5407 [hep-ph].

[74] Lorenzo Calibbi, Paride Paradisi, and Robert Ziegler. "Lepton Flavor Violation in Flavored Gauge Mediation". In: (2014). arXiv: 1408.0754 [hep-ph].

[75] Zohar Komargodski and Nathan Seiberg. "mu and General Gauge Mediation". In: *JHEP* 0903 (2009), p. 072. DOI: 10.1088/1126-6708/2009/03/072. arXiv: 0812.3900 [hep-ph].

[76] N. Seiberg. "Electric-magnetic duality in supersymmetric nonAbelian gauge theories". In: *Nucl.Phys.* B435 (1995), pp. 129–146. DOI: 10.1016/0550-3213(94)00023-8. arXiv: hep-th/9411149 [hep-th].

[77] Nathan Seiberg. "Exact results on the space of vacua of four-dimensional SUSY gauge theories". In: *Phys.Rev.* D49 (1994), pp. 6857–6863. DOI: 10.1103/PhysRevD.49.6857. arXiv: hep-th/9402044 [hep-th].

[78] Jared Evans, David Shih, and Arun Thalapillil. "Work in progress". In: ().

[79] Michael Dine and Ann E. Nelson. "Dynamical supersymmetry breaking at low-energies". In: *Phys.Rev.* D48 (1993), pp. 1277–1287. DOI: 10.1103/PhysRevD.48.1277. arXiv: hep-ph/9303230 [hep-ph].

[80] Michael Dine, Ann E. Nelson, and Yuri Shirman. "Low-energy dynamical supersymmetry breaking simplified". In: *Phys.Rev.* D51 (1995), pp. 1362–1370. DOI: 10.1103/PhysRevD.51.1362. arXiv: hep-ph/9408384 [hep-ph].

[81] Michael Dine et al. "New tools for low-energy dynamical supersymmetry breaking". In: *Phys.Rev.* D53 (1996), pp. 2658–2669. DOI: 10.1103/PhysRevD.53.2658. arXiv: hep-ph/9507378 [hep-ph].

[82] B.C. Allanach. "SOFTSUSY: a program for calculating supersymmetric spectra". In: *Comput.Phys.Commun.* 143 (2002), pp. 305–331. DOI: 10.1016/S0010-4655(01)00460-X. arXiv: hep-ph/0104145 [hep-ph].

[83] S. Ambrosanio, Graham D. Kribs, and Stephen P. Martin. "Three body decays of selectrons and smuons in low-energy supersymmetry breaking models". In: *Nucl.Phys.* B516 (1998), pp. 55–69. DOI: 10.1016/S0550-3213(98)00041-8. arXiv: hep-ph/9710217 [hep-ph].

[84] Georges Aad et al. "Search for supersymmetry in events with large missing transverse momentum, jets, and at least one tau lepton in 20 fb^{-1} of $\sqrt{s} = 8$ TeV proton-proton collision data with the ATLAS detector". In: *JHEP* 1409 (2014), p. 103. DOI: 10.1007/JHEP09(2014)103. arXiv: 1407.0603 [hep-ex].

[85] J. Alwall et al. "The automated computation of tree-level and next-to-leading order differential cross sections, and their matching to parton shower simulations". In: *JHEP* 1407 (2014), p. 079. DOI: 10.1007/JHEP07(2014)079. arXiv: 1405.0301 [hep-ph].

[86] Serguei Chatrchyan et al. "Search for anomalous production of events with three or more leptons in pp collisions at sqrt(s) = 8 TeV". In: *Phys.Rev.* D90 (2014), p. 032006. DOI: 10.1103/PhysRevD.90.032006. arXiv: 1404.5801 [hep-ex].

[87] Gino Isidori, Yosef Nir, and Gilad Perez. "Flavor Physics Constraints for Physics Beyond the Standard Model". In: *Ann.Rev.Nucl.Part.Sci.* 60 (2010), p. 355. DOI: 10.1146/annurev.nucl.012809.104534. arXiv: 1002.0900 [hep-ph].

[88] Marcela S. Carena, M. Quiros, and C.E.M. Wagner. "Effective potential methods and the Higgs mass spectrum in the MSSM". In: *Nucl.Phys.* B461 (1996), pp. 407–436. DOI: 10.1016/0550-3213(95)00665-6. arXiv: hep-ph/9508343 [hep-ph].

[89] Vardan Khachatryan et al. "Searches for a heavy scalar boson H decaying to a pair of 125 GeV Higgs bosons hh or for a heavy pseudoscalar boson A decaying to Zh, in the final states with h $\to \tau\tau$". In: (2015). arXiv: 1510.01181 [hep-ex].

[90] Vardan Khachatryan et al. "Search for Neutral MSSM Higgs Bosons Decaying to $\mu^+\mu^-$ in pp Collisions at $\sqrt{s} = 7$ and 8 TeV". In: (2015). arXiv: 1508.01437 [hep-ex].

[91] Vardan Khachatryan et al. "Search for Neutral MSSM Higgs Bosons Decaying into A Pair of Bottom Quarks". In: *JHEP* 11 (2015), p. 071. DOI: 10.1007/JHEP11(2015)071. arXiv: 1506.08329 [hep-ex].

[92] Georges Aad et al. "Search for neutral Higgs bosons of the minimal supersymmetric standard model in pp collisions at $\sqrt{s} = 8$ TeV with the ATLAS detector". In: *JHEP* 11 (2014), p. 056. DOI: 10.1007/JHEP11(2014)056. arXiv: 1409.6064 [hep-ex].

[93] Georges Aad et al. "Search for an additional, heavy Higgs boson in the $H \to ZZ$ decay channel at $\sqrt{s} = 8$ TeV in *pp* collision data with the ATLAS detector". In: (2015). arXiv: 1507.05930 [hep-ex].

[94] Georges Aad et al. "Measurements of the Higgs boson production and decay rates and coupling strengths using *pp* collision data at $\sqrt{s} = 7$ and 8 TeV in the ATLAS experiment". In: (2015). arXiv: 1507.04548 [hep-ex].

[95] Vardan Khachatryan et al. "Precise determination of the mass of the Higgs boson and tests of compatibility of its couplings with the standard model predictions using proton collisions at 7 and 8 TeV". In: *Eur.Phys.J.* C75.5 (2015), p. 212. DOI: 10.1140/epjc/s10052-015-3351-7. arXiv: 1412.8662 [hep-ex].

[96] The ATLAS and CMS Collaborations. "Measurements of the Higgs boson production and decay rates and constraints on its couplings from a combined ATLAS and CMS analysis of the LHC pp collision data at $\sqrt{s} = 7$ and 8 TeV". In: (2015).

[97] Thomas Appelquist and J. Carazzone. "Infrared Singularities and Massive Fields". In: *Phys. Rev.* D11 (1975), p. 2856. DOI: 10.1103/PhysRevD.11.2856.

[98] Howard Georgi and Marie Machacek. "DOUBLY CHARGED HIGGS BOSONS". In: *Nucl.Phys.* B262 (1985), p. 463. DOI: 10.1016/0550-3213(85)90325-6.

[99] M.J.G. Veltman and F.J. Yndurain. "RADIATIVE CORRECTIONS TO W W SCATTERING". In: *Nucl.Phys.* B325 (1989), p. 1. DOI: 10.1016/0550-3213(89)90369-6.

[100] John McDonald. "Gauge singlet scalars as cold dark matter". In: *Phys.Rev.* D50 (1994), pp. 3637–3649. DOI: 10.1103/PhysRevD.50.3637. arXiv: hep-ph/0702143 [HEP-PH].

[101] T.D. Lee. "A Theory of Spontaneous T Violation". In: *Phys.Rev.* D8 (1973), pp. 1226–1239. DOI: 10.1103/PhysRevD.8.1226.

[102] T.D. Lee. "CP Nonconservation and Spontaneous Symmetry Breaking". In: *Phys.Rept.* 9 (1974), pp. 143–177. DOI: 10.1016/0370-1573(74)90020-9.

[103] Pierre Fayet. "A Gauge Theory of Weak and Electromagnetic Interactions with Spontaneous Parity Breaking". In: *Nucl.Phys.* B78 (1974), p. 14. DOI: 10.1016/0550-3213(74)90113-8.

[104] Ricardo A. Flores and Marc Sher. "Higgs Masses in the Standard, Multi-Higgs and Supersymmetric Models". In: *Annals Phys.* 148 (1983), p. 95. DOI: 10.1016/0003-4916(83)90331-7.

[105] John R. Ellis et al. "Higgs Bosons in a Nonminimal Supersymmetric Model". In: *Phys. Rev.* D39 (1989), p. 844. DOI: 10.1103/PhysRevD.39.844.

[106] Christophe Grojean, Geraldine Servant, and James D. Wells. "First-order electroweak phase transition in the standard model with a low cutoff". In: *Phys.Rev.* D71 (2005), p. 036001. DOI: 10.1103/PhysRevD.71.036001. arXiv: hep-ph/0407019 [hep-ph].

[107] Donal O'Connell, Michael J. Ramsey-Musolf, and Mark B. Wise. "Minimal Extension of the Standard Model Scalar Sector". In: *Phys.Rev.* D75 (2007), p. 037701. DOI: 10.1103/PhysRevD.75.037701. arXiv: hep-ph/0611014 [hep-ph].

[108] Vernon Barger et al. "LHC Phenomenology of an Extended Standard Model with a Real Scalar Singlet". In: *Phys.Rev.* D77 (2008), p. 035005. DOI: 10.1103/PhysRevD.77.035005. arXiv: 0706.4311 [hep-ph].

[109] Georges Aad et al. "Constraints on new phenomena via Higgs boson couplings and invisible decays with the ATLAS detector". In: (2015). arXiv: 1509.00672 [hep-ex].

[110] John F. Gunion and Howard E. Haber. "The CP conserving two Higgs doublet model: The Approach to the decoupling limit". In: *Phys.Rev.* D67 (2003), p. 075019. DOI: 10.1103/PhysRevD.67.075019. arXiv: hep-ph/0207010 [hep-ph].

[111] G. C. Branco et al. "Theory and phenomenology of two-Higgs-doublet models". In: *Phys. Rept.* 516 (2012), pp. 1–102. DOI: 10.1016/j.physrep.2012.02.002. arXiv: 1106.0034 [hep-ph].

[112] Brian Henning, Xiaochuan Lu, and Hitoshi Murayama. "What do precision Higgs measurements buy us?" In: (2014). arXiv: 1404.1058 [hep-ph].

[113] Gustavo C. Branco, Luis Lavoura, and Joao P. Silva. "CP Violation". In: *Int. Ser. Monogr. Phys.* 103 (1999), pp. 1–536.

[114] Howard E. Haber and Deva O'Neil. "Basis-independent methods for the two-Higgs-doublet model. II. The Significance of tan beta". In: *Phys.Rev.* D74 (2006), p. 015018. DOI: 10.1103/PhysRevD.74.015018. arXiv: hep-ph/0602242 [hep-ph].

[115] Sacha Davidson and Howard E. Haber. "Basis-independent methods for the two-Higgs-doublet model". In: *Phys.Rev.* D72 (2005), p. 035004. DOI: 10.1103/PhysRevD.72.099902, 10.1103/PhysRevD.72.03500410.1103/PhysRevD.72.099902, 10.1103/PhysRevD.72.035004. arXiv: hep-ph/0504050 [hep-ph].

[116] D. M. Asner et al. "ILC Higgs White Paper". In: *Community Summer Study 2013: Snowmass on the Mississippi (CSS2013) Minneapolis, MN, USA, July 29-August 6, 2013*. 2013. arXiv: 1310.0763 [hep-ph]. URL: http://inspirehep.net/record/1256491/files/arXiv:1310.0763.pdf.

[117] Joachim Kopp. "Efficient numerical diagonalization of hermitian 3 x 3 matrices". In: *Int.J.Mod.Phys.* C19 (2008), pp. 523–548. DOI: 10.1142/S0129183108012303. arXiv: physics/0610206 [physics].

[118] Jacob Baron et al. "Order of Magnitude Smaller Limit on the Electric Dipole Moment of the Electron". In: *Science* 343 (2014), pp. 269–272. DOI: 10.1126/science.1248213. arXiv: 1310.7534 [physics.atom-ph].

[119] Andreas Crivellin, Ahmet Kokulu, and Christoph Greub. "Flavor-phenomenology of two-Higgs-doublet models with generic Yukawa structure". In: *Phys.Rev.* D87.9 (2013), p. 094031. DOI: 10.1103/PhysRevD.87.094031. arXiv: 1303.5877 [hep-ph].

[120] J. P. Lees et al. "Evidence for an excess of $\overline{B} \to D^{(*)}\tau^-\overline{\nu}_\tau$ decays". In: *Phys. Rev. Lett.* 109 (2012), p. 101802. DOI: 10.1103/PhysRevLett.109.101802. arXiv: 1205.5442 [hep-ex].

[121] J. P. Lees et al. "Measurement of an Excess of $\overline{B} \to D^{(*)}\tau^-\overline{\nu}_\tau$ Decays and Implications for Charged Higgs Bosons". In: *Phys. Rev.* D88.7 (2013), p. 072012. DOI: 10.1103/PhysRevD.88.072012. arXiv: 1303.0571 [hep-ex].

[122] M. Huschle et al. "Measurement of the branching ratio of $\overline{B} \to D^{(*)}\tau^-\overline{\nu}_\tau$ relative to $\overline{B} \to D^{(*)}\ell^-\overline{\nu}_\ell$ decays with hadronic tagging at Belle". In: *Phys. Rev.* D92.7 (2015), p. 072014. DOI: 10.1103/PhysRevD.92.072014. arXiv: 1507.03233 [hep-ex].

[123] Roel Aaij et al. "Measurement of the ratio of branching fractions $\mathcal{B}(\overline{B}^0 \to D^{*+}\tau^-\overline{\nu}_\tau)/\mathcal{B}(\overline{B}^0 \to D^{*+}\mu^-\overline{\nu}_\mu)$". In: *Phys. Rev. Lett.* 115.11 (2015). [Addendum: Phys. Rev. Lett.115,no.15,159901(2015)], p. 111803. DOI: 10.1103/PhysRevLett.115.159901,10.1103/PhysRevLett.115.111803. arXiv: 1506.08614 [hep-ex].

[124] R Aaij et al. "Measurement of Form-Factor-Independent Observables in the Decay $B^0 \to K^{*0}\mu^+\mu^-$". In: *Phys. Rev. Lett.* 111 (2013), p. 191801. DOI: 10.1103/PhysRevLett.111.191801. arXiv: 1308.1707 [hep-ex].

[125] Roel Aaij et al. "Test of lepton universality using $B^+ \to K^+\ell^+\ell^-$ decays". In: *Phys. Rev. Lett.* 113 (2014), p. 151601. DOI: 10.1103/PhysRevLett.113.151601. arXiv: 1406.6482 [hep-ex].

[126] Vardan Khachatryan et al. "Search for Lepton-Flavour-Violating Decays of the Higgs Boson". In: *Phys. Lett.* B749 (2015), pp. 337–362. DOI: 10.1016/j.physletb.2015.07.053. arXiv: 1502.07400 [hep-ex].

[127] Marat Freytsis, Zoltan Ligeti, and Joshua T. Ruderman. "Flavor models for $\overline{B} \to D^{(*)}\tau\overline{\nu}$". In: *Phys. Rev.* D92.5 (2015), p. 054018. DOI: 10.1103/PhysRevD.92.054018. arXiv: 1506.08896 [hep-ph].

[128] Herbi K. Dreiner et al. "Supersymmetric Jarlskog invariants: The Neutrino sector". In: *Phys. Rev.* D76 (2007), p. 015006. DOI: 10.1103/PhysRevD.76.015006. arXiv: hep-ph/0703074 [HEP-PH].